The evolution of apomixis in the *Asplenium monanthes* fern complex

Robert James Dyer

A thesis submitted in fulfilment of the requirements for the degree of Doctor of Philosophy and the diploma of Imperial College London

Department of Life Sciences
Imperial College London

March 2013

Asplenium monanthes. Copper plate by Daniel Mackenzie from the original drawing by Sydney Parkinson made during Captain James Cook's first voyage across the Pacific, 1768-1771.

Abstract

Asexually reproducing eukaryotes provide a window into the evolution and maintenance of sexual reproduction, and are challenging our concept of a species. In plants, asexual reproduction (apomixis) is known to cause taxonomic problems and has been indicated to have a disparately high frequency in homosporous ferns. The reasons for such a high frequency of apomictic taxa are unclear, and only add to the enigmatic nature of these ferns. Contemporary studies in ferns are focussing on such questions, and are providing valuable insights into the evolutionary dynamics of apomictic ferns. In this thesis, I investigate the evolution of apomixis in the *Asplenium monanthes* complex. First, I perform a biosystematic study of the complex, based upon plastid and nuclear DNA sequence data, reproductive mode and polyploidy. I present evidence for reticulate evolution and multiple apomictic lineages. Second, I address the problem of species delimitation in an apomictic species complex. I performed a comparative analysis of AFLP data and sequence data using a variety of species delimitation methods. Results supported the inferences of independent lineages and reticulate evolution made in the previous chapter, but the AFLP data did not support inferences of parentage. Third, I investigated the evolution of genome size in the complex based on DNA C-value data, and tested the utilisation of spore size data to infer ploidy level based on the relationship between genome size and spore size. Genome size variation was shown not only to be due to polyploidy, but also due to expansion of the monoploid genome / chromosome size. Moreover, the evolution of spore size and genome size were not correlated, indicating that spore size is not a good indicator of ploidy level in apomictic complexes. Finally, I investigate the origins of apomixis in *A.monanthes* based upon AFLP data, sequence data and DNA C-values. I find evidence that the observed genetic and karyological diversity is explained by a single origin of apomixis followed by the spread of apomixis by hybridisation with closely related sexual species by the male function. There is also evidence for post genetic divergence by other mechanisms such as genetic segregation, somatic mutation and unequal meiosis. This thesis presents the first thorough investigation of this complex and has increased our understanding of the evolutionary dynamics of apomixis in ferns.

Declaration of Authorship

I confirm that the research presented in this thesis is my own work, and any assistance received has been appropriately acknowledged. Co-authors who have contributed to manuscripts prepared for publication have been acknowledged at the beginning of each chapter.

Signed: **Robert Dyer**

Date: **18/12/2012**

Acknowledgements

I am incredibly grateful to so many people who have helped, guided, inspired and supported me over the past four years. The thesis would simply not have been completed without them.

First and foremost, I am truly indebted to Harald who has always made time for me, and whose passion and enthusiasm for this field of research has been an inspiration. Second, to Vincent who has navigated me through and kept me on my toes throughout. I thank you both for tolerating my relaxed concept of the deadline, and for you understanding during my more stressed moments. It has been an unforgettable journey and I will always appreciate the opportunity that you have given me.

I have been privileged to meet and become friends with many wonderful people both in the museum and at Silwood Park. I leave both with a bag full of cherished memories. In the museum, I thank Anne, Sabine, Steve, Li, Ying, Jeannine, Norman, Cecile, Andie, Steve Russell, Alex Aitken, Tiina, Mark Carine, Alex Monro, Mark Lewis and Mark Spencer for all your help in the lab, discussions and general warmth. Thank you to all in the sequencing lab, Gabrielle, and Anna and Eileen in the postgraduate office. The museum would certainly not have been the same without the cake Wednesday girls, the mycology massive, and not forgetting Messrs Tom, Guy and Murray. Thank you all for some very happy times.

In Silwood, I want to say a special thank you to Helen, Alex and Martyn who have really spurred me through the last phases, and generally kept me smiling. Also to Tim, CT, Rich, Omar, Paul, Jan, Andrew, Betty, Luis, Lyndsey, Yael, Hanno, and Guillame for helpful discussions and for ‘thinking big’. Thank you to the Mark, Charlie, Bearded Richard, Andy and everyone else in the cricket and football teams for lots of fun, the odd drink, and I’m pleased to say, even the odd victory.

I would also like to thank Ilia and Jaume for the lovely time I spent at Kew. Thank you both for your friendliness and all your help with the manuscript.

I must also thank Carl, James, Anders, George, Paul, Alex and Jorge for their invaluable help in the field, and those at Duke who helped me to edit the first chapter into a paper.

I honestly don't think I'd have made it here in as healthy a state, if at all, without the sustenance provided by my housemates, Charlie and Victoria. I will be forever grateful for your kindness, endless home cooked meals, and all the laughter we shared. Lunch times will not be the same without Tommy Walsh. Thank you also to all my other housemates.

I have been incredibly fortunate to have the continuous support of so many close friends and family. Thank you James and La, and family, Fox Lloyd and family (including Richard), the Leighton family, Ben, Kate and Brenny, Julia and Matt, Alex, Polly and Otis, Uncle Kelvin, Auntie Lydia and Uncle Ray, and many more.

To Vicky, thank you for supporting and enduring me. Your love and understanding has kept me going.

A special mention goes to my grandparents who always encouraged me, and who I will always remember.

And finally, to Mum, Dad, Naomi, Paul (and Wiggins), I am a very lucky person to have you all. You are a truly wonderful family.

Contents

List of Figures

List of Tables

“Science is a big thing if you can travel a Winter Journey in her cause and not regret it. I am not sure she is not bigger still if you can have dealings with scientists and continue to follow in her path.”

Apsley Cherry-Garrard (1922).

CHAPTER 1

General Introduction

1.1 Asexual reproduction and the paradox of sex

> "An author who knows his own mind about everything can present a clear and consistent case. I have felt more that I was carrying a debate with myself, presenting the arguments first on one side and then on the other... Indeed, on the most fundamental questions – the nature of the forces responsible for the maintenance of sexual reproduction and genetic recombination – my mind is not made up."
>
> John Maynard Smith (1978).

The evolution of sex and its predominance in eukaryotes has been a major focus of evolutionary biology research for over a century. The transition to asexuality in many eukaryotic lineages has caused much debate concerning what is now generally known as the 'Paradox of sex'. This paradox comprises a number of theoretical short-term evolutionary benefits for asexual reproduction over sexual reproduction. These include the two-fold cost of sex and the maintenance of favourable gene combinations in asexuals (Stebbins, 1957; Maynard Smith, 1978). Arguments to explain the predominance of sex in eukaryotes include Muller's ratchet (Muller, 1932, 1964) and Kondrashov's hatchet (Kondrashov, 1982), both of which form part of the theory for a long-term benefit of sex, due to recombination (Hartfield & Keightley, 2012). This infers that asexual organisms should accumulate a higher load of deleterious mutations leading to higher extinction rate (Felsenstein, 1974; Barton & Charlesworth, 1998; Otto & Lenormand, 2002; Bachtrog, 2003), and less heritable variation, which theoretically leads to low speciation rates due to a lower chance of fixation of advantageous mutations in a changing environment (Fisher, 1930; Muller, 1932; Stebbins, 1957; Maynard Smith, 1978; Crow, 1992; Orr & Presgraves, 2000).

The general observation of a concentration of asexual organisms at the very tips of the phylogeny supports the long term advantage of sex or cost to asexuality, and has lead to the common notion of asexuality being an 'evolutionary dead end' (Williams, 1975; Maynard Smith, 1978). The phylogenetic pattern would suggest a relatively young age to these asexual lineages and therefore to be consistent with the notion of a higher extinction risk in the absence of sexual recombination. However, the existence of ancient obligate asexual taxa such as *ostracods, orbiatid* mites and *Timema* stick insects and sometimes entirely clonal asexual lineages such as *bdelloid rotifers*, have all seemingly defied initial theory (Judson & Normark, 1996; Welch & Meselson, 2000; Fontaneto *et al.*, 2007). Such paradoxical lineages or 'asexual scandals' have therefore been the subject of intensive study, revealing evidence for: genetic variability within clonal populations (Van Doninck *et al.*, 2004), divergent selection within asexual populations (Fontaneto *et al.*, 2007), and possibly a lesser effect of deleterious mutation accumulation on lineage longevity than previously thought (Barraclough *et al.*, 2007). These findings challenge the argument of asexuality being an evolutionary dead end, and have ensured that the paradox of sex remains a major focus of research in evolutionary biology.

1.2 Asexual reproduction in plants

Asexual reproduction in plants appears in a variety of distinct forms. In this thesis, I follow Mogie (1992) in defining asexual reproduction as comprising the production of an embryo from a single cell whose nucleus is not formed by syngamy. Vegetative reproduction, a common form of asexual reproduction, does not involve development from a single cell stage and is not considered herein.

The taxonomic distribution of apomictic taxa across plant lineages is uneven, with estimations of 0.1% in angiosperms, up to 10% in ferns, and with little if no evidence in gymnosperms, mosses, liverworts or hornworts (Walker, 1966a; Lovis, 1977; Asker & Jerling, 1992; Mogie, 1992; Pichot *et al.*, 2001; Park & Kato, 2003; Liu *et al.*, 2008). The reasons for this disparate distribution are unknown, but it is likely that the intrinsic reproductive and life cycle differences impart distinct evolutionary constraints between the various plant groups. The effect of these constraints are reflected in the diversity observed in mechanisms of asexuality,

and the associated variation in terminology, both within and between plant groups (Asker & Jerling, 1992; Mogie, 1992; Carman, 1997).

Asexual reproduction in angiosperms is termed apomixis, which is defined as the production of seed without reductive meiosis or fertilisation, (Gustafsson, 1946, 1947a,b; Asker & Jerling, 1992; Whitton *et al.*, 2008). The mechanisms of apomixis in this lineage are varied but can be defined in two primary forms: gametophytic apomixis and sporophytic apomixis (Asker & Jerling, 1992; Carman, 1997). Gametophytic apomixis (diplospory or apospory) is the most common form of apomixis, and involves the formation of an unreduced megagametophyte (egg sac) by altering or bypassing meiosis. The unreduced egg cell then develops by parthenogenesis (without fertilisation). In the less common sporophytic apomixis the embryo is formed directly from somatic cells, rather than from the megagametophyte, a process that usually arises in parallel with the production of a reduced (sexual) embryo.

Apomixis in angiosperms can be obligate (constrained to apomixis) or facultative (capable of sexual reproduction and apomixis). The facultative nature of most apomictic angiosperms has allowed for several reversals to obligate sexual reproduction across the phylogeny (Hörandl & Hojsgaard, 2012). Apomixis has a scattered taxonomic distribution in angiosperms and is well studied in the following genera: *Hypericum* (Matzk *et al.*, 2003; Robson, 2006; Barcaccia *et al.*, 2006), *Ranunculus* (Hörandl *et al.*, 2009; Hörandl & Emadzade, 2012), *Rubus* (Weber, 1996), and *Taraxacum* (Van Dijk, 2003; Verduijn *et al.*, 2004). Such studies have revealed that the evolution of apomixis is strongly associated with polyploidy and hybridisation, and that many apomicts retain sexual function via functional male gametes, which allows the potential for the spread of apomixis. The emerging consensus is that apomixis in angiosperms appears to be a highly dynamic process that does not necessarily conform to the view of asexual lineages as evolutionary dead ends (Whitton *et al.*, 2008; Hörandl & Hojsgaard, 2012).

In ferns, asexual reproduction has previously been described as apogamy and not apomixis (Winkler, 1908), following the distinctive properties of the reproductive biology and life cycle of ferns (discussed in detail subsequently). However, Lovis (1977) provides a compelling argument for a more unified terminology through the application in ferns of the term

apomixis as used in angiosperms. These arguments address distinct parallels in the nature of asexual reproduction between the two lineages, and hereafter I will refer to asexual reproduction in ferns as apomixis.

1.3 Apomictic reproduction in homosporous ferns

1.3.1 An introduction to ferns

Ferns (monilophytes) are the most diverse group of vascular plants after angiosperms, with estimations of species diversity exceeding 10,000 species (Pryer *et al.*, 2004; Schneider *et al.*, 2004b; Smith *et al.*, 2006). The group includes: horsetails (Equisetum), Marattioid ferns (e.g. *Angiopteris*), ophioglossoid ferns (e.g. *Botrychium* and *Ophioglossum*), whisk ferns (e.g. *Pstilotum* and *Tmesipteris*), and the most species rich lineage, leptosporangiate ferns (Pryer *et al.*, 2004; Smith *et al.*, 2006).

The ancestral mode of reproduction in the monilophytes and other land plants is homospory. The vast majority of extant ferns are homosporous, with the exception of one lineage, which has evolved a heterosporous mode of reproduction. Homosporous plants produce spores that are uniform in size and germinate to form a bisexual gametophyte (explained subsequently). Conversely, heterosporous plants (including seed plants) produce spores of different sizes, microspores and megaspores, which lead to the development of unisexual gametophytes. The difference between the two distinguishes a major variation in reproductive mode, which confers a profound effect on the evolutionary constraints of these plants (Mogie, 1990; Haufler, 2002).

The evolution of the homosporous fern genome is somewhat of an enigma (Nakazato *et al.*, 2008; Barker & Wolf, 2010; Barker, 2013). These plants are renowned for their high chromosome numbers, and the mean chromosome number in this lineage (n=57.05) is significantly higher than for other plant groups (including heterosporous ferns, n=13.6; and angiosperms, n=15.99) (Klekowski & Baker, 1966; Nakazato *et al.*, 2008). Indeed, one homosporous fern, *Ophioglossum reticulatum*, has the highest chromosome number (n=ca.1400) of all eukaryotes (Abraham & Ninan, 1954). The reasons for such high chromosome numbers, and the disparity compared to other plant groups, remains a major

focus for researchers in this field (Nakazato *et al.*, 2008). Polyploidy (Soltis & Soltis, 1987; Otto & Whitton, 2000; Wood *et al.*, 2009) and paleopolyploidy (Haufler & Soltis, 1986; Haufler, 1987; Pichersky *et al.*, 1990; McGrath *et al.*, 1994; McGrath & Hickok, 1999) have long been considered to play a role in the evolution of homosporous fern genomes. Nevertheless, recent studies have indicated that polyploidy may be no more prevalent than in angiosperms (Nakazato *et al.*, 2006; Barker, 2009; Barker & Wolf, 2010). Such findings contradict 'Haufler's hypothesis' (1987), which considers the high chromosome numbers of homosporous ferns to have arisen via multiple paleopolyploidy events, followed by subsequent gene silencing and genome diploidisation. Instead, the current synthesis suggests that homosporous ferns have less dynamic genomes, undergo different processes of diploidisation (Pichersky *et al.*, 1990; Barker & Wolf, 2010), and experience chromosomal loss at a reduced rate, when compared with angiosperms (Nakazato *et al.*, 2006, 2008; Leitch & Leitch, 2013).

1.3.2 Reproduction in homosporous ferns

The reproductive life cycle of homosporous ferns is described by the 'alternation of generations', which is distinguished by two distinct free-living multicellular forms: the gametophyte and the sporophyte. In a sexual life cycle the gametophyte is haploid (n) and produces haploid gametes by mitosis, and the sporophyte is diploid (2n). The diploid sporophyte produces haploid spores by meiosis during sporogenesis. These spores are dispersed and, dependent on a favourable settling environment, will germinate into gametophytes. The gametophyte stage can be bisexual, as it has the potential to produce both archegonia (female gametes) and antheridia (male gametes). Successful fertilisation of the archegonium by an antheridium results in the development of a diploid sporophyte, completing the life cycle.

The putative bisexual nature of the gametophyte confers a range of breeding systems, some of which are not present in seed bearing plants. These modes of sexual production include inter-gametophytic crossing (gametes from different parents = outbreeding), inter-gametophytic selfing (gametes from the same parent but different gametophytes), intra-gametophytic selfing (gametes from the same parent and the same gametophyte). Despite the potential for extreme inbreeding by intra-gametophytic selfing, most ferns evade self-fertilisation by avoiding

expression of both gender organs on the same gametophyte. Thus ferns have been shown to be predominantly out-crossers and/or display mixed breeding systems (Haufler & Soltis, 1984; Gastony & Gottlieb, 1985; Wubs *et al.*, 2010).

1.3.3 Apomictic reproduction in homosporous ferns

The sexual life cycle, as described above, is the ancestral (pleisiomorphic) condition in homosporous ferns. Previous research has shown that all but one of the documented apomictic ferns are obligate apomicts (Lloyd, 1973; Lovis, 1977), and provides no record of the reverse transition back to sexual reproduction. The transition from a sexual life cycle to apomixis involves the evolution of two phenomena: diplospory and apogamy (Fig. 1.1). Diplospory represents the production of unreduced spores by the alteration or avoidance of meiosis during sporogenesis, and apogamy represents the spontaneous development of a sporophyte without syngamy (fertilization) (Lovis, 1977).

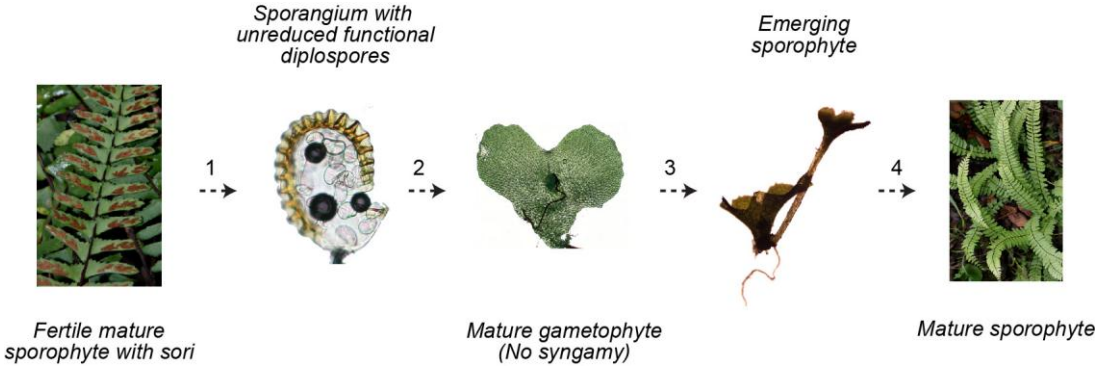

Figure 1.1. The apomictic fern life cycle. (1) The production of unreduced spores (diplospores) by diplospory. (2) The dispersal and germination of spores into an independent and unreduced gametophyte. (3) The emergence of a sporophyte by apogamy. (4) Growth and development into a mature sporophyte.

Diplospory involves a departure from the normal pathway of sporogenesis in ferns, in which the sequence of cell divisions leading to the formation of meio-spores is altered resulting in the production of unreduced (2n) spores (Döpp, 1932; Manton, 1950; Braithwaite, 1964) (Fig. 1.2). Apomicts exhibiting diplospory usually produce 32 unreduced (2n) spores per sporangium, which is in contrast to the vast majority of sexual ferns that produce 64 haploid (n) spores per sporangium (Knobloch, 1966; Vida, 1970). Diplospory generally occurs via

one of two pathways, the more common ‘Döpp-Manton’ sporogenesis, or by the ‘Braithwaite scheme’ of sporogenesis (Figure 1.2).

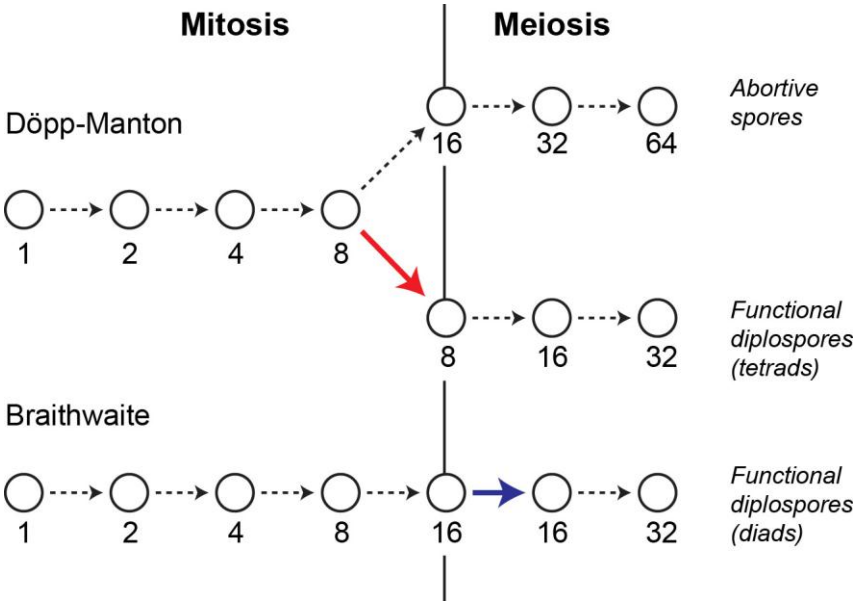

Figure 1.2. Sporangial development in apomictic ferns, adapted from Walker (1966a). The identified two mechanisms of diplospory, ‘Döpp-Manton sporogenesis’ and ‘Braithwaite sporogenesis’ are outlined. The numbers below each circle represent the number of cells per sporangium. Broken arrows indicate normal nuclear divisions. The solid red line indicates a compensatory nuclear division by endomitosis, and solid blue line indicates the formation of a restitutional nucleus.

Döpp-Manton sporogenesis involves a pre-meiotic doubling of chromosomes via an endomitosis resulting in the production of 32 unreduced diplospores. This process has important implications for apomictic polyploids that have an uneven number of genomes (i.e. triploids, pentaploids etc.), or in interspecific hybridisation events where there is a lack of homology between two converging genomes. This is because a pre-meiotic duplication results in an even number of homologous chromosomes, which allows regular bivalents to be formed during meiosis. The preservation of meiosis also has important consequences for the accumulation of genetic diversity in established apomictic lineages. The gametophytes that develop from unreduced Döpp-Manton spores form non-functional archegonia (female gametophytes) but functional antheridia (male gametes) (Laird & Sheffield, 1986). The maintenance of the male function has important implications for the spread of apomixis by hybridisation (Mogie, 1992). Braithwaite sporogenesis involves an entirely different sequence of cytological events by which unreduced apomictic spores are produced. The archesporial cell undergoes the four mitotic divisions normally, but then undergoes a restitutional meiosis,

whereby the first meiotic division does not occur but the second meiotic division is normal, resulting in the production of 32 unreduced diplospores. This form of diplospory often leads to the production of variable spore number, and conversely to Döpp-Manton spores, results in the development of non-functional antheridia.

Apogamy involves the initiation of sporophytic growth from a gametophyte without fertilisation and indeed without change in the chromosome complement (Manton, 1950; Regalado Gabancho *et al.*, 2010). Despite the formation of archegonia on gametophytes of apomictic spores, the topmost cells of mature archegonia are collapsed, which is thought to account for the loss of archegonial function (Laird & Sheffield, 1986). Instead, the sporophyte is initiated through the development of vegetative cell on the gametophyte. It is noteworthy that apogamy has long been documented and can often be induced in sexual species (Somer *et al.*, 2009).

1.3.4 The evolution of apomixis in homosporous ferns

The evolution and maintenance of apomixis in this group are of major interest to researchers in the field of plant evolution. The disproportionately high frequency of apomixis observed in homosporous ferns when compared to other plant groups is hugely intriguing. This intrigue becomes paradoxical, when considering that in theory homospory confers a 50% cost to asexuality (Mogie, 1990). The first cost of asexuality in homosporous plants is that each sporangium produces 50% less spores, and hence 50% less gametophytes. The second cost is that, in contrast to heterosporous plants, male gametes in asexual homosporous plants are not reduced. Cross fertilisation between asexual lineages and sexual relatives by unreduced male gametes would therefore result in an increase in ploidy level. The ploidy level of asexual lineages could therefore increase incrementally and become deleteriously high.

Historically, the evolutionary origins of apomixis have been associated to hybridisation, polyploidy, and female sterility (Manton, 1950; Lovis, 1977; Mogie, 1992). This is due to the meiotic chromosome behaviour observed in apomictic taxa, the high proportion of triploid apomictic taxa, and because apomictic taxa are usually found in complex reticulation networks with other apomictic and sexually reproducing lineages (Walker, 1966a; Liu *et al.*, 2012). Examples of such apomictic polyploid groups include; *Argyochosma* (Sigel *et al.*,

2011), *Astrolepis* (Beck *et al.*, 2011b), *Bommeria* (Gastony & Haufler, 1976), the *Cheilanthes yavapensis* complex (Grusz *et al.*, 2009), *Cyrtomium fortunei* complex (Ootsuki *et al.*, 2011), *Pellaea andromedifolia* (Tryon, 1957; Gastony & Gottlieb, 1985), and the *P.glabella* complex (Gastony, 1988). However, there are also a smaller number of diploid apomicts, including: a few specimens of *Dryopteris affinis* subsp.*affinis* (Manton, 1950; Schneller & Krattinger, 2010), the diplodised triploid apomicts observed in *Dryopteris pacifica* (Lin *et al.*, 1992), the possible rare case of facultative apomixis documented in *Matteuccia orientalis* (Lloyd, 1974), and several examples in the genus *Pteris*, notably including *P.cretica* (Walker, 1962; Suzuki & Iwatsuki, 1990; Yao-Moan Huang *et al.*, 2006; Huang *et al.*, 2011; Chao *et al.*, 2012).

There is growing support for an association between the establishment of apomixis and reticulate evolution across the homosporous ferns, and that the occurrence of apomixis is correlated to the species richness of lineages (Liu *et al.*, 2012). It has also become clear that the evolution of apomixis is a dynamic process, and that the interpretation of genetic patterns often reveals a range of genotypes and morphotypes. These patterns can be caused by a number of factors including: multiple origins of apomixis, due to ongoing apomict formation by co-existing sexual progenitor species; the spread of apomixis via the male function (Walker, 1962; Gastony & Gottlieb, 1985; Watano & Iwatsuki, 1988; Suzuki & Iwatsuki, 1990); post-origin divergence due to ongoing somatic mutation (see Schneller & Krattinger, 2010), unequal meiosis (Lin *et al.*, 1992), and homoeologous chromosome pairing (Klekowski, 1973; Ishikawa *et al.*, 2003; Ootsuki *et al.*, 2011, 2012).

1.4 The *Asplenium monanthes* complex: A model system for studying apomixis in ferns

1.4.1 Taxonomy and cytology

Asplenium (Aspleniaceae) is one of the most species rich genera in the leptosporangiate ferns, comprising approximately 700 species (Schneider *et al.*, 2004a). The *A.monanthes* complex is part of the ‘black stemmed’ spleenwort group that also includes the *A.normale* complex, the *A.trichomanes* complex, *A.viride*, and the Hawaiian *Diellia* complex (Schneider *et al.*, 2004a, 2005). Currently the complex lacks comprehensive revision, but roughly corresponds to 'Grupo 5' of Adams (1995) and species are well described in the treatment of the fern flora of

Mexico by Mickel and Smith (2004). The complex consists of up to 22 terrestrial and saxicolous species (based on Mickel and Smith 2004), including three documented apomictic species: *A.monanthes* (n=2n=108 and 2n=144), which forms 32 unreduced spores via the Döpp-Manton scheme of sporogenesis (Manton, 1950; Manton & Vida, 1968; Wagner *et al.*, 1970; Tryon *et al.*, 1973; Lovis, 1977; Smith & Mickel, 1977; Manton *et al.*, 1986); *A.resiliens* (n=2n=108) (Morzenti & Wagner, 1962; Wagner, 1963, 1966; Morzenti, 1966; Wagner & Wagner, 1966; Walker, 1966b; Wagner *et al.*, 1970; Windham, 1983; Haufler & Soltis, 1986), and a rare pentaploid apomict species, *A.heteroresiliens* (n=2n=180). The latter is thought to be a hybrid between the apomictic triploid *A.resiliens* and the sexual tetraploid/hexaploid *A.heterochroum* (2n=144 or 216) (Morzenti & Wagner, 1962; Morzenti, 1966). Besides these species, the complex includes the diploid sexual *A.formosum* (2n=72) (Manton, 1959; Walker, 1966b; Ghatak, 1977; Ammal & Bahavanandan, 1991; Guillén & Daviña, 2005) and several less well-studied taxa such as *A.castaneum*, *A.blepharodes*, *A.fibrillosum*, *A.hallbergii*, *A.palmeri*, *A.polyphyllum*, and *A.soleirolioides*. Little to no evidence exists concerning the reproductive biology and ploidy level of these taxa.

1.4.2 Geographic distribution

The centre of species diversity for this complex is in southern Mexico. However, species are distributed from southern North America, thorough Central and South America (Stolze, 1981; Tryon *et al.*, 1993; Wagner *et al.*, 1993; Stolze *et al.*, 1994; Adams, 1995; Smith *et al.*, 1999; Mickel & Smith, 2004; Zuloaga *et al.*, 2008; Jørgensen *et al.*, 2010; Kessler & Smith, 2011). Apomictic triploid *A.monanthes* and the sexual diploid *A.formosum* show a wider distribution than the other species within this range, as they also occur in other localities throughout the subtropics, including Africa and various islands in the Atlantic and Indian oceans.

1.5 Outline of thesis

In this thesis I investigate the evolutionary origins of apomixis in the *A.monanthes* complex. The complex is primed for discovery, and offers huge potential for new insights into the paradoxical prevalence of apomixis in homosporous ferns. I have approached the investigation in four parts:

In the second chapter, I assess the occurrence of apomixis within the *A.monanthes* complex, and the association of apomixis to reticulate evolution. I use spore measurements, gametophyte observations and phylogenetic analysis of plastid and nuclear DNA sequence data.

In the third chapter, I address the problems of species delimitation within an apomictic complex. I use a comparative analysis of multilocus and single locus DNA data and a variety of delimitation methods to determine independently evolving apomictic and sexually reproducing lineages.

In the fourth chapter I explore the variation in genome size within and between the various lineages of the *A.monanthes* complex. I also investigate the relationship between genome size and spore size to test the inference of ploidy level from spore size in homosporous ferns.

In the fifth chapter I address the problems in elucidating the evolutionary origins of apomixis in ferns. I consider the evolutionary origins of *A.monanthes* by testing hypotheses on the accumulation of genetic variation within an apomictic lineage.

CHAPTER 2

Apomixis and reticulate evolution in the *Asplenium monanthes* fern complex

Published in Annals of Botany, under the co-authorship of Vincent Savolainen & Harald Schneider.

2.1 Summary

Asexual reproduction is a prominent evolutionary process within land plant lineages and especially in ferns. Up to 10% of the ~10,000 fern species are assumed to be obligate asexuals. In the *Asplenium monanthes* species complex, previous studies identified two triploid, apomictic species. The purpose of this study is to elucidate the phylogenetic relationships in the *A.monanthes* complex and to investigate the occurrence and evolution of apomixis within this group. DNA sequences of three plastid markers and one nuclear single copy gene were used for phylogenetic analyses. Reproductive modes were assessed by examining gametophytic and sporophyte development, while polyploidy was inferred from spore measurements. *Asplenium monanthes* and *A.resiliens* are confirmed to be apomictic. *Asplenium palmeri*, *A.hallbergii*, and specimens that are morphologically similar to *A.heterochroum* are also found to be apomictic. Apomixis is confined to two main clades of taxa related to *A.monanthes* and *A.resiliens*, respectively, and is associated to reticulate evolution. Two apomictic *A.monanthes* lineages, and two putative diploid sexual progenitor species are identified in the *A.monanthes* clade. We infer multiple origins of apomixis, in both alloploid and autoploid forms, within the *A.resiliens* and *A.monanthes* clades.

2.2 Introduction

Asexually reproducing organisms are at the forefront of evolutionary theory and continue to be the subject of new inquiries (Judson & Normark, 1996; Fontaneto *et al.*, 2007; Schwander *et al.*, 2011). Although the evolutionary transition to obligate asexual reproduction is relatively rare across eukaryotes, it appears to be an important evolutionary process in plants (Mogie, 1990, 1992; Asker & Jerling, 1992). However, the taxonomic distribution of apomictic (asexual) taxa across plant lineages is uneven, with estimations of 0.1% in angiosperms, up to 10% in ferns, and with little if no evidence in gymnosperms, mosses, liverworts or hornworts (Walker, 1966a; Lovis, 1977; Asker & Jerling, 1992; Mogie, 1992; Pichot *et al.*, 2001; Park & Kato, 2003).

Sexual reproduction is ancestral in homosporous ferns and the transition to apomixis requires the evolution and alternation of two distinct phenomena: diplospory and apogamy. They represent the avoidance of meiotic reduction during sporogenesis (diplospory), and the spontaneous development of a sporophyte without fertilization (apogamy) (Lovis, 1977). All but one of the documented apomict fern taxa are obligate (Lloyd, 1973; Lovis, 1977), and the reverse transition from apomixis to sexual reproduction has not been observed.

The transition to apomixis has long been associated with hybridisation, polyploidy, and female sterility (Mogie, 1992). This is due to the meiotic chromosome behaviour observed in apomictic taxa, the high proportion of triploid apomictic taxa, and because apomictic taxa are usually found in complex reticulation networks with other apomictic and sexually reproducing lineages (Manton, 1950; Lovis, 1977; Walker, 1979; Grusz *et al.*, 2009). A recent study by Beck *et al.* (2011a) supports the role of hybridisation in apomictic origins, showing that it drives the transition to apomixis in diploid *Boechera* species.

The interpretation of genetic patterns in other apomictic lineages often reveals a cryptic range of genotypes and morphotypes (Grusz *et al.*, 2009; Schneller & Krattinger, 2010). These patterns can be caused by a number of factors including: ongoing apomict formation caused by co-existing sexual progenitor species (clonal turnover); extinction or rarity of sexual progenitors; hybridisation between apomicts and closely related sexual taxa through functional antheridia; ongoing somatic mutation; meiotic recombination and random

segregation of homologues as observed in Dopp-Manton sporogenesis; and homoeologous chromosome pairing (Klekowski, 1970; Klekowski & Hickok, 1974; Ishikawa *et al.*, 2003). Crucial to the understanding of these patterns, is the level of gene flow to and from apomictic lineages. In elucidating origins of apomixis, it is important therefore to consider two hypotheses: a single origin and the subsequent diversification of apomictic lineages, or multiple origins by hybridisation between different sexual relatives.

In this study, we aim to investigate the occurrence and origins of apomixis in the *Asplenium monanthes* complex, for which a modern taxonomic treatment is overdue. The complex consists of up to 22 terrestrial and saxicolous species that occur mainly in Mesoamerica, with its centre of diversity in southern Mexico (based on Mickel & Smith, 2004). The complex is part of the 'black stemmed' spleenwort group that also includes the *A.normale* complex, *A.trichomanes* complex, *A.viride*, and the Hawaiian *Diellia* complex (Schneider *et al.*, 2004a, 2005). The *A.monanthes* complex roughly corresponds to 'Grupo 5' of Adams (1995) and contains two documented triploid apomictic species, *A.monanthes* (n=2n=108 and 2n=144) (Manton, 1950; Manton & Vida, 1968; Wagner *et al.*, 1970; Tryon *et al.*, 1973; Smith & Mickel, 1977; Lovis *et al.*, 1977; Manton *et al.*, 1986) and *A.resiliens* (n=2n=108). It also contains a rare pentaploid apomict species, *A.heteroresiliens.* The latter is thought to be a hybrid between the apomictic triploid *A.resiliens* and the sexual tetraploid/hexaploid *A.heterochroum* (2n=144 or 216) (Morzenti & Wagner, 1962; Wagner, 1963, 1966; Morzenti, 1966; Wagner & Wagner, 1966; Walker, 1966b; Wagner *et al.*, 1970; Windham, 1983; Haufler & Soltis, 1986). Besides these species, the complex includes the diploid sexual *A.formosum* (2n=72) (Manton, 1959; Walker, 1966b; Ghatak, 1977; Ammal & Bahavanandan, 1991; Guillén & Daviña, 2005), and several less well-studied taxa such as *A.castaneum, A.blepharodes, A.fibrillosum, A.hallbergii, A.palmeri, A. polyphyllum,* and *A.soleirolioides* (Mickel & Smith, 2004). Little to no evidence exists concerning the reproductive biology and ploidy level of these taxa.

Asplenium monanthes is a widespread and presumed long-lived apomictic species that forms 32 unreduced spores via the Döpp-Manton scheme of sporogenesis (Manton, 1950). Currently the complex lacks comprehensive revision and so here we follow the treatment of the fern flora of Mexico by Mickel and Smith (2004). Although Mexico is the centre of species

diversity for this complex, species are distributed from southern North America, through Central and South America (Stolze, 1981; Tryon *et al.*, 1993; Wagner *et al.*, 1993; Stolze *et al.*, 1994; Adams, 1995; Smith *et al.*, 1999; Mickel & Smith, 2004; Zuloaga *et al.*, 2008; Jørgensen *et al.*, 2010; Kessler & Smith, 2011). Apomictic triploid *A.monanthes* and the sexual diploid *A.formosum* show a wider distribution than the other species within this range and are distinct as they also occur in other localities throughout the subtropics, including Africa and various islands in the Atlantic and Indian oceans. Current knowledge makes this group a prime candidate to explore the origins and long-term fate of apomictic ferns, along with aspects of their biogeography and ecology.

Here, we use plastid and nuclear sequence data to reconstruct species relationships within the *A.monanthes* complex. This phylogenetic framework is used in combination with some experiments to determine the reproductive modes and ploidy levels in the taxa. Then, we evaluate the following hypotheses: (1) apomixis has multiple origins within this complex; (2) apomixis is associated to reticulate evolution; (3) apomictic lineages have sexual progenitors present in the complex.

2.3 Material and methods

2.3.1 Taxonomic Sampling

In total 140 specimens were studied, representing approximately 50% of the species in the *A.monanthes* complex (Mickel & Smith, 2004) (Appendix, Table A1). The approximated taxonomic coverage may be inflated as the result of the limited knowledge on the taxonomy of this group. First, some taxa were considered to be part of the complex based on morphology alone. Secondly, several of the un-sampled taxa were known from a single or a few samples in herbaria. Studies on the putative sister lineage, the *Asplenium trichomanes* complex, showed the limitations of morphological based studies in assessing species diversity of *Asplenium* species complexes (Lovis *et al.*, 1977; Schneider, unpublished). Most specimens were collected during fieldwork in Mexico, El Salvador and Costa Rica. DNA samples were preserved in silica gel, and voucher specimens were deposited at the herbarium of the Natural History Museum in London (BM), as well as at MEXU, LAGU and INBIO. Additional silica dried material was provided by colleagues (collectors, localities and

additional voucher information are given in the Appendix, Table A1). Some samples were obtained from herbarium specimens stored at BM. Unfortunately we were unable to obtain material for *A.gentryi, A.heteroresiliens, A.nesioticum, A.oligosorum, A.olivaceum, A.pringlei, A.sanchezii, A.stolonipes, A.tryonii, A.underwoodii* and *A.vespertinum*. These species are either rare and/or have restricted geographic ranges that were not visited (Mickel & Smith, 2004). All included samples were carefully identified using the keys provided in Mickel and Smith (2004), and by critical comparison with herbarium collections held at the BM. If needed, specimen identifications were restudied in the context of the obtained DNA sequences, to address inconsistencies in results and identifications. Outgroup taxa were chosen based on Schneider *et al*. (2004a, 2005).

2.3.2 DNA extraction, PCR amplification and sequencing

Total genomic DNA was extracted from leaf tissue using CTAB (Doyle, 1987). Three plastid markers commonly used in ferns were successfully amplified using polymerase chain reactions (PCR): (i) the *psbA-trnH* intergenic spacer (IGS) region (~600 nucleotides) (Aldrich *et al.*, 1988), (ii) the *rps4* plus *rps4-trnS IGS* region (~1000 nucleotides) (Smith & Cranfill, 2002), and (iii) the *trnL-trnF* region including the *trnL* intron and the *trnL-trnF* IGS region (~900 nucleotides) (Taberlet *et al.*, 1991; Trewick *et al.*, 2002). Samples from *A.formosum* proved difficult to amplify for *trnL-trnF*, so only the *trnL* IGS was amplified using *E* and *F* primers (Taberlet *et al.*, 1991; Trewick *et al.*, 2002).

PCR was carried out using Promega Gotaq® Green Master Mix, and amplification was performed using an ABI Veriti Thermo Cycler (Applied Biosystems, Warrington, Cheshire, UK) using protocols from Shaw *et al*. (2007). We also sequenced a fragment of the low copy nuclear gene *pgiC* (~600 nucleotides) for a subset of specimens. Specimens were chosen in order to attain sufficient phylogenetic coverage, based on the relationships observed in the plastid dataset. The generated fragment included the introns spanning exons 14 and 16. The region was amplified using primers *pgiC14FN–16RN* (Ishikawa *et al.*, 2002) and PCR conditions as above were used. Successfully amplified products were isolated by gel extraction using a QIAquick gel extraction kit (www.qiagen.com). Isolated bands were then cloned using the Promega pGEM®–T Vector system to isolate multiple copies present within the nuclear genome. Only one PCR amplicon per individual was cloned, which unfortunately

increases the potential effect of PCR copy preference (Brysting *et al.*, 2011). Where possible eight colonies were randomly chosen from the plated transformants and amplified by diluting colonies in 30µl of sterile water and using 1.5µl of this colony suspension as DNA template. The plasmid specific primers, *puc/M13*, were used to amplify the inserted fragments using the thermo-cycling conditions: 3 min initial denaturation at 94°C, followed by 35 cycles with 15 seconds denaturation at 94°C, 30 seconds annealing at 55°C, 1 min elongation at 72°C and no final extension.

Products were eluted in 40µl of deionised water and then purified using Montage PCR micro 96 Plates. Purified products were quantified using NanoDrop ND-8000 (Thermo Scientific). Sequencing reactions were set up using 2ng purified PCR product per 100bp, Buffer (2x) - 3.5ul, Primer - 1ul of 1uM stock solution, Big Dye version 1.1 - 0.5ul, and the final volume made up to 10ul with deionised water. Cycle sequencing reactions were run on an Applied Biosystems® 9700 96-well Dual Block Thermal Cycler (Life Technologies Ltd, Paisley, UK) as follows: 28 cycles of 10 seconds denaturation at 96°C, 5 seconds annealing at 50°C, and 4 minutes elongation at 60°C. Both forward and reverse strands were sequenced. The fragments were assembled and edited using Sequencher v4.8 (Gene Codes Corporation) and aligned manually using MacClade 4.08 (Maddison & Maddison, 1989, 2005). All newly generated sequences were confirmed using BLAST searches in GenBank (Benson *et al.*, 2011). The three-plastid regions were analysed both separately and in combination. All alignments were checked visually for ambiguous regions, which were excluded from all analyses. Gaps in the alignment were treated as missing data. All sequences are available from Genbank (see Appendix, Tables A1 and A2 for accession numbers).

2.3.3 Phylogenetic analyses

Topological congruence among the three plastid regions was evaluated using bootstrap resampling with maximum parsimony (MP) (Felsenstein, 1985a) using PAUP* 4.0b8 (Swofford, 1993, 2002). The bootstrap heuristic searches were as follows: 1,000 replicates, 10 random sequence-addition per replicate, TBR branch swapping and MULTrees option on, collapse zero-length branches off, and saving all trees. The strict bootstrap consensus trees of the individual regions were compared by eye to detect topological conflicts among the three regions using the criteria outlined by Mason and Kellogg (1996). We did not find any major

topological incongruence between regions (Appendix, Figures A1, A2, and A3); therefore the three plastid regions were compiled into a single matrix for analysis. Specimens that did not have sequence data for all three regions were not included in the combined analysis. This dataset was then reduced to represent unique haplotypes only (Appendix, Table A3); this resulted in a dataset of 54 specimens.

The *pgiC* dataset was reduced to represent unique clones per specimen. To designate unique clones we had to consider the possibility of polymerase error, which can result in two clones of the same allele being amplified with some base pair differences. In order not to confuse these for different alleles, clones that had very similar sequences were only treated as unique if they were separated by significant branch support (Bayesian posterior probability = >0.6). If sequence differences between these clones had no significant branch support then they were treated as being the same allele, and any observed base differences were inferred to be due to polymerase error. The disadvantage of this method is that real alleles that are recovered only once (due to PCR bias) may be disregarded if supported within a clade of other alleles. No chimeric sequences were observed. According to these criteria the full dataset was reduced from 385 clones to 141, representing only one sequence per unique clone per specimen (Appendix, Table A2).

Maximum likelihood (ML) analyses on the combined plastid and nuclear datasets were carried out in PhyML 3.0 with standard search options and parameters estimated simultaneously from the data (Guindon *et al.*, 2005, 2010). The nucleotide substitution model with the least number of parameters that best fit the data was determined using a likelihood ratio test and AIC criterion as implemented in jModeltest version 3.7 (Posada & Crandall, 1998; Posada, 2008), and branch support was estimated using 300 bootstrap replicates (Appendix, Table A4).

Bayesian analysis (BY) was performed on the same two datasets using substitution models according to BIC criterion determined in jModeltest (Appendix, Table A4). Analyses were run in MrBayes 3.1 (Huelsenbeck & Ronquist, 2001; Ronquist & Huelsenbeck, 2003), with Markov Chain Monte Carlo (MCMC) run for 5 million generations and sampled every 500 generations to approximate the posterior probabilities of trees. The two analyses were run

simultaneously and a conservative burn-in phase of 25% was implemented in both datasets to disregard trees prior to convergence on the maximum likelihood. Remaining trees were then compiled to give 7,500 trees for each run, from which a 50% majority rule consensus was calculated.

2.3.4 Reproductive modes

Diplospory involves a departure from the normal pathway of sporogenesis in ferns, resulting in the production of unreduced (2n) spores (Döpp, 1932; Manton, 1950; Braithwaite, 1964). In derived ferns (see Pryer *et al.*, 2004), the number of spores per sporangium often can be used as reliable indicator for the occurrence of diplospory because the number of spore mother cells and the number of cell divisions is highly conserved (Schneider *et al.*, 2009). Thus, the vast majority of sexual ferns produce 64 haploid spores per sporangium. In contrast, apomicts exhibiting diplospory produce 32 unreduced spores per sporangium (Döpp, 1932; Manton, 1950; Tryon, 1956; Knobloch, 1966; Vida, 1970). We determined the number of spores per sporangia for most of the collected specimens. Where possible whole sporangia were isolated but in some instances no unopened sporangia were found due to the age of some of the specimens. The sporangia/spore samples were mounted using Glycerine jelly and spore number per sporangia was counted for up to ten sporangia per specimen using a transmission light microscope.

Apogamy involves the initiation of sporophytic growth from a gametophyte without fertilisation and indeed without change in chromosome numbers (Manton, 1950; Regalado Gabancho *et al.*, 2010). To confirm the presence/absence of apogamous growth, we carried out experiments in which prothalli were grown from spores, allowing direct observations on the gametophyte stage of the fern life cycle. Spores were filtered and sterilised using diluted HCl and then applied to the surface of sterilised potted compost and sealed in a re-sealable plastic bag. The pots were kept in dappled light to shaded conditions at 10–20˚C. The pots were monitored regularly and growth typically began after four weeks and took between 8–24 weeks until prothalli were mature. For determination of reproductive mode, select mature prothalli were mounted on slides and observed in water. Euparal mounting media (ANSCO Laboratories, Manchester, UK) was used to obtain images. The prothalli were then examined for the presence of antheridia and archegonia and evidence of sporophyte emergence (see

examples in Fig. 2.1). Where sporophytes occurred, their emergent position, character and shape were recorded. Observation of the outgrowth of the sporophyte from vegetative cells of the gametophyte is considered as the best approach to identify apogamous reproduction in ferns (Huang *et al.*, 2011), although apogamy can be induced in sexual fern gametophytes under some conditions (Somer *et al.*, 2009; Kawakami *et al.*, 2011).

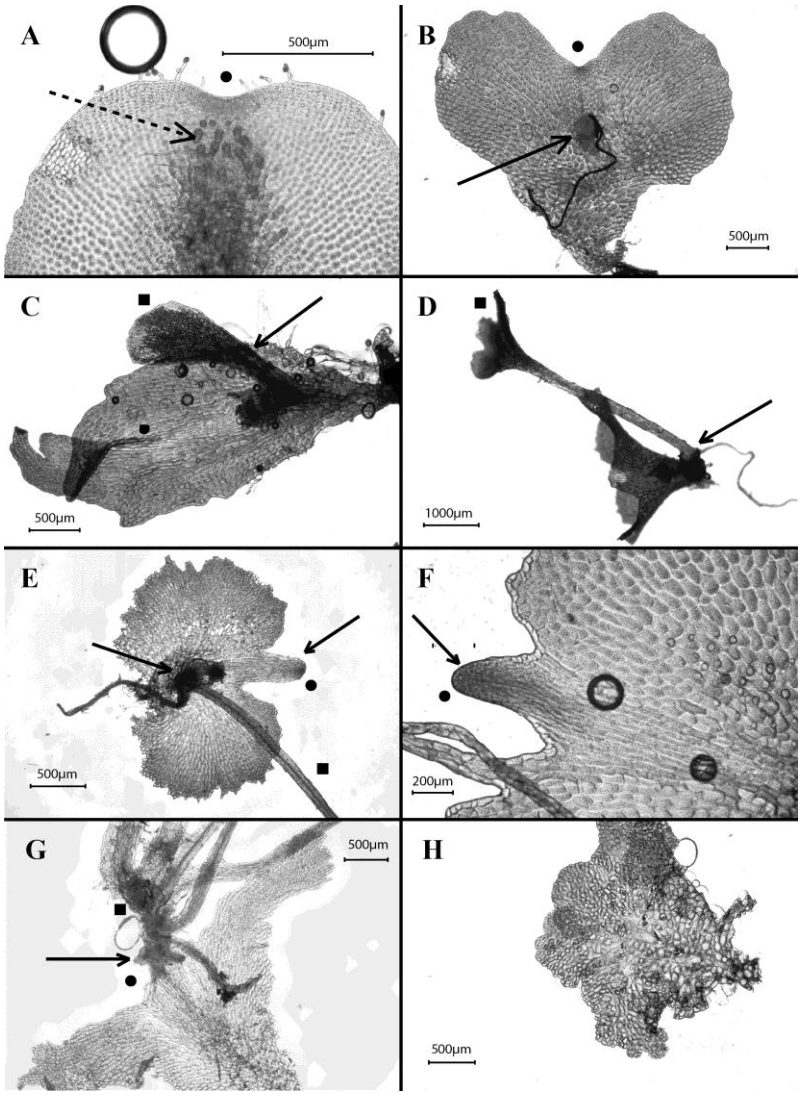

Figure 2.1. Sexual versus apogamous prothalli. Pictures of cultivated prothalli from different specimens (Appendix, Table A7); A) sexual *A.formosum*, RD28, the dashed arrow indicates a group of archegonia; B) apogamous *A.monanthes*, RD110; C) apogamous *A.monanthes*, RD101b; D) apogamous *A.resiliens*, RD127; E) apogamous *A.resiliens*, RD128; F) apogamous *A.monanthes*, RD132; G) apogamous *A.resiliens* RD107; H) apogamous *A.monanthes*, RD17. Solid circles indicate apical meristems and sporophytes are indicated by solid squares. Plain arrows indicate apogamous growth.

2.3.5 Ploidy level

In ferns, the size of spores and stomatal guard cells can often be employed to infer differences in ploidy levels among closely related species (Barrington *et al.*, 1986; Yao-Moan Huang *et al.*, 2006). Spore measurements were successfully employed in several recent studies on the evolution of apomixis in ferns (Beck *et al.*, 2010; Sigel *et al.*, 2011) despite the occurrence of aborted spores, which may add some error to the estimate range (Huang *et al.*, 2011). In the *Asplenium trichomanes* complex, the sister group to the *A.monanthes* complex, it was possible to distinguish ploidy level according to spore size classes, with a mean spore length of 29.4µm in diploids and 41.6µm in tetraploids (Moran, 1982; Tutin *et al.*, 1993).

Here, spores were measured for a representative sampling of 49 specimens (i.e., maximising phylogenetic coverage). Spores from individual specimens were mounted using glycerine jelly and measured for length and width using AxioVision on a calibrated light-microscope (v4.8.2, www.zeiss.com). An average of 25 spores per specimen were measured, although with some specimens very few spores were recovered. Box plots of width and length were plotted separately to determine the variance within each. Ploidy level was inferred based on statistical analysis of spore length variation. Analyses included a one-way ANOVA and Tukey-Kramer analyses at 95% confidence levels using R (R Core Development Team, 2011). Ploidy level was also estimated based upon calibrations of the mean values and variation in spore measurements, to known spore measurements and ploidy levels in the *A.trichomanes* complex (Moran, 1982; Tutin *et al.*, 1993).

2.3.6 Reticulate evolution

In order to illustrate reticulate evolution (Hörandl *et al.*, 2005; Pirie *et al.*, 2009; Huson & Scornavacca, 2011) we reconstructed a phylogenetic network using SplitsTree version 4.12.6 (Huson & Bryant, 2006). Plastid and nuclear datasets were reduced to a subset of compatible samples (Appendix, Tables A5 and A6). One sample for each unique combination of plastid vs nuclear loci was included. However, unique combinations did not include those that varied in nuclear copy number, only those that varied in nuclear copy distribution, i.e. nuclear copies that occurred in different clades. The nuclear dataset was further divided into four subsets, so that each specimen was represented only once in a dataset, i.e. multiple copies were present in separate datasets. The optimal trees resulting from ML bootstrap analyses of the plastid and

nuclear datasets were used as input files. A reticulation network was computed using the 'RECOMB2007' method as implemented in SplitsTree (Kloepper & Huson, 2008). The resulting network was then used to inform the manual construction of a reticulation cladogram, which summarises the reticulate relationships between and within species of this complex.

2.4 Results

2.4.1 Plastid phylogenetic analyses

Analysis of the combined plastid dataset using BY (Fig. 2.2) and ML (Appendix, Fig. A4) resulted in trees with similar topology: see Fig. 2.2 for posterior support values, and the Appendix, Fig. A4 for bootstrap support values. *Asplenium formosum* (pFO) was found to be the sister to the remainder of the *A.monanthes* complex, which formed a polytomy consisting of three well-supported clades: the *A.castaneum clade,* the *A.resiliens* clade, and the *A.monanthes* clade (Fig. 2.2). The *A.castaneum* clade consisted of distinct lineages of *A.polyphyllum* (pPO) and *A.soleirolioides* (pSO), two *A.castaneum* subclades (pCA1 and pCA2), and two lineages containing a paraphyletic *A.fibrillosum* (pFI) (Fig. 2.2). In analysis of the *psbA-trnH* dataset, *Asplenium blepharodes* is recovered within the *A.castaneum* clade (Appendix, Fig. A1). The *A.resiliens* clade consisted of three lineages: two distinct *A.resiliens* subclades (pRE1 and pRE2), and one mixed subclade consisting of *A.palmeri* and *A.*aff.*heterochroum* specimens (pPA) (Fig. 2.2). Three exceptions were observed, but not present in the combined analysis: two *A.palmeri* specimens (CJR2494 and ES486) were recovered in the pRE2 subclade (Appendix, Figures A1, A2, and A3), and one *A.resiliens* specimen (CJR2504) was recovered in subclade pPA (Appendix, Fig. A3). The *A.monanthes* clade consisted of two isolated accessions designated spec.nov.1 (pSP1) and spec.nov.2 (pSP2), and three well-supported monophyletic groups. These included two subclades of *A.monanthes* (pMO1 and pMO2), and one subclade of *A.hallbergii* (pHA) (Fig. 2.2).

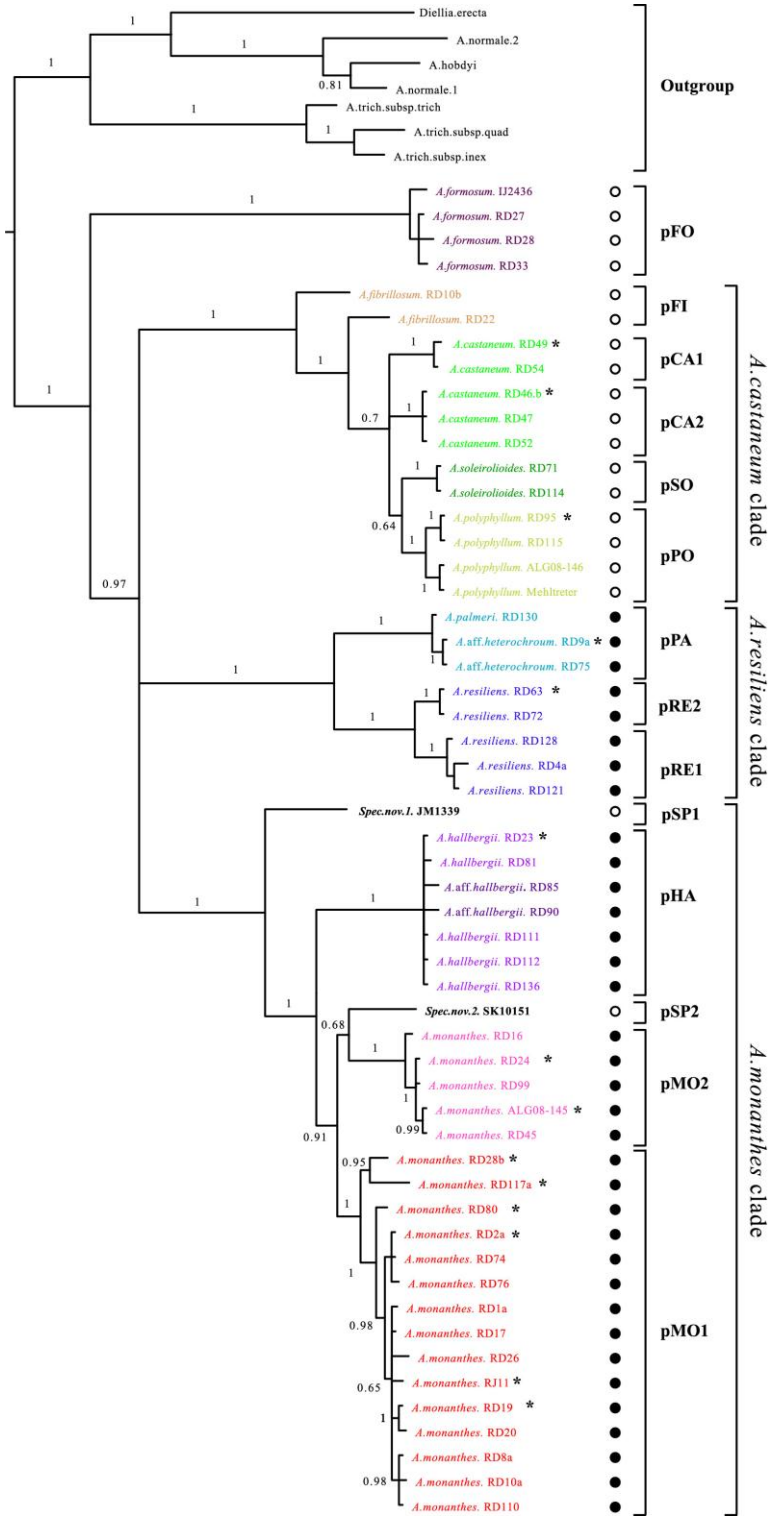

Figure 2.2. Bayesian phylogenetic tree based on the combined plastid data. Posterior support values of p > 0.6 are shown. Tips are labelled with species names followed by a voucher accession, and colour-coded according to species. Subclades are abbreviated and summarised to the right of the tree. Abbreviations for subclades correspond to those used in the text. Stars indicate tips representing multiple haplotypes (Appendix, Table A3). Filled black circles indicate apomictic specimens, and unfilled circles indicate specimens inferred to have a sexual mode of reproduction.

2.4.2 Nuclear phylogenetic analyses

BY (Fig. 2.3) and ML (Appendix, Fig. A5) analysis of the *pgiC 14FN–16RN* dataset (ca 600bp) resulted in trees of similar topology. However, the subclades recovered were not analogous to the subclades present in the plastid-based phylogenetic trees. There was evidence of reticulate evolution as individual specimens often had multiple copies of nuclear sequences that were distributed in different subclades. It must be recognised that this pattern may also be explained by the loss of paralogs in different lineages. We argue that the repeated occurrence of this pattern across the phylogeny suggests that this is due to reticulate evolution. Reticulate evolution generally was restricted to species within the three major clades (*A.castaneum, A.resiliens* and *A.monanthes*) identified in the plastid analysis, although one *A.fibrillosum* accession (RD10b) shared one nuclear copy with the *A.palmeri*/*A.*aff.*heterochroum* subclade (nPA).

Sequences obtained from *A.castaneum* specimens were recovered in three different subclades, two of which (nPO and nSO) were sister to the remainder of the complex. *Asplenium polyphyllum* sequences were also found in these two subclades, and *A.soleirolioides* sequences were present in subclade nSO. The remainder of the complex formed an unresolved polytomy. The third subclade of *A.castaneum* (nCA) was recovered within this polytomy as the weakly supported (posterior probability = 0.75) putative sister to a clade comprised of *A.hallbergii* clone sequences, and one *A.monanthes* sequence (nHA). The polytomy also included: one clade of *A.fibrillosum* clone sequences (nFI); one clade comprising sequences of *A.monanthes* and spec.nov.1 (nMO1); one clade comprising sequences of *A.monanthes, A.hallbergii,* and one sequence of spec.nov.2 (nMO2); and a clade comprising sequences of *A.formosum, A.resiliens, A.palmeri, A.*aff.*heterochroum,* and one sequence of *A.fibrillosum*. The latter clade was a polytomy consisting of four subclades: nFO, formed of *A.formosum* sequences only; nRE1, formed of *A.resiliens* sequences and one *A.palmeri* sequence; nRE2, formed of *A.resiliens* sequences only; and nPA, formed of *A.palmeri* and *A.*aff.*heterochroum* sequences, one sequence of *A.resiliens,* and one sequence of *A.fibrillosum* (see Fig. 2.3 for details).

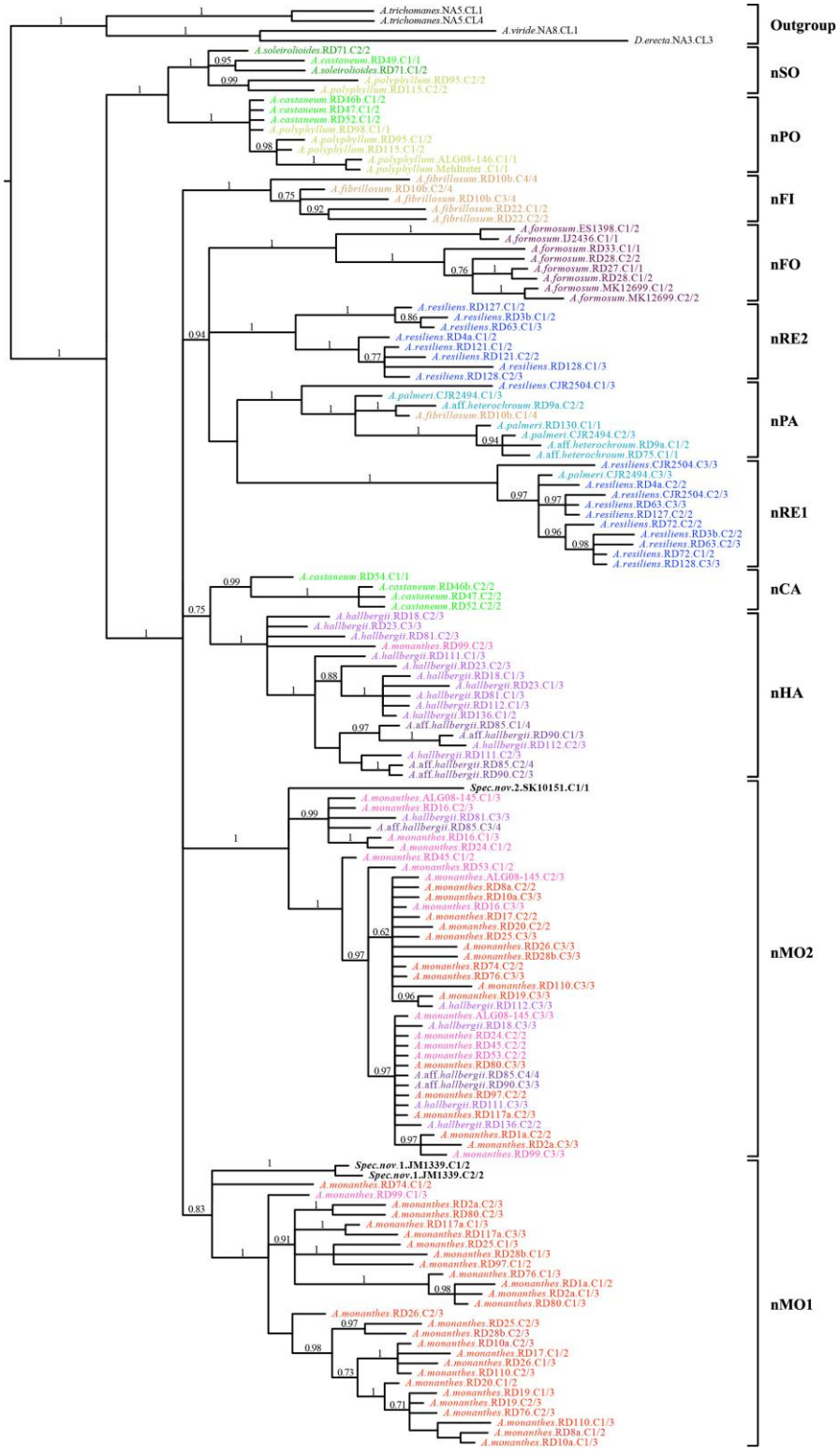

Figure 2.3. Bayesian phylogenetic tree based on the nuclear data. Posterior support values of p > 0.6 are shown. Tips are labelled with species names, followed by a voucher accession (e.g. RD112), and indication of the clone identifier out of the total number of clones (e.g. C2/3 = clone no 2 out of 3 unique clones; see text for details). Tips are colour coded according to species. Subclades are abbreviated and summarised to the right of the tree.

2.4.3 Evidence for reticulate evolution

The unique clones (i.e., nuclear copies) within individual specimens were interpreted as different alleles. The distribution of these unique clones showed evidence of reticulation between clades (Fig. 2.3 and Appendix, Table A5). Although, as mentioned previously, it is possible that such patterns are caused by the loss of paralogs in different lineages. These reticulate relationships are summarised in a hybridisation network (Fig. 2.4, Appendix, Fig. A6 and Table A6).

The nuclear copy distribution of *A.formosum* specimens and *A.fibrillosum* specimen RD22 showed no evidence of reticulation, and these specimens only had one or two copies. The *A.fibrillosum* accession designated RD10b had four copies, one of which was recovered in the nPA clade. *Asplenium castaneum* specimens appeared in three forms according to copy number and distribution. One showed evidence of reticulation sharing one copy in subclade nCA and the other in subclade nPO. Of the remaining inferred *A.castaneum* forms, one had only a single clone sequenced (present in sub-clade nCA), and the other showed no evidence of reticulation, having a single copy in subclade nSO. *Asplenium polyphyllum* specimens were present in two forms: one with a single copy in subclade nPO, whereas the other showed reticulation with one copy in subclade nPO and a second copy in subclade nSO. *Asplenium soleirolioides* showed no reticulation.

Asplenium resiliens specimens showed clear evidence of reticulation, with all but one specimen having one, two or three copies distributed between subclades nRE1 and nRE2. The exception was specimen CJR2504, which had one sequence in subclade nPA, and two in sub-clade nRE1. Most specimens of *A.palmeri* and *A.*aff.*heterochroum* showed no evidence of reticulation. There was one exception, whereby one *A.palmeri* specimen (CJR2494) had three copies, two distributed in sub-clade nPA, and one in sub-clade nRE1. Details are shown in Fig. 2.3 and a summary is presented in Fig. 2.4.

Extensive reticulation was observed between the *A.monanthes* and *A.hallbergii* clades designated nMO1, nMO2 and nHA. *Asplenium monanthes* specimens with the plastid pMO1 haplotype had up to two nuclear copies in clade nMO1 and a third in nMO2. *Asplenium hallbergii* specimens showed reticulation, having up to two nuclear copies in the nHA clade,

and a single copy in clade nMO2. Specimen RD23 was the exception, having three copies only in the nHA clade. One of the *A.*aff.*hallbergii* specimens (RD85) had four nuclear copies, two of which were derived from the nHA clade and two from the nMO2 clade. In addition to these clear cases of reticulate evolution, there were a few specimens that showed no evidence of reticulation. *Asplenium monanthes* specimens with the plastid haplotype pMO2 were monophyletic (2-3 copies) in clade nMO2, and spec.nov.2 (of subclade nMO2) and spec.nov.1 (of subclade nMO1) had one and two copies of *pgiC*, respectively. The exception in pMO2 was specimen RD99, which had a nuclear copy in each of the clades nMO1, nMO2 and nHA.

2.4.4 Evidence for diplospory and apogamy

Diplospory was inferred for taxa producing 32 spores per sporangium, these included: *A.monanthes, A.hallbergii, A.*aff.*hallbergii, A.resiliens, A.palmeri* and *A.*aff.*heterochroum* (Table 2.1 and Appendix, Table A5). No diplospory was evident in *A.formosum, A.fibrillosum, A.castaneum, A.polyphyllum, A.soleirolioides*, spec.nov.1 or spec.nov.2, all of which had counts of 64 spores per sporangium. One specimen of *A.*aff.*hallbergii* (RD85) yielded counts of both 32 and 64 spores per sporangium from the same individual; all of these spores appeared viable.

Our spore germination experiments showed that *A.formosum* produced normal sexual organs, and showed no evidence of apogamous growth (Fig. 2.1A). All studied specimens of *A.hallbergii, A.*aff.*heterochroum, A.monanthes and A.resiliens* produced gametophytes without sexual organs (see Fig. 2.1B, C, D, E, F, G, H). Sporophytes in these taxa emerged through either a callus like sporophytic growth from the central or lower region of the gametophyte (Fig. 2.1B, C, D, E), or by extension of the apical meristem (Fig. 2.1E, F, G). In some cases, prothalli were deformed where the apical cell appears to have become detached (Fig. 2.1H). Apomictic reproduction appeared to be obligate in all cases, with apogamous prothalli exclusive to specimens exhibiting evidence of diplospory (Table 2.1 and Appendix, Table A7).

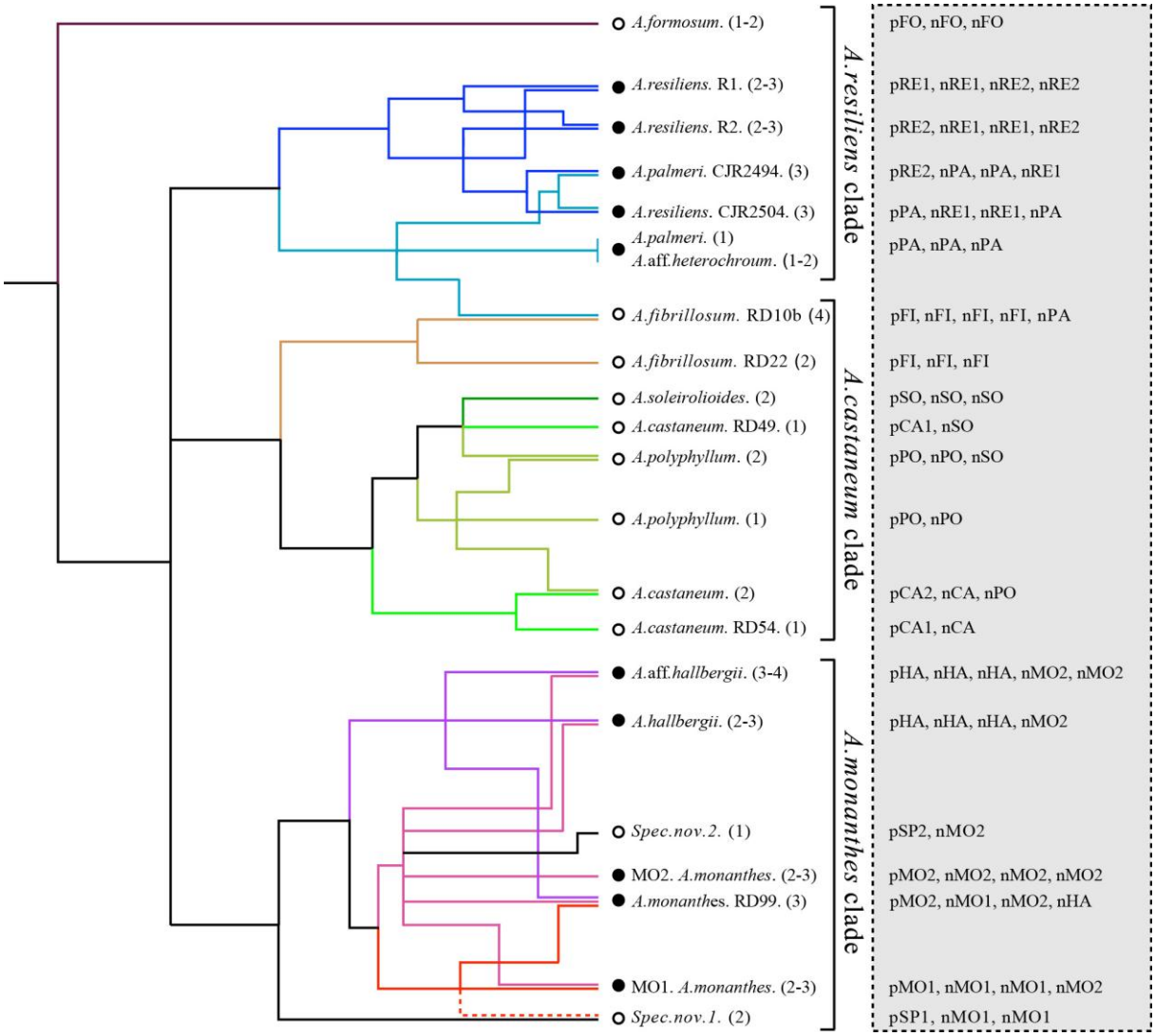

Figure 2.4. A reticulation network illustrating the evolutionary history of the *A.monanthes* complex. This summarises a hybridisation network (Appendix, Fig. A6) performed in SplitsTree (Huson & Bryant, 2006) and illustrates hypothetical hybrid relationships observable by comparison between nuclear and plastid trees (Figures 2.1 and 2.2). The terminals illustrated are inferred as different species forms. Where copy numbers for one species forms are variable, we have included the range of values in parentheses after the species label. Branches are colour coded according to species. Filled black circles indicate apomictic species, and unfilled circles indicate species inferred to have a sexual mode of reproduction. The plastid group and nuclear copy distribution is summarised adjacent to terminal labels. Dashed red line indicates inferred association of this spec.nov.1 to the MO1 *A.monanthes* lineage.

Table 2.1. Spore characteristics and apogamy as recovered in this study by investigating spore characters, and cultivation and observations of gametophytes. Mean spore length and width are reported as ranges where multiple specimens were measured per species, and as single values where only one specimen was measured per species. † Indicates taxa for which chromosome counts are available: *A.formosum* 2n=72 (Manton, 1959; Walker, 1966b; Ghatak, 1977; Ammal & Bahavanandan, 1991; Guillén & Daviña, 2005); *A.monanthes* n=2n=108 and 2n=144 (Manton, 1950; Manton & Vida, 1968; Wagner *et al.*, 1970; Tryon *et al.*, 1973; Manton *et al.*, 1986; Mickel & Smith, 2004) and *A.resiliens* n=2n=108 (Morzenti & Wagner, 1962; Wagner, 1963, 1966; Morzenti, 1966; Wagner & Wagner, 1966; Walker, 1966b; Wagner *et al.*, 1970). * Wagner et al. (1993) reported 64 spores for *A.palmeri* whereas Mickel and Smith (2004) show no spore count.

Species	Spore number	Apogamy	Mean Spore length range (µm)	Mean Spore width range (µm)
A.castaneum	64	-	36.54 – 46.53	28.39 – 37.69
A.fibrillosum	64	-	44.34 – 47.90	34.85 – 37.97
A.formosum †	64	No	27.85 – 32.20	20.64 – 25.02
A.hallbergii	32	Yes	39.15 – 46.83	27.07 – 32.84
*A.*aff.*hallbergii*	32/64	Yes	43.32 – 44.97	30.45 – 31.86
*A.*aff.*heterochroum*	32	Yes	37.43 – 38.62	25.89– 27.83
A.monanthes (MO1) †	32	Yes	38.02 – 47.38	26.68 – 32.08
A.monanthes (MO2) †	32	Yes	38.45 – 48.54	26.63 – 34.72
A.palmeri *	32	-	-	-
A.polyphyllum	64	-	35.87 – 39.87	25.06 – 30.06
A.resiliens †	32	Yes	39.78 – 44.70	28.17 – 31.10
A.soleirolioides	64	-	36.88	27.55
Spec.nov.1	64	-	31.26	21.42
Spec.nov.2	64	-	29.22	20.77

2.4.5 Inferring ploidy level

Analysis of spore length variation between the different species showed that the spores of *A.formosum* are significantly smaller than those of all other species ($p<0.001$), with the exception of spec.nov.1 and spec.nov.2 (Table 2.1, Fig. 2.5 and Appendix, Table A8 and Fig. A7). Spec.nov.1 and spec.nov.2 had significantly smaller spore sizes ($p<0.001$) than all other specimens within the *A.monanthes* MO1 clade and the *A.monanthes* MO2 clade respectively. Mean spore lengths in *A.formosum*, spec.nov.1 and spec.nov.2 were <32µm, comparable to those of sexual diploids in the related *A.trichomanes* complex (see Fig. 2.5). We infer from these results that these three taxa represent sexually reproducing diploids.

The remainder of the *A.monanthes* complex showed significant spore size variation between (<0.001) and within species (<0.05, with the exception of *A.*aff.*heterochroum*, *A.soleirolioides* and *A.fibrillosum*). However this variation was difficult to classify into

distinguishable groups and so inference of ploidy level was not possible. All remaining species did have large mean spore sizes (35 - 52µm), and were significantly larger ($p<0.001$) than inferred diploid species (*A.formosum*, spec.nov.1 and spec.nov.2) (Table 2.1, Fig. 2.5, and Appendix, Table A8 and Fig. A7). We therefore infer that the remaining species were all polyploids.

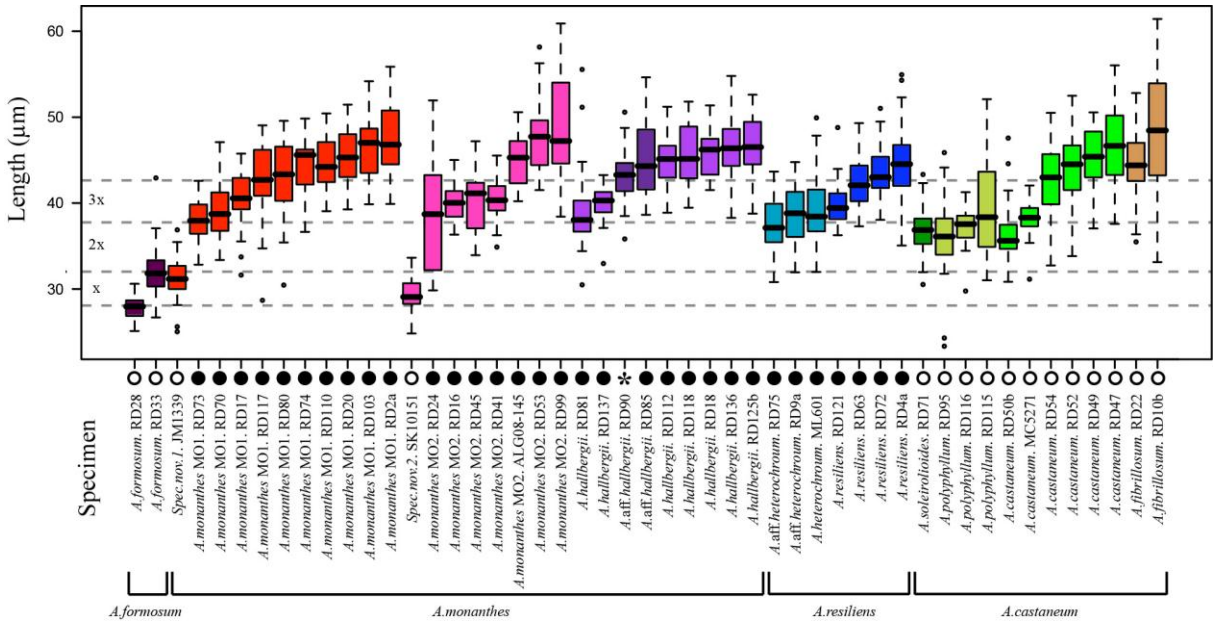

Figure 2.5. Boxplots illustrating variation in spore length of species/specimens of the *A.monanthes* complex. Each boxplot is labelled below with its corresponding species name and specimen voucher, and coloured according to species as in Fig. 2.2. Boxplots are grouped together according to clades and ordered from lowest to highest mean lengths. Each boxplot represents the variation of measurements of spores within each specimen, the thick horizontal line is the median, the box indicates the variation observed between the 25th and 75th percentiles, the whiskers show the variation range, and small circles identify extreme outliers. Dashed lines running across the graph illustrate average spore measurements in comparison to the ploidy levels of the spores, based on average counts of triploid *A.resiliens* (spore ploidy = 3x) specimens, hexaploid *A.heterochroum* (spore ploidy = 3x) specimens (Morzenti, 1966), and diploids and tetraploids of the *A.trichomanes* complex (spore ploidy = x and 2x, respectively) (Tutin *et al.*, 1993). Filled black circles indicate apomictic specimens that produce 32 spores per sporangium. Unfilled circles indicate specimens that produce 64 spores sporangium and are inferred to have a sexual mode of reproduction. The star indicates a specimen that produces both 32 and 64 spores per sporangium.

2.5 Discussion

2.5.1 Evolutionary relationships and reticulate evolution

Plastid sequence data identified four main lineages within this complex and some of these lineages have also been recovered in the *pgiC* dataset. The backbone of the *pgiC*-based tree is a polytomy and this nuclear marker only provides limited evidence to reconstruct relationships among these species. This region has not commonly been used in ferns and other studies have encountered similar problems resolving species evolutionary relationships (Juslén *et al.*, 2011). However, *pgiC* is better suited to trace reticulate evolution when compared with the plastid marker data) (also see Juslén *et al.*, 2011).

In the plastid phylogenetic tree, *A.formosum* was recovered as the putative sister to three clades that broadly correspond to taxonomic species assemblages of *A.castaneum, A.resiliens* and *A.monanthes*. Relationships among these three clades are unresolved, though the lineages themselves are strongly supported. The nuclear phylogenetic tree shows evidence of extensive reticulate evolution within these clades but not between them, except for one hybrid specimen originally identified as *A.fibrillosum* (Fig. 2.3 and Fig. 2.4). We are able to infer parentage of putative hybrids based on the phylogenetic distribution of nuclear clones. However, it is important to consider that the power of these inferences is potentially limited by PCR copy preference (Brysting *et al.*, 2011), or processes such as diploidisation, which could produce misleading results.

According to spore number and cultivation experiments, apomixis has evolved in the *A.monanthes* and *A.resiliens* clades but appears to be absent in the *A.castaneum* clade. Several previously published chromosome counts indicate that *A.formosum* is a sexual diploid (2n=72) (Manton, 1959; Walker, 1966b; Ghatak, 1977; Ammal & Bahavanandan, 1991; Guillén & Daviña, 2005), which is consistent with the spore measurements and gametophyte experiments reported here. We did not find any evidence to support suggestions of *A.formosum* as one parent of *A.monanthes*.

Fern spore size has been successfully used to determine ploidy level in several recent studies on apomixis in xeric ferns (Beck *et al.*, 2010; Sigel *et al.*, 2011). Also, studies correlating

cytofluorometry and spore measurements in the *Asplenium trichomanes* complex have indicated that spore size provides a useful estimator of ploidy level among the black-stemmed rock spleenworts (Ekrt & Stech, 2008). However, it is not always clear if spore size is reliable for inferring ploidy level (Barrington *et al.*, 1986), and in this study we were only able to use spore size measurements to distinguish between diploid and polyploid specimens, and were not able to infer polyploid levels.

2.5.2 The A.resiliens clade

We report that *A.palmeri* and *A.heterochroum*-like morphotypes produce 32 spores per sporangium and show an apomictic mode of reproduction. An unpublished chromosome count of n=2n=108 for *A.palmeri* (M.D. Windham, pers. comm.) confirms that at least some specimens assigned to this taxon are apomictic triploids. Wagner *et al.* (1993) reported 64 spore counts per sporangium in the Flora of North America treatment of this species, whereas Mickel and Smith (2004) did not record the spore number for this species. *Asplenium heterochroum* was previously known as a sexual polyploid (4x and 6x) with 64 spores (Morzenti & Wagner, 1962; Wagner, 1963, 1966; Morzenti, 1966; Wagner & Wagner, 1966; Walker, 1966b; Wagner *et al.*, 1970). Our conflicting results may reflect reported taxonomic difficulties (Stolze, 1981; Tryon *et al.*, 1993; Stolze *et al.*, 1994) and suggest that these species require further cytological study. This complex was not exhaustively sampled, and inference of reticulate relationships and apomictic origins call for caution.

2.5.3 The A.castaneum clade

The distinction between *A.polyphyllum* and *A.castaneum* has previously posed taxonomic difficulties (Mickel & Smith, 2004), and our reconstruction of phylogenetic relationships was unable to resolve these. Our spore size data provide the first evidence for polyploidy in this species complex. Spore data indicates that *A.fibrillosum*, *A.polyphyllum*, *A.soleirolioides* and *A.castaneum* are polyploids.

The plastid phylogenetic tree identifies species lineages broadly corresponding to proposed morphological groups. *Asplenium castaneum* comprises two subclades, with members of the pCA1 subclade more similar to *A.fibrillosum* in appearance, and representatives of the pCA2

subclade more likely to be misidentified as *A.polyphyllum*. However, the nuclear phylogenetic tree indicates extensive reticulation and multiple hybrid formation (Fig. 2.4). The observed pattern is similar in complexity to the pervasive reticulation observed in the *A.trichomanes* polyploid complex (Lovis, 1977). Denser sampling of specimens and additional cytological information (e.g. chromosome counts) are required to reconstruct the relationships within this widespread complex.

2.5.4 The A.monanthes clade

This clade comprises two *A.monanthes* lineages (MO1 and MO2) and one *A.hallbergii* (HA) lineage, which are supported in both plastid and nuclear genomes. It also contains two accessions (spec.nov.1 and spec.nov.2), which are isolated in the plastid genome but associated to MO1 and MO2 in the nuclear genome. Specimens of *A.monanthes* and *A.hallbergii* are apomictic and appear to be triploid and possibly tetraploid, as indicated by previous chromosome counts for *A.monanthes* (Manton, 1950; Smith & Mickel, 1977). Both the MO1 and *A.hallbergii* lineages consist of allopolyploid hybrids formed with the MO2 lineage, which itself appears to be autoploid (Fig. 2.4 and Fig. 2.6). Specimen RD99 is an exception to the inference of autoploidy in lineage MO2, as it contains clones from three lineages. This could indicate PCR bias in the cloning method, but we would expect that the high sample number within this lineage would overcome this bias. RD99 could therefore represent a case of gene flow from an apomictic lineage, through hybridisation with a sexual relative, via functional antheridia.

The *A.*aff.*hallbergii* specimens (RD85 and RD90) are nested within the *A.hallbergii* lineage, but appear physically larger in size and show up to four nuclear copies, implying that they could be tetraploid variants (Fig. 2.4 and Fig. 2.5). One of these specimens (RD90) produced both 32 and 64-spored sporangia. Both types of spores appeared normal and viable. This would suggest that RD90 is producing both reduced and unreduced spores and thus might be a facultative apomict, though separate cultivation experiments are necessary to test this hypothesis.

Spec.nov.1 (JM1339) and spec.nov.2 (SK10151) are inferred to be sexual diploids, and have affinities to the nuclear *A.monanthes* lineages nMO1 and nMO2 respectively (Fig. 2.4 and

Fig. 2.6). Although no morphological analysis was performed, some patterns were observed during visual identification of these specimens. Spec.nov.2 is morphologically similar to some *A.monanthes* specimens, but spec.nov.1 appears distinct, having previously been identified as *A.polyphyllum* (Monterrosa *et al.*, 2009). Further study confirmed the morphological differences of the later specimen from *A.monanthes* and *A.polyphyllum* (as defined in Mickel & Smith, 2004). The *A.hallbergii* group is morphologically distinct from the two *A.monanthes* groups (Mickel & Smith, 2004). Morphological distinctions between the MO1 and MO2 lineages are unclear, but it further investigation may uncover correlations between morphological and genetically identified taxa.

In general, our approach using cpDNA and nrDNA markers improved our understanding of the relationships within the group, especially when polyploidy is considered. Further improvements will be likely achieved by expanding the taxonomic sampling, using a more sensitive method to determine polyploidy (e.g. flow cytometry) and by using several nuclear markers. Single nuclear markers can result in misleading interpretations as a result of factors such as incomplete lineage sorting which resemble patterns of ongoing hybridisation (Nitta *et al.*, 2011).

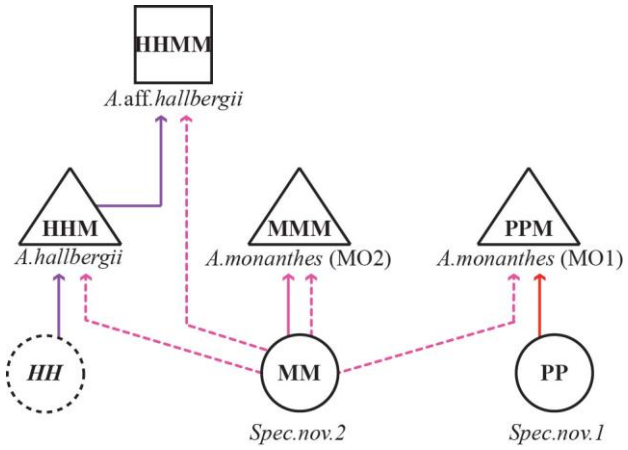

Figure 2.6. A reticulogram illustrating the apomictic polyploid species relationships and hypothetical origins of apomixis within the *A.monanthes* clade. Extant cytotypes are used to illustrate hypothesised lineage origins and parental relationships. The inferred ploidy levels within the three lineages are represented using circles for diploids, triangles for triploids and squares for tetraploids. The diploids are sexually reproducing species whereas the triploids and tetraploid forms are apomictic. The dashed circle represents a hypothesised (either un-sampled or extinct) parent cytotype. Dashed arrows indicate paternal parent relationships. Solid arrows indicate maternal parents (i.e., unreduced gametophytes).

2.5.5 Origins of apomixis

The occurrence of apomixis in this complex can be explained in two ways: (1) a single origin with a complex history of reversals and post-origin differentiation/divergence of apomictic lineages, or; (2) multiple independent origins from more than one sexual progenitor species (e.g. Beck *et al.*, 2011b,a; Sigel *et al.*, 2011).

(1) The weak resolution among clades and putative sister relationships of the *A.monanthes* clade and *A.resiliens* clade may be seen as arguments for a single origin of apomixis in these ferns. This would then imply that the various apomictic lineages were the result of diversification within an asexual lineage (Fontaneto *et al.*, 2007). However this would require the sexual taxa (spec.nov.1 and spec.nov.2) within the *A.monanthes* clades to have undergone evolutionary reversals from asexual to sexual reproduction (Fig. 2.1 and Fig. 2.4). To our knowledge, this process has not been documented for apomictic ferns yet.

(2) The alternative hypothesis of multiple origins is supported by evidence for the association of apomixis with reticulate evolution in both the *A.resiliens* and *A.monanthes* clades. Here, apomictic taxa are present in multiple polyploid and hybrid forms, including putative autoploid and alloploid lineages. Although reticulation is common throughout the complex (including sexual taxa), and there are some non-hybrid apomictic lineages present, the pattern of hybridisation observed does not correspond to the single origin hypothesis.

We therefore favour this second scenario of multiple origins within the whole complex. Within the *A.monanthes* clade in particular, there is evidence for three lineages. The pattern of nuclear copy distribution between these lineages indicates three origins of apomixis from up to three different sexual progenitor species (Fig. 2.6 and Appendix, Tables A5 and A6). Under the assumption of rarity of regaining sexual reproduction in obligate apomictic lineages, the observed pattern does not support a single origin, and gene flow between asexual and sexual lineages by hybridisation (via functional antheridia) with sexual relatives. This inference is strengthened by the lack of antheridia observations in gametophyte studies. However, one specimen (RD99) has nuclear copies from all three apomictic lineages. This indicates that apomixis may have spread via functional hybridisation in some instances.

Nuclear copies from the MO2 lineage are present in both the *A.monanthes* MO1 and the *A.hallbergii* apomictic lineages (Fig. 2.4 and Fig. 2.6). This indicates that the *A.monanthes* MO2 lineage is crucial in alloploid apomictic origin. The *A.monanthes* MO2 lineage itself is a putative autoploid lineage. Although the precise pathways to autoploid apomict origin are difficult to infer, this process almost certainly involved the cross-fertilisation of normal haploid gametophytes and unreduced gametes, the latter produced either by sexual diploids or autotetraploids (Fig. 2.6).

The affinity of the sexual diploids, spec.nov.1 and spec.nov.2, to the *A.monanthes* MO1 and MO2 lineages respectively, indicates that these accessions may represent sexual progenitor species for each group. No putative diploid sexual progenitor specimen was observed for the *A.hallbergii* lineage but due to the clear difference in morphology and distinction in both the plastid and nuclear genomes, we suggest the participation of at least one additional undetected sexual progenitor. The *A.castaneum* subclade nCA (weakly supported as sister to *A.hallbergii* by the nuclear gene analysis) and the putative facultative tetraploid *A.*aff.*hallbergii* are potential progenitors (Fig. 2.4).

Similar patterns are observed within the *A.resiliens* clade, although we make no inferences here, as more exhaustive sampling of species within this clade is necessary.
These hypotheses of origin need to consider the limits of single gene markers; additional studies would benefit from the use of several nuclear genes or a better marker system (such as co-dominant microsatellites) that sample a larger portion of the genomes. We also need to be aware that the dynamics of genomic re-arrangement in apomictic polyploids may create patterns similar to those observed by entirely different processes such as homoeologous chromosome pairing (Ishikawa *et al.*, 2003). The large ranges of spore size in some specimens such as RD24 and RD99 (Fig. 2.5) suggest that such processes may be present in this group and may also effect spore development.

These caveats aside, our results are congruent to those of several recent studies on cheilanthoid ferns (Grusz *et al.*, 2009; Beck *et al.*, 2011b; Sigel *et al.*, 2011) and filmy ferns (Nitta *et al.*, 2011) that reported multiple-recent origins of apomixis (both alloploidy and autoploid) from a variety of ancestral diploid progenitor species.

2.6 Conclusion

Within this complex there appear to be a number of relatively well-established apomictic lineages of independent origins. However, we find no strong evidence for long-lived apomictic lineages that outlast or replace their diploid progenitors completely. Sexual progenitors are rare and the lack of evidence for functional antheridia in apomictic prothalli provides little evidence for ongoing clonal turnover. Apomictic lineages are associated to reticulate evolution. However, we are as yet unable to determine the precise mechanisms of origin or, for that matter, whether this association of apomixis to reticulation is the cause or the effect of apomictic origins within this complex.

Our study is limited by the fact that nuclear copy distribution is not the best indicator of parentage/reticulation patterns, and our conclusions should be viewed primarily as a foundation for further investigation. Our findings also call for some taxonomic studies in the complex. For example, following on the collection of two previously unknown sexual diploid taxa for the flora of El Salvador (Monterrosa *et al.*, 2009), more extensive sampling is needed and may lead to the discovery of several new taxa that are either rare and/or have small distribution ranges. We believe that future work would benefit from using population genetic approaches and more in-depth cytological analysis to fully disentangle the mechanisms by which asexuality evolves and is maintained.

CHAPTER 3

Species delimitation in an apomictic complex: A comparative analysis of AFLP data and DNA sequence data to determine species boundaries in the *Asplenium monanthes* fern complex

Prepared for submission to the American Journal of Botany, under the co-authorship of Vincent Savolainen and Harald Schneider.

3.1 Summary

The delimitation of species within an apomictic species complex is notoriously difficult. Problems arise due to variation in reproductive mode, high levels of phenotypic plasticity, and the prevalence of polyploidy and hybridisation. In this study we employ a unified species concept, which identifies independently evolving lineages as species. We performed a comparative analysis of multilocus AFLP data and single locus DNA sequence data through the application of a variety of species delimitation methods. Our results indicate that the multilocus AFLP and the single locus sequence data identify similar independently evolving lineages and confirm previous inferences of reticulate lineages. However, the AFLP data does not support previous inferences of sexual diploid progenitor species, highlighting the shortcomings of using dominant markers for parentage analysis. Species delimitation analyses also reveal further diversity in the *A.monanthes* lineages, indicating the potential occurrence of post origin genetic divergence or recurrent hybrid origins. In conclusion the AFLP data supports previous inferences of independently evolving lineages within *A.monanthes* and *A.resiliens*, and species delimitation methods identify further genetic diversity within *A.monanthes* lineages. In summary, our study highlights the value of conducting comparative analyses of different DNA data in apomictic complexes.

3.2 Introduction

Delimiting species in an apomictic complex is a taxonomic nightmare. Apomixis is a form of asexual reproduction in plants, and apomictic taxa are usually found in complicated reticulate networks with other apomictic and sexually reproducing taxa (e.g. Lovis, 1977; Asker & Jerling, 1992; Mogie, 1992; Beck *et al.*, 2011a). The occurrence of clonally reproducing lineages, hybridisation, and polyploidy, all in uncertain measures, makes the inference of species relationships and species boundaries in such complexes very difficult (Manton, 1950; Stebbins, 1950; Rieseberg *et al.*, 2006; Hörandl *et al.*, 2009; Verhoeven *et al.*, 2010).

Phylogenetic analysis can expose underlying patterns of reticulate evolution and the presence of genotypic diversity. However, these patterns are difficult to interpret without knowledge of the intrinsic biology of individual samples, such as: reproductive mode and ploidy level (Paun *et al.*, 2006; Hörandl *et al.*, 2009; Grusz *et al.*, 2009; Beck *et al.*, 2010; Sigel *et al.*, 2011). Even when prior knowledge of each sample is available, the diversity in biological attributes, including uniparental reproduction and a reticulate evolutionary history between taxa, hinders the application of available species concepts (Hörandl *et al.*, 2009). This is especially apparent when trying to define an apomictic species, and has historically restricted species delimitation in apomictic complexes (Gastony & Windham, 1989; Hörandl, 1998).

The application of the recently established unified species or general lineage concept (Pons *et al.*, 2006; Fontaneto *et al.*, 2007; De Queiroz, 2007; Birky *et al.*, 2010; Reeves & Richards, 2011; Hausdorf, 2011) has gone a long way to resolving this issue. This defines a species as a separately evolving meta-population or evolutionarily distinct lineage, and only employs secondary species criteria, such as reproductive mode and ploidy level, as evidence for lineage independence. Nevertheless, the application of this concept to a phylogenetic hypothesis of species relationships is still problematic, as reticulate phylogenetic patterns are not sufficiently described by the bifurcating patterns of cladogenesis (e.g. Cronquist, 1987; McDade, 1990). Hybridisation can cause gene trees and the actual species tree to contradict each other; indeed such incongruences are commonly used to identify reticulation events. Conversely, other processes including incomplete lineage sorting can also cause the same patterns, and confusion between these processes has often led to incorrect assumptions of, or overlooked incidences of hybridisation (Blanco-Pastor *et al.*, 2012).

In this study we are interested in testing previous inferences of species boundaries, species relationships, and reticulate evolution in the *Asplenium monanthes* complex (Dyer *et al.*, 2012). These inferences were based on morphological classification, reproductive mode, polyploidy, monophyly of plastid sequence data, incongruences between plastid and nuclear sequence data, and the paraphyly of nuclear alleles. Multiple hybrid lineages were inferred for the apomictic assemblages associated to *A.resiliens* (including *A.*aff.*heterochroum* and *A.palmeri*) and *A.monanthes* (including *A.hallbergii*), respectively. Two putative sexual diploid progenitors were identified for *A.monanthes* and *A.hallbergii* lineages, informally named as spec.nov.1 and spec.nov.2. *Asplenium formosum* was confirmed to be a sexual diploid and *A.polyphyllum* and *A.castaneum* were inferred to be sexual polyploids with a probable reticulate history.

Here, these inferences will be tested using a comparative analysis of genome-wide multilocus Amplified Fragment Length Polymorphism (AFLP) data and single locus plastid and nuclear sequence datasets, through the application of a variety of species delimitation methods.
Whilst AFLPs are commonly used to investigate intraspecific relationships, they are increasingly being used for phylogenetic inference of interspecific relationships (see Meudt & Clarke, 2007). This is due to mounting evidence that AFLP data is phylogenetically informative and can often improve the resolution of phylogenetic inferences from sequence data (Després *et al.*, 2003; Pelser, 2003; Koopman, 2005), especially at shallow nodes, e.g. in rapid radiations. More recent studies have indicated that AFLPs can also be informative for the resolution of species relationships at deeper nodes, and the potential for the application of a molecular clock for divergence time estimation in AFLP data (Kropf *et al.*, 2009; Dasmahapatra *et al.*, 2009; García-Pereira *et al.*, 2010).

The use of DNA markers for species delimitation in complicated taxonomic groups is becoming more common (Meudt *et al.*, 2009; Monaghan *et al.*, 2009; Sauer & Hausdorf, 2010, 2012; Niemiller *et al.*, 2012) due to the emergence of a variety of delimitation methods that are applicable to multilocus and single locus data (Pons *et al.*, 2006; Fontaneto *et al.*, 2007; Falush *et al.*, 2007; Birky *et al.*, 2010; O'Meara, 2010; Hausdorf & Hennig, 2010;

Meudt, 2011). The methods use different aspects of the data (e.g. genetic distance, branching rate, coalescence, etc.) to provide different lines of evidence supporting species boundaries.
The general aim in this study is to investigate whether AFLP data is congruent with sequence data. Specifically we want to test: (1) inferences of species by investigating whether various methods of species delimitation define consistent species within and between AFLP data and DNA sequence datasets; (2) inferences of species relationships and incongruences between plastid and nuclear data; (3) inferences of reticulate evolution due to incongruence between plastid and nuclear sequence data.

3.3 Materials and Methods

3.3.1 Sampling

Individual samples for AFLP analysis were chosen in order to attain sufficient taxonomic and phylogenetic coverage. Accessions sampled from a previous phylogenetic study (Dyer *et al.*, 2012) were used together with new samples, which included newly collected accessions from El Salvador and Costa Rica (Table 3.1). New samples were identified according to Mickel and Smith (2004) based on the assignment of two new species (Dyer *et al.*, 2012). The study sample consisted of 63 individuals in total, comprising the following species: *Asplenium castaneum, A.fibrillosum, A.formosum, A.hallbergii*, *A.*aff.*heterochroum, A.monanthes A.palmeri, A.polyphyllum, A.resiliens*, and two newly identified taxa, spec.nov.1 and spec.nov.2. Previous chromosome counts have shown *Asplenium formosum* to be a sexual diploid (2n=72) and *A.monanthes, A.palmeri* and *A.resiliens* to be triploid apomicts (n=2n=108) (see Dyer *et al.*, 2012). Spore size measurements showed spec.nov.1 and spec.nov.2 to be sexual diploids, and *A.castaneum, A.fibrillosum, A.hallbergii* (apomictic) and *A.*aff.*heterochroum* (apomictic) *A.polyphyllum* to be polyploids (Dyer *et al.*, 2012). The two newly recovered species are still awaiting formal description, which will be carried out in an independent study. The formal description required the comparison of the morphology of the newly discovered species with the type specimens of previously established species.

Published DNA sequence data (Dyer *et al.*, 2012) corresponding to individuals sampled for AFLP analysis were used for comparative analysis. Sequence alignments included three plastid markers and one nuclear gene (Table 3.1): (i) the *psbA-trnH* intergenic spacer (IGS)

region (~600 nucleotides) (Aldrich *et al.*, 1988), (ii) the *rps4* plus *rps4-trnS IGS* region (~1000 nucleotides) (Smith & Cranfill, 2002), (iii) the *trnL-trnF* region including the *trnL* intron and the *trnL-trnF* IGS region (~900 nucleotides) (Taberlet *et al.*, 1991; Trewick *et al.*, 2002), and (iv) the low copy nuclear gene *pgiC* (Ishikawa *et al.*, 2002), which included the introns spanning exons 14 and 16 (~600 nucleotides). A fifth dataset constituted the combination of all three plastid markers.

Table 3.1. Sampling information. Species are identified using Mickel and Smith (2004) and voucher number, collector ID, collection location and Genbank accession number (where applicable) are given.

Species	Voucher	Collector	*psbA-trnH*	*rps4-trnS*	*trnL-trnF*	*pgiC*
A.castaneum	RD46.a	R.J.Dyer	JQ767568	JQ767699	JQ767816	-
A.castaneum	RD48	R.J.Dyer	JQ767572	JQ767703	JQ767820	-
A.castaneum	RD49	R.J.Dyer	JQ767573	JQ767704	JQ767821	JQ767198
A.castaneum	RD50	R.J.Dyer	JQ767574	JQ767706	JQ767823	-
A.castaneum	RD52	R.J.Dyer	JQ767575	JQ767707	JQ767824	JQ767206-7
A.castaneum	RD91	R.J.Dyer	JQ767577	JQ767709	JQ767826	-
A.castaneum	RD116	R.J.Dyer	JQ767579	JQ767711	JQ767828	-
A.castaneum	RD144.2	R.J.Dyer	-	-	-	-
A.castaneum	RD144.6	R.J.Dyer	-	-	-	-
A.castaneum	RD144.7	R.J.Dyer	-	-	-	-
A.castaneum	RD147	R.J.Dyer	-	-	-	-
A.castaneum	RD151	R.J.Dyer	-	-	-	-
A.castaneum	MC5205	M.Christenhusz	-	-	-	-
A.castaneum	MC5271	M.Christenhusz	-	-	-	-
A.fibrillosum	RD22	R.J.Dyer	JQ767581	JQ767713	JQ767830	JQ767221-2
A.formosum	IJ2436	I.Jimenez	JQ767583	JQ767716	JQ767832	JQ767233
A.formosum	MK12699	M.Kessler	JQ767585	-	JQ767833	JQ767235-6
A.formosum	RC1922	R.C.Forzza	-	-	-	-
A.formosum	RD27	R.J.Dyer	JQ767586	JQ767717	JQ767834	JQ767238
A.formosum	RD28	R.J.Dyer	JQ767587	JQ767718	JQ767835	JQ767244-5
A.formosum	RD33	R.J.Dyer	JQ767588	JQ767719	JQ767836	JQ767251
A.formosum	RD157	R.J.Dyer	-	-	-	-
A.formosum	RD158	R.J.Dyer	-	-	-	-
A.formosum	RD160	R.J.Dyer	-	-	-	-
A.hallbergii	RD23	R.J.Dyer	JQ767593	JQ767723	JQ767841	JQ767274-6
*A.*aff.*hallbergii*	RD85	R.J.Dyer	JQ767589	JQ767720	JQ767837	JQ767251-5
A.hallbergii	RD120	R.J.Dyer	JQ767599	JQ767729	JQ767848	-
*A.*aff.*heterochroum*	ML601	M.Lehnert	JQ767606	JQ767734	JQ767855	-
*A.*aff.*heterochroum*	RD9.A	R.J.Dyer	JQ767604	JQ767732	JQ767853	JQ767311 & -3
*A.*aff.*heterochroum*	RD75	R.J.Dyer	JQ767605	JQ767733	JQ767854	JQ767319
*A.*cf.*monanthes*	MC5307	M.Christenhusz	-	-	-	-
A.monanthes	RD1.A	R.J.Dyer	JQ767619	JQ767743	JQ767865	JQ767329-30
A.monanthes	RD45.1	R.J.Dyer	JQ767636	JQ767760	JQ767878	JQ767407-8
A.monanthes	RD70A	R.J.Dyer	JQ767638	JQ767762	JQ767879	-
A.monanthes	RD73.1	R.J.Dyer	JQ767639	JQ767763	JQ767880	-
A.monanthes	RD117.1	R.J.Dyer	JQ767657	JQ767780	JQ767897	JQ767450-2
A.monanthes	RD119.A	R.J.Dyer	JQ767658	JQ767781	JQ767898	-
A.monanthes	RD139	R.J.Dyer	-	-	-	-
A.palmeri	CJR2494	C.J.Rothfels	-	JQ767792	JQ767909	JQ767455-7
A.palmeri	RD130	R.J.Dyer	JQ767670	JQ767793	JQ767910	JQ767462

A.polyphyllum	MC5365	M.Christenhusz	-	-	JQ767914	-
A.polyphyllum	RD95	R.J.Dyer	JQ767676	JQ767797	JQ767916	JQ767483-4
A.polyphyllum	RD98	R.J.Dyer	JQ767677	-	JQ767917	JQ767491
A.polyphyllum	RD115	R.J.Dyer	JQ767678	JQ767798	JQ767918	JQ767498-9
A.polyphyllum	RD140	R.J.Dyer	-	-	-	-
A.polyphyllum	RD141	R.J.Dyer	-	-	-	-
A.polyphyllum	RD145.2	R.J.Dyer	-	-	-	-
A.polyphyllum	RD145.5	R.J.Dyer	-	-	-	-
A.polyphyllum	RD145.8	R.J.Dyer	-	-	-	-
A.polyphyllum	RD146	R.J.Dyer	-	-	-	-
A.polyphyllum	RD154	R.J.Dyer	-	-	-	-
A.resiliens	RD63	R.J.Dyer	JQ767685	JQ767803	JQ767926	JQ767522-4
A.resiliens	RD72	R.J.Dyer	JQ767687	JQ767805	JQ767928	JQ767530-1
A.resiliens	CJR2504	C.J.Rothfels	-	-	JQ767922	JQ767506-8
A.resiliens	RD121	R.J.Dyer	JQ767689	JQ767807	JQ767930	JQ767535-6
A.resiliens	RD127	R.J.Dyer	JQ767691	JQ767809	-	JQ767538-9
A.resiliens	RD128	R.J.Dyer	JQ767692	JQ767810	JQ767932	JQ767545-7
Spec.nov.1	JM1339	J.Monterosa	JQ767697	JQ767814	JQ767937	JQ767553-4
Spec.nov.1	MP p2.3	R.J.Dyer	-	-	-	-
Spec.nov.1	MPp2.7.2	R.J.Dyer	-	-	-	-
Spec.nov.2	MS.1.1	R.J.Dyer	-	-	-	-
Spec.nov.2	MS.2.1	R.J.Dyer	-	-	-	-
Spec.nov.2	SK10151	S.Knapp	JQ767698	JQ767815	JQ767938	JQ767559

3.3.2 AFLP fingerprints

Total genomic DNA was extracted from leaf tissue using a modified version of the CTAB protocol (Doyle, 1987). This method includes the use of DNeasy Mini Spin Columns (Qiagen, Crawley, West Sussex, UK), according to the manufacturer's protocol. Amplified fragment length polymorphisms (AFLPs) were generated for samples following Vos *et al*. (1995) and the PE Applied Biosystems protocol (Life Technologies Ltd, Paisley, UK). This procedure involved three steps including: restriction ligation, where total DNA is digested and ligated to double stranded adaptor pairs; pre-selective PCR amplification of DNA fragments; and finally selective PCR amplification of DNA fragments. Total DNA for each sample was quantified using NanoDrop ND-8000 (Thermo Scientific), and approximately 500ng of DNA was dried down and diluted to a volume of 5.5µl for restriction ligation. Restriction ligation reactions (11µl in total) included the addition of 1.1µl T4 DNA ligase buffer (Promega), 1.1µl 0.5M NaCl, 1.5µl 1mg/ml BSA, 1U *MseI* (Promega), 5U *EcoI* (Promega), 1U T4 DNA ligase (Promega), 1µl *MseI* adaptor, 1µl *EcoI* adaptor, and incubation at 37°C for 2 hours. TE buffer (189µl per 11µl reaction) was added to stop the reactions.

Pre selective amplification was conducted using Applied Biosystems AFLP mapping kit for regular genomes (Life Technologies Ltd, Paisley, UK), using 7.5µl core mix and 0.5µl of pre-

selective primer pairs (*EcoR1*-A and *Mse1*-C). The success of pre-selective amplification was verified on 1.5% agarose gel. TE buffer (95 µl per 5µl reaction) was added to stop the reactions. Selective amplification reactions included 7.5µl of PCR master mix (2X) (Fermentas), 0.5µl of 5µM *Mse1*-CXX primer, 0.5µl of fluorescently labelled 1µM *EcoR1*-XXX (+ Dye) primer and 1.5µl of diluted pre-selective product. Primer trials were conducted for 42 different primer combinations on 8 randomly chosen samples. The most successful primer pair combinations, based on the quality and quantity of bands produced (see Bonin *et al.*, 2007), were found to have congested AFLP fingerprints making scoring difficult. We therefore added an extra nucleotide to the *Mse1* primers to increase selectivity and reduce the number of fragments amplified. 14 primer pair combinations with modified *Mse1* (CXXX) primers were trialled, and the two best fluorescently labelled primer pair combinations were chosen for selective amplification of all samples: *EcoR1*-ACC (NED- Yellow) / *Mse1*-CACC, and *EcoR1*-ACC (NED- Yellow) / *Mse1*-CTCG. PCR reactions were carried out on a Veriti® 96-well Thermal Cycler (Applied Biosystems), and products were run on an automated sequencer with GeneScan Rox-500 (Applied Biosystems) internal size-standard to enable identification of fluorescently labelled AFLP fragments.

AFLP banding patterns were scored using Genemapper V4 (Applied Biosystems). Size standards were automatically checked and manually confirmed to be correct for each sample. Peaks were scored automatically in gene mapper for bands between 50-500 base pairs long and 1 base pair in width, generating a presence/absence matrix across the dataset. These were then checked manually and peaks were scored in context of the whole dataset according to Bonin *et al*. (2007). Samples were scored blindly in order to avoid bias. Error rates and reproducibility were assessed by comparison of banding pattern between eight (12.7%) repeated samples. Loci with error rates >0.125% were eliminated from the datasets (Bonin *et al.*, 2007), leading to an overall error rate of 2.3% per multilocus genotype, and 204 polymorphic loci in total.

3.3.3 Analysis of AFLP data

Restriction fragment data, such as AFLP data has several intrinsic properties that can severely limit its use for phylogenetic analysis (see Koopman, 2005). Two of the major limitations include the non-independence of AFLP fragments and the non-homology of shared AFLP

fragments, described as fragment size homoplasy (Vekemans *et al.*, 2002). Lack of fragment homology has been observed both within individuals and between individuals (Mechanda & Baum, 2004), and fragment homology between distantly related species is shown to decrease over time (Althoff, 2007). Other limitations include the unequal probability in the loss/gain of fragments, and the dominant nature of AFLP markers (problems differentiating between homozygous and heterozygous fragments). Tests to diagnose such properties in AFLP datasets have been advocated by a number of studies, including testing for phylogenetic signal in AFLP data (Koopman, 2005) and testing for a correlation between AFLP distances and DNA sequence divergence (Meudt *et al.*, 2009; Dasmahapatra *et al.*, 2009).

Here, the suitability of the AFLP dataset for phylogenetic and cluster analysis was tested by comparison of pairwise AFLP distances and pairwise sequence distances. AFLP data was transformed into Jaccard (Jaccard, 1908) and Hamming distances (Hamming, 1950), and the combined plastid sequence dataset and the nuclear sequence dataset were transformed into Hamming distances in SplitsTree (Huson & Bryant, 2006). We test for a correlation between pairwise AFLP distance matrices and pairwise sequence divergence matrices using the mantel test (Legendre & Legendre, 1998) implemented in the vegan package (Oksanen *et al.*, 2012) in R (R Core Development Team, 2011). We also look for evidence of phylogenetic conflict with previous findings (Dyer *et al.*, 2012) using NeighborNet analysis in SplitsTree (results not shown) (Huson & Bryant, 2006).

Neighbor-joining (NJ) analyses with 500 bootstrap replicates were performed using Jaccard distances in SplitsTree (Huson & Bryant, 2006), and Nei-Li distances (Nei & Li, 1979) in Paup v4.0b10 (Swofford, 2002). Jaccard distances are a measure of the similarity between individuals, calculated by pairwise comparisons based on the presence of a band in at least one individual. This method is therefore not effected by homoplasic absent bands. Nei Li distances are similar but give more weight to the shared presence of bands and therefore place more emphasis on the similarity rather than the dissimilarity between individuals (see Bonin *et al.*, 2007).

Maximum parsimony (MP) was performed in PAUP using a heuristic search as follows: 1,000 replicates, 10 random sequence-addition per replicate, TBR branch swapping and

MULTrees option on, collapse zero-length branches off, characters were treated as equally weighted, and a strict consensus tree was calculated. Bootstrap support was estimated using 500 bootstrap replicates and a heuristic search with 10 random sequence-addition per replicate, TBR branch swapping, and MULTrees option off.

Bayesian analyses (BY) were run using the restriction site model for binary data in MrBayes 3.1 (Ronquist & Huelsenbeck, 2003; Huelsenbeck & Ronquist, 2005) with default settings. Analyses were run with a Markov Chain Monte Carlo (MCMC) run for 10 million generations and sampled every 500 generations to approximate the posterior probabilities of trees. The two analyses were run simultaneously and convergence on the maximum likelihood was assessed using Tracer v1.5 (Rambaut & Drummond, 2007), resulting in a conservative burn-in phase of 25% being implemented to disregard trees prior to convergence. The remaining trees, 15,000 trees for each run, were then compiled and a 50% majority rule consensus was calculated. We also performed a combined phylogenetic analysis of AFLP and sequence data in order to test for increased branch support and resolution of species relationships. The datasests were compiled in a text file and a mixed datatype was specified. Bayesian analyses were conducted on: (i) combined AFLP and nuclear DNA sequences (34 individuals plus out-group taxa), and (ii) combined AFLP and plastid sequences (56 individuals plus out-group taxa).

Bayesian inference of clusters (k) was performed using Structure 2.3.4 (Pritchard *et al.*, 2000; Falush *et al.*, 2007; Hubisz *et al.*, 2009). Version 2.3.4 of this software enables detection of genetically homogenous groups in dominant marker data such as AFLPs. It also allows for the inclusion of polyploidy individuals where genotypes may be ambiguous, through specification of the 'RECESSIVEALLELES' option. Analyses were run for 300000 MCMC generations after a burn-in period of 100000 generations, with independent allele frequencies and an admixture model of ancestry. Up to 16 clusters (k=1 to k=16) were assumed and analyses were repeated five times for each value of k. Convergence of the estimated Ln probability of the data (Ln P(D)) was confirmed by visualising the Ln P(D) plots of each run. The best estimate of the number of clusters present in our data was determined according to changes in the log likelihood and the ΔK values for each value of k (Evanno *et al.*, 2005).

Principle coordinates analysis (PCO) was performed using Jaccard distances obtained from the AFLP data (see above). Principle coordinates were computed in PCO3 (Anderson, 2003), with the first two and three axes plotted respectively, and individuals assigned according to taxonomic species.

Recent studies have also used Gaussian clustering for the delimitation of species in dominant markers datasets (Hausdorf & Hennig, 2010; Sauer & Hausdorf, 2012). Here we perform Gaussian mixture model cluster analysis using 'Mclust' (Fraley & Raftery, 1998) as implemented in the 'prabclus' package (Hennig & Hausdorf, 2012) in R (R Core Development Team, 2011). The mixture estimation was performed for 0 to 30 clusters with and without a noise component specified (to identify outliers), and using both metric and non-metric (Kruskal, 1964) multidimensional scaling (MDS) of Jaccard distances, with the number of MDS dimensions (NMDS) tested for four (r=4) and five (r=5) dimensions respectively.

3.3.4 Analysis of DNA sequence data

Ultrametric phylogenetic trees with divergence time estimates were generated for each dataset using Beast v1.7.4 (Drummond *et al.*, 2012), with specific models of evolution assessed in jModelTest 0.1 (Posada, 2008, 2009). Analyses were conducted with a relaxed lognormal clock and estimated rates, Monte Carlo Markov chains (MCMC) run for 200 million generations and sampled every 20,000 generations, using a coalescent tree prior. The relaxed lognormal clock priors were calibrated to *Asplenium dielerecta* (Schneider *et al.*, 2005).The combined plastid dataset was analysed with unlinked substitution models and linked tree priors. Output was analysed using Tracer v1.5 to ensure the effective sample of all estimated parameters (ESS) was over 200. The maximum clade credibility tree with posterior probability limits of 0.5 and mean node heights was produced from analysis of combined tree files in TreeAnnotator v1.7.4, with a burnin set to 1000 trees (10%).

Species delimitation of single locus datasets was investigated using a single threshold generalized mixed Yule coalescent (GMYC) model (Pons *et al.*, 2006; Fontaneto *et al.*, 2007). The GMYC model delineates species boundaries by estimating the transition in branching rates from species level (Yule model) to population level (coalescence model) evolutionary

processes. Single locus consensus trees with a coalescent prior generated in beast (see above) were transformed to binary format using the 'multi2di' function implemented in the 'ape' package (Paradis *et al.*, 2004) in R, and the GMYC model was fitted to each, as implemented by the 'gmyc' function in the 'splits' package (Ezard *et al.*, 2009) in R.

Species delimitation of the combined plastid dataset was investigated using Brownie 2.1.1 (O'Meara *et al.*, 2006), a non-parametric coalescent method that performs a heuristic search of a given set of gene tree topologies to estimates species limits. The consensus trees for each plastid marker (generated in Beast) were used as input trees, and a heuristic search was conducted with the number of random starting trees (NReps) set to 100, all possible taxon reassignments on leaf splits explored (Subsample = 1), and the minimum number of samples per species (MinSamp) set to 1. We performed 20 independent runs in order to find the optimal delimited species clusters.

3.4 Results

3.4.1 Phylogenetic analyses using AFLP data

We found evidence that increasing sequence divergence is correlated to increasing pair-wise distances in the AFLP data, supporting the use of the AFLP datasets in phylogenetic analyses. A positive correlation was found between pairwise interspecific AFLP distances (Jaccard and Hamming distances) and the pairwise interspecific distances of the plastid sequence dataset (Fig. 3.1A) (AFLP Jaccard distances: p=0.001 and r=0.74; AFLP Hamming distances: p=0.001 and r =0.48). A positive correlation was also found between pairwise interspecific AFLP distances and the pairwise interspecific distances of the nuclear *pgiC* dataset (Fig. 3.1B) (AFLP Jaccard distances: p=0.001 and r=0.47; AFLP Hamming distances: p=0.001 and r =0.27). Visualisation of phylogenetic signal in the AFLP data, using NeighborNet analysis, revealed no major topological conflict with the findings of previous phylogenetic analysis of DNA sequence data (results not shown).

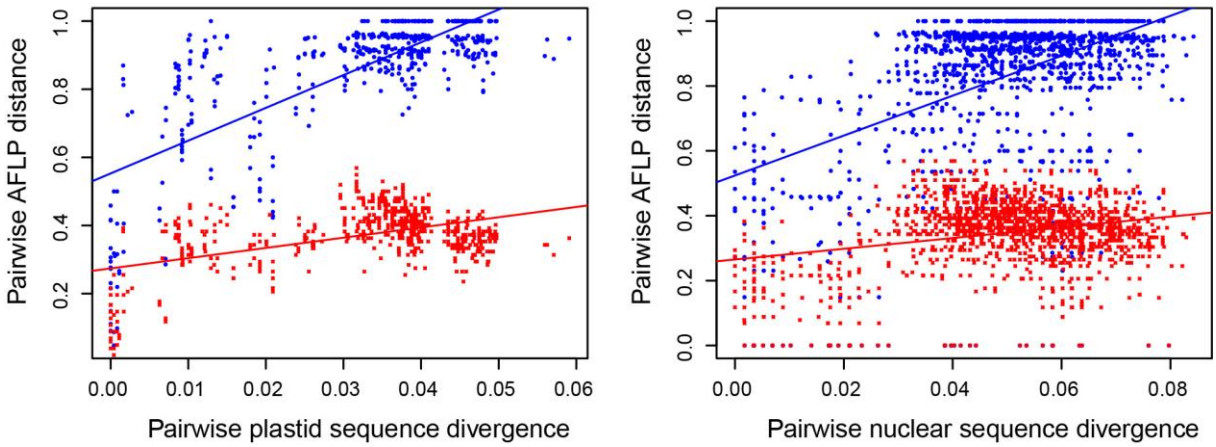

Figure 3.1. Matrix correlation between pairwise DNA sequence distances and AFLP distances. (A) The correlation between pairwise interspecific AFLP distances and the pairwise interspecific distances of the plastid DNA sequence dataset. AFLP Jaccard distances are plotted in blue (p=0.001 and r=0.74), and AFLP Hamming distances are plotted in red (p=0.001 and r =0.48). (B) The correlation between pairwise interspecific AFLP distances and the pairwise interspecific distances of the nuclear single copy gene *pgiC* dataset. AFLP Jaccard distances are plotted in blue (p=0.001 and r=0.47), and AFLP Hamming distances are plotted in red (p=0.001 and r =0.27).

Neighbor-joining analysis of the whole AFLP dataset using Jaccard and Nei-Li distance measures resulted in very similar tree topologies, differing only in branch support values. We therefore only present the NJ tree derived from Jaccard distances (Fig. 3.2). The recovered tree topology supports mostly monophyletic species clusters, corresponding to previously identified putative species. Species relationships were not well resolved and *A.polyphyllum* and *A.castaneum* were each recovered in three paraphyletic groups respectively. *Asplenium hallbergii* was recovered within *A.monanthes*, as was a previously un-sampled accession identified as spec.nov.2 (Spec.nov.2.p.2.1). All other spec.nov.2 accessions were recovered in a separate well-supported group. *A.resiliens* accessions were grouped together and supported as sister to a group consisting of *A.heterochroum* and *A.palmeri*.

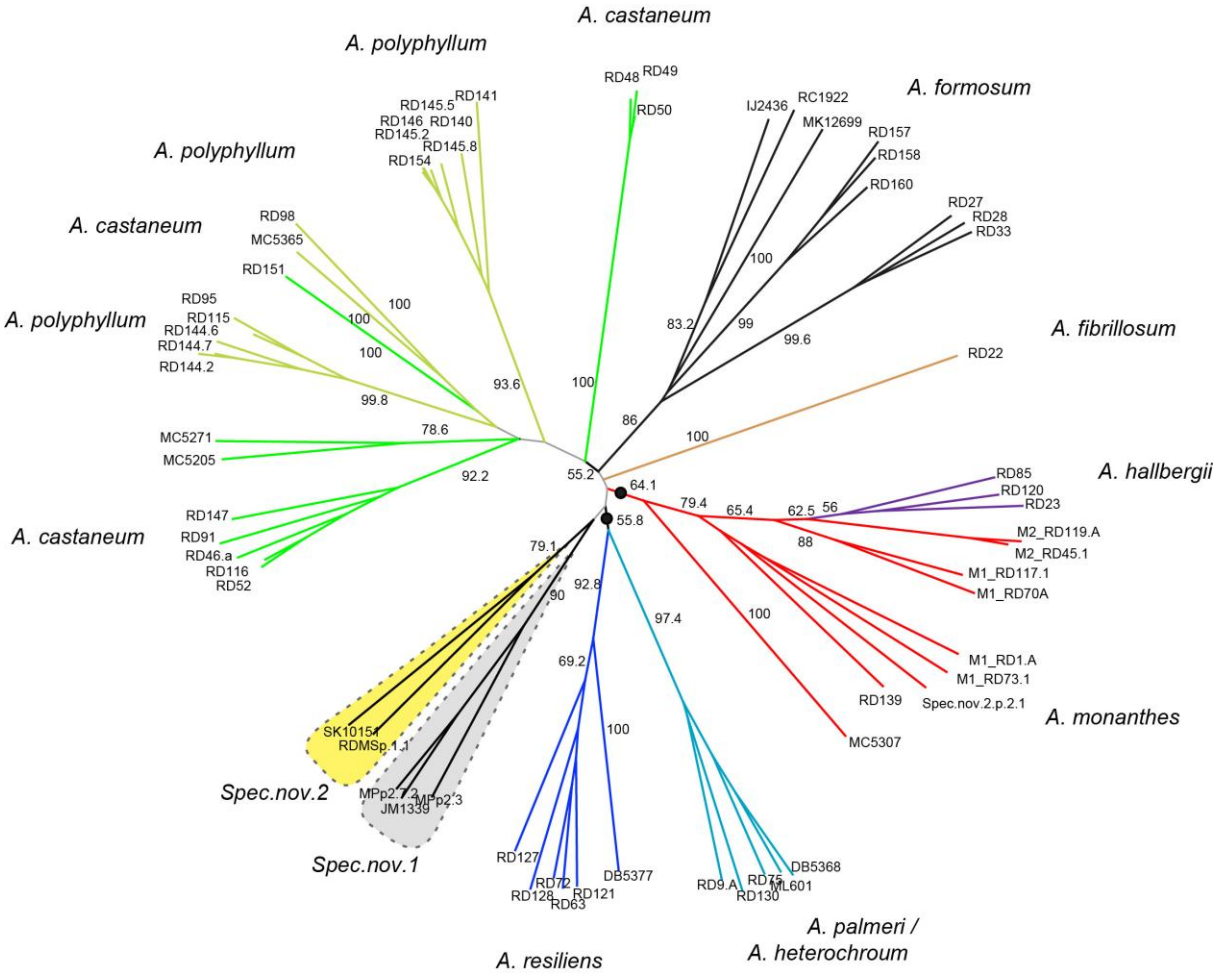

Figure 3.2. Neighbor joining tree of AFLP data performed using Jaccard distances and 500 bootstrap replicates in SplitsTree (Huson & Bryant, 2006). Bootstrap values over 50% are shown. Black filled circles indicate apomictic lineages. Clusters are coloured and labelled according to species assignments as inferred in Dyer et al. (2012). Terminals are labelled with voucher codes (Table 3.1).

The BY and MP trees (Fig. 3.3) were less resolved than the NJ tree, but did recover support for some of the same species groups observed. However, the majority of species were recovered in a large polytomy, and no further information on species relationships were retrieved. The BY combined analyses of AFLP and DNA sequence data with nuclear and plastid sequence data respectively (Fig. 3.4) improved support for the main clades recovered in analysis of sequence data alone. Combined analysis of the plastid DNA sequence data and AFLP data (Fig. 3.4A) recovered a near identical topology to analysis of the combined plastid sequence data alone, but with support for the relationships between the three major clades: (i) the *A.castaneum clade*, (ii) the *A.resiliens* clade, and (iii) the *A.monanthes* clade. Strong support was shown for the *A.castaneum* clade as sister to both the *A.resiliens* clade and the *A.monanthes* clade. Species accessions were monophyletic with the exception of *A*.cf.*monanthes* MC5307, which was recovered in a clade with accessions of *A.fibrillosum* and *A.polyphyllum*.

Combined analysis of the *pgiC* sequence data and AFLP data (Fig. 3.4B) recovered a similar tree to analysis of sequence data alone, but provided a higher resolution of species relationships. The major difference was that *A.monanthes* and *A.hallbergii* accessions were found in a monophyletic clade, and spec.nov.1 and Spec.nov.2 were nested with support in a clade with *A.fibrillosum*. Also, the support for *A.formosum* as sister to *A.resiliens*, *A*.aff.*heterochroum* and *A.palmeri* was strengthened.

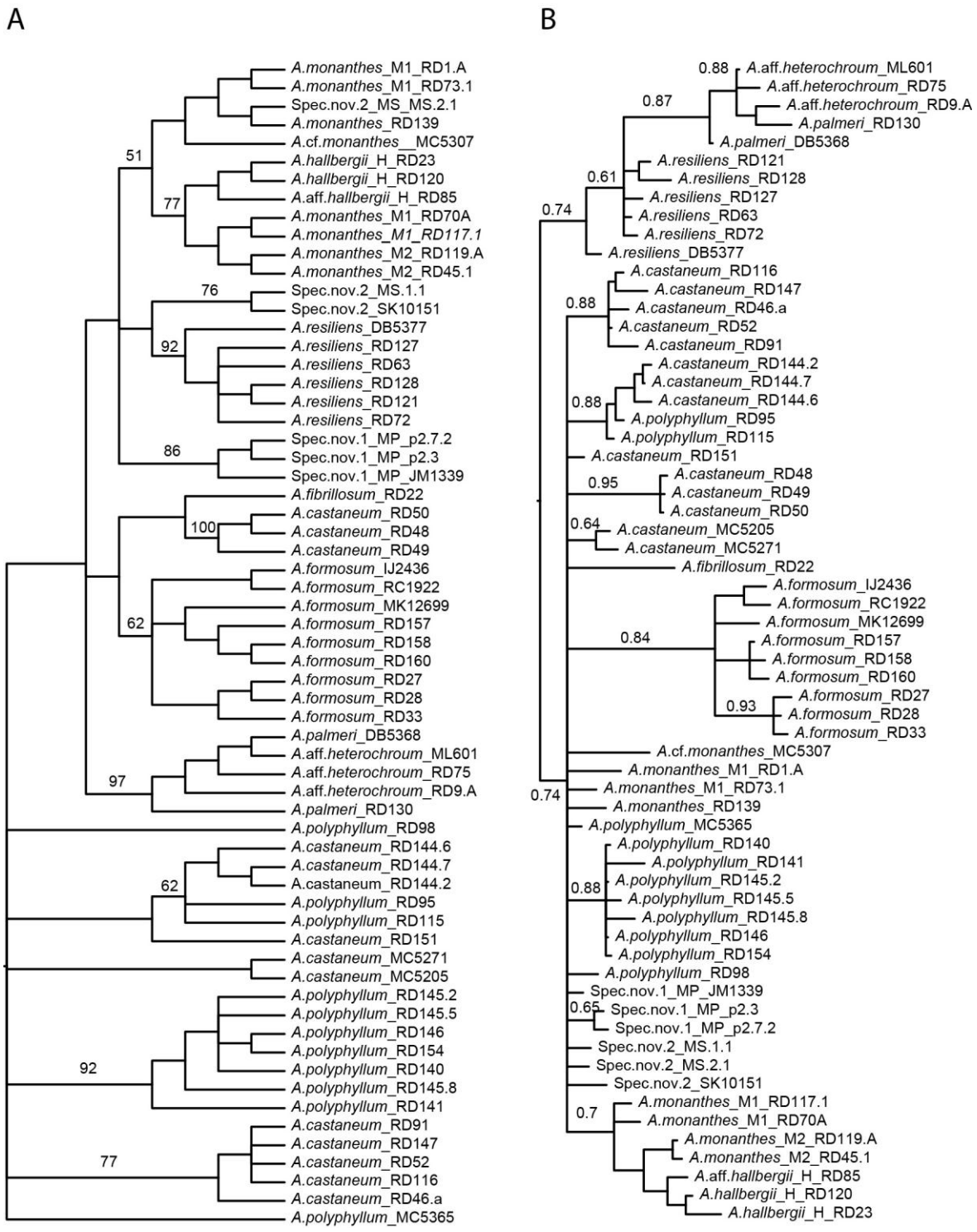

Figure 3.3. Phylogenetic analysis of AFLP data. (A) Maximum parsimony strict consensus tree using a midpoint rooting option, bootstrap values >50% are shown for the main clades. (B) Bayesian 50% majority rule consensus tree using a midpoint rooting option, posterior confidence values p >0.6 are shown for the main clades.

Figure 3.4. Combined phylogenetic analysis of AFLP and sequence data. Trees are rooted to outgroup taxa. (A) Bayesian 50% majority rule consensus tree of combined AFLP and plastid DNA sequence data. Clades are labelled according to the findings of Dyer *et al*. (2012): (i) the *A.castaneum* clade, (ii) the *A.resiliens* clade, (iii) the *A.monanthes* clade (B) Bayesian 50% majority rule consensus tree of combined AFLP and nuclear *pgiC* sequences. Posterior confidence values p >0.8 are shown. Black filled circles indicate apomictic lineages.

3.4.2 Species delimitation using AFLP data

The compilation and visual inspection of the output from Structure analyses showed that although there was a distinct rise at K=2, there was not a distinct value of K at which the mean estimated posterior probability of the data reached a clear maximum value (Fig. 3.5A). Calculation of the ΔK statistic estimated the number of clusters to be K=2 (Fig. 3.5B). The clusters at K=2 are composed of one cluster that consist of all *A.castaneum* and *A.polyphyllum* specimens, and one cluster that is comprised of all remaining species. These clusters correspond to the major clades recovered in the *pgiC* gene tree and in the combined *pgiC* and AFLP tree (Fig. 3.4B).

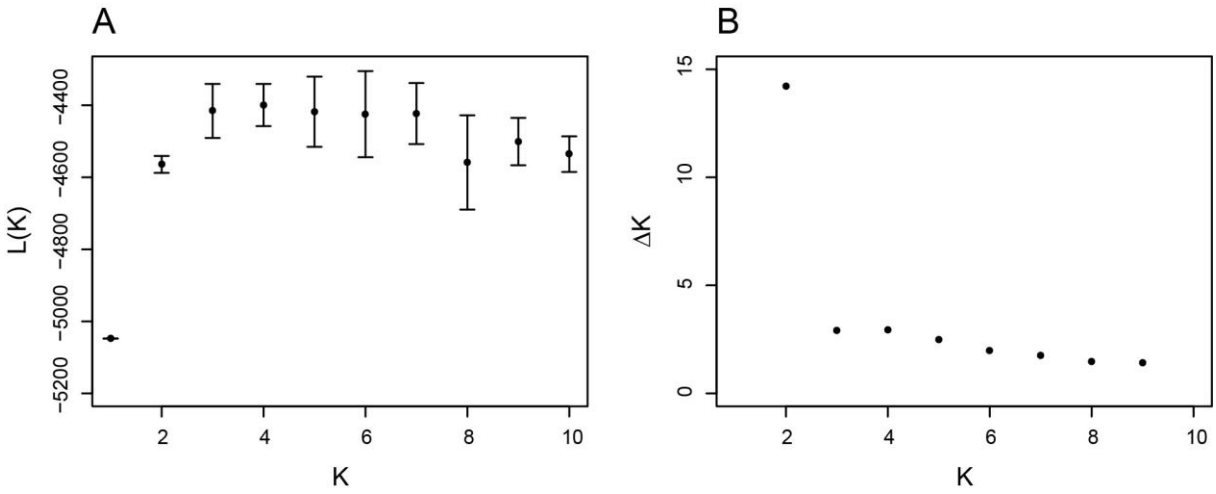

Figure 3.5. Results of the Structure analysis of AFLP data. The true number of clusters present in our data was estimated according to (A) changes in the log likelihood, and (B) the ΔK values for each value of K (Evanno *et al.*, 2005).

PCO analysis of AFLP data showed that most species are clearly separated into distinct clusters (Fig. 3.6A, B). Gaussian clustering analysis of the AFLP data using both metric and non-metric MDS methods with no noise component, and for r=4 (stress = 11.92%) and r=5 (stress = 9.45%), resulted in the identification of 10 clusters (Figures 3.6C and 3.7, and Table 3.2). When 4 NMDS dimensions (r=4) were specified using a metric MDS method: *A.*aff.*heterochroum* accessions and *A.palmeri* accessions were combined in one cluster; two species specific clusters containing *A.castaneum* and *A.polyphyllum* were identified respectively, but two separate clusters were also recovered combining accessions of both species; all *A.formosum* accessions were recovered in one species specific cluster; all

A.resiliens accessions were recovered in one species specific cluster; *A.monanthes* specimens were identified in two clusters, one combined with *A.hallbergii* accessions, and one combined with one accession of spec.nov.2 (MS2.1); and finally spec.nov.1, spec.nov.2, one *A.*cf.*monanthes* accession (MC5307) and *A.fibrillosum* were combined in one cluster. When five NMDS dimensions (r=5) were specified using a metric MDS method, identical clusters were recovered with the exception of the composition of clusters containing *A.monanthes*, *A.hallbergii* and one accession of spec.nov.2.

In general, the clusters recovered using a metric MDS method are supportive of the clades recovered in the combined *pgiC* and AFLP tree (Fig. 3.4B). When a non-metric MDS method was used with four and five NMDS dimensions specified respectively, the composition of clusters remained very similar to that recovered in analyses using the metric MDS method. Exceptions included the following: *A.fibrillosum* was combined in the otherwise species-specific cluster containing three accessions of *A.castaneum* (RD48, RD49, and RD50); *A.*cf.*monanthes* accession MC5307 was combined with all other *A.monanthes* and *A.hallbergii* accessions together with the isolated accession of spec.nov.2 (MS2.1) in one cluster. Analysis performed with four NMDS dimensions also grouped the two clusters of combined *A.castaneum* and *A.polyphyllum* into one cluster.

In analysis using a noise component to identify outliers, the metric MDS method resulted in eight (r=4) and seven (r=5) individuals being included in the noise component, and the non-metric MDS method resulted in 21 (r=4) and 28 (r=4) individuals being included in the noise component.

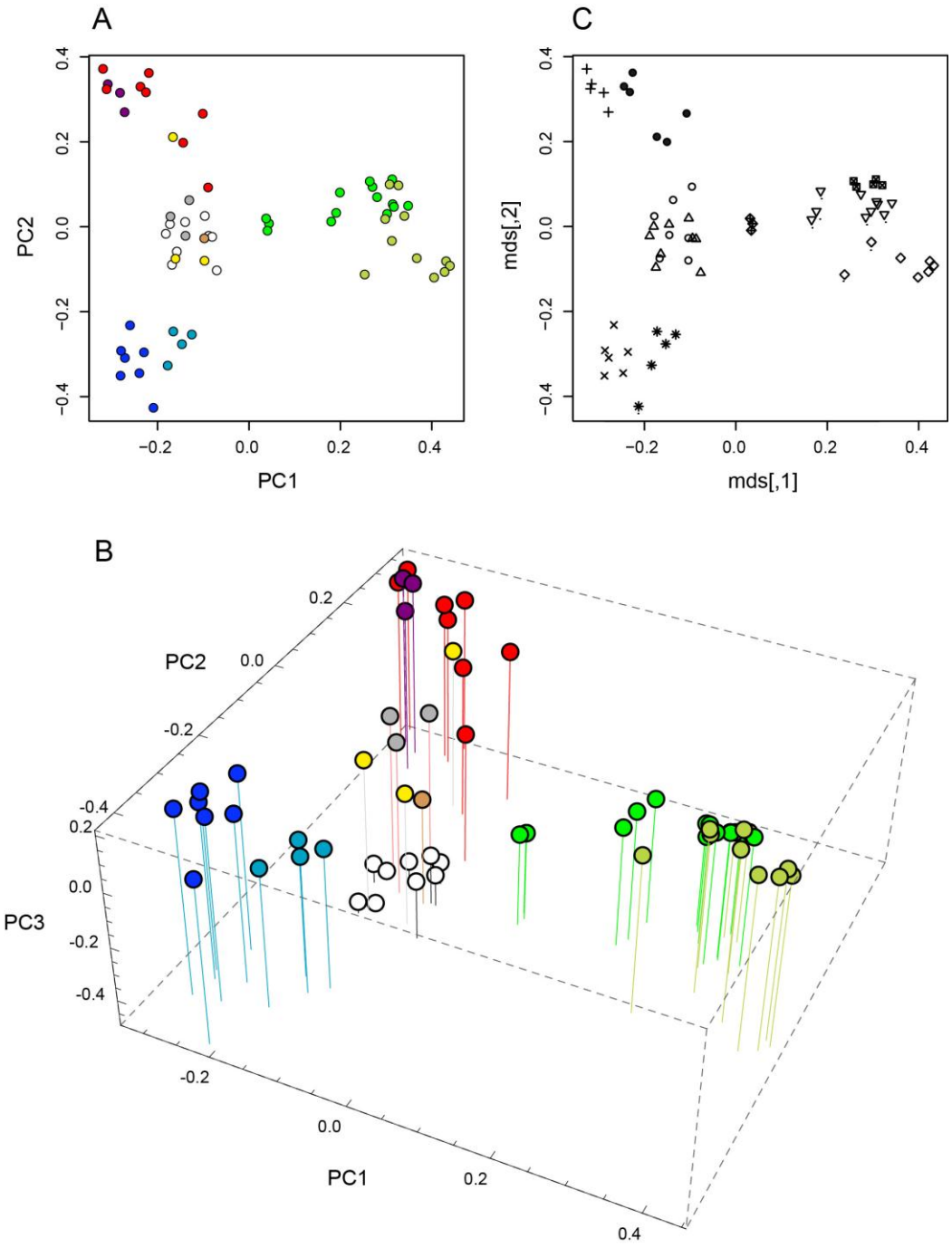

Figure 3.6. (A and B) Results of principle components analysis of AFLP Jaccard distances computed in PCO3 (Anderson, 2003), plotting the principle components of the first two axes (A) and the first three axes (B). Individual principle components are coloured according to species inferred in Dyer et al. (2012): Dark blue = *A.resiliens*; Light blue = *A.palmeri* / *A.*aff.*heterochroum*; White = *A.formosum*; Yellow = spec.nov.2; Grey = spec.nov.1; Red = *A.monanthes*; Purple = *A.hallbergii*; Bright green = *A.castaneum*; Olive green = *A.polyphyllum*. (C) Gaussian analysis of AFLP data. Results from the metric multidimensional scaling of Jaccard distances and NMDS=5 are shown. The first two dimensions are plotted with clusters represented by different symbols. Individuals with small black circles underneath were included as noise when analysis was run with a noise component. Clusters generally correspond to morphological species (see A, B and Fig. 3.7).

3.4.3 Species delimitation using sequence data

We used the GMYC model to delineate species based on single locus ultrametric trees obtained from BY analysis with a relaxed lognormal clock and coalescent prior in Beast. A log-likelihood ratio test of the GMYC model against a null model of coalescence showed that the null model could not be rejected for *psbA-trnH* (p=0.64) and *pgiC* gene trees (p=0.78). However, the GMYC model produced a significantly better fit for *trnL-trnF* (likelihood ratio=11.08, p=0.01) and *rps4F-trnS* trees (likelihood ratio=23.03, p=0.004). The GMYC model estimated 12 clusters and 16 entities for the *rps4-trnS* tree, and 11 clusters and 15 entities for the *trnL-trnF* tree (Fig. 3.7, and Table 3.2). Species delimitation in both trees was relatively concordant with previous species inferences (Dyer *et al.,* 2012) with the following exceptions: *A.monanthes*, *A.castaneum*, *A.formosum* and *A.resiliens* were divided into sub-species in both trees; in the *trnL-trnF* tree, *A.palmeri* and *A*.aff.*heterochroum* were grouped together, and *A.polyphyllum* was grouped with *A*.cf.*monanthes* accession MC5307; in the *rps4-trnS* tree, *A.fibrillosum* was grouped with *A*.cf.*monanthes* accession MC5307.

Non-parametric species delimitation of the multilocus (combined plastid) sequence dataset resulted in the identification of 15/16 species (Fig. 3.7, and Table 3.2). These species clusters are consistent to those recovered in GMYC analysis of single locus datasets. Although most delimited species were consistently recovered, there were some species that were not always consistent in their composition (*A*.aff.*heterochroum*, *A.hallbergii*, *A.castaneum)*. In these cases the most common species delimitation was summarised in Fig. 3.7.

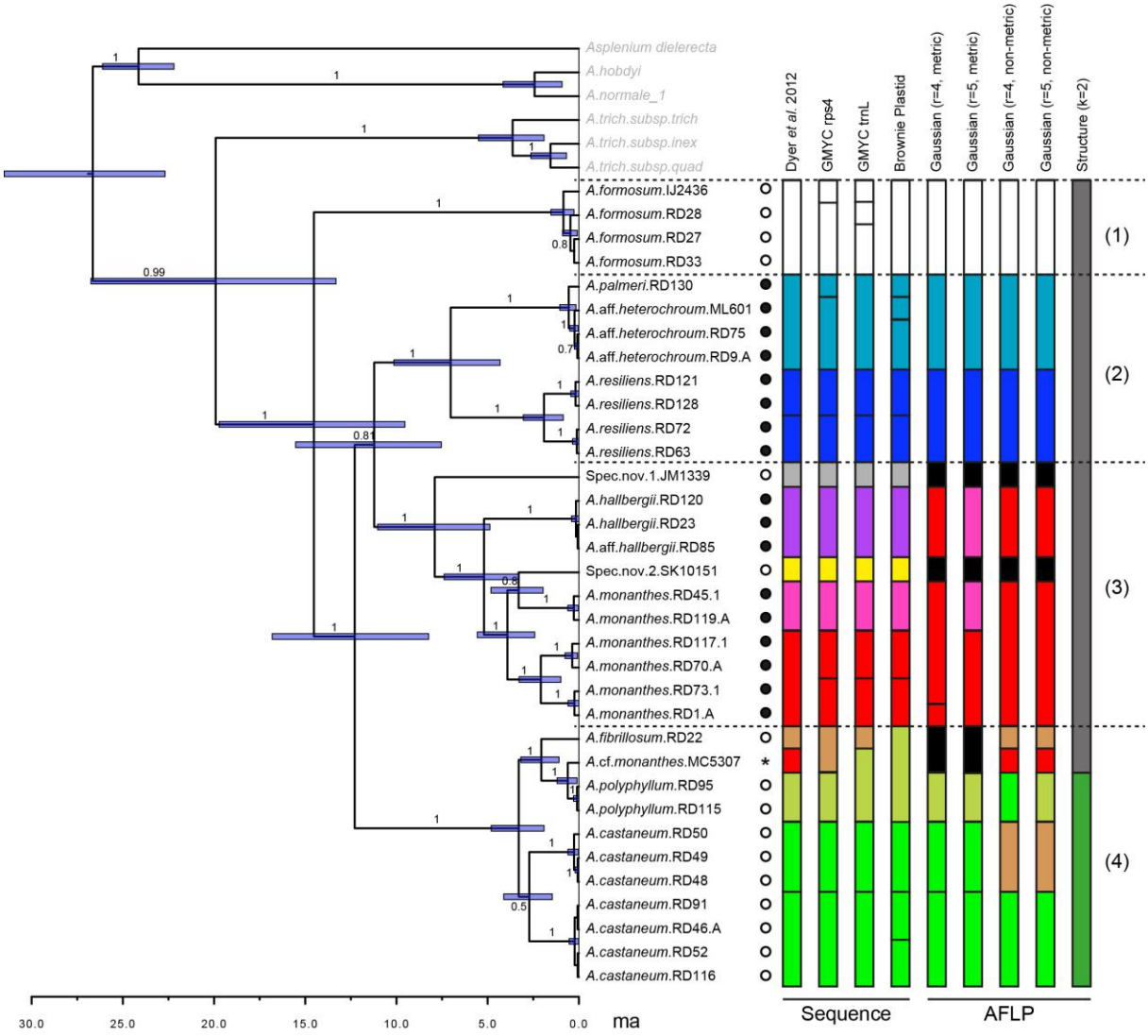

Figure 3.7. A comparison of species delimitations of sequence and AFLP datasets based on an ultrametric phylogenetic tree of combined plastid sequence data, with divergence time estimates using a coalescent tree prior, and a relaxed lognormal clock and estimated rates, as estimated in Beast v1.7.4 (Drummond *et al.*, 2012). The clock is calibrated according to an estimate for *Asplenium dielerecta* (Schneider *et al.*, 2005). Scale of the ultrametric tree corresponds to million year to the present (ma). Major clades are labelled as: (1) *A.formosum*, (2) the *A.resiliens* clade, (3) the *A.monanthes* clade, (4) the *A.castaneum* clade. Species assignments are coloured according to morphological species and according to the most common species when species are grouped. Black horizontal lines indicate subdivisions within species. Black filled circles indicate taxa with an apomictic mode of reproduction, and empty circles indicate sexually reproducing taxa. The asterisk (*) indicates a previously unsampled individual with unknown ploidy level or reproductive mode.

Table 3.2. Summary of species delimitation results. Data type is indicated as AFLP data, single locus sequence data, or 'Plastid' (signifying combined analysis of the three plastid loci: *psbA-trnH*, *trnL-trnF*, and *rps4-trnS*). For Gaussian cluster analysis, r signifies the number of dimensions specified, and the number of clusters given in brackets is the actual number of clusters recovered (extra clusters are recovered as noise). For Brownie analysis results were not always consistent and the range of clusters recovered is given.

Data	Method	Parameters	No. of individuals	No. of clusters	Species fused	Species subdivided
rps4-trnS	GMYC	Single	40	16	2	4
trnL-trnF	GMYC	Single	40	15	4	4
Plastid	Brownie	Non parametric	40	15/16	3	4
AFLP	Gaussian	Metric r=4	63	10	9	3
AFLP	Gaussian	Metric r=5	63	10	9	3
AFLP	Gaussian	Non-metric r=4	63	7 (10)	9	1
AFLP	Gaussian	Non-metric r=5	63	9 (10)	9	2
AFLP	STRUCTURE	k=2	63	2	11	0

3.5 Discussion

The occurrence of reticulate evolution and mixed reproductive systems within apomictic fern complexes often hinders the delimitation of species boundaries and species relationships. We have investigated this problem in the *Asplenium monanthes* complex through a comparative analysis of AFLPs and DNA sequence data, using a variety of different species delimitation methods. In general, these data and analysis methods produce congruent results and find support for the findings of Dyer *et al*. (2012).

3.5.1 Species delimitation

Species delimitation of DNA sequence data supported inferences of species made by Dyer *et al.* (2012). The application of the GMYC model to *rps4-trnS* and *trnL-trnF* locus trees and the non-parametric method (Brownie) to multilocus sequence data recovered generally congruent species (Fig. 3.7). This includes the distinction of spec.nov.1 and spec.nov.2 as species, highlighting the importance of ploidy level and reproductive mode as secondary species criteria. Moreover, the inference of distinct hybrid lineages within *A.resiliens* and *A.monanthes* respectively is also supported, but with a further sub-division of the *A.monanthes* lineage into three species (Fig. 3.7). However, the GMYC model provided no significant improvement to the null model of coalescence for *psbA-trnH* and *pgiC* trees, so

provided no information on species boundaries. This is probably owing to the low levels of diversity observed in these loci.

Species delimitation of the AFLP dataset varied according to the method applied (Fig. 3.7, Table 3.2). Structure analysis resulted in the delimitation of only two species, whilst Gaussian cluster analyses (Figures 3.6C and 3.7) resulted in seven to ten species. This result corresponds to previous studies which show that Gaussian analysis are more suitable for species delimitation within dominant marker and interspecific data (Hausdorf & Hennig, 2010; Sauer & Hausdorf, 2012). Gaussian cluster analysis of the AFLP data was generally congruent with species delimitation in the sequence datasets, but with the general uniting of sub-divisions. This included sub-divisions in *A.resiliens* and *A.monanthes* respectively. In metric analysis several species were united, notably spec.nov.1, spec.nov.2, *A.fibrillosum* and *A*.cf.*monanthes* MC5307. The unification of these four species has implications for species relationships and reticulate evolution, and is discussed in the following sections.

The higher number of species delimited in sequence data compared to AFLP data must also be considered. Single locus data carries a higher risk than multilocus data of overestimating, underestimating, or inaccurate species delimitation (Roe & Sperling, 2007; Roe *et al.*, 2010). Equally, species delimitation using multilocus AFLP data may underestimate species in cases of a low sample number of individuals or low numbers of examined loci (Hausdorf & Hennig, 2010).

3.5.2 Species relationships

The resolution of species relationships from phylogenetic analysis in Dyer *et al*. (2012) was uncertain due to the presence of polytomies and topological incongruences between plastid and nuclear phylogenies. The reduced subset of samples used for this study provided stronger resolution of species relationships in the plastid dataset, showing the *A.resiliens* clade to be sister to the *A.monanthes* clade. This is possibly due to a more equal sampling of species than in previous analysis, and has implications for the origins of apomixis (discussed later).

Unfortunately, tree-building analyses of the AFLP data alone did not resolve species relationships. The NJ analysis of AFLP data did recover congruent species clusters to

sequence data, but relationships between species were not well supported (Fig. 3.2). Bayesian and maximum parsimony analyses showed similar results but again did not provided resolution in species relationships (Fig. 3.3). However, the combined Bayesian analysis of AFLP data and plastid or nuclear datasets, respectively, produced well-resolved trees (Fig. 3.4). These trees were very similar to those of respective sequence data trees, but increased branch support values were recovered for the main clades in both trees.

The combination of AFLP data with the nuclear sequence data tree (Fig. 3.4B) resulted in spec.nov.1 and spec.nov.2 being recovered with *A.fibrillosum* in a separate clade to *A.monanthes* and *A.hallbergii*. As mentioned previously, this clade was also delimited as a separate cluster in Gaussian analysis (metric method) (Figures 3.6C and 3.7), and highlights the concordance of species delimitation of AFLP data with the combined AFLP and nuclear sequence tree (Fig. 3.4B). This is also true of species delimitation in Structure, which delimits the two main clades of the tree (Fig. 3.7). However, it is not the case for Gaussian analysis using a non-metric method, which recovers *A.fibrillosum* within *A.castaneum* and *A*.cf.*monanthes* MC5307 with other *A.monanthes* individuals.

3.5.3 Reticulate evolution

Hybridisation was inferred in Dyer *et al*. (2012) based on incongruences between the nuclear and plastid data. Species delimitation of the plastid sequence data supports the monophylly and sub-division of inferred hybrid lineages in the plastid dataset (in *A.resiliens*, *A.monanthes*, and *A.castaneum/ A.polyphyllum*) (Fig. 3.7). However, species delimitation of the nuclear *pgiC* sequence data was uninformative, as the GMYC model did not provide a significantly better fit than the null model of coalescence. This means that incomplete lineage sorting cannot be ruled out for this data.

AFLP data generally reflects diversity in the nuclear genome, which would indicate that *A.monanthes* and *A.resiliens* have homogeneous genotypes. The incongruence between these findings and the diversity observed in the plastid genome (maternally inherited) supports the inference of hybridisation in both of these lineages (Figures 3.6C and 3.7). However, Gaussian analysis using a metric method did recover some additional diversity within *A.monanthes*, which might indicate the occurrence of unequal meiosis (Lin *et al.*, 1992), or

genetic segregation as seen in *Cyrtomium fortunei* (Ootsuki *et al.*, 2012). This assertion is also supported by the delimitation of further clusters in the plastid data (Fig. 3.7). The analysis of AFLP data for *A.castaneum* and *A.polyphyllum* accessions resulted in more heterogeneous patterns, making species delimitation difficult. It is likely that this supports inferences of reticulation between these two taxa but further scrutiny of these two taxa is required. The association of *A.fibrillosum* and *A.*cf.*monanthes* MC5307 with spec.nov.1 and spec.nov.2, in the AFLP data indicates previously undocumented hybridisation with the *A.castaneum* clade.

3.5.4 Origins of apomixis and sexual progenitors

Multiple origins of apomixis were inferred in Dyer *et al*. (2012) due to the occurrence of diploid sexual putative progenitor species (spec.nov.1 and spec.nov.2) associated to distinct hybrid lineages of *A.monanthes* and *A.hallbergii*, and the distinction of *A.resiliens* lineages and *A.palmeri* and *A.*aff.*heterochroum*. Although the AFLP data highlights the close association of putative sexual progenitors spec.nov.1 and spec.nov.2 with the *A.monanthes* and *A.hallbergii* lineages (Figures 3.4B and 3.7), they are recovered as separate clusters. This introduces uncertainty as to their involvement in the origin of apomixis in *A.monanthes* lineages. However, the variation in ploidy levels between putative sexual diploid progenitors and the triploid apomictic lineages may affect the validity of AFLPs in detecting parentage. Further insight into these inferences would be gained from the use of co-dominant markers.

The inference of multiple origins of apomixis is supported in this study; however, a single origin of apomixis for *A.monanthes* lineages and the *A.resiliens* lineages cannot be ruled out. This assertion is supported by the resolution of species relationships observed in the plastid data showing *A.monanthes* and *A.resiliens* as sister to each other, and the clustering of these species in structure analysis of the AFLP data. However, the close association of sexual species, *A.fibrillosum*, *A.formosum*, spec.nov.1, spec.nov.2 and the un-sampled *A.heterochroum* mean that further analysis into parentage of hybrid lineages needs to be undertaken.

3.6 Conclusions

Comparative analysis of sequence data and AFLP data resulted in generally congruent delimitation of species, and supported the inferences of distinct lineages and hybridisation made in Dyer *et al*. (2012). However, evidence for additional genetic diversity within the *A.monanthes* lineages, supported in both the AFLP data and the sequence data, also indicated that genetic segregation or unequal meiosis within apomictic taxa could not be ruled out. Moreover, species delimitation was not applicable for the nuclear *pgiC* tree, indicating that inferences of hybridisation from this data need to be tested against lineage sorting and genetic segregation.

The inference of sexual progenitors species spec.nov.1 and spec.nov.2 was not supported in the AFLP data. However, this may indicate shortcomings in the use of AFLPs for the detection of parentage in the presence of variation in ploidy level.

Inference of a species tree was not possible from phylogenetic analysis of AFLP data alone. However, the AFLP data did support the species relationships observed in the nuclear phylogeny. In order to move towards a species tree, a greater understanding of reticulate relationships is required. This could be achieved through intraspecific analysis of AFLP data and/or a greater sampling of nuclear genes, and the application of a number of recent methods that are able to detect hybridisation and even distinguish between reticulation and incomplete lineage sorting (see Blanco-Pastor *et al.*, 2012).

CHAPTER 4

Genome size expansion and the evolutionary relationship between nuclear DNA content and spore size in the *Asplenium monanthes* fern complex (Aspleniaceae)

Prepared for submission to New Phytologist under the co-authorship of Jaume Pellicer, Ilia J. Leitch, Vincent Savolainen, & Harald Schneider.

4.1 Summary

Genome size measurements are an under exploited tool in homosporous ferns. The application of this tool shows great potential to provide an overview of the mechanisms that define genome evolution in these ferns, and test evolutionary hypotheses based on the correlated evolution between genome size and a range of traits, such as spore size. The purpose of this study is to investigate the relationship between genome size and spore size and explore the evolution of genome size within the *Asplenium monanthes* fern complex and related lineages. We use flow cytometry to measure DNA amount of specimens, and comparative methods to test for correlation between genome size and spore size across the phylogeny. Our findings show that spore size and genome size are not correlated and thus they challenge the widely held assumption that spore size can be used to infer ploidy levels within apomictic fern complexes. The data also provide evidence for marked genome size variation between lineages of the *A.monanthes* complex and its relatives. We argue that the observed genome size variation is likely to have arisen via both polyploidy and chromosome size expansion. That latter is consistent with retrotransposon-driven chromosome/genome size expansion which to date, has not been considered to be an important process of genome evolution within homosporous ferns. We infer that genome evolution, at least in some homosporous fern lineages, is a more dynamic process than existing studies would suggest. However, it is uncertain to what degree our findings are associated with the prevalence of apomixis in this lineage.

4.2 Introduction

Homosporous ferns are renowned for their high chromosome numbers, with *Ophioglossum reticulatum* having the highest chromosome number (2n=ca.1400) so far reported for any eukaryote (Ghatak, 1977). Moreover, the mean chromosome number for homosporous ferns (n=57.05) is significantly higher than for any other plant group (including heterosporous ferns, n=13.6; and angiosperms, n=15.99) (Klekowski and Baker 1966). Nevertheless, the reasons for such disparity between these different plant groups still remain enigmatic, and are a major focus of ongoing research in this field (e.g. Nakazato *et al.*, 2008; Barker & Wolf, 2010; Barker, 2013).

The application of novel genome-wide analytical methods, including genome size analysis, is providing significant insight into the processes that shape homosporous fern genomes (Nakazato *et al.*, 2008; Barker & Wolf, 2010; Bainard *et al.*, 2011a). Although our knowledge of genome sizes in ferns is limited (< 1% of species have been analysed), available data suggest that patterns of genome size evolution, which include (i) polyploidisation; (ii) changes in chromosome size; and, (iii) paleopolyploidsation, are not operating uniformly across all fern lineages (Bennett & Leitch, 2001, 2010; Obermayer *et al.*, 2002; Bainard *et al.*, 2011a; Leitch & Leitch, 2013). In contrast to the extreme diversity of genome sizes encountered in angiosperms, which range c. 2,400-fold (Pellicer *et al.*, 2010), genome sizes in ferns (monilophytes) are less variable, ranging just c. 94-fold (Bennett & Leitch, 2010; Leitch & Leitch, 2013).

In fact, if we focus within homosporous ferns, this variation in nuclear DNA contents only spans c. 25-fold, from 1C=2.95pg in *Athyrium filix-femina* (Grime *et al.*, 1988) to 1C=72.68 pg in *Psilotum nudum* var. *rubra* (Obermayer *et al.*, 2002). The 1C-value is the DNA content of the un-replicated reduced chromosome compliment (see Greilhuber *et al*., 2005). While some of this diversity arises from polyploidy (e.g. *Ophioglossum petiolatum*, 2n=32*x*=c. 960, and 1C=65.55pg, see Obermayer *et al.*, 2002), genome size changes can also arise within the same ploidy level in some genera. For example, the 1.5-fold range of genome sizes encountered in *Davallia* have taken place at the diploid level (2n = 80) with the different genome sizes between species reflected in contrasting chromosome sizes (Obermayer *et al.*, 2002). Such differences may arise through different balances between transposable element

activity (especially retrotransposons) leading to genome and chromosome size increases, and DNA elimination, as frequently observed in angiosperms (Grover & Wendel, 2010; Leitch & Leitch, 2012). Nevertheless, available cytogenetic data indicates that despite a few examples (Britton, 1953) most homosporous ferns are characterized by possessing small and rather conserved chromosome sizes with little evidence of retrotransposon activity (Wagner & Wagner, 1980; Brandes *et al.*, 1997; Nakazato *et al.*, 2008; Bainard *et al.*, 2011a). This observation is supported by the relatively small variation in the monoploid genome size reported for homosporous ferns (1C*x*=2.95pg - 21.02pg; 1C*x*-value is the DNA content of one unreplicated chromosome set *sensu* Greilhuber *et al.*, 2005), and the absence of any apparent relationship between 1C*x*-value and chromosome numbers (Bainard *et al.*, 2011a).

In ferns, studies on closely related species in *Dryopteris* (Ekrt *et al.*, 2009, 2010) and *Polypodium* (Bures *et al*., 2003) have shown that genome size can be a powerful marker for taxonomic delimitations. However, as far as we are aware, no study to date has investigated the evolution of genome size and whether it is correlated with breeding system or any morphological traits, in a closely related group of fern species. This is in contrast to studies in angiosperms which have demonstrated that genome size is correlated with several ecological and morphological traits, such as seed mass and stomatal density (e.g. Beaulieu *et al.*, 2007, 2008; Zedek *et al.*, 2010; Greilhuber & Leitch, 2013). Such studies would be highly informative in ferns, as traits such as spore size and stomatal cell size are often used to infer changes in ploidy levels among closely related species (Moran, 1982; Barrington *et al.*, 1986; Beck *et al.*, 2010). This is based on the implicit assumption that species with higher ploidy levels (and hence larger genomes) will have larger spores, although this has never been systematically tested for genome size within a phylogenetically well defined group.

In this study we investigate the evolution of genome size and spore size within the *Asplenium monanthes* complex and related lineages (Fig. 4.1), a group of closely related species whose phylogenetic relationships have been recovered (Dyer *et al.*, 2012). These studies have uncovered evidence of reticulate evolution, and multiple apomictic lineages in this complex of black-stemmed rock spleenworts. In addition, polyploidy is known to occur, based on previously reported chromosome counts in some taxa (see Material and Methods in Dyer *et al.*, 2012).

Our work had two aims. First we wanted to test the widely held assumption that DNA amount and spore size are correlated. To do this we compared DNA content and spore length for multiple taxa within the *A.monanthes* complex. Our second aim was to investigate genome size evolution within this group of ferns to determine to what extent genome size variation reflects changes in chromosome size or ploidy levels. To do this we used genome size estimations made for taxa with known ploidy level (i.e. karyologically determined) to infer DNA ploidies for those species without available chromosome counts. The data were then analysed within the phylogenetic framework of Dyer *et al*. (2012) to provide insights into genome size dynamics.

4.3 Material and Methods

4.3.1 Taxa studied

The *Asplenium* species included in the present study are listed in Table 4.1. They were selected based on the phylogenetic investigation of the complex by Dyer *et al.* (2012) and whether the species could be successfully cultivated (see Table 4.1). Spec.nov1 and spec.nov.2, which belong to the *A.monanthes* complex, are reported by Dyer *et al*. (2012) to be sexual diploids (based on spore size and nuclear DNA sequence analysis) and considered to be putative progenitor species to the two distinct apomictic lineages of *A.monanthes*, referred to as MO1 and MO2 (see Fig. 4.1).

Chromosome counts and derived ploidy levels are reported for: *A.formosum*, 2n=2*x*=72 (Manton, 1959; Walker, 1966b; Ghatak, 1977; Ammal & Bahavanandan, 1991; Guillén & Daviña, 2005); *A.monanthes*, mainly n=2n=3*x*=108, although there is a single count of 2n=4*x*=144 (Manton, 1950; Manton & Vida, 1968; Wagner *et al.*, 1970; Tryon *et al.*, 1973; Smith & Mickel, 1977; Lovis *et al.*, 1977; Manton *et al.*, 1986); *A.resiliens*, n=2n=3*x*=108 and *A.heterochroum*, 2n=4*x*=144/2n=6*x*=216, 2n=5*x*=180 (Morzenti & Wagner, 1962; Wagner, 1963, 1966; Morzenti, 1966; Wagner & Wagner, 1966; Walker, 1966b; Wagner *et al.*, 1970; Windham, 1983; Haufler & Soltis, 1986).

Fresh material was unavailable for *A.fibrillosum, A.polyphyllum, A.soleirolioides*, spec.nov.1, spec.nov.2, and some accessions of *A.formosum* (see Table 4.1), so silica dried samples were

used instead. In total, the study sample comprised 31 fresh samples cultivated from specimen spores, and seven silica-dried samples.

Table 4.1. A summary of the specimens analysed including, mean 2C DNA content and mean spore length measurements per specimen (both with standard deviation values). Voucher numbers are linked to accession numbers for sequences deposited at Genbank (Dyer *et al.*, 2012). In cases where alternate voucher numbers appear in brackets, these accessions were used for phylogenetic analysis. CV% indicates the mean coefficient of variation of the 2C DNA peak for each specimen. Reproductive mode was determined from spore number per sporangia, and some prothalli observations (Dyer *et al.*, 2012). MO1 and MO2 refer to the two clades within the *A.monanthes* complex identified by the phylogenetic analysis of Dyer *et al.* (2012).

Species	Voucher	Spore Length (μm)	2C-value (pg)	CV%	Reproductive mode
A.fibrillosum *	RD10b	47.90 ± 8.14	37.78 ± 0.18	6.95	Sexual
A.formosum	RD28	27.85 ± 1.26	13.46 ± 0.03	3.77	Sexual
A.formosum	RD33	32.20 ± 3.80	13.19 ± 0.03	2.73	Sexual
A.formosum †	RD157 (IJ2436)	34.65 ± 3.37	13.93 ± 0.23	3.15	Sexual
A.formosum †	RD158 (ES1398)	33.56 ± 3.78	13.87 ± 0.11	2.24	Sexual
A.hallbergii	RD23	48.69 ± 5.18	26.05 ± 0.06	3.72	Apomictic
*A.*aff.*hallbergii*	RD90	43.32 ± 3.1	26.17 ± 0.12	3.47	Apomictic
A.hallbergii	RD93 (RD112)	47.63 ± 4.81	26.23 ± 0.19	3.40	Apomictic
A.hallbergii	RD111	41.33 ± 3.91	26.00 ± 0.06	3.24	Apomictic
*A.*aff.*heterochroum*	RD9a	38.62 ± 3.35	18.67 ± 0.08	3.11	Apomictic
*A.*aff.*heterochroum*	RD75	37.43 ± 3.19	14.38 ± 0.05	2.39	Apomictic
A.monanthes (MO1) I	RD70	39.03 ± 3.35	30.72 ± 0.78	3.94	Apomictic
A.monanthes (MO1) I	RD101b	39.44 ± 2.96	29.68 ± 0.12	4.19	Apomictic
A.monanthes (MO1) I	RD104	41.85 ± 3.73	30.11 ± 0.32	4.15	Apomictic
A.monanthes (MO1) II	RD80	43.15 ± 4.53	28.03 ± 0.06	2.75	Apomictic
A.monanthes (MO1) II	RD94	45.79 ± 3.31	27.96 ± 0.19	3.36	Apomictic
A.monanthes (MO1) III	RD1a	48.54 ± 5.94	26.54 ± 0.16	4.05	Apomictic
A.monanthes (MO1) III	RD17	40.31 ± 3.34	26.84 ± 0.52	4.35	Apomictic
A.monanthes (MO1) III	RD20	45.53 ± 3.38	26.45 ± 0.39	3.77	Apomictic
A.monanthes (MO1) III	RD73	38.09 ± 2.42	26.91 ± 0.14	4.08	Apomictic
A.monanthes (MO1) III	RD76	40.78 ± 5.07	27.21 ± 0.13	3.82	Apomictic
A.monanthes (MO1) III	RD89	45.30 ± 3.24	26.82 ± 0.02	3.14	Apomictic
A.monanthes (MO1) III	RD103	46.39 ± 3.54	26.90 ± 0.14	3.64	Apomictic
A.monanthes (MO1) III	RD110	44.54 ± 2.85	26.62 ± 0.16	4.04	Apomictic
A.monanthes (MO1) III	RD132	43.97 ± 4.27	27.41 ± 0.26	4.03	Apomictic
A.monanthes (MO2) I	RD53 (RD45)	47.76 ± 4.27	27.40 ± 0.09	3.53	Apomictic
A.monanthes (MO2) I	RD99	48.54 ± 5.88	26.09 ± 0.24	5.29	Apomictic
A.monanthes (MO2) I	RD125	42.80 ± 4.36	27.43 ± 0.18	4.39	Apomictic
A.monanthes (MO2) I	RD135	38.94 ± 3.69	27.32 ± 0.06	3.92	Apomictic
A.monanthes (MO2) II	RD96	42.11 ± 4.82	18.58 ± 0.09	3.00	Apomictic
A.polyphyllum *	RD98 (RD95)	35.42 ± 3.58	29.95 ± 0.10	4.02	Sexual
A.resiliens	RD128	45.07 ± 2.96	13.90 ± 0.07	2.75	Apomictic
A.resiliens	RD63	42.39 ± 2.93	13.70 ± 0.12	2.80	Apomictic
A.resiliens	RD107	43.45 ± 4.35	14.50 ± 0.04	3.07	Apomictic

A.resiliens	RD127 (RD64)	42.26 ± 4.59	13.87 ± 0.07	2.85	Apomictic
A.soleirolioides *	RD82 (RD71)	39.37 ± 2.89	50.29 ± 0.16	4.03	Sexual
Spec.nov.1 †	RD162 (JM1339)	30.87 ± 2.80	17.67 ± 0.19	4.26	Sexual
Spec.nov.2 †	RD163 (SK10151)	29.71 ± 2.63	22.20 ± 0.28	3.54	Sexual

* Data for these species (which belong to the *A castaneum* clade) should only be considered as very approximate values, as they were estimated from 2 year old silica dried material.

† Data for these species were estimated from 6 month old silica dried material.

4.3.2 Flow cytometry: genome size and DNA ploidy

The nuclear DNA content of 38 specimens was measured following the one-step procedure described by Dolezel *et al.* (2007). Individual sporophytes were prepared as follows: several pinnae (after removing the rachis) were co-chopped using new razor blades, together with the appropriate calibration standard (*Pisum sativum* 'Ctirad', 2C=9.09 pg) (Doležel *et al.*, 1998), in a Petri dish containing 2mL of 'General purpose buffer' (GPB) (Loureiro *et al*., 2007) supplemented with of 3% PVP-40 . The suspension of nuclei was then filtered through a 30 µm nylon mesh, stained with100 µl of propidium iodide (Sigma; 1 $mg \cdot mL^{-1}$), and treated with 34 µl of 3 $mg \cdot mL^{-1}$ ribonuclease A (RNase A; Sigma). Samples were kept on ice for 30 min and 5,000 particles recorded using a Partec Cyflow SL3 flow cytometer (Partec GmbH) fitted with a 100 mW green solid state laser (532 nm, Cobolt Samba). Flow histograms were analysed with the FlowMax software (v. 2.4, Partec GmbH). Three sporophytes were measured separately for each specimen, and three replicates of each were processed. Measurements obtained from fresh and silica dried materials of the same specimens were compared to determine the extent to which the preservation method influenced the relative fluorescence (i.e. nuclear DNA content) estimate.

We compared 1C*x*-values between different specimens of the same species (with karyologically determined ploidy levels) to check for cryptic ploidy levels. In order to infer DNA ploidy levels (i.e. ploidy levels inferred only from DNA amount cf. Suda *et al.*, 2006) for the species without chromosome counts, we compared their holoploid genome size (the DNA content of the whole chromosome compliment, with chromosome number n, see Greilhuber *et al*., 2005) and mean spore length (see section below), with those of taxa within the same clades whose ploidy level had been karyologically determined.

4.3.3 Spore measurements

To analyse the relationship between spore size and genome size we combined the spore size data from Dyer *et al*. (2012), with additional spore measurements made for the remaining specimens sampled in this study. Spores from individual specimens were mounted onto slides using glycerine jelly. Each spore length was measured using AxioVision on a calibrated light-microscope (v4.8.2, Zeiss). An average of 25 spores were measured per specimen, and a mean spore length was calculated (Table 4.1). Special care was taken to identify putative abortive spores that were then excluded from the analyses. Individual box plots were compiled to show spore size variation within each specimen, as well as the interquartile range and the median.

4.3.4 The relationship between DNA amount and spore length

We investigated the relationship between DNA amount and spore length by comparing the results obtained from analysing the raw data with those obtained using phylogenetic independent contrasts (PIC), which takes phylogenetic relationships into account. Different DNA amount values were used for specimens based on their mode of reproduction: apomictic ferns produce unreduced spores, and so 2C-values were used for analysis; sexually reproducing ferns produce reduced spores, and hence 1C-values were used for analysis. The raw data were not normally distributed; therefore, in order to linearize the data for PIC analysis (Quader *et al.*, 2004), the mean measurements for DNA amount were log transformed.

4.3.5 Regression analysis of raw data

We used a linear model (LM) regression analysis to test for the correlation between traits in all sampled specimens. We then fitted a line of best fit using a standardised major axis (SMA) to obtain a slope estimate and r^2 value (Beaulieu *et al*., 2008; Connolly *et al*., 2008). The SMA reduces the residuals in both the dependent and independent variables (rather than just the dependent variable, as in the LM model), and is therefore useful here as it is unknown which variable is important. An SMA was fitted using the (S)MATR package in R (Falster, Warton, and Wright, 2006; Warton *et al*., 2011).

4.3.6 Regression analysis incorporating phylogenetic data

To incorporate phylogenetic information into the regression analysis using PIC, we first reconstructed a phylogenetic tree of the sampled taxa. Bayesian inference (BY) was performed on a combined matrix of three plastid regions for the species listed in Table 4.1 (see Dyer *et al.*, 2012, for voucher and accession numbers), using substitution models determined in jModeltest according to BIC criterion (Posada, 2008). Sequence data were incomplete for some of the taxa sampled in this study (i.e. not all three plastid regions were present). On these occasions, sequence data from very closely related taxa (based on analysis of individual plastid regions) were used as substitutes in phylogenetic reconstruction (see Table 4.1). Analysis was carried out in MrBayes 3.1 (Huelsenbeck & Ronquist, 2001; Ronquist & Huelsenbeck, 2003), with Markov Chain Monte Carlo (MCMC) run for 5 million generations and sampled every 500 generations to approximate the posterior probabilities of trees. Two analyses were run simultaneously, and a conservative burn-in phase of 25% was implemented to disregard trees prior to convergence on the maximum likelihood. Remaining trees were then compiled to give 7,500 trees for each run, from which a 50% majority rule consensus was calculated.

In order to determine whether PIC analysis was appropriate, we tested for 'phylogenetic signal' (= κ value), i.e., trait similarity among closely related species (Blomberg *et al.*, 2003). We used the 'Analysis of Traits' model in Phylocom (Webb *et al.*, 2008), using the 'Picante package' in R (Kembel *et al.*, 2010), to asses phylogenetic signal for a series of different branch length transformations. Significant phylogenetic signal was shown for all branch length transformation (Table 4.2), supporting phylogenetic regression by the PIC method (Felsenstein, 1985b; Garland *et al.*, 1992).

PICs were calculated using the PDAP: PDTREE module in Mesquite v.2.75 (Midford *et al.*, 2005; Maddison & Maddison, 2011). This method uses branch lengths to standardise contrasts between closely related taxa and is able to deal with the soft polytomies present in our phylogeny (Garland and Díaz-Uriarte 1999). We had several zero-length terminal branches, so it was necessary to transform branch lengths in Mesquite, in order to generate the PICs. To test whether branch lengths had adequately standardised the contrasts, we performed regression analysis on the PICs of both characters against their standard deviation.

Logarithmic, Pagel (1992) and Nee (Read & Nee, 1995) transformation of branch lengths resulted in an insignificant relationship for spore length, but was significant for DNA content (see Table 4.2) indicating that the contrasts had not been significantly standardised. However, the branch transformation methods of Grafen (Grafen, 1989), showed no significant relationship between contrasts and their standard deviations for both characters (DNA content, p=0.289; Spore length, p=0.090) (see Table 4.2), indicating the contrasts had been adequately standardised by branch lengths. The contrasts were then standardised by dividing them by their respective standard deviations. The sign of the DNA amount contrasts were made positive, and the spore length contrasts were compared in the same direction across the node (Garland *et al.*, 1992). Regression analysis of standardised contrasts (forced through the origin) was performed to test for the correlated evolution of traits in R (Garland *et al.*, 1992; Midford *et al.*, 2005). The slope estimate and r^2 value was obtained using SMA analysis in R (as above), and forced through the origin.

Table 4.2. Phylogenetically independent contrasts (PICs) analysis of the relationship between genome size and spore length. DNA amount values were log transformed prior to analysis. GS=genome size, and SL=spore length. 1C or 2C DNA values were used depending on the reproductive mode: 2C-values are used for apomictic taxa, and 1C-values are used for sexual taxa. Results are given for four branch length transformation methods, as discussed in the Materials and Methods. Significant P values are given in bold.

Branch Transformation method	Phylogenetic signal (κ)				PIC standardisation			
	GS		SL		GS		SL	
	κ	*P*	κ	*P*	r^2	*P*	r^2	*P*
Log	2.500	**0.001**	0.773	**0.001**	0.314	**0.024**	0.207	0.076
Pagel	2.814	**0.001**	0.800	**0.001**	0.196	**0.008**	0.021	0.408
Nee	2.317	**0.001**	0.988	**0.001**	0.176	**0.014**	0.019	0.434
Grafen	1.131	**0.001**	0.273	**0.003**	0.035	0.289	0.080	0.090

4.4 Results

4.4.1 Shifts in genome size associated with the preservation of material

Since fresh material was not available for all the specimens studied, the impact of silica drying on the relative fluorescence of nuclei was investigated. Genome size estimates were very similar between fresh leaf material and material that had been stored in silica for 6 months. This was shown for *A.formosum* where genome size estimates for RD28 and RD33 (2C=13.46pg and 13.19pg respectively) were very similar to those obtained from the 6 month old silica dried samples of *A.formosum* RD157 and RD158 (2C=13.93pg and 13.87pg respectively) (Table 4.3). We therefore inferred no meaningful shift in the genome size measurements for specimens stored in silica for six months and thus genome size estimates obtained from four 6 month old silica samples (*A.formosum*, RD157 and RD158; spec.nov.1, RD162; and spec.nov.2, RD163) were used in all analyses.

In contrast, samples processed using 2 year old silica material showed that 2C-values had an average increase of 18.6% (ranging from 7.83–30.09%), when compared to fresh material (Table 4.3). Indeed, the quality of measurements in 2 year old silica samples was also shown to decrease, when compared to fresh samples and samples 6 month in age. That is, mean CV% (the mean coefficient of variation of the 2C DNA peak for each specimen) of the 2C peaks in the flow histograms increased markedly for samples preserved in silica material for 2 years (fresh samples=3.37; silica samples 6 month old=3.29; Silica samples 2ya=5.65), although similarities between fresh material and silica material (6 months old) are based on comparison of different specimens. Data from 2 year old material were therefore excluded from further analysis. However, we decided to keep data for three species belonging to the *A.castaneum* clade (*A.fibrillosum*, RD10b; *A.soleirolioides*, RD82; and *A.polyphyllum* RD98), for which no fresh material was available (see Table 4.1 and Fig. 4.1) to give an indication of their approximate genome sizes in this clade. These data were not however used in further analysis.

Table 4.3. Observed shifts in 2C DNA content shown in response to drying and storage of leaf material in silica. CV% indicates the coefficient of variation of the 2C DNA peak in the flow histogram. Percentage increase indicates the percentage difference between fresh 2C DNA content and silica-dried 2C DNA content.

		Fresh material		Silica dried material			
Species	Voucher	2C-value (pg)	CV%	2C-value (pg)	CV%	Silica age	Percentage increase (%)
A.formosum	RD28	13.46 ± 0.03	3.77	17.23 ± 0.12	3.41	2 years	21.88
A.formosum	RD33	13.19 ± 0.03	2.73	18.87 ± 0.19	6.74	2 years	30.09
A.monanthes	RD70	30.72 ± 0.78	3.94	33.33 ± 0.10	5.98	2 years	7.83
A.monanthes	RD94	27.96 ± 0.19	3.36	33.44 ± 0.14	6.75	2 years	16.4
A.resiliens	RD107	14.50 ± 0.04	3.07	17.43 ± 0.17	5.39	2 years	16.81
A.formosum	RD157	(13.19-13.46)*	-	13.93 ± 0.23	3.15	6 months	(0.06-0.10)
A.formosum	RD158	(13.19-13.46)*	-	13.87 ± 0.11	2.24	6 months	(0.06-0.09)
Spec.nov.1	RD162	-	-	17.67 ± 0.19	4.26	6 months	-
Spec.nov.2	RD163	-	-	22.20 ± 0.28	3.54	6 months	-

* Range of 2C-values obtained from the analysis of fresh leaf material of the same species but different accessions.

4.4.2 Variation in genome size and spore size

Within the *A.formosum* and *A.resiliens* clades, the ranges of 2C-values were similar (13.19-13.93 pg and 13.70-14.50pg respectively), but the ranges of mean spore lengths were different (27.85-34.56µm and 42.26-45.07µm respectively) (Fig. 4.1). All accessions of *A.resiliens* formed a well supported monophyletic lineage (clade A, Fig. 4.1), with accessions of *A.*aff.*heterochroum* occupying a sister position (clade B, Fig. 4.1). Of the two specimens investigated of *A.*aff.*heterochroum*, one (RD75, 2C=14.38pg) had a similar 2C DNA content to *A.resiliens* (mean 2C of four individuals=13.99pg), while the other was distinctly higher (RD9a, 2C=18.67pg). In contrast to this genome size variability, both specimens showed very similar spore lengths (37.43-38.62µm), which were smaller compared with the mean value for the *A.resiliens* specimens analysed (43.29µm).

Within the *A.monanthes* clade, the smallest genome size was found in the diploid spec.nov.1, which has been shown to be sister to the rest of the clade (Fig. 4.1). Diploid sexual, spec.nov.2 showed a distinctly larger genome size (22.20pg). The specimens of *A.hallbergii* and *A.*aff.*hallbergii*, which form a sister clade to the main clades of *A.monanthes* (MO1 and MO2), showed very little variation in nuclear DNA contents (2C=26.00-26.23pg), but a relatively large variation in spore length (41.33-48.69µm). Within the *A.monanthes* MO1

lineage, three sub-clades with similar, but distinct 2C value ranges could be identified: MO1 (I), 29.68-30.72pg; MO1 (II), 27.96-28.03pg; and MO1 (III), 26.45-27.41pg. Spore size across these three sub-clades varied from 38.09µm to 48.54µm. The nuclear DNA content of individuals within the *A.monanthes* (MO2) clade was found to be similar (2C=26.09-27.43pg), with the exception of a single specimen (RD96, designated MO2 II), which had a significantly smaller genome size (2C=18.58pg) (Fig. 4.1 and Table 4.1). Spore size varied from 38.94-48.54µm, and the value for specimen RD96 also fell within this range (42.11µm).

Asplenium fibrillosum, A.soleirolioides, and *A.polyphyllum,* which together comprise the *A.castaneum* clade, were observed to have the highest 2C values in the complex (37.78pg for *A.fibrillosum,* 29.95pg for *A.polyphyllum,* and 50.29pg for *A.soleirolioides*) (Table 4.1 and Fig. 4.1), but since these estimates were made from material that had been stored on silica for 2 years their reliability is questioned (as noted above). Interestingly, the mean spore length of the *A.fibrillosum* specimen was also very large (47.90µm), although those for *A.soleirolioides* and *A.polyphyllum* were distinctly smaller (39.37µm and 35.42µm).

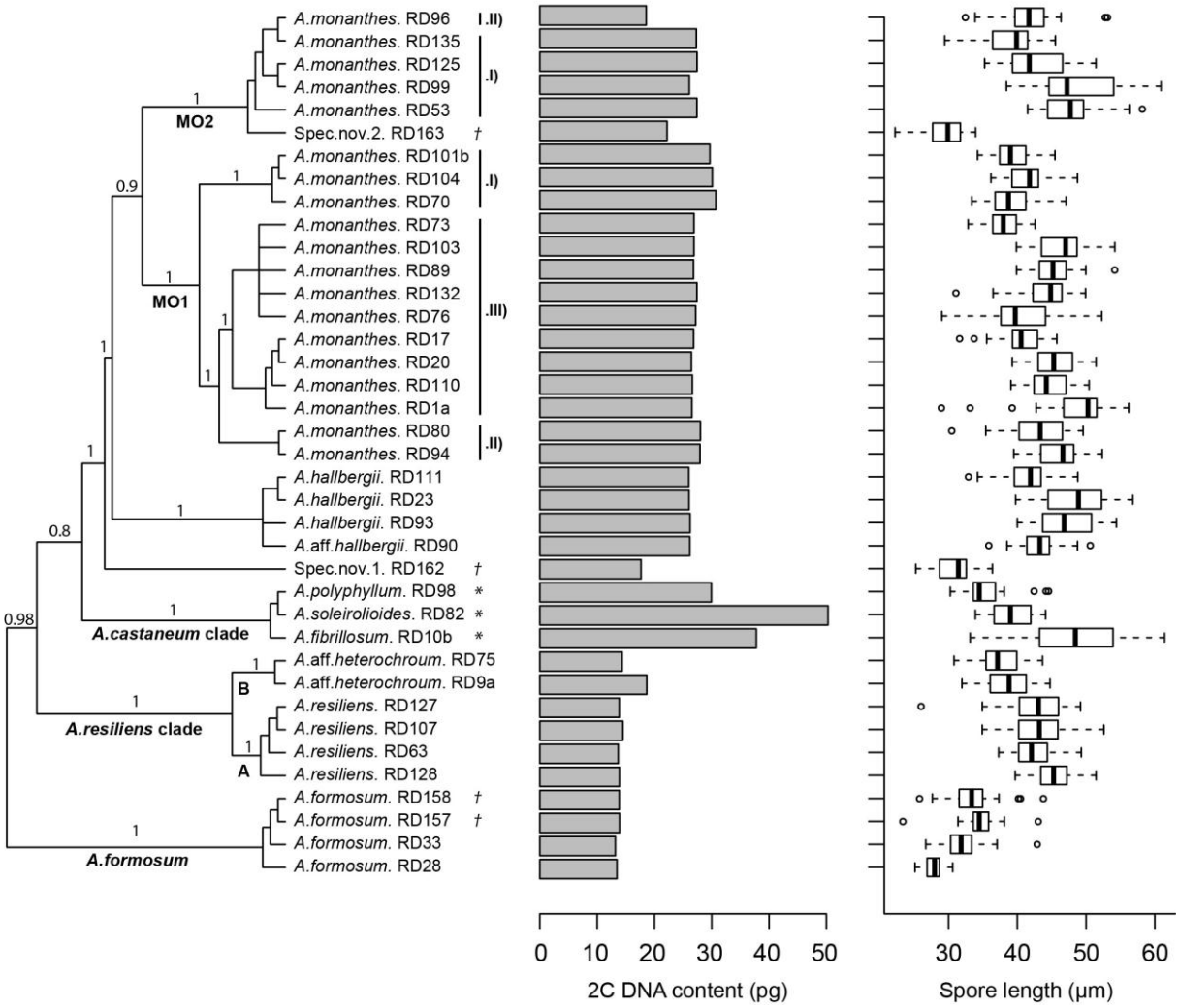

Figure 4.1. Phylogenetic framework (based on BY analysis) of the plastid genome, as presented in Dyer *et al*. (2012), of the *Asplenium monanthes* complex and related lineages, together with nuclear DNA content and spore length for each specimen analysed. Tree is rooted according to (Dyer *et al.*, 2012). Posterior branch support (≥0.8) is shown. 2C DNA content for each specimen is represented by a bar chart, whilst spore length data are shown as box plots. Each boxplot represents the variation of measurements of spores within each specimen, the thick horizontal line is the median, the box indicates the variation observed between the 25th and 75th percentiles, the whiskers show the variation range, and small circles identify extreme outliers. MO1 and MO2 indicate the two distinct *A.monanthes* clades and these are further divided into sub-clades I and II, and also III in the case of MO1 only. Asterisks (*) indicate samples for which 2C DNA content should be considered as approximate, as measurements were made from silica material (2 years old). *† symbols* indicate samples for which 2C DNA content measurements were made from silica material (6 months old).

4.4.3 Correlation between DNA amount and spore size

Regression analysis of the raw data showed a positive correlation ($p=4.57x10^{-6}$, $r^2=0.542$, slope=10.986, 95% CI's=8.665-13.929) between DNA amount and spore length (Fig. 4.2A). However, phylogenetically independent contrasts analysis indicated no significant relationship between contrasts (Grafen branch transformation, p=0.101) (Fig. 4.2B and Table 4.2). This indicated that divergences in DNA amount are not associated with divergences in spore length, and therefore there is no correlated evolution between DNA amount and spore length.

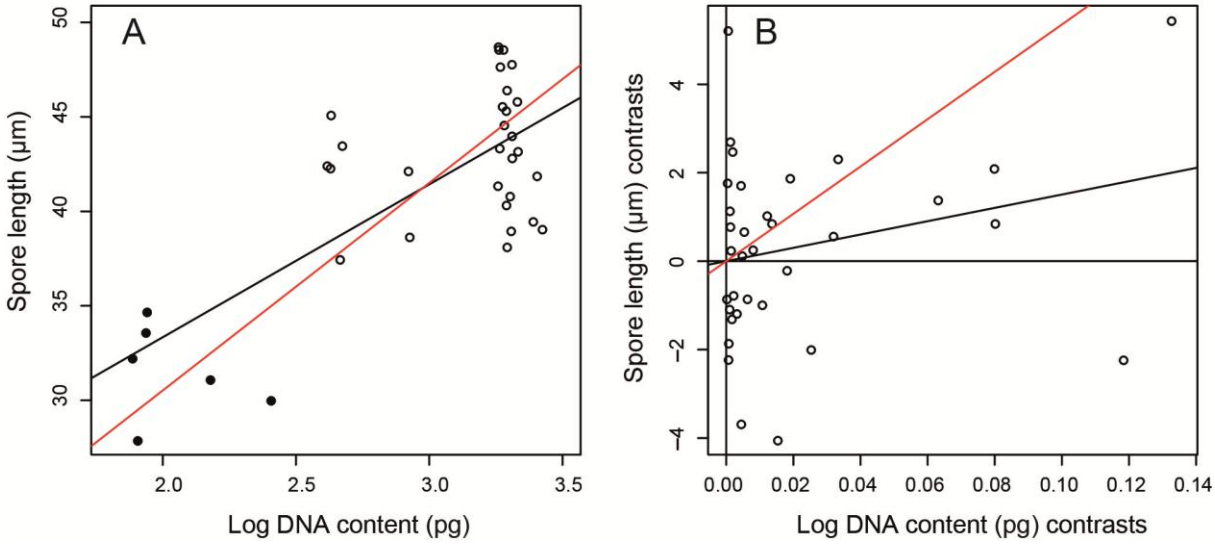

Figure 4.2. Regression analyses of 38 specimens showing the positive relationship between DNA amount and spore length for both (A) the raw data ($p=4.57x10^{-6}$, $r^2=0.542$, slope=10.986, 95% CI's=8.665-13.929), and (B) data from the phylogenetically independent contrasts analysis (Branch transformation of Grafen; SMA, p=0.101) (see Table 4.2). DNA amount values were logged prior to analysis, and the values used for DNA amount were based on reproductive mode: i.e. 2C-values were used for apomictic taxa, and 1C-values were used for sexually reproducing taxa. Lines of best fit are indicated using LM (black line) and SMA (red line) models, and in B only, the SMA is forced through the origin. In plot A, open circles represent apomictic taxa, and filled black circles represent sexually reproducing taxa.

4.4.4 Genome size and ploidy level

Monoploid genome size (1C*x*-values) and ploidy levels were not inferred for *A.fibrillosum*, *A.soleirolioides* and *A.polyphyllum*, due to the shifts observed in the 2C DNA contents of these species, as a consequence of their storage for 2 years in silica (see above). Ploidy levels and 1C*x*-values were inferred for all other subclades analysed (Table 4.4 and Fig. 4.3).

Within the *A.resiliens* clade, different ploidy levels were inferred for the two *A*.aff.*heterochroum* specimens. One specimen of *A*.aff.*heterochroum* (RD75; 2C=14.38pg) had a similar 2C-value to *A.resiliens* (mean 2C=13.99pg), a species reported to be triploid, suggesting that RD75 could also be a triploid. In contrast, the other *A*.aff.*heterochroum* specimen analysed (RD9a), had a significantly higher 2C-value of 18.67pg), and this was therefore considered to be tetraploid.

The suggestion that most *A.monanthes* specimens are triploid is based on the observation that, with the exception of one report of a tetraploid count, all counts for this species have been n=2n=3*x*=108. Under this assumption, the mean 1C*x*-values for MO1 sub-clades I, II and III are 10.06pg, 9.33g, and 8.95pg, respectively (Table 4.4). A triploid level is also assumed for MO2 (I), based on the 2C-values, resulting in a mean1C*x*-value of 9.02pg. The *A.monanthes* MO2 (II) sub-clade, which comprised a single specimen (RD96), had a significantly lower 2C-value of 18.58pg, and we infer that this specimen is likely to be a diploid cytotype. This would result in a 1C*x* value of 9.29pg, which is in broad agreement with the monoploid genome sizes calculated for the remaining *A.monanthes* sub-clades (Table 4.4). Nevertheless, it is noted that the mean spore size of RD96 (42.11μm) conflicts with this finding. In *A.hallbergii*, the similarity of its mean 2C-value (26.11pg) and mean spore size (45.24μm) to that of the triploid *A.monanthes* lineages (MO1 and MO2.I) suggests this species is also a triploid. As for the two new species, spec.nov.1 and spec.nov.2, they differ in 2C-values (17.67pg and 22.20pg respectively) but have similarly small spore sizes. They are currently inferred to be diploid although further data are needed to confirm or refute this.

Overall, the results show that monoploid genome size varies 2.4-fold (4.66-11.10pg), with little variation in 1C*x*-values within clades, but considerable variation between some of them (Table 4.4 and Fig. 4.3). For example, compared with the small 1C*x*-values in the *A.resiliens* clade (4.66-4.79pg), the mean 1C*x*-value for diploid *A.formosum* (6.81pg) was markedly higher. A larger monoploid genome size was also noted in the between the *A.monanthes* clade compared with the *A.resiliens* clade. Indeed, the largest monoploid genome sizes were encountered within the *A.monanthes* clade (8.70-11.10pg), with spec.nov.2 having the highest 1Cx-value (11.10 pg) of all, which is more than double the mean monoploid genome size of the *A.resiliens* clade.

Table 4.4. A summary of the genome size and spore size data obtained for specimens belonging to the *Asplenium monanthes* clade and related lineages. Mean 2C DNA content (pg) and mean spore length (μm) were only calculated for sub-clades distinguished by low genome size variation (Fig. 4.1). This resulted in separate inferences of genome size and ploidy for the two *A.*aff.*heterochroum* specimens (RD75 and RD9a), and *A.monanthes* subclades: MO1 (I); MO1 (II); MO1 (III); MO2 (I), and MO2 (II) (Fig. 4.1). Published chromosome counts (*A.formosum*, 2n=2*x*=72; *A.monanthes*, n=2n=3*x*=108; *A.resiliens*, n=2n=3*x*=108) were used to estimate ploidy and hence calculate monoploid genome size (i.e. 2C-value divided by ploidy level). For lineages with unknown ploidy levels, monoploid genome size and ploidy level were estimated according related species. Estimates of ploidy underlined in bold are based on the spore number and spore measurements (Dyer *et al.*, 2012).

Species	Mean 2C-value (pg)	Mean CV%	Inferred Ploidy (x)	Holoploid 1C-value (pg)	1C-value SE	Monoploid 1Cx-value (pg)	1Cx-value SE	Mean spore length
A.formosum	13.61 ± 0.10	2.97	2	6.81	0.09	6.81	0.09	32.07
***A.resiliens* clade**								
A resiliens	13.99 ± 0.08	2.87	3	7.00	0.09	4.66	0.06	43.29
*A.*aff.*heterochroum* RD9a	18.67 ± 0.08	3.11	4	9.34	-	4.67	-	38.62
*A.*aff.*heterochroum* RD75	14.38 ± 0.05	2.39	3	7.19	-	4.79	-	37.43
***A.monanthes* clade**								
A.hallbergii	26.11 ± 0.11	3.46	3	13.06	0.03	8.70	0.02	45.24
MO1 I	30.17 ± 0.41	4.09	3	15.09	0.15	10.06	0.10	40.11
MO1 II	28.00 ± 0.13	3.06	3	14.00	0.02	9.33	0.01	44.47
MO1 III	26.86 ± 0.21	3.88	3	13.43	0.05	8.95	0.03	43.72
MO2 I	27.06 ± 0.14	4.28	3	13.53	0.16	9.02	0.11	44.51
MO2 II	18.58 ± 0.09	3.00	2	9.29	-	9.29	-	42.11
Spec.nov.1	17.67 ± 0.19	4.26	**2**	8.84	-	8.84	-	30.87
Spec.nov.2	22.20 ± 0.28	3.54	**2**	11.10	-	11.10	-	29.71

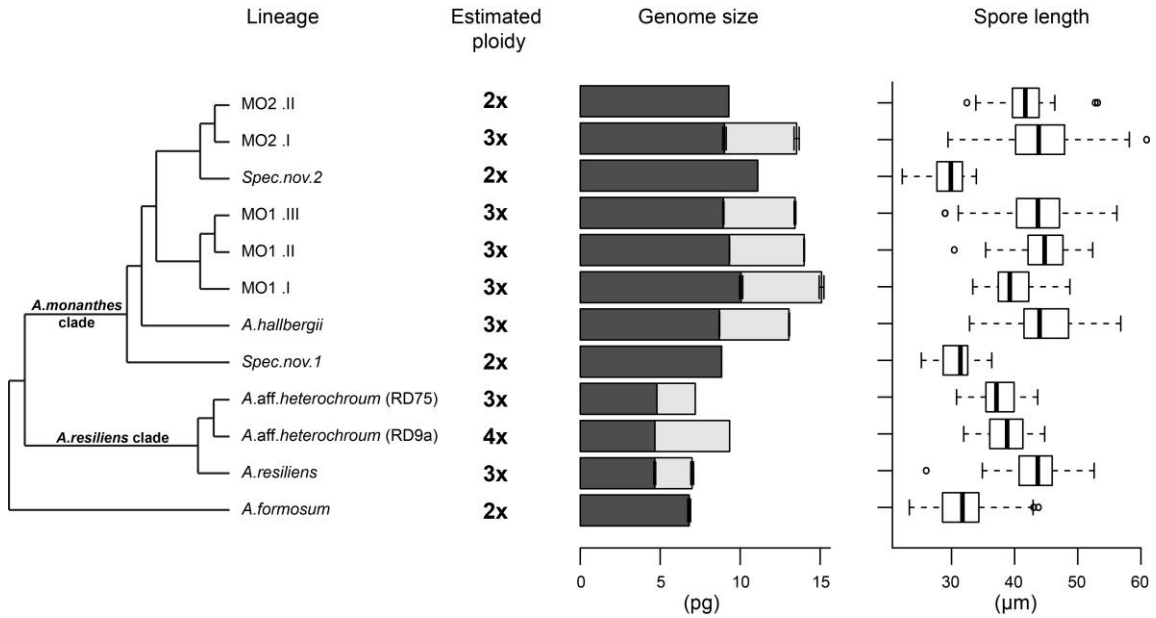

Figure 4.3. A summarized phylogenetic tree of the *Asplenium monanthes* complex and related lineages (as presented in Dyer *et al.*, 2012) together with the inferred ploidy levels (based on published chromosome data), mean holoploid genome size (1C-value; entire bar black and grey), and inferred monoploid genome size (1C*x*-value; black bars) and the mean spore length (µm) of each operational unit. Posterior branch support >0.8 is shown. Tree is rooted according to Dyer *et al.* (2012). For diploids only black bars are present as the 1C-value is equal to the 1C*x*-value. Standard error bars are included for 1C-value and 1C*x*-value means, except for lineages represented by one specimen only. Details of the box plots for spore size are given in the legend to Figure 4.1.

4.5 Discussion

4.5.1 Considerations for the use of silica dried material for genome size estimation

Recently, the question as to whether it is possible to use silica preserved material to measure genome size in absolute units has become the focus of intense debate (Cires *et al.*, 2009; Bainard *et al.*, 2011b; Sánchez-Jiménez *et al.*, 2012). In order to avoid ambiguous interpretations, some authors only advocate the use of fresh material to estimate genome size (Doležel *et al.*, 2007), and restrict the use of silica-dried material to estimating DNA ploidy levels (e.g. Suda *et al.*, 2006). However, studies claiming for slightly more relaxed operational standards have recently appeared (Bainard *et al.*, 2011a,b). These approaches would help overcome some of the constraints imposed by the need for fresh material,

especially when the quality of measurements is not compromised (i.e. <10% of variation between fresh and silica-dried tissues).

In the current analysis some of the accessions were only available as silica dried material (either 6 months or 2 years old), so the reliability of the genome size estimates obtained from such material was investigated. We were able to compare both fresh and 2-years old silica-dried tissues belonging to the same accession, for three separate species (Table 4.3). We found a significant increase in fluorescence intensity in all silica-dried samples relative to the fresh material, which resulted in genome size estimates up to c. 30% larger (Table 4.3). In addition, as previously reported, %CVs were also seen to increase, and in most cases these exceeded acceptable values (i.e. >5%). We therefore conclude that for *Asplenium*, the use of 2 year old silica dried material is unsuitable for obtaining accurate genome size estimations.

In contrast, samples of *A.formosum* stored for 6 months in silica gave similar results to those obtained from fresh material (although the analyses were conducted on different accessions, Table 4.3). In addition, there was no evidence of any reduction in the quality of the flow histogram with the CVs for both fresh and silica samples being similar. Nevertheless, while these results suggest that the short term storage of *Asplenium* samples in silica is suitable for genome size estimations, the extent to which these findings can be extrapolated to other plant genera, including other ferns remains unknown.

4.5.2 Relationship between DNA amount and spore size

Numerous studies in angiosperms have shown a positive correlation between genome size and a number of morphological traits, including seed mass, cell size and stomatal density (e.g. Beaulieu *et al.*, 2007, 2008; Knight & Beaulieu, 2008; Hodgson *et al.*, 2010). Beyond the angiosperms, such studies are relatively rare (e.g. Bures *et al.*, 2003; Ekrt *et al.*, 2009), and while spore size is often used as a proxy for inferring ploidy level (e.g. Moran, 1982; Barrington *et al.*, 1986; Beck *et al.*, 2010), there have been no empirical studies to date that test these inferences using genome size. In this study we investigated the relationship between genome size and spore size to determine the extent to which such an assumption is valid.

We found a significant and positive correlation between nuclear DNA amount and spore length using the raw data. However, when evolutionary relationships were considered, using phylogenetically independent contrasts (PICs), no significant correlation was found. The

discrepancy between analyses highlights the importance of using PICs to determine the evolutionary association between traits (Garland *et al.*, 1992).

The insignificant relationship observed between DNA amount and spore size calls into question the use of spore size for inferences of ploidy level within homosporous ferns. Previous authors have pointed out that this inference should be restricted to very close relatives, and the distinction between diploids and their autoploid offspring (Moran, 1982; Barrington *et al.*, 1986). Our findings are consistent with these suggestions. In addition, our study sample is mainly comprised of apomictic accessions, and due to a low sample number of sexually reproducing species we are unable to test for the effect of reproductive mode on the relationship between traits.

Considerable variation was found in spore length, both within and between specimens of the apomictic lineages. In part this variation may be a consequence of the non-globulose shape of the monolete spores found in this complex, making precise measurements difficult. However, the variation may also be due to the variable nature of Döpp Manton sporogenesis in triploid apomicts of homosporous ferns (Döpp, 1932; Manton, 1950). The variation in spore size within and between these taxa is reflected by the inability to determine ploidy level, beyond the difference between diploid and polyploids, from spore size measurements in this complex (Dyer *et al.*, 2012).

Overall, our findings challenge the utility of spore size for inferences of ploidy level within ferns. Nevertheless, further investigations are needed to test our findings for spore size in a greater number of lineages, and also determine the effect, if any, of reproductive mode on the relationship between DNA amount and spore size.

4.5.3 Genome size and chromosome size evolution in the Asplenium monanthes complex

The high chromosome numbers, and conserved chromosome size reported for homosporous ferns has contributed to the hypothesis that the evolution of fern genomes is less dynamic than the evolution of angiosperm genomes (Nakazato *et al.*, 2008; Barker & Wolf, 2010; Leitch & Leitch, 2013). The inferred constancy of chromosome size is based on physical measurements (Wagner & Wagner, 1980), the low number of reported retrotransposons (Brandes *et al.*, 1997), and the correlation between chromosome size and genome size (Nakazato *et al.*, 2008).

Bainard *et al*. (2011a) showed that although there is a significant relationship between chromosome number and holoploid genome size, there is no correlation between chromosome number and the monoploid genome size in monilophytes. The authors suggested that these relationships show that genome size expansion is mainly driven by polyploidy, and that stepwise increases observed in 1C*x*-values across monilophytes might be indicative of paleopolyploidy.

In this study, some of the 1C-value variation within clades clearly arises from polyploidisation, with ploidy levels ranging from 2*x* to 4*x* (Table 4.4), as inferred by comparing the genome size data with previously published chromosome counts for the species studied, when available. Given the comprehensive variety (quantity and geographic spread) of available karyological data we consider our inferences (by means of the DNA content) legitimate, and illustrative of the ploidy levels within the group. However, variation is also observed in the 1C*x*-values, indicating chromosome size variation between clades, which could have arisen either through increases or decreases in genome size (Fig. 4.3). Nevertheless, the 1C*x*-values of specimens within the *A.resiliens* clade (1Cx= 4.66-4.79pg) are similar to those reported for *A.trichomanes* ssp *quadrivalens* (1C*x*=4.53pg; a species within the closely related *A.trichomanes* complex and other *Asplenium* species (Bennett & Leitch, 2010; Bainard *et al.*, 2011a) which suggests that, *A.formosum* and species within the *A.monanthes* clade may have undergone an expansion in monoploid genome size.

Indeed, this finding of variation in 1C*x*-values, independent of ploidy, between closely related species suggests that monoploid genome size variation does occur within these homosporous ferns and provides further evidence that chromosome size may not be as conserved as widely reported (e.g. Nakazato *et al.*, 2008). Such variation could arise via retrotransposon-driven changes in genome and hence chromosome size, as suggested for *Equisetum* and *Pstilotum* (Manton, 1950; Brownsey & Lovis, 1987; Guillon, 2007; Leitch & Leitch, 2013). Retrotransposon proliferation and elimination is linked with genomic and environmental factors such as effective population size, environmental stress, hybridisation and polyploidy (Kalendar *et al.*, 2000; Leitch & Bennett, 2004; Grandbastien *et al.*, 2005; Lockton *et al.*, 2008; Grover & Wendel, 2010; Petit *et al.*, 2010). Given that the apomictic *A.monanthes* clade and related lineages show strong patterns of reticulate evolution, it is possible that these

processes may be acting as triggers for retrotransposon activity leading to the range of 1Cx-values observed. Indeed, given the extent of hybridization and reticulate evolution reported in homosporous ferns in general (Lovis, 1977), it seems likely that retrotransposon driven changes in genome size is probably more widespread across ferns but has been largely overlooked due to the low level of sampling.

The use of genome size data as a taxonomic tool has been documented in angiosperms (e.g. Bures *et al.*, 2003; Ekrt *et al.*, 2010), and here it proved useful in determining the presence of putative cryptic species (*A*.aff.*heterochroum*, and MO2,II) and, as mentioned above, in inferring ploidy-level for taxa without chromosome numbers available. Even so, ploidy inferences must be done cautiously when comparing a range of species, as even closely related taxa with different ploidy levels can display similar genome sizes leading to incorrect ploidy determinations (Suda *et al.*, 2006). Indeed, *A.formosum* and apomict *A.resiliens* clearly illustrated this situation as both taxa have very similar 2C-values (mean 2C=13.61pg and 13.99pg respectively) (Figures 4.1 and 4.3). Without additional information it might be tempting to assume they had the same ploidy level. Yet, complementary information from published chromosome counts strongly supported the presence of different ploidy levels, with *A.formosum* being a sexual diploid and *A.resiliens* a triploid apomict.

Different ploidy levels were identified among *A*.aff.*heterochroum* specimens (RD75=3x and RD9a=4x), when compared to the genome size of the sister species *A.resiliens*. In the *A.monanthes* complex moderate variation in 1C-values was noted between the accessions identified as *A.monanthes* (Fig. 4.1). However, in all but one case (i.e. RD96), these specimens were inferred to be triploid. It is suggested that such DNA variation has most likely arisen from differences in the DNA contents of the progenitor species that gave rise to the triploids, a claim supported by the different 1C-values reported for the putative diploid progenitor species, spec.nov.1 and spec.nov.2 (Dyer *et al.*, 2012). The exception noted in specimen RD96, which belonged to the MO2.II lineage of *A.monanthes*, was inferred to be a diploid apomict, due to a significantly smaller 2C-value (18.58pg) than the mean 2C of the remaining triploid taxa (27.64 pg). This suggestion is consistent with the occurrence of diploid apomicts in other ferns, including taxa of the *Dryopteris affinis* complex (Ekrt *et al.*, 2009; Schneller & Krattinger, 2010) and the *Pteris cretica* complex (Huang *et al.*, 2011).

4.6 Conclusion

Our findings indicate that the evolution of genome size and spore size are not correlated within the *A.monanthes* complex. These findings challenge the utility of spore size for inferences of ploidy level within ferns. However, the prevalence of apomixis within this complex may be the cause of these findings, and the effect, if any, of reproductive mode on the relationship between DNA amount and spore size is currently unclear.

Our study also provides important insight into the dynamism of the fern genome. Previous studies, based on a small taxonomic sample of genome size data, have suggested that chromosome size expansion plays only a minor role in the evolution of the fern genome; with most genome size variation generated through cycles of polyploidy. Yet, in the *A.monanthes* complex and related lineages we have found evidence to suggest that genome size variation is not explained by polyploidy alone, but also by mechanisms inducing changes in the amount of DNA per chromosome (chromosome size), without altering the number of chromosomes per genome. This finding indicates the potential for retrotransposon-driven chromosome/ genome size expansion within homosporous ferns. This would have large implications for our understanding of the evolution of the homosporous fern genome in general, and it highlights the need for a substantial increase in genome size studies, in order to determine the full extent to which these processes operate across the diversity of ferns.

CHAPTER 5

Investigating the origins of apomixis in the homosporous fern *Asplenium monanthes*

Prepared for submission to Evolution, under the co-authorship of Helen Hipperson, Alex Papadopulos, Martyn Powell, Vincent Savolainen & Harald Schneider.

5.1 Summary

Homosporous ferns offer an ideal model to study the evolution of apomixis, due to its relatively high frequency in this group compared to other plant groups. Furthermore, the high frequency of apomixis in this group is paradoxical due to the theoretical 50% cost of asexuality that is associated to homospory. Apomixis in ferns has been linked to reticulate evolution and selection due to female sterility. Nevertheless, stronger inferences into the evolutionary properties of apomixis cannot be made as little is known about the mechanisms of transition to apomixis. In this study we outline a number of mechanisms that are likely to be responsible for the accumulation of genetic diversity in apomictic homosporous fern species. These include: 1) Multiple origins of apomixis by the repeated formation of otherwise sterile hybrids between sexual species; 2) Genetic divergence within an established apomictic lineage derived from a single origin; 3) A single origin of apomixis and spread of apomixis via the male function. We use a genome wide approach to investigate the influence of these mechanisms on patterns of genetic diversity in the apomictic triploid fern *Asplenium monanthes*. Our approach uses a comparative analysis of multilocus AFLP data, single locus plastid and nuclear DNA sequence data, and DNA C-values, using a number of species delimitation methods. The AFLP data showed variable support for sexual progenitor species inferred from the DNA sequence data. Comparative analysis of all datasets indicated that most of the genetic diversity in *A.monanthes* is derived form a single transition to apomixis followed by post origin divergence through hybridisation via the male function. There is also some support for post-origin genetic divergence by other processes, such as genetic segregation and unequal meiosis. Overall our findings are consistent with recent findings in other apomictic fern complexes and with the hypothesis of a 50% cost of asexuality, going some way to explaining the high frequency of apomixis in ferns. They also highlight the potential for the establishment of new apomictic lineages and the need to reconsider the view of apomixis as an evolutionary dead end.

5.2 Introduction

The taxonomic distribution of apomixis in land plants is markedly uneven, with a disproportionately high frequency of up to 10% in homosporous ferns according to some authors (Walker, 1966a; but see Liu *et al.*, 2012). This is paradoxical, as in theory apomictic reproduction in homosporous plants incurs a cost of 50%, and apomixis is selected for as an alternative to female sterility, rather than as an alternative to sexual reproduction (Mogie, 1990, 1992). Mogie's hypothesis is supported by the strong association between hybridisation and apomixis, and the distinct lack of facultative apomicts observed in homosporous ferns (Manton, 1950; Lovis, 1977; Liu *et al.*, 2012). The importance of hybridisation in the evolutionary origins of apomixis in ferns is therefore evident, but whether the transition to apomixis is the direct result of a hybridisation event or only fixed by hybridisation is not clear.

The evolutionary history of apomictic ferns is often shrouded by high levels of complexity, often as a result of genotypic diversity and multiple ploidy levels (Grusz *et al.*, 2009; Schneller & Krattinger, 2010; Ootsuki *et al.*, 2011; Sigel *et al.*, 2011; Chao *et al.*, 2012; Dyer *et al.*, 2012; Beck *et al.*, 2012). This leads to the question: How is genetic diversity in apomictic ferns assembled over time? Here we consider that genetic diversity can be generated by three independent mechanisms, which are not mutually exclusive.

(1) Multiple origins of apomixis by the repeated formation of otherwise sterile hybrids between sexual species (Darnaedi *et al.*, 1990). Here, the same sexual progenitor species could potentially hybridise multiple times, forming a distinct apomictic lineage each time. (2) Genetic divergence within an established apomictic lineage (derived from a single origin). Sporogenesis in *A.monanthes* is likely to occur via the Döpp-Manton pathway (Döpp, 1932; Manton, 1950), which involves the termination of the fourth mitosis and results in the formation of a restitution nucleus. The reductional meiosis step is not altered, resulting in the potential for genetic variability due to somatic mutation (Schneller & Krattinger, 2010), unequal meiosis (Lin *et al.*, 1992), and/or genetic segregation by homoeologous chromosome pairing (Klekowski, 1973; Ishikawa *et al.*, 2003; Ootsuki *et al.*, 2011, 2012). (3) A single origin of apomixis and spread of apomixis via the male function (Walker, 1962; Gastony & Gottlieb, 1985; Watano & Iwatsuki, 1988; Suzuki & Iwatsuki, 1990). Although apomictic

ferns lack functional archegonia (female organs), the male function has been shown to be unaffected by the transition to apomixis in at least some ferns (Laird & Sheffield, 1986). Consequently, functional male antheridia (unreduced male gametes) of apomictic taxa can potentially hybridise with closely related sexual species, producing polyploid apomictic progeny.

In this study we use a genome wide approach to investigate the influence of these mechanisms on patterns of genetic diversity in the apomictic triploid fern *Asplenium monanthes*. Previous analysis of nuclear and plastid DNA sequence data for this species (Dyer *et al.*, 2012) revealed significant patterns of genotypic diversity within *A.monanthes*, which also comprised the somewhat morphologically distinct apomict *A.hallbergii* (hereafter described as a lineage of *A.monanthes*). It also revealed the association of two putative sexual diploid progenitor species, spec.nov.1 and spec.nov.2. Inclusive of *A.hallbergii*, three distinct hybrid lineages of *A.monanthes* were inferred. However, the study of interspecific AFLP data (see chapter 3) showed that other sources of genetic variation, such as genetic segregation, could not be ruled out. This data also indicated the possibility for further instances of hybridisation, possibly via functional male gametes, with more distantly related species, including individual accessions of *A*.cf.*polyphyllum* and *A*.cf.*fibrillosum* (chapter 3).

Chapter 4 indicated low genome size variation within triploid accessions of *A.monanthes*, but also identified one diploid accession of apomictic *A.monanthes*, indicating that diploidisation or unequal meiosis may have occurred in some instances (see Chapter 4). It also showed the genome size of triploid *A.monanthes* to be double that of closely related triploid apomict *A.resiliens*.

In this study, we will investigate the influence of the three mechanisms mentioned above in the evolutionary origins of apomixis and the accumulation of genetic diversity in *A.monanthes*. First, if genetic diversity were the result of multiple origins of apomixis via the repeated formation of otherwise sterile hybrids between sexual progenitor species, we would expect multiple and rather uniform genetic clusters of apomictic taxa. We would also expect the karyotype of the apomictic hybrids to reflect the combined karyotypes of the sexual progenitor species. However, dependent on the age and number of transitions we might

expect to see some genetic divergence between clusters. Second, if genetic diversity were accumulated by a single origin of apomixis and post-origin divergence, we would consider processes such as somatic mutation (Schneller & Krattinger, 2010), unequal meiosis (Lin *et al.*, 1992), and/or genetic segregation by homoeologous chromosome pairing (Klekowski, 1973; Ishikawa *et al.*, 2003; Ootsuki *et al.*, 2011, 2012). We would expect that genetic diversity would accumulate in the cpDNA via substitution events (and not by picking up cpDNA from different parents), and in the nuclear DNA via substitution events and modification via somatic rearrangements. If unequal meiosis had occurred we would also expect changes in ploidy level. Third, if genetic diversity is accumulated by a single origin of apomixis and the spread of apomixis via the male function, we would expect the plastid data to indicate the maternal parents, and the nuclear sequence data and AFLP data, which largely reflects genetic patterns in the nuclear genome, to indicate the paternal parents. Furthermore, hybridisation via unreduced male spermatozoids would always result in an increase in ploidy level of the progeny.

5.3 Material and Methods

5.3.1 Sampling

The study sample was compiled based on the results of DNA sequence data analyses (Dyer *et al.*, 2012) and interspecific AFLP data analyses (see Chapter 3) in the *A.monanthes* complex. In total 159 individual specimens were sampled, including 73 individuals that comprised population level samples from 13 separate populations (see Table 5.1). The species that were sampled included: *A.monanthes*, *A.hallbergii*, one putative hybrid accession of *A.*cf.*fibrillosum* (RD22), one putative hybrid accession of *A.*cf.*polyphyllum* (AM5249), and the two newly identified putative progenitor species spec.nov.1 and spec.nov.2.

Samples were collected and acquired from a broad geographical range across the recorded distribution of *A.monanthes* (see Table 5.1 and Dyer *et al.*, 2012). Published plastid and nuclear DNA sequence data (Dyer *et al.*, 2012) corresponding to individuals sampled for AFLP analysis were used for comparative analysis (see Table 5.1).

Table 5.1. Sampling information. Species are identified using Mickel and Smith (2004) and Dyer *et al*. (2012). Clade code, voucher number, population information, collector ID, collection location and Genbank accession number for individual markers (where applicable) are given. Clade code is reported based on findings of DNA sequence data analysis (Dyer *et al.*, 2012), which includes all accessions except those coded as M and all population samples of SP1 and SP2, for which no sequence data is available. Asterisks (*) indicate diploid apomictic accession (see Chapter 4).

Species	Clade	Voucher	Population	Collector	Origin	*psbA-trnH*	*rps4-trnS*	*trnL-trnF*	*pgiC*
*A.*cf.*fibrillosum*	FIB	RD22	-	R.J.Dyer	Mexico, Jalisco	JQ767581	JQ767713	JQ767830	JQ767221-2
A.hallbergii	H	RD18.3	-	R.J.Dyer	Mexico, Jalisco	JQ767592	-	JQ767840	JQ767267-9
A.hallbergii	H	RD23	-	R.J.Dyer	Mexico, Jalisco	JQ767593	JQ767723	JQ767841	JQ767274-6
*A.*aff.*hallbergii*	H	RD85	-	R.J.Dyer	Mexico, Oaxaca	JQ767589	JQ767720	JQ767837	JQ767252-5
*A.*aff.*hallbergii*	H	RD90	-	R.J.Dyer	Mexico, Oaxaca	JQ767590	JQ767721	JQ767838	JQ767259-61
A.hallbergii	H	RD93	-	R.J.Dyer	Mexico, Oaxaca	JQ767595	-	JQ767843	-
A.hallbergii	H	RD101a	-	R.J.Dyer	Mexico, Oaxaca	JQ767596	JQ767725	JQ767844	-
A.hallbergii	H	RD111	-	R.J.Dyer	Mexico, Mexico DF	JQ767597	JQ767726	JQ767845	JQ767290-2
A.hallbergii	H	RD112	-	R.J.Dyer	Mexico, Mexico DF	JQ767598	JQ767727	JQ767846	JQ767297-9
A.hallbergii	H	RD113b	-	R.J.Dyer	Mexico, Mexico DF	-	JQ767728	JQ767847	-
A.hallbergii	H	RD118.1	-	R.J.Dyer	Mexico, Mexico DF	-	-	-	-
A.hallbergii	H	RD120	-	R.J.Dyer	Mexico, Mexico DF	JQ767599	JQ767729	JQ767848	-
A.hallbergii	H	RD136.1	-	R.J.Dyer	Mexico, Queretaro	JQ767600	JQ767730	JQ767849	JQ767304-5
A.hallbergii	H	RD138	-	R.J.Dyer	Mexico, Queretaro	JQ767601	JQ767731	JQ767850	-
A.hallbergii	H	THO2730	-	T.Kromer	Mexico	JQ767602	-	JQ767851	-
A.hallbergii	H	THO2731	-	T.Kromer	Mexico	JQ767603	-	JQ767852	-
*A.*cf.*monanthes*	M	MC5307	-	M.Christenhusz	Guatemala	-	-	-	-
A.monanthes	M	CJR3580	-	C.J.Rothfels	Ecuador, Carchi	-	-	-	-
A.monanthes	M	MK13252	-	M.Kessler	Mexico	-	-	-	-
A.monanthes	M	RD139	-	R.J.Dyer	Costa Rica	-	-	-	-
A.monanthes	M	RD142	-	R.J.Dyer	Costa Rica	-	-	-	-
A.monanthes	M	RD148	-	R.J.Dyer	Costa Rica	-	-	-	-
A.monanthes	M	RD149	-	R.J.Dyer	Costa Rica	-	-	-	-
A.monanthes	M	RD153	-	R.J.Dyer	Costa Rica	-	-	-	-
A.monanthes (MO1)	M1	CJR3673	-	C.J.Rothfels	Ecuador	JQ767608	JQ767735	JQ767856	-
A.monanthes (MO1)	M1	EG51	-	E.Grangaud	La Reunion	-	-	-	-
A.monanthes (MO1)	M1	Heiko.2	-	H.Muth	Mexico	JQ767612	JQ767739	JQ767859	-
A.monanthes (MO1)	M1	IJ1269	-	I.Jimenez	Bolivia	JQ767613	JQ767740	-	-
A.monanthes (MO1)	M1	RD1a	-	R.J.Dyer	Mexico, Hidalgo	JQ767619	JQ767743	JQ767865	JQ767329-30
A.monanthes (MO1)	M1	RD2	7 (a,b,d,e,f,g,h)	R.J.Dyer	Mexico, Hidalgo	JQ767620	JQ767744	JQ767866	JQ767333-5
A.monanthes (MO1)	M1	RD8	6 (a,b,c,e,f,h)	R.J.Dyer	Mexico, Guanajuato	JQ767621	JQ767745	JQ767867	JQ767338-9

A.monanthes (MO1)	M1	RD10a	-	R.J.Dyer	Mexico, Guanajuato	JQ767622	JQ767746	JQ767868	JQ767344-6
A.monanthes (MO1)	M1	RD17	-	R.J.Dyer	Mexico, Jalisco	JQ767624	JQ767748	JQ767870	JQ767357-8
A.monanthes (MO1)	M1	RD19.1	-	R.J.Dyer	Mexico, Jalisco	JQ767625	JQ767749	JQ767871	JQ767365-7
A.monanthes (MO1)	M1	RD20.2	-	R.J.Dyer	Mexico, Jalisco	JQ767626	JQ767750	JQ767872	JQ767373-4
A.monanthes (MO1)	M1	RD21.1	-	R.J.Dyer	Mexico, Jalisco	JQ767627	JQ767751	-	JQ767383-5
A.monanthes (MO1)	M1	RD25.1	-	R.J.Dyer	Mexico, Jalisco	JQ767629	JQ767753	-	-
A.monanthes (MO1)	M1	RD26.1	-	R.J.Dyer	Mexico, Jalisco	JQ767630	JQ767754	JQ767874	JQ767391-3
A.monanthes (MO1)	M1	RD29a	-	R.J.Dyer	Mexico, Nayarit	JQ767632	JQ767756	-	-
A.monanthes (MO1)	M1	RD30	-	R.J.Dyer	Mexico, Nayarit	JQ767633	JQ767757	-	-
A.monanthes (MO1)	M1	RD32	-	R.J.Dyer	Mexico, Nayarit	JQ767634	JQ767758	JQ767876	-
A.monanthes (MO1)	M1	RD70a	-	R.J.Dyer	Mexico, Guerrero	JQ767638	JQ767762	JQ767879	-
A.monanthes (MO1)	M1	RD73	5 (a-e)	R.J.Dyer	Mexico, Oaxaca	JQ767639	JQ767763	JQ767880	-
A.monanthes (MO1)	M1	RD74	-	R.J.Dyer	Mexico, Oaxaca	JQ767640	JQ767764	JQ767881	JQ767414-5
A.monanthes (MO1)	M1	RD76.1	-	R.J.Dyer	Mexico, Oaxaca	JQ767641	JQ767765	JQ767882	JQ767420-2
A.monanthes (MO1)	M1	RD80	5 (2-6)	R.J.Dyer	Mexico, Oaxaca	JQ767642	JQ767766	JQ767883	JQ767426-8
A.monanthes (MO1)	M1	RD88	5 (a,b,d,e,f)	R.J.Dyer	Mexico, Oaxaca	JQ767644	JQ767768	JQ767885	-
A.monanthes (MO1)	M1	RD89	-	R.J.Dyer	Mexico, Oaxaca	JQ767645	JQ767769	JQ767886	-
A.monanthes (MO1)	M1	RD97	-	R.J.Dyer	Mexico, Oaxaca	JQ767649	JQ767773	-	JQ767432-3
A.monanthes (MO1)	M1	RD101b	-	R.J.Dyer	Mexico, Oaxaca	JQ767651	JQ767775	JQ767891	-
A.monanthes (MO1)	M1	RD103	-	R.J.Dyer	Mexico, Oaxaca	JQ767653	JQ767777	JQ767893	-
A.monanthes (MO1)	M1	RD104.1	-	R.J.Dyer	Mexico, Oaxaca	JQ767654	JQ767778	JQ767894	-
A.monanthes (MO1)	M1	RD110.1	-	R.J.Dyer	Mexico, Mexico DF	JQ767656	JQ767779	JQ767896	JQ767445-7
A.monanthes (MO1)	M1	RD117.1	-	R.J.Dyer	Mexico, Mexico DF	JQ767657	JQ767780	JQ767897	JQ767450-2
A.monanthes (MO1)	M1	RD126a	-	R.J.Dyer	Mexico, Queretaro	JQ767660	JQ767783	JQ767900	-
A.monanthes (MO1)	M1	RD131.1	-	R.J.Dyer	Mexico, Queretaro	JQ767661	JQ767784	JQ767901	-
A.monanthes (MO1)	M1	RD132.2	-	R.J.Dyer	Mexico, Queretaro	JQ767662	JQ767785	JQ767902	-
A.monanthes (MO1)	M1	RJ11	-	R.Jonas	Bolivia	JQ767665	JQ767788	JQ767905	-
A.monanthes (MO1)	M1	THO2660	-	T.Kromer	Mexico	JQ767666	JQ767789	JQ767906	-
A.monanthes (MO1)	M1	THO2743	-	T.Kromer	Mexico	JQ767668	JQ767791	JQ767907	-
A.monanthes (MO2)	M2	ALG08-145	-	A.L.Grusz	Costa Rica	JQ767611	JQ767738	JQ767858	JQ767321-3
A.monanthes (MO2)	M2	ES462	-	E.Schuettpelz	USA, Arizona	JQ767610	JQ767737	JQ767857	-
A.monanthes (MO2)	M2	IJ2419	-	I.Jimenez	Bolivia	JQ767614	-	-	-
A.monanthes (MO2)	M2	LJ03-38	-	Launert & Jahns	Mexico, Oaxaca	JQ767615	JQ767741	JQ767860	-
A.monanthes (MO2)	M2	MADBUI	2 (1,2)	P.Acock	Portugal, Madeira	JQ767616	-	JQ767861	-
A.monanthes (MO2)	M2	RD16	6 (1-6)	R.J.Dyer	Mexico, Jalisco	JQ767623	JQ767747	JQ767869	JQ767349-1
A.monanthes (MO2)	M2	RD24	6 (1-6)	R.J.Dyer	Mexico, Jalisco	JQ767628	JQ767752	JQ767873	JQ767375-6
A.monanthes (MO2)	M2	RD41		R.J.Dyer	Mexico, Jalisco	JQ767635	JQ767759	JQ767877	-
A.monanthes (MO2)	M2	RD45.1	9 (1-9)	R.J.Dyer	Mexico, Jalisco	JQ767636	JQ767760	JQ767878	JQ767407-8
A.monanthes (MO2)	M2	RD53		R.J.Dyer	Mexico, Jalisco	JQ767637	JQ767761	-	JQ767412-3

A.monanthes (MO2)	M2	RD83a		R.J.Dyer	Mexico, Oaxaca	JQ767643	JQ767767	JQ767884	-
A.monanthes (MO2)	M2	RD92a		R.J.Dyer	Mexico, Oaxaca	JQ767646	JQ767770	JQ767887	-
A.monanthes (MO2)	M2 *	RD96		R.J.Dyer	Mexico, Oaxaca	JQ767648	JQ767772	JQ767889	-
A.monanthes (MO2)	M2	RD99		R.J.Dyer	Mexico, Oaxaca	JQ767650	JQ767774	JQ767890	JQ767439-1
A.monanthes (MO2)	M2	RD102.1		R.J.Dyer	Mexico, Oaxaca	JQ767652	JQ767776	JQ767892	-
A.monanthes (MO2)	M2	RD109		R.J.Dyer	Mexico, Mexico DF	JQ767655	-	JQ767895	-
A.monanthes (MO2)	M2	RD119a	9 (a,b,d,e,f,g,h,I,j)	R.J.Dyer	Mexico, Mexico DF	JQ767658	JQ767781	JQ767898	-
A.monanthes (MO2)	M2	RD125a		R.J.Dyer	Mexico, Queretaro	JQ767659	JQ767782	JQ767899	-
A.monanthes (MO2)	M2	RD135.1		R.J.Dyer	Mexico, Queretaro	JQ767663	JQ767786	JQ767903	-
A.monanthes (MO2)	M2	RD137.1		R.J.Dyer	Mexico, Queretaro	JQ767664	JQ767787	JQ767904	-
A.monanthes (MO2)	M2	THO2728		T.Kromer	Mexico	JQ767667	JQ767790	-	-
*A.*cf.*polyphyllum*	POL	AM5249		A.Monro	Panama, Bocas del toro	JQ767671	JQ767794	JQ767911	-
Spec.nov.1	SP1	JM1339		J.Monterosa	El Salvador	JQ767697	JQ767814	JQ767937	JQ767553-4
Spec.nov.1	SP1	RD162	14 (MP 1-14)	R.J.Dyer	El Salvador	-	-	-	-
Spec.nov.2	SP2	SK10151		S. Knapp	El Salvador	JQ767698	JQ767815	JQ767938	JQ767559
Spec.nov.2	SP2	RD163	7 (1-7)	R.J.Dyer	El Salvador	-	-	-	-
Spec.nov.2	SP2	RD164	4 (1-4)	R.J.Dyer	El Salvador	-	-	-	-

5.3.2 AFLP data generation

See Chapter 3.

5.3.3 AFLP data analysis

Pairwise AFLP distances and pairwise sequence distances (of the combined plastid and nuclear sequence datasets respectively) were compared in order to assess the suitability of the AFLP dataset for phylogenetic and tree building analyses. AFLP data was transformed into Jaccard (Jaccard, 1908) and Hamming distances (Hamming, 1950), and the combined plastid sequence dataset and the nuclear sequence dataset were transformed into Hamming distances in SplitsTree (Huson & Bryant, 2006). The mantel test (Legendre & Legendre, 1998), implemented in the vegan package (Oksanen *et al.*, 2012) in R (R Core Development Team, 2011), was used to test for a correlation between pairwise AFLP distance matrices and pairwise sequence divergence matrices.

Neighbor-joining (NJ) analyses, maximum parsimony (MP) analyses, and principle coordinates analysis (PCO) were performed as in Chapter 3. Bayesian inference of clusters (k) was also performed as in Chapter 3, but only up to 10 clusters (k=1 to k=10) was assumed. Gaussian mixture model cluster analysis was performed as in chapter 3, but using a non-metric (Kruskal, 1964) multidimensional scaling (MDS) of Jaccard distances, with the number of MDS dimensions (NMDS) only tested for 4 dimensions (r=4).

5.3.4 DNA sequence data analysis

Ultrametric phylogenetic trees with divergence time estimates were generated for each single locus dataset and a combined plastid dataset (three plastid loci) using Beast v1.7.4 (Drummond *et al.*, 2012), as in Chapter 3. We did not use a Yule prior as the GMYC uses a coalescent as the null model to explain branching patterns (Pons *et al.*, 2006), and the coalescent tree prior is therefore the more conservative option.

In order to determine independently evolving lineages, the single threshold generalized mixed yule coalescent (GMYC) model (Pons *et al.*, 2006; Fontaneto *et al.*, 2007) was applied to each single locus ultrametric tree using the ‘gmyc’ function in the ‘splits’ package (Ezard *et al.*, 2009) in R. The GMYC model determines independently evolving lineages based on the

transition in branching rates from species level (yule model) to population level (coalescence model) evolutionary processes. Where applicable trees were transformed to binary format using the 'multi2di' function implemented in the 'ape' package (Paradis *et al.*, 2004) in R.

5.4 Results

5.4.1 Tree building analyses

The application of phylogenetic analysis methods to the AFLP data was supported by the significant correlation between pairwise AFLP distances and pairwise sequence distances. A significant positive correlation was found between pairwise AFLP distances and: (1) pairwise distances of the plastid sequence dataset (Fig. 5.1A) (AFLP Jaccard distances: p=0.001 and r=0.5; AFLP Hamming distances: p=0.002 and r =0.28): (2) the pairwise distances of the nuclear *pgiC* dataset (Fig. 5.1B) (AFLP Jaccard distances: p=0.001 and r=0.22; AFLP Hamming distances: p=0.002 and r =0.12).

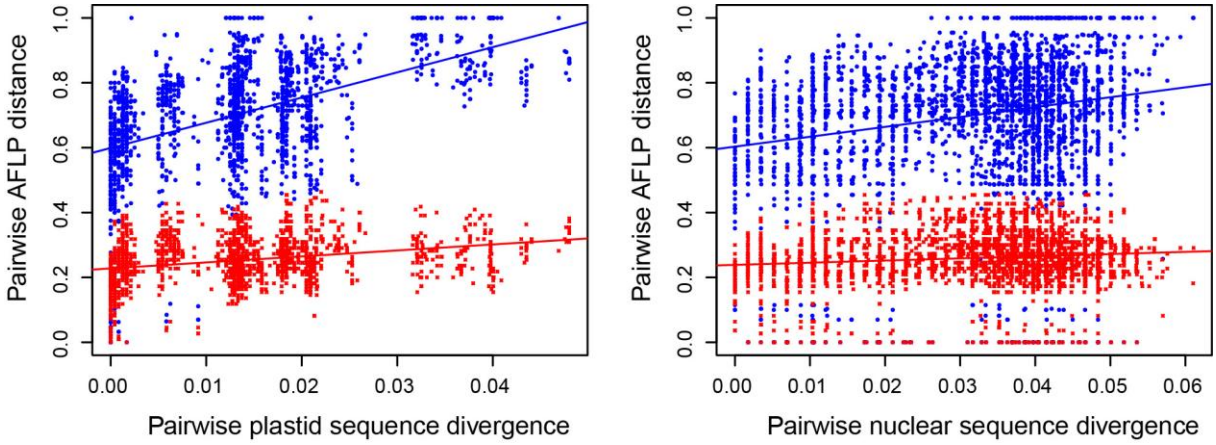

Figure 5.1. Matrix correlation between pairwise DNA sequence distances and AFLP distances. (A) Pairwise AFLP distances plotted against the pairwise distances of the plastid DNA sequence dataset. AFLP Jaccard distances are plotted in blue (p=0.001 and r=0.5), and AFLP Hamming distances are plotted in red (p=0.002 and r =0.28). (B) Pairwise AFLP distances plotted against the pairwise distances of the nuclear single copy gene *pgiC* dataset. AFLP Jaccard distances are plotted in blue (p=0.001 and r=0.22), and AFLP Hamming distances are plotted in red (p=0.002 and r =0.12).

NJ analysis of the AFLP dataset using Jaccard distances (Fig. 5.2) and Nei-Li distances (results not shown) resulted in very similar trees. Accessions of spec.nov.1 and individual accessions of *A.*cf.*fibrillosum* (RD22) and *A.*cf.*polyphyllum* (AM5249) were recovered as independent lineages respectively. Spec.nov.2 accessions were recovered in two independent clusters that correspond to the two populations sampled (RD163 and RD164). One previously un-sampled accession of *A.monanthes* (RD153) was supported within the cluster corresponding to the first population of spec.nov.2 (RD163). *Asplenium monanthes* lineages MO1 and MO2 and *A.hallbergii* (as defined by previous analysis of plastid sequence data) were supported in a number of exclusive and mixed clusters. Despite this, individuals that were characterised by the respective plastid lineages did appear to be associated, and occurrences of mixed clusters were due to a small number of individuals.

MP analyses recovered five most parsimonious trees. Deeper relationships were ambiguous as illustrated by the collapse of the deeper nodes in the strict consensus tree obtained from the MP trees (Fig. 5.3). Several clades however were robust and had bootstrap values >50%. These clades correspond to clusters recovered in the NJ analyses.

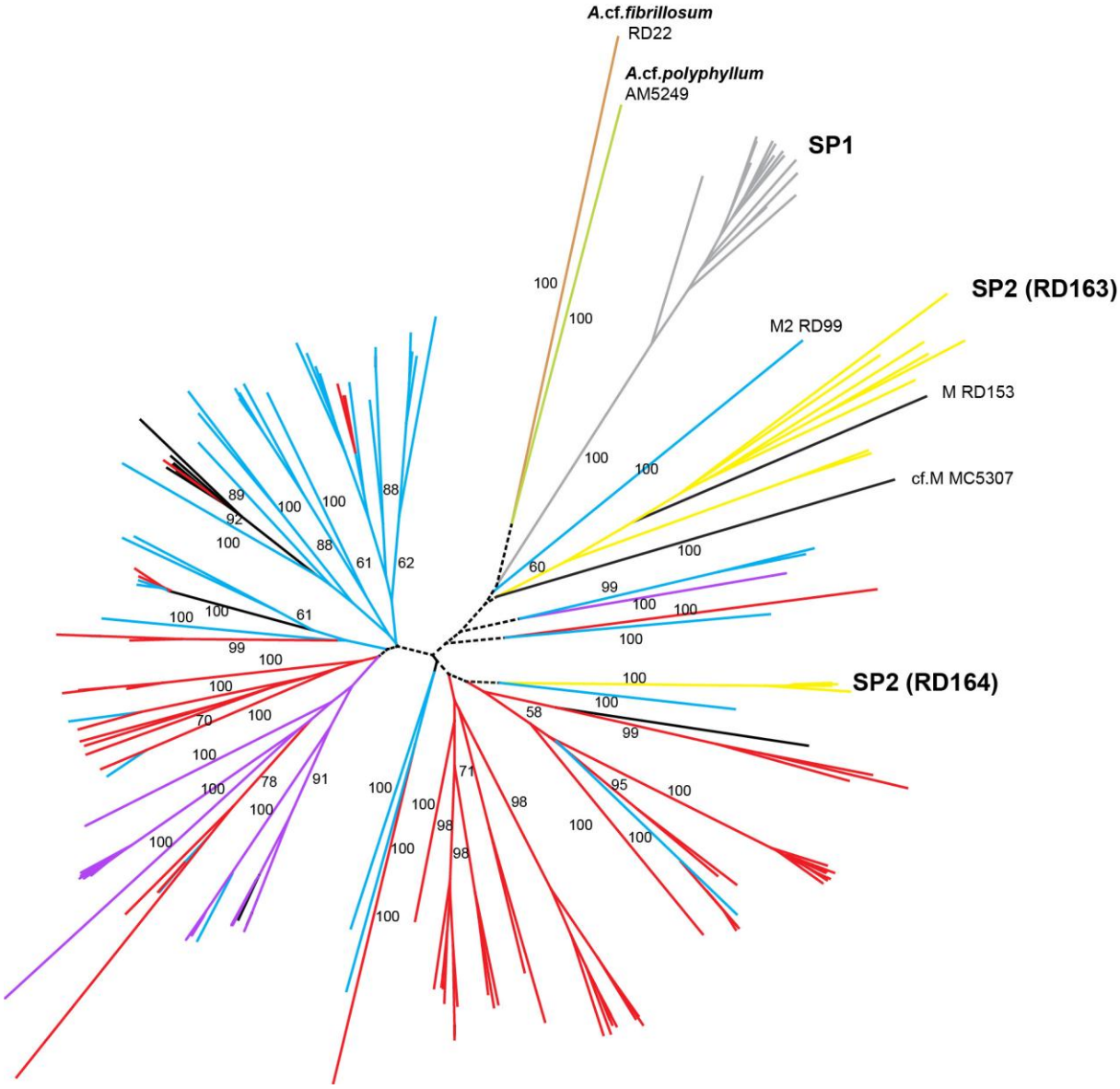

Figure 5.2. Neighbor joining tree of AFLP data performed using Jaccard distances and 500 bootstrap replicates in SplitsTree (Huson & Bryant, 2006). Bootstrap values over 50% are shown. Clusters are coloured according to species assignments as inferred in Dyer et al. (2012): Red = *A.monanthes* MO1; Blue = *A.monanthes* MO2; Black = *A.monanthes* (not assigned due to lack of sequence data); Purple = *A.hallbergii*; Yellow = spec.nov.2; Grey = spec.nov.1; Brown = *A*.cf.*fibrillosum*; Green = *A*.cf.*polyphyllum*.

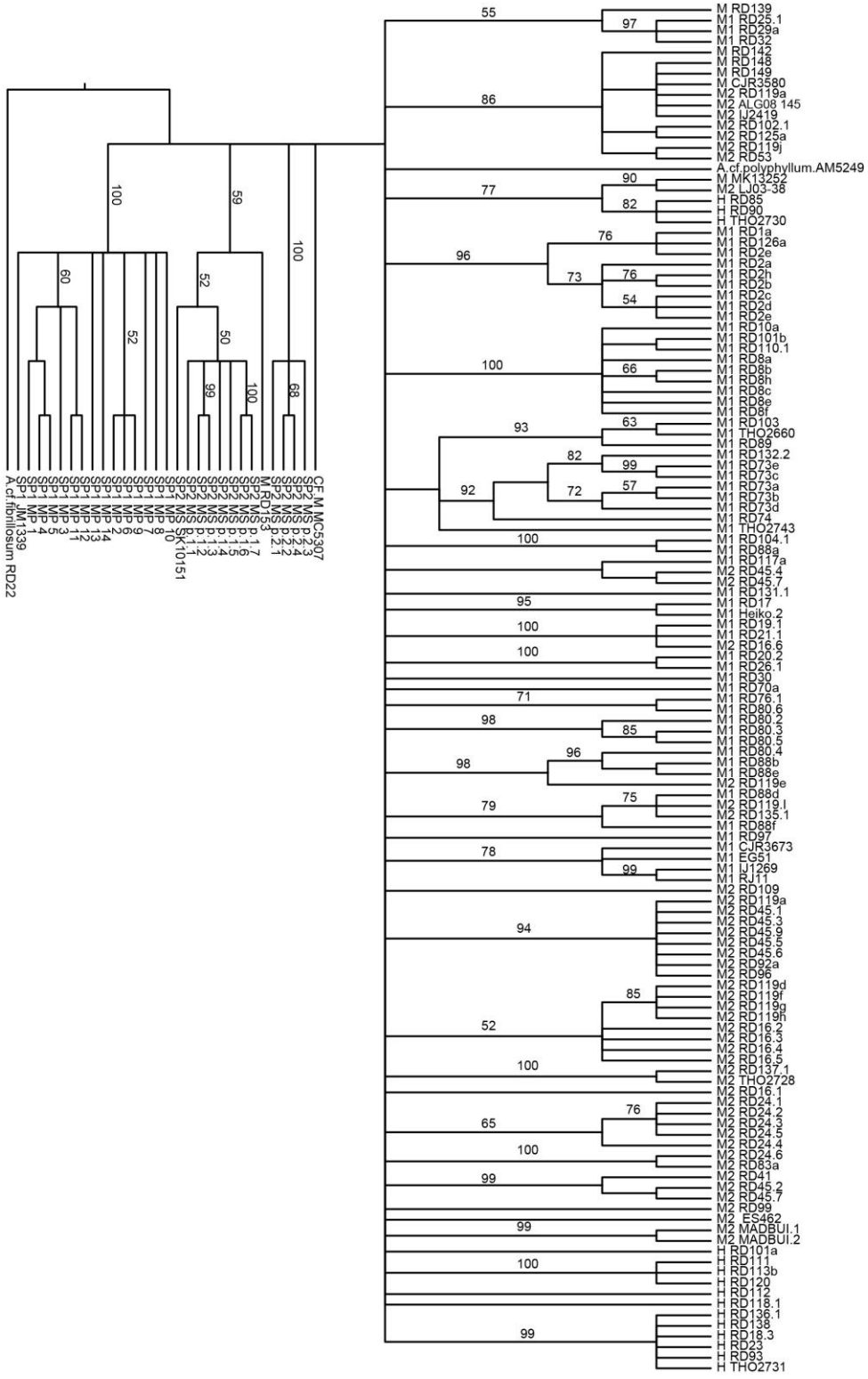

Figure 5.3. Maximum parsimony phylogenetic analysis of the AFLP data. The strict consensus tree of the 5 most parsimonious trees is shown using a midpoint rooting option, and bootstrap values >50% are indicated for the main clades. Terminals are labelled with accession vouchers and lineage codes: SP1 = spec.nov.1; SP2 = spec.nov.2; CF. M = *A.*cf.*monanthes*; M = *A.monanthes* (lineage unassigned); M1 = *A.monanthes* MO1; M2 = *A.monanthes* MO2; H = *A.hallbergii.*

5.4.2 Multilocus clustering analyses

The compilation and visual inspection of the output from Structure analyses showed that although there was a distinct rise at K=2 and K=3, there was not a distinct value of K at which the mean estimated posterior probability of the data reached a clear maximum value (Fig. 5.4A). Calculation of the ΔK statistic estimated the number of clusters to be K=3, with K=4 showing a smaller but relatively high value of ΔK (Fig. 5.4B).

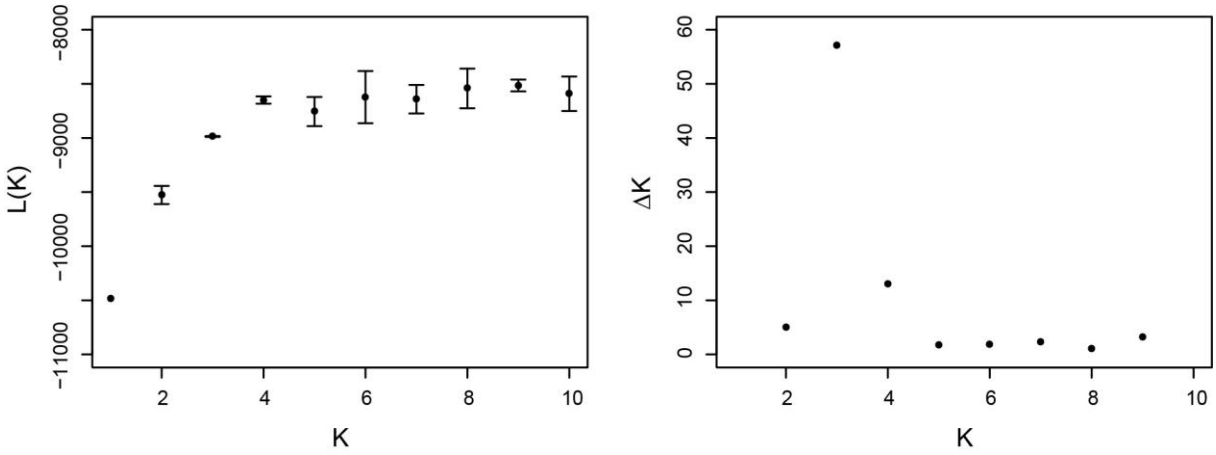

Figure 5.4. The results of Structure analysis of the AFLP data for increasing values of K (1 to 10). The true number of clusters (K) present in our data was estimated according to (A) changes in the log likelihood values, and (B) the ΔK values for each value of K (Evanno *et al.*, 2005). Standard deviation for log likelihood is illustrated with error bars.

Based on these results we evaluated the composition of clusters for K=2, K=3, and K=4 (Fig. 5.5 and Table 2). The clusters at K=2 were composed of one cluster that consists of spec.nov.1, spec.nov.2 (RD163 only), one accession of *A.monanthes* (RD153) and the sole accession of *A. polyphyllum* (AM5249). The latter two accessions, together with *A.*cf.*fibrillosum* (RD22), *A.*cf.*monanthes* (MC5307) and one accession of *A.monanthes* (RD99) showed extensive admixture. The second cluster was composed of all remaining accessions of *A.monanthes*, *A.hallbergii* and the second population of spec.nov.2 (RD164). Low levels of admixture were shown in this population of spec.nov.2, and also in several *A.monanthes* and *A.hallbergii* accessions.

When three clusters were assumed (K=3), the first cluster described for K=2 was maintained, and the second cluster described for K=2 was sub-divided into two clusters. One of these clusters was comprised of approximately half of the *A.monanthes* MO1 accessions, the

second population of spec.nov.2 (RD164), and one accession of *A.monanthes* MO2 (RD16.6). The other cluster included the remaining *A.monanthes* MO1 accessions, all but one *A.monanthes* MO2 accessions, and *A.hallbergii*. High levels of admixture were shown between these two clusters in many *A.monanthes* MO1 accessions.

When four clusters were assumed (K=4), spec.nov.1 was identified as a separate cluster, but the remaining clusters differed in composition between runs. We therefore do not consider this to be the optimal value of k to investigate the delineation of distinct lineages. Structure analyses were re-run with only *A.monanthes* and *A.hallbergii* specimens to test for the effect of the other species, and no change in results was shown.

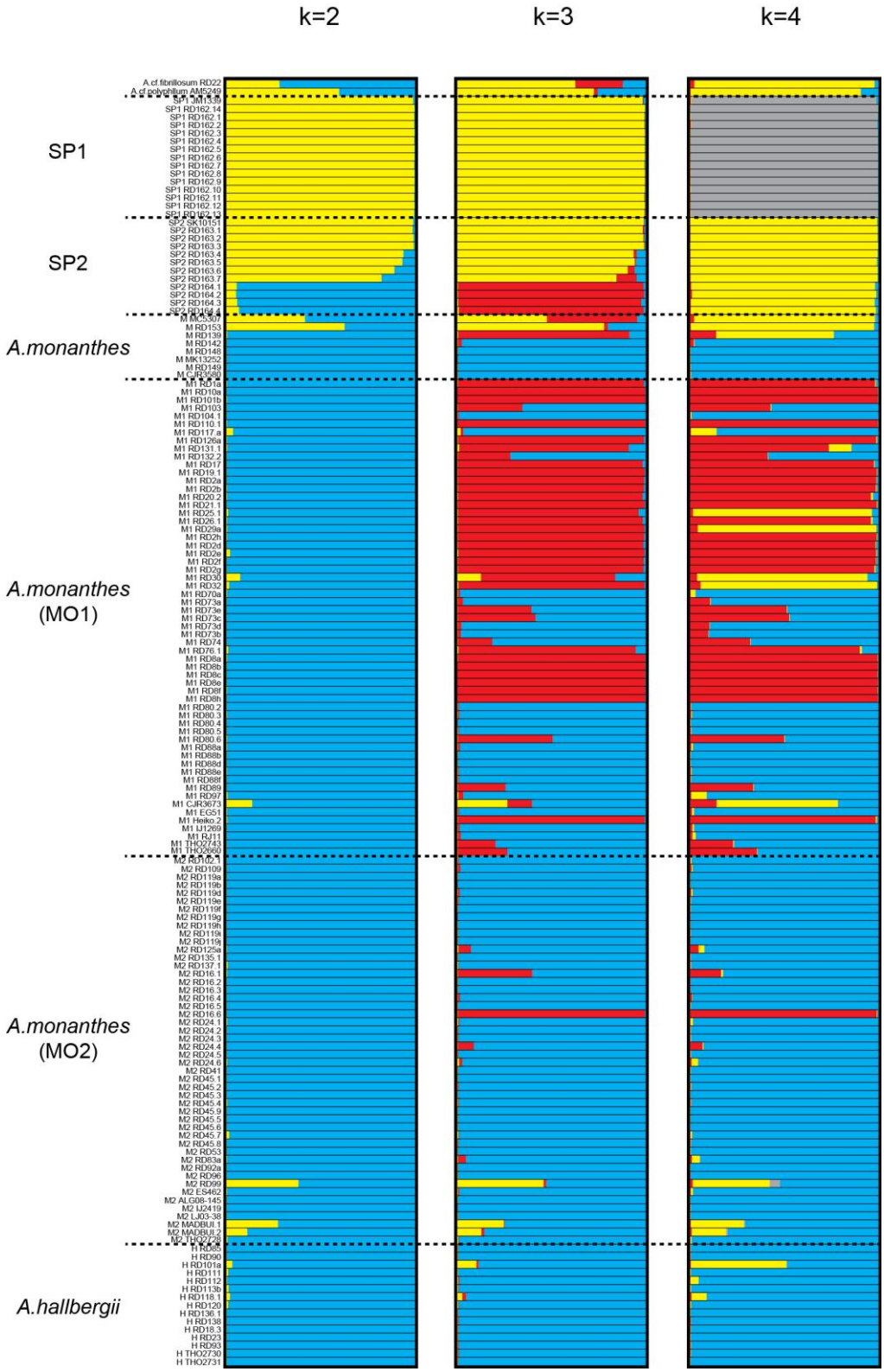

Figure 5.5. Genetic clusters inferred by Structure analysis at K=2, K=3 and K=4 for *Asplenium monanthes* lineages. Each bar plot shows fractional assignment to various clusters for each value of K respectively. Individuals within each bar plots are labelled with voucher codes and organised according to distinct lineages inferred by Dyer *et al*. (2012).

PCO analysis of the whole AFLP dataset (Fig. 5.6A) showed that spec.nov.1 formed a distinct cluster, separated form the remaining species. The remaining principle components were compressed due to distinct nature of the principle components of spec.nov.1. We therefore performed another PCO analysis without spec.nov.1 (Fig. 5.6B, C). This showed that spec.nov.2 (RD163 only) and all but one of the *A.hallbergii* accessions formed distinct clusters respectively, but that there was substantial overlap between *A.monanthes* MO1 and MO2 lineages, and one hallbergii accession (RD101a) and spec.nov.2 (RD164). Overlapping accessions corresponded to the accessions of *A.monanthes* MO1 found in the paraphyletic cluster or accessions showing admixture in structure analysis (Fig. 5.5).

Gaussian cluster analysis of AFLP data using non-metric multidimensional scaling (MDS) of Jaccard distances, for four MDS (r=4), resulted in the partitioning of: (1) the full dataset into eight clusters (Stress = 12.66; and 10 clusters without a noise component) (Fig. 5.7A and Table 5.2); and (2) the reduced dataset (with spec.nov.1 accessions removed) into 11 clusters (Stress = 12.6; and 18 clusters without a noise component) (Fig. 5.7B and Table 5.2). In analysis of the full dataset 18.2% of the individuals were included in the noise category, including all accessions of Spec.nov.2, and individual accessions of *A*.cf.*monanthes* (MC5307), *A*.cf.*fibrillosum* (RD22) and *A*.cf.*polyphyllum* (AM5249). Accessions classified as *A.monanthes* MO1 were partitioned into five clusters in total (Fig. 5.7A): three monophyletic clusters; one cluster that included one accession of *A.monanthes* MO2 (RD16.6); and, one cluster that included several accessions of *A.monanthes* MO2 and *A.hallbergii*. The remaining accessions of *A.hallbergii* and *A.monanthes* MO2 were recovered in single monophyletic clusters respectively, and the final cluster included all accessions of spec.nov.1 (Fig. 5.7A).

In analysis of the reduced dataset 16.6% of the individuals were included in the noise category, including individual accessions of *A*.cf.*monanthes* (MC5307), *A*.cf.*fibrillosum* (RD22), and *A*.cf.*polyphyllum* (AM5249). The 11 clusters (Fig. 5.7B) comprised: one monophyletic cluster of spec.nov.2, three monophyletic clusters of *Asplenium monanthes* MO1; three monophyletic clusters of *Asplenium monanthes* MO2; two clusters including both *A.monanthes* MO1 and MO2; one monophyletic cluster of *A.hallbergii*; and, one cluster including accessions of both *A.monanthes* MO1 an MO2 lineages, and *A.hallbergii*.

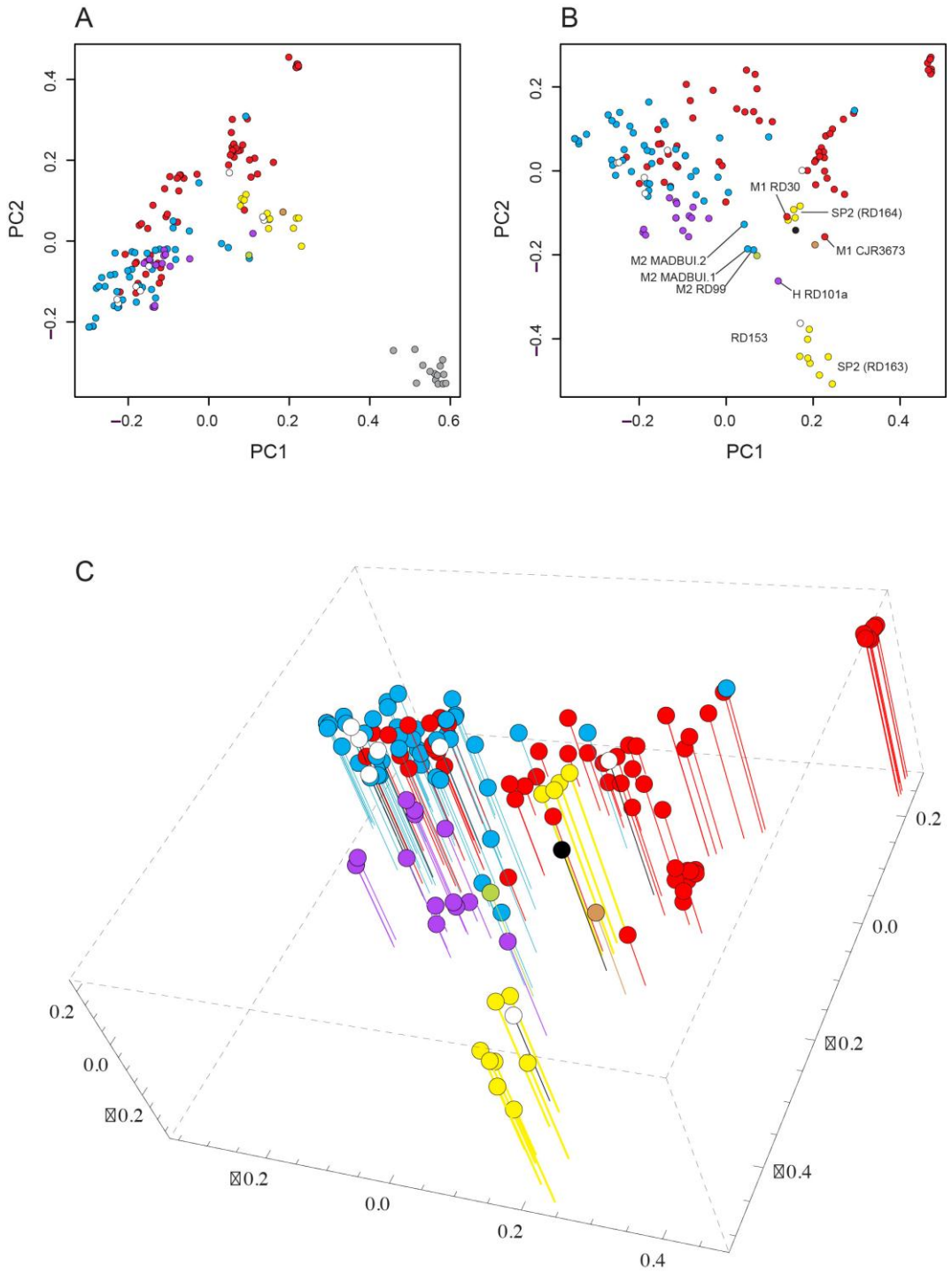

Figure 5.6. Principle components analysis of AFLP Jaccard distances computed in PCO3 (Anderson, 2003). (A) A plot of the first two principle components axes of the full dataset. (B and C) Plots of the first two axes of the principle components (B), and the first three axes of the principle components (C), of the reduced dataset without accessions of spec.nov.1. Individual principle components are coloured according to species inferred in Dyer *et al*. (2012): Red = *A.monanthes* MO1; Blue = *A.monanthes* MO2; Black = *A.*cf.*monanthes*; White = *A.monanthes* (not assigned due to lack of sequence data); Purple = *A.hallbergii*; Yellow = spec.nov.2; Grey = spec.nov.1; Brown = *A.*cf.*fibrillosum*; Green = *A.*cf.*polyphyllum*.

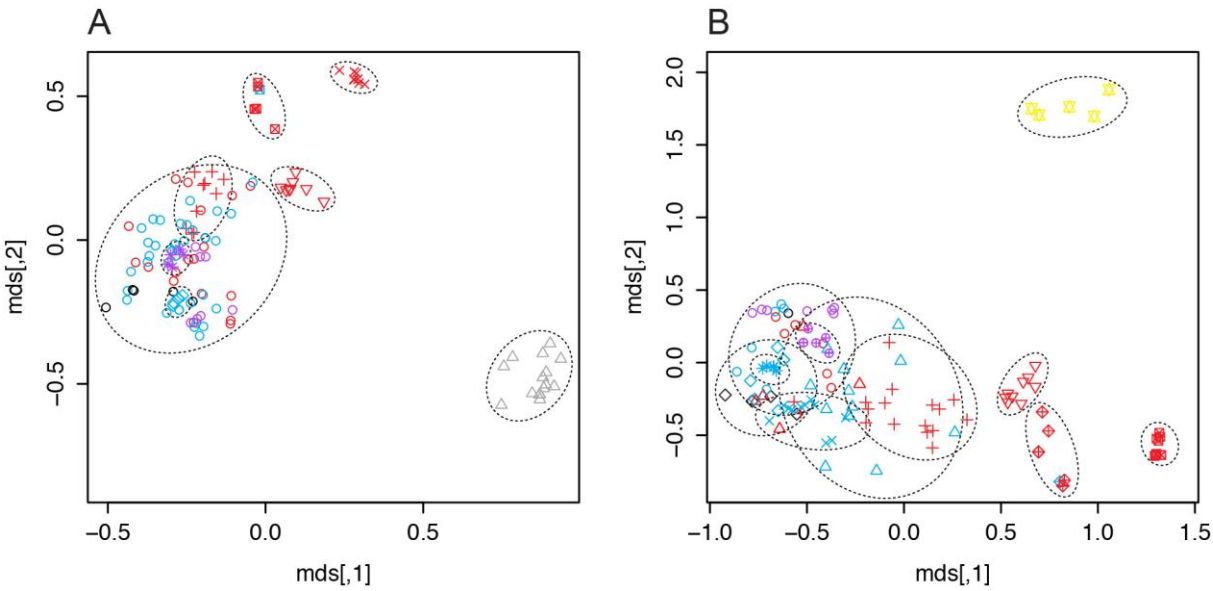

Figure 5.7. Gaussian cluster analysis of AFLP data using a non-metric multidimensional scaling of Jaccard distances, with four MDS (r=4) and a noise component specified. The first two MDS dimensions are plotted for: (A) Gaussian cluster analysis of the full dataset; (B) Gaussian cluster analysis without accessions of spec.nov.1. Clusters are represented by different symbols and bounded within dashed lines. Individual components are coloured according to species inferences made in Dyer *et al*. (2012): Red = *A.monanthes* MO1; Blue = *A.monanthes* MO2; Black = *A.monanthes* (not assigned due to lack of sequence data); Purple = *A.hallbergii*; Yellow = spec.nov.2; Grey = spec.nov.1.

5.4.3 Analysis of single locus DNA sequence data

A log-likelihood ratio test of the GMYC model against a null model of coalescence showed that the null model could not be rejected for *psbA-trnH* (p=0.79) and *pgiC* gene trees (p=0.86). However, the GMYC model fitted significantly better for the *rps4F-trnS* tree (likelihood ratio=10.39, p=0.016) and the *trnL-trnF* tree (likelihood ratio=7.94, p=0.047). The GMYC model estimated 7 clusters and 12 entities (minus out-group taxa) for the *rps4-trnS* tree, and 9 clusters and 13 entities (minus out-group taxa) for the *trnL-trnF* tree (Fig. 5.8, and Table 5.2). The clusters broadly corresponded to previous assignments of species, the major exception being that *A.monanthes* MO1 accessions were subdivided into 6 clusters in both trees (the composition of these clusters differed slightly between trees). Also one *A.monanthes* MO2 accession (RD16) was assigned as a single entity in both trees, and *A*.cf.*monanthes* (MC5307), *A*.cf.*fibrillosum* (RD22), and *A*.cf.*polyphyllum* (AM5249) were grouped in the *rps4-trnS* tree and *A*.cf.*monanthes* (MC5307), *A*.cf.*fibrillosum* (RD22) were grouped in the *trnL-trnF* tree.

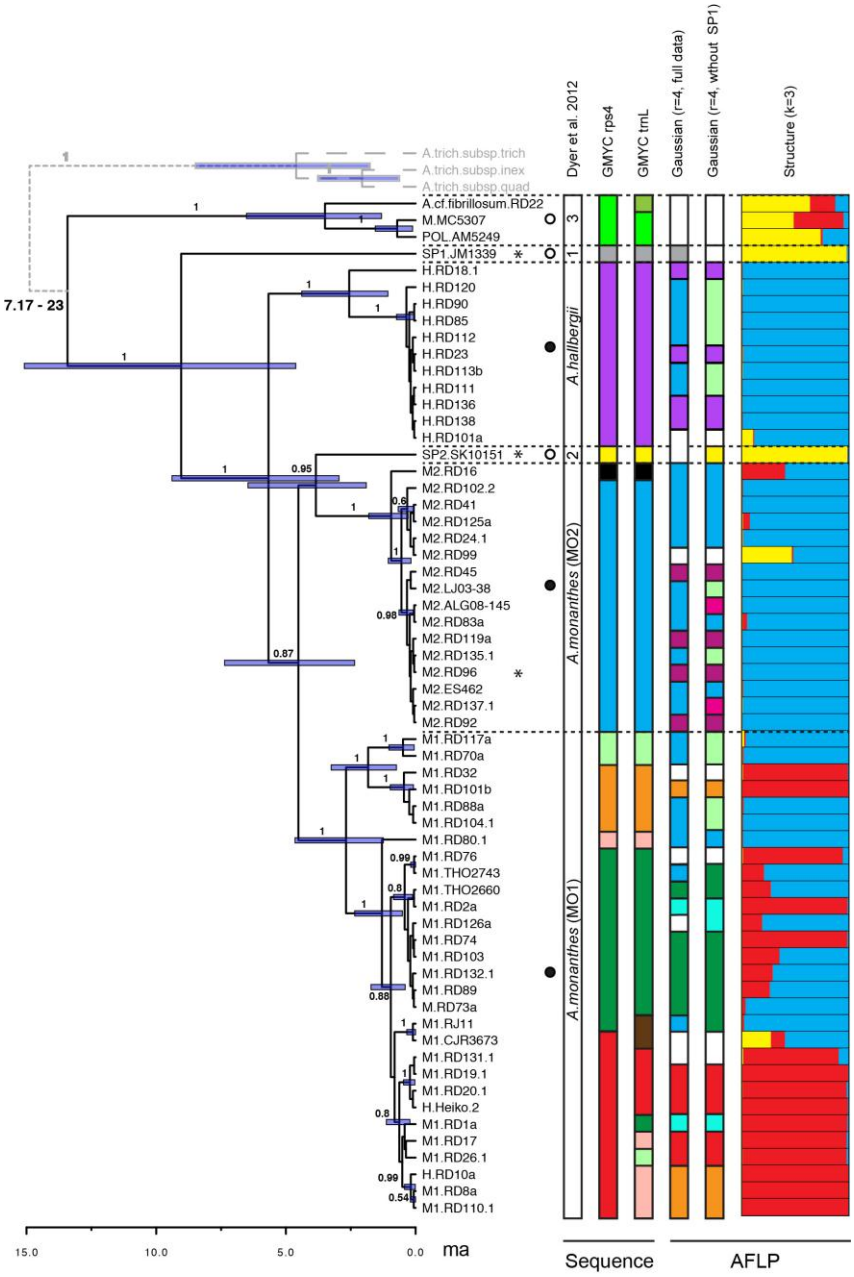

Figure 5.8. A comparison of independent lineage delineation according to analysis of DNA sequence data and multilocus AFLP data. The results from various delineation methods are mapped onto an ultrametric phylogenetic tree of combined plastid sequence data, with divergence times estimated using a coalescent tree prior, and a relaxed lognormal clock and estimated rates, as estimated in Beast v1.7.4 (Drummond *et al.*, 2012). The clock is calibrated according to an estimate for *Asplenium dielerecta* (Schneider *et al.*, 2005). Scale of the ultrametric tree corresponds to million year to the present (ma). Posterior branch support >0.5 is shown. Major clades are labelled according to lineages inferred in Dyer *et al*. (2012): Clade1 = spec.nov.1, Clade 2 = spec.nov.2, and Clade 3 = *A*.cf.*fibrillosum* (RD22), *A*.cf.*monanthes* (MC5307), and *A*.cf.*polyphyllum* (AM5249). In Gaussian analysis, individuals incorporated within the noise component are indicated in white. Structure results are presented in the form of a bar plot, illustrating admixture by fractional assignment to clusters. Apomictic lineages are indicated with filled black circles, and sexually reproducing lineages are indicated with empty white circles. Stars indicate diploid individuals.

Table 5.2. Summary of results from various analysis methods of AFLP and DNA sequence data. Data type is indicated as: (1) AFLP data, including full dataset or reduced dataset (Spec.nov.1 accessions removed); or (2) single locus sequence data, including *psbA-trnH*, *trnL-trnF*, and *rps4-trnS*. In GMYC analyses, the number of clusters displayed includes clusters and single entities. In Gaussian cluster analysis the number of clusters given in brackets is the number of clusters recovered when no noise component was specified.

Data	Method	Parameters	Samples	Clusters	Species Fused
Sequence (*rps4-trnS*)	GMYC	Single threshold	67	12	3
Sequence (*trnL-trnF*)	GMYC	Single threshold	67	13	2
AFLP (full dataset)	Gaussian	Non-metric r=4	159	8 (10)	2 (5)
AFLP (without SP1)	Gaussian	Non-metric r=4	144	11 (18)	2 (4)
AFLP	STRUCTURE	k=2	159	2	6
AFLP	STRUCTURE	k=3	159	3	6
AFLP	STRUCTURE	k=4	159	4	5

5.5 Discussion

In this study we investigated a total of 159 individuals of *A.monanthes* and putative progenitor species, to infer the mechanism for the accumulation of genetic variation in this apomictic lineage. The three hypotheses outlined in the introduction were explored using four types of evidence: multilocus AFLP data, DNA sequences of plastid loci, DNA sequences of a single nuclear gene, and DNA C-Values. In discussing the results it is pertinent first to acknowledge some of the limitations in our study and the methods used. These limitations are mainly derived from uncertainties arising from analysing AFLP data for a group of individuals with a range of reproductive mode and polyploid levels. AFLPs are dominant markers, and therefore the comparison of dissimilarity measures between diploids and polyploids can be misleading with regards to the interpretation of hybridisation and parentage (Kosman & Leonard, 2005; Meudt & Clarke, 2007). Furthermore, the study sample size may lead to the over- or underestimation of independent lineages in both AFLP and sequence data. In the AFLP data this may lead to clustering bias based on only a few bands in insufficiently sampled individuals (*A.*cf.*fibrillosum* RD22 is a good example of this).

5.5.1 Identifying diploid sexual putative progenitors

Until recently, *Asplenium monanthes* was known as a triploid apomict with a single report of a diploid chromosome count from southern Mexico (Mickel & Smith, 2004). Dyer *et al*.

(2012) inferred two sexual diploids, spec.nov.1 and spec.nov.2, as putative progenitors to *A.monanthes* lineages MO1 and MO2, respectively, due to their association to these lineages in the nuclear and plastid data. Despite this affinity in the nuclear *pgiC* gene, the AFLP data did not provide support for spec.nov.1 as a progenitor species to *A.monanthes.* One population of spec.nov.2 (RD163) was weakly supported as being a progenitor species to *A.monanthes*. It was isolated in cluster analysis, but inspection of the raw data showed that *A.monanthes* accessions shared between 9 to 46% of AFLP bands found in spec.nov.2 accessions (see Guo *et al.,* 2006). The close association of a new accession (RD153) from Costa Rica, previously identified as *A.monanthes*, is supported within this cluster, indicating that this accession is the inferred diploid sexual spec.nov.2, demonstrating that it is more widely distributed than previously thought. The second population of spec.nov.2 (RD164) was supported within the *A.monanthes* MO1 lineage in the AFLP data (Fig. 5.5). This population of spec.nov.2 was identified based on collection location only due to morphological similarity with *A.monanthes*. It must therefore be assumed this has been a misidentification and is *A.monanthes*. Sequence, cytological and spore size data on accessions from this population would clarify this situation.

The affinity of spec.nov.2 to *A.monanthes* lineages in the plastid and nuclear *pgiC* gene, but the isolation and only weak support as a progenitor species in the multilocus cluster analyses is surprising (Figures 5.7 and 5.8). This might be due to the dominant nature of AFLP data, whereby the difference in ploidy level may be distorting the degree of genetic overlap observed in both spec.nov.1 and spec.nov.2 (see Kosman & Leonard, 2005). It may also indicate that the transition to apomixis is not recent, and genetic differences may be due to the build up of somatic mutations in both the sexual and apomictic lineages.

5.5.2 Multiple origins of apomixis via repeated hybridisation events between sexual progenitor species

Under this hypothesis we would expect multiple rather uniform genetic clusters of apomictic taxa. If progenitor species were both diploids then the resulting interspecific sterile hybrid would be diploid, and would have half the chromosome complement of both parents. If the parents were one diploid and one tetraploid then a triploid hybrid would be produced, as observed in *Dryopteris yakusilvicola* (Darnaedi *et al.,* 1990).

The vast majority of cytological work has indicated the prevalence of triploid cytotypes within *A.monanthes* lineages, with the exception of very rare occurrences of one documented apomictic diploid (see chapter 4) and one tetraploid (Mickel & Smith, 2004). The occurrence of the tetraploid does indicate that triploids could be the result of hybridisation between a sexual diploid and tetraploid, although we would expect a higher occurrence of tetraploids in this case. The large diversity observed in the plastid and nuclear sequence data, and to a lesser extent in the AFLP data, and the low outcrossing rates observed in tetraploid ferns makes repeated origins by this scenario unlikely. The presence of a single record of an apomictic diploid could be the result of an interspecific hybridisation between two sexual diploids. However, this could also be the result of post-origin processes (discussed subsequently).

5.5.3 Genetic divergence within an established apomictic lineage (single origin)

Under the hypothesis we would expect that from a single origin, genetic diversity would accumulate in the cpDNA via substitution events (and not by picking up cpDNA from different parents), and in the nuclear DNA via substitution events and modification via somatic rearrangements. We would also expect changes in ploidy level if unequal meiosis had occurred.

The genetic diversity observed in the plastid sequence data indicates the influence of different parental genomes, making it unlikely that these processes are responsible for the main patterns of diversity observed in *A.monanthes*. However, these processes could be operating within the independent plastid *A.monanthes* lineages, as indicated by the recovery of several clusters in the sequence data and AFLP data, and the variation in the cytological data (see chapter 4).

The discovery of a diploid apomict in *A.monanthes* MO2 (Fig. 5.8 and Table 5.1) (see Chapter 4) provides putative evidence for unequal meiosis as recorded in *Dryopteris pacifica* (Lin *et al.*, 1992). The diploid *A.monanthes* accession is recovered in cluster specific to *A.monanthes* MO2 lineage, which indicates that unequal meiosis may have resulted in the establishment of a diploid lineage. Genetic segregation, as reported in *Cyrtomium fortunei* (Ootsuki *et al.*, 2012) and *Dryoteris niponensis* (Ishikawa *et al.*, 2003), is also indicated in *A.monanthes*. It is supported by the observation of two genotypes within a population of

A.monanthes MO2 (RD16), whereby different individuals are supported in different genetic clusters. However, this pattern may also be explained by the co-occurrence of lineages derived from different parents. Despite the putative evidence for genetic divergence within established apomictic lineages, a more stringent test for the occurrence of these mechanisms would require cytological data for each individual, and comparative analysis of the genetic data of parents and progeny (see Ootsuki *et al.*, 2012).

5.5.4 Single origin and spread of apomixis by the male function

This hypothesis considers that apomictic ferns produce unreduced male gametes but that female gametes are sterile. The model assumes that apomixis is paternally inherited by hybridisation between unreduced male gametes and closely related sexual species. We would therefore expect the plastid data to indicate the maternal parents and the nuclear sequence data and AFLP data, which largely reflects genetic patterns in the nuclear genome, to indicate the paternal parents. Furthermore, hybridisation via unreduced male spermatozoids would always result in an increase in ploidy level of the progeny.

In *A.monanthes*, the patterns of genetic diversity and the observation of mainly triploid cytotypes show support for this hypothesis. The identification of distinct patterns of genetic diversity in the plastid sequence data indicates independent apomictic lineages derived from up to three maternal progenitor species. The nuclear sequence data supports this and indicates a common paternal parent (spec.nov.2) in all three lineages and the putative parental role of spec.nov.1 for *A.monanthes* MO1. In the AFLP data, despite less support for sexual progenitor species, a large number of accessions from all plastid *A.monanthes* lineages are clustered together in one group (Figures 5.5 and 5.8). This would indicate a single paternal progenitor species. The increased diversity observed in the *A.monanthes* MO1 lineage, in the plastid and AFLP data, could indicate other mechanisms of genetic diversity accumulation are operating (discussed above), but could also be explained by repeated hybridisation events via the male function in this lineage. This is also true for *A.hallbergii* and *A.monanthes* MO2 lineages, as the AFLP data shows distinct clusters within each lineage respectively.

Structure analysis of the AFLP data (Fig. 5.5) indicated that several accessions of the *A.monanthes* lineages showed admixture from outside the group. This indicates less frequent

and perhaps more recent hybridisation events (by the male function) with more distantly related maternal progenitors, including individual accessions of *A.*cf.*polyphyllum* and *A.*cf.*fibrillosum* respectively.

5.5.5 Is apomixis in homosporous ferns a non-adaptive trait that is fixed and spread via the male function?

Mogie's hypothesis of a 50% cost of asexuality (Mogie, 1990, 1992) posits that apomixis is only selected for as an alternative to female sterility in homosporous plants. In the *A.monanthes* complex, the observation of mainly triploid cytotypes for all lineages supports this hypothesis, and is consistent with the scenario that a diploid asexual species hybridised with closely related sexual diploid species via the male function. A similar mechanisms may also be considered to explain the assembly of other triploid apomictic ferns, such as in the *Dryopteris affinis* complex (Schneller & Krattinger, 2010), the *Cheilanthes yavapensis* complex (Grusz *et al.*, 2009), and the *Pteris cretica* and *Pteris cadieri* complexes (Suzuki & Iwatsuki, 1990; Chao *et al.*, 2012).

The question then arises whether the asexual diploid progenitor in this scenario was the result of an interspecific hybridisation event between two sexual species, or was the result of a mutation for asexuality in a sexual diploid species, giving rise to an asexual diploid population? If the former were true then we would not expect to find sexual progenitor species associated to autoploid triploid cytotypes. Our data would indicate that the latter case is true, as the *A.monanthes* MO2 lineage appears to be an autoploid formed by the progenitor species spec.nov.2. However, this inference is based on only a single nuclear gene and any strong inferences of parentage and mechanism of origin would require the analysis of co-dominant data such as microsatellites.

The diploid apomict recovered in the *A.monanthes* MO2 clade might provide putative support for the former argument of origin by interspecific hybridisation. Conversely, if asexuality had emerged due to mutation in a sexual diploid, Mogie's hypothesis implies that this diploid apomict would only be selected for if a mutation for female sterility also occurred. The likelihood for this is up for debate. Of course, as discussed above, the occurrence of this apomictic diploid could be explained by diploidisation of a triploid cytotypes by unequal meiosis. This uncertainty together with the rare occurrence of sexual diploids associated to the

A.monanthes lineages makes strong inferences about the origins of apomixis very difficult. Explanations for the rarity of sexual progenitor species are speculative, but may be explained by the heterosis effect due to increases in ploidy, or the potential for 'sexual competition' via the male function of apomicts (Mogie, 1992).

5.6 Conclusions

In conclusion our data indicates that a major driver of these patterns is the spread of apomixis by the male function. However, we cannot reject the hypotheses that genetic diversity is also accumulated by post origin genetic divergence due to genetic segregation, unequal meiosis or somatic mutation. Further scrutiny is required to prove that these processes are also occurring in this complex. Given the rarity of sexual diploids, it appears unlikely that the patterns of genetic diversity observed are explained by multiple origins via repeated interspecific hybridisation between sexual species.

The evidence for the spread of apomixis by the male function is consistent with the strong association of apomictic lineages to hybridisation and polyploidy, which is also consistent with Mogie's hypothesis (Mogie, 1990, 1992). This hypothesis stipulates a 50% cost of asexuality and the selection for apomixis only as an alternative to female sterility. The inferred autoploid nature of *A.monanthes* MO2 lineage indicates that the apomixis has emerged due to a mutation for asexuality in a sexual diploid, which has been spread by hybridisation (via the male function) with sexual diploid species. However, a single origin by interspecific hybridisation and subsequent spread via the male function cannot be ruled out.
An important consideration of these findings is the potential for the establishment of new apomictic lineages, and the possible distinction between the origin of apomixis and the age of apomictic lineages. The accumulation of new genetic diversity from sexual lineages and potential for diploidisation in apomictic lineages, means that the actual transition to apomixis may be older than appears (Kimura & Crow, 1964; Janko *et al.*, 2008). That is a single transition to apomixis and spread via the male function may give the appearance of multiple transitions across the phylogeny. In this case, the inference of a separate origin of apomixis in a closely related apomict, *A.resiliens*, needs to be investigated.

Another consideration is the evolutionary potential of established apomictic lineages. In a previous study of this lineage (Dyer *et al.*, 2012), no antheridia were observed on gametophytes of *A.monanthes* specimens. This might be explained by erosion of the gametophytic function, which is consistent with the build up of deleterious mutations due to higher rates of genetic segregation observed in gametophytes (Ootsuki *et al.*, 2012). This would support the view of apomictic lineages as evolutionary dead ends. However, the lack of antheridia may have been caused by cultivation conditions.

Nevertheless, the importance of the male function in younger apomictic lineages, and the implications for the perpetuation of an apomictic gene, challenges this idea of apomixis as an evolutionary dead end, and may go some way to explain the disproportionately high frequency of apomixis in ferns.

CHAPTER 6

General Discussion

6.1 Synopsis

In this thesis I aimed to investigate the paradoxically high frequency of apomixis in homosporous ferns, using the *Asplenium monanthes* species complex as a model study system. I approached the investigation in four parts: To begin with I conducted a multiple-level biosystematic survey of the apomictic *A.monanthes* complex, using spore size measurements to infer ploidy level, spore number counts and gametophytic observations to infer reproductive mode, and single locus DNA sequence data (three plastid loci and one nuclear locus) to infer phylogenetic relationships (Dyer *et al.*, 2012). In the second part, I addressed the problem of species delimitation within a polyploid, apomictic species complex, using a comparative analysis between single locus and multilocus DNA data and a variety of species delimitation methods (chapter 3). In the third part, I investigated the evolution of genome size (DNA amount) within the *A.monanthes* species complex, and tested the utility of spore size for the inference of polyploid levels in homosporous ferns (chapter 4). Finally, I investigated the origins of apomixis in this complex by testing hypotheses on the accumulation of genetic diversity in an apomictic species (chapter 5). Below, I present a summary of the main findings of this thesis, and discuss their wider implications. I also consider future directions for further studies on this complex, and on apomixis in homosporous ferns and all plants.

6.2 Species delimitation in an apomictic species complex

In investigating evolutionary hypotheses on the evolution of apomixis it is first important to identify independently evolving species. Species delimitation within an apomictic fern complex is notoriously difficult due to variation in ploidy levels, the common association of apomixis with hybridisation, and mixed reproductive modes (discussed in chapter 3). In order to address this problem it is necessary to use a multi-faceted approach that combines several sources of information, including, karyotype, genotype, and reproductive mode (Gastony & Windham, 1989; Grusz *et al.,* 2009). The biosystematic study of the *A.monanthes* complex in Dyer *et al.* (2012) employed this multi faceted approach, enabling the most extensive insight into this complex to date. Previous studies had documented chromosome counts (see chapter 1 and Dyer *et al.*, 2012 for details), identifying two triploid apomictic taxa (*A.monanthes* and *A.resiliens*), one pentaploid apomictic taxon (*A.heteroresiliens*) and one sexual diploid taxon (*A.formosum*). However, the biological attributes of the other taxa in this complex were unknown or unreported.

The utilisation of spore size, spore number, gametophytic observations (Dyer *et al.*, 2012), and DNA C-value measurements (chapter 4) proved highly informative in the identification of previously unverified apomictic taxa and several cryptic species in this complex. The assessment of reproductive mode also identified other taxa to be apomictic, including *A.hallbergii, A.palmeri* (confirmed by chromosome counts of M.D. Windham, pers. comm.) and accessions similar in their morphology to the sexual *A.heterochroum* (designated *A.*aff.*heterochroum*). Crucially, this method also identified two isolated accessions associated to *A.monanthes* (in the plastid and nuclear data), to be sexually reproducing. Spore measurements and 2C-DNA value measurements (chapter 4) confirmed these to be two new sexual diploid species (designated spec.nov.1 and spec.nov.2). A formal description of these two species is still missing but will be approached in the near future. Spore size data also confirmed *A.formosum* to be a sexual diploid, but showed that the remaining taxa were all to be polyploid. The failure to specify distinct ploidy levels above diploid level (chapter 2) was supported by the insignificant relationship between spore size and DNA C-value for taxa of this complex (Chapter 4). Chromosome counts would have been the best indicator of ploidy level here, but unfortunately due to difficulties in obtaining suitable material, these were not attained. DNA C-value data did however provide a good alternative to chromosome counts

for the inference of ploidy level variation. These data identified the vast majority of *A.monanthes* to be triploid, but identified a single specimen to be an apomictic diploid. The data also showed all *A.hallbergii* accessions to be triploid, and showed variation in ploidy level in accessions of *A.*aff.*heterochroum*, including one tetraploid and one triploid.

Phylogenetic analysis of three plastid loci and one nuclear locus revealed species relationships, patterns of reticulate evolution, and exposed genetic diversity within several taxa, including apomicts, *A.monanthes* and *A.resiliens*. These data also supported spec.nov.1 and spec.nov.2 to be independently evolving lineages. Hybrid lineages were inferred from the disparity between plastid data (maternally inherited) and the distribution of nuclear alleles (paternally inherited), revealing three separate hybrid forms of *A.monanthes* (*A.monanthes* MO1, *A.monanthes* MO2, and *A.hallbergii*), at least two hybrid forms of *A.resiliens*, and extensive reticulation between *A.castaneum* and *A.polyphyllum* (Dyer *et al.*, 2012). The application of species delimitation methods to the plastid sequence data and AFLP data supported the inference of these hybrid forms (Chapters 3 and 5). These methods also indicated further genotypic diversity in *A.monanthes* lineages in the sequence data and the AFLP data (Dyer *et al.*, 2012, and chapters 3 and 5).

In summary, the inference of ploidy level and reproductive mode variation between and within taxa was successfully mapped on to a phylogenetic hypothesis to identify independent evolutionary lineages. Genetic diversity did reflect the variation observed in reproductive mode, especially with respect to sexual progenitor species (spec.nov.1 and spec.nov.2), but did not always identify the variation in ploidy level. Additional independently evolving lineages were identified from genetic data alone, and the disparity between plastid and nuclear/AFLP data was highly informative for identification of hybrid lineages. These findings highlight the need for an extensive sampling effort, in order to detect rare diversity in karyotype, genotype and reproductive mode, and the absolute necessity of such a multi-faceted approach for inferences into the evolution of apomixis in homosporous ferns.

6.3 The evolutionary origins of apomixis in homosporous ferns

Once independently evolving lineages had been determined it was then possible to test hypotheses on the evolutionary origins of apomixis in this complex. The inference of hybrid lineages within both *A.monanthes* and *A.resiliens* from genetic diversity observed in the sequence data (Dyer *et al.*, 2012) indicated multiple origins of apomixis. Within *A.monanthes* lineages (MO1, MO2 and *A.hallbergii*), diploid sexual species spec.nov.1 and spec.nov.2 were supported as putative progenitors to MO1 and MO2 respectively. In order to test these inferences, a more thorough investigation was conducted using an increased sampling effort of the *A.monanthes* lineages, and a comparative analysis of AFLP and sequence data (chapter 5). The evolutionary origins of apomixis in *A.monanthes* were investigated by testing hypotheses on the accumulation of genetic diversity in an apomictic lineage. I considered three hypotheses: (1) Multiple origins of apomixis by repeated formation of hybrids between sexual species; (2) A single origin and genetic divergence by processes such as somatic mutation, genetic segregation and unequal meiosis; (3) A single origin and spread of apomixis by hybridisation via the male function with closely related sexual species. The results presented in chapter 5 indicated that a single origin of apomixis in the *A.monanthes* lineages was likely, and that patterns in genetic diversity were primarily explained by the spread of apomixis by the male function. Current genetic diversity supports the hypothesis that triploid *A.monanthes* lineages were formed from hybridisation events between diploid apomicts and sexual diploids. This supports the scenario for a spontaneous emergence of apomixis in a diploid population and the subsequent spread and fixation (by female sterility) of the mutation by hybridisation (via functional male antheridia) with an individual from the sexual diploid progenitor lineage. The presence of multiple hybrid forms indicates that that apomixis was also spread by interspecific hybridisation with other closely related sexual species. The presence of karyotypic and genotypic diversity within these independent hybrid lineages also indicates that other mechanisms of post-origin divergence may be operating, including somatic mutation, unequal meiosis and genetic segregation by homoeologous chromosome pairing. This is especially apparent with the identification of a diploid apomict (Dyer *et al.*, 2012 and chapter 4).

The implications of these findings are very important for the wider understanding of the evolution and high frequency of apomixis in homosporous ferns. The spread of apomixis by

the male function is consistent with the strong association of apomictic lineages to hybridisation and polyploidy (Lovis, 1977; Liu *et al.*, 2012), and with Mogie's hypothesis of a 50% cost of asexuality in homosporous plants (Mogie, 1990, 1992), As discussed in chapter 5, the potential for the establishment of new apomictic lineages through the accumulation of new genetic diversity from sexual lineages could negate the long term disadvantages of asexuality, such as the build up of deleterious mutations (Muller, 1932; Kondrashov, 1982). When this is considered together with the potential for diploidisation in apomictic lineages (Lin *et al.*, 1992), the actual transition to apomixis may be older than appears (Kimura and Crow, 1964; Janko et al., 2008). In this case, the inference of a separate origin of apomixis in *A.resiliens* needs to be investigated. The significance of the male function and its implication for the perpetuation of an apomictic gene, therefore challenges the idea of apomixis as an evolutionary dead end, and may go some way to explain the disproportionately high frequency of apomixis in ferns. This is consistent with the emerging consensus of the evolutionary dynamics in angiosperms (Hörandl & Hojsgaard, 2012).

Inconsistencies with this hypothesis include the lack of functional antheridia on apomictic gametophytes of all lineages in this complex (Dyer *et al.*, 2012). This observation might be explained by erosion of the gametophytic function due to the build up of deleterious mutations, which is consistent with the higher rates of genetic segregation observed in gametophytes (Ootsuki *et al.*, 2012). Another consideration to this hypothesis is that, although a rare pentaploid apomict (*A.heteroresiliens*), inferred to be associated to *A.resiliens* and the sexual tetraploid *A.heterochroum*, is observed in the complex, no pentaploid apomicts are observed in *A.monanthes*. Considering the data available for apomictic taxa in the *A.monanthes* complex it would appear that hybrid polyploid apomicts are all formed from diploid apomicts progenitors. These observations might give insight into the evolutionary dynamics of apomixis and constraints on its spread via the male function.

6.4 The evolution of genome size in closely related homosporous ferns

The evolution of the homosporous fern genome is highly enigmatic The high chromosome numbers, and conserved chromosome size observed led to the hypothesis that the evolution of the fern genome is less dynamic than that of the angiosperm genome (Nakazato *et al.*, 2008; Barker & Wolf, 2010; Leitch & Leitch, 2013). In chapter 4, I presented a study on the

evolution of genome size in an apomictic fern complex. As well as allowing the investigation of the relationship between genome size and biological traits, such as spore size, and the inference of ploidy level in some taxa (mentioned above), this study offers important insight into the dynamism of the fern genome. The findings of this chapter show evidence to suggest that genome size variation is not only explained by polyploidy, but also by mechanisms inducing changes in the amount of DNA per chromosome (chromosome size), without altering the number of chromosomes per genome. This is observed in high levels of variation in the monoploid genome size of closely related species, with the apomictic triploid lineages of *A.monanthes* showing a two-fold expansion in genome size compared to the genome size of apomictic triploid lineages of *A.resiliens*.

Previous studies have argued that chromosome size expansion plays a minor role in the evolution of the fern genome (e.g. Nakazato *et al.*, 2008). The data presented in chapter 4 would contradict this hypothesis, having large implications for our understanding of the evolution of the homosporous fern genome. The findings indicate the potential for retrotransposon-driven chromosome/ genome size expansion within homosporous ferns. As discussed in chapter 4, retrotransposon proliferation and elimination is linked with genomic and environmental factors such as effective population size, environmental stress, hybridisation and polyploidy (Kalendar *et al.*, 2000; Leitch & Bennett, 2004; Grandbastien *et al.*, 2005; Lockton *et al.*, 2008; Grover & Wendel, 2010; Petit *et al.*, 2010). Given that the apomictic *A.monanthes* clade and related lineages show strong patterns of reticulate evolution, it is possible that these processes may be acting as triggers for retrotransposon activity leading to the range of 1Cx-values observed. Indeed, given the extent of hybridization and reticulate evolution reported in homosporous ferns in general (Lovis, 1977), it seems likely that retrotransposon driven changes in genome size is probably more widespread across ferns but has been largely overlooked due to poor taxonomic sampling.

6.5 Further work and future direction

The paradoxical prevalence of apomixis in homosporous ferns and the enigmatic nature of the genome in these ferns, make this a highly rewarding and exciting group to study. This thesis has provided the first detailed biosystematic survey of the *Asplenium monanthes* complex,

and insight into the evolutionary dynamics of apomixis and the evolution of the homosporous fern genome in general. Much of the work has involved the general assessment of species boundaries and species relationships in this complex. It is clear that this will be an ongoing process, and this study by no means provides a definite classification of the species complex. Indeed, the study has shown that a higher sampling effort revealed increased genotypic and karyotypic diversity, making it likely that extra diversity exists but is yet to be sampled. Nevertheless, the biosystematic survey of this complex has provided a solid foundation on which to test some evolutionary inferences, as well as a springboard for further work.

The disparity in the monoploid genome size of closely related species in this complex is highly intriguing and should be the subject of further scrutiny/ inquiry. It is clear that chromosome counts are required to strengthen the inferences made in chapter 4. Future work could then establish the mode of chromosome size expansion, specifically testing for retrotransposon proliferation/ deletion. This work could provide crucial insight into the evolutionary dynamics of the fern genome, but also the effect of these processes on the evolution of apomixis, or vice versa.

The mechanism of origin of apomixis in homosporous ferns is poorly understood. Chapter 5 highlights the importance of the male function and hybridisation in the spread of apomixis, and explains most of the genetic diversity in the *A.monanthes* complex. Strong inferences of origin are hampered by the uncertain inference of putative progenitor species. Future work using co-dominant genome wide markers, such as microsatellites, would provide a crucial indicator of parentage. Further work could also apply the hypotheses tested in chapter 5 to all known apomictic fern lineages. Such a macro-evolutionary approach would allow fantastic insight into some of the more general patterns in the evolutionary origins of apomixis, including the potential effect of biogeography and environment (see Liu *et al.*, 2012).

APPENDIX

Table A1. Sampling data for phylogenetic datasets. Specimens are identified according to Mickel and Smith (Mickel & Smith, 2004). Location information is given as Country and Province of origin, where possible. Genbank accession numbers are indicated for the different plastid regions. Voucher deposition at the herbarium BM (P. Acock, M. Christenhusz, R.J. Dyer, R.Jonas, K. Mehltreter, A. Monro), COLO (T.J.Lemieux), DUKE (A.Z.Grusz, C. Rothfels, E. Schuettpelz, M. Windham), GOET (I.Jimenez, M.Kessler, T.Kroemer, E.Launert & I.Jahn, M. Lehnert, H.Muth, L. Otto), LAGU (S. Knapp, J.Monterosa), MEXU (JS, Leon). Herbaria abbreviated as in Index Herbariorum (http://sciweb.nybg.org/science2/IndexHerbariorum.asp).

Species	Voucher	Collector	Origin	*psbA-trnH*	*rps4-trnS*	*trnL-trnF*
A.blepharodes	JL4079	J.L.Leon	Mexico, BCS	JQ767567	-	-
A.castaneum	RD46a	R.J.Dyer	Mexico, Jalisco	JQ767568	JQ767699	JQ767816
A.castaneum	RD46b	R.J.Dyer	Mexico, Jalisco	JQ767569	JQ767700	JQ767817
A.castaneum	RD46c	R.J.Dyer	Mexico, Jalisco	JQ767570	JQ767701	JQ767818
A.castaneum	RD47	R.J.Dyer	Mexico, Jalisco	JQ767571	JQ767702	JQ767819
A.castaneum	RD48	R.J.Dyer	Mexico, Jalisco	JQ767572	JQ767703	JQ767820
A.castaneum	RD49	R.J.Dyer	Mexico, Jalisco	JQ767573	JQ767704	JQ767821
A.castaneum	RD50a	R.J.Dyer	Mexico, Jalisco	-	JQ767705	JQ767822
A.castaneum	RD50b	R.J.Dyer	Mexico, Jalisco	JQ767574	JQ767706	JQ767823
A.castaneum	RD52	R.J.Dyer	Mexico, Jalisco	JQ767575	JQ767707	JQ767824
A.castaneum	RD54	R.J.Dyer	Mexico, Jalisco	JQ767576	JQ767708	JQ767825
A.castaneum	RD91	R.J.Dyer	Mexico, Oaxaca	JQ767577	JQ767709	JQ767826
A.castaneum	RD113a	R.J.Dyer	Mexico, Mexico DF	JQ767578	JQ767710	JQ767827
A.castaneum	RD116	R.J.Dyer	Mexico, Mexico DF	JQ767579	JQ767711	JQ767828
A.fibrillosum	RD10b	R.J.Dyer	Mexico, Guanajuato	JQ767580	JQ767712	JQ767829
A.fibrillosum	RD22	R.J.Dyer	Mexico, Jalisco	JQ767581	JQ767713	JQ767830
A.formosum	L2304	Lemieux	Costa Rica	JQ767582	JQ767714	-
A.formosum	ES1398	E.Schuettpelz	Brasil	-	JQ767715	JQ767831
A.formosum	IJ2436	I.Jimenez	Bolivia	JQ767583	JQ767716	JQ767832
A.formosum	LO20	Lisa Otto	Mexico	JQ767584	-	-
A.formosum	MK12699	M.Kessler	Madagasgar	JQ767585	-	JQ767833
A.formosum	RD27	R.J.Dyer	Mexico, Nayarit	JQ767586	JQ767717	JQ767834
A.formosum	RD28	R.J.Dyer	Mexico, Nayarit	JQ767587	JQ767718	JQ767835
A.formosum	RD33	R.J.Dyer	Mexico, Jalisco	JQ767588	JQ767719	JQ767836
*A.*aff.*hallbergii*	RD85	R.J.Dyer	Mexico, Oaxaca	JQ767589	JQ767720	JQ767837
*A.*aff.*hallbergii*	RD90	R.J.Dyer	Mexico, Oaxaca	JQ767590	JQ767721	JQ767838
A.hallbergii	MK13519	M.Kessler	Mexico	JQ767591	JQ767722	JQ767839
A.hallbergii	RD18	R.J.Dyer	Mexico, Jalisco	JQ767592	-	JQ767840
A.hallbergii	RD23	R.J.Dyer	Mexico, Jalisco	JQ767593	JQ767723	JQ767841
A.hallbergii	RD81	R.J.Dyer	Mexico, Oaxaca	JQ767594	JQ767724	JQ767842
A.hallbergii	RD93	R.J.Dyer	Mexico, Oaxaca	JQ767595	-	JQ767843
A.hallbergii	RD101a	R.J.Dyer	Mexico, Oaxaca	JQ767596	JQ767725	JQ767844
A.hallbergii	RD111	R.J.Dyer	Mexico, Mexico DF	JQ767597	JQ767726	JQ767845
A.hallbergii	RD112	R.J.Dyer	Mexico, Mexico DF	JQ767598	JQ767727	JQ767846
A.hallbergii	RD113b	R.J.Dyer	Mexico, Mexico DF	-	JQ767728	JQ767847
A.hallbergii	RD120	R.J.Dyer	Mexico, Mexico DF	JQ767599	JQ767729	JQ767848
A.hallbergii	RD136	R.J.Dyer	Mexico, Queretaro	JQ767600	JQ767730	JQ767849
A.hallbergii	RD138	R.J.Dyer	Mexico, Queretaro	JQ767601	JQ767731	JQ767850
A.hallbergii	THO2730	T.Kromer	Mexico	JQ767602	-	JQ767851
A.hallbergii	THO2731	T.Kromer	Mexico	JQ767603	-	JQ767852
*A.*aff.*heterochroum*	RD9a	R.J.Dyer	Mexico, Guanajuato	JQ767604	JQ767732	JQ767853
*A.*aff.*heterochroum*	RD75	R.J.Dyer	Mexico, Oaxaca	JQ767605	JQ767733	JQ767854
A.heterochroum	ML601	M.Lehnert	Ecuador	JQ767606	JQ767734	JQ767855
A.monanthes	AM26	A.Monro	Mexico	JQ767607	-	-
A.monanthes	CJR3673	C.J.Rothfels	Ecuador	JQ767608	JQ767735	JQ767856
A.monanthes	DT-D4945	D.Tejero-Diez	Mexico, Oaxaca	JQ767609	JQ767736	-

A.monanthes	ES462	E.Schuettpelz	USA, Arizona	JQ767610	JQ767737	JQ767857
A.monanthes	ALG08-145	A.L.Grusz	Costa Rica	JQ767611	JQ767738	JQ767858
A.monanthes	Heiko2	H.Muth	Mexico	JQ767612	JQ767739	JQ767859
A.monanthes	IJ1269	I.Jimenez	Bolivia	JQ767613	JQ767740	-
A.monanthes	IJ2419	I.Jimenez	Bolivia	JQ767614	-	-
A.monanthes	LJ03-38	Launert & Jahns	Mexico, Oaxaca	JQ767615	JQ767741	JQ767860
A.monanthes	MADBU1	P.Acock	Portugal, Madeira	JQ767616	-	JQ767861
A.monanthes	MC5290	M.Christenhusz	Guatemala	-	-	JQ767862
A.monanthes	ML741	M.Lehnert	Ecuador	JQ767617	-	JQ767863
A.monanthes	PA14	P.Acock	France, La Reunion	JQ767618	JQ767742	JQ767864
A.monanthes	RD1a	R.J.Dyer	Mexico, Hidalgo	JQ767619	JQ767743	JQ767865
A.monanthes	RD2a	R.J.Dyer	Mexico, Hidalgo	JQ767620	JQ767744	JQ767866
A.monanthes	RD8a	R.J.Dyer	Mexico, Guanajuato	JQ767621	JQ767745	JQ767867
A.monanthes	RD10a	R.J.Dyer	Mexico, Guanajuato	JQ767622	JQ767746	JQ767868
A.monanthes	RD16	R.J.Dyer	Mexico, Jalisco	JQ767623	JQ767747	JQ767869
A.monanthes	RD17	R.J.Dyer	Mexico, Jalisco	JQ767624	JQ767748	JQ767870
A.monanthes	RD19	R.J.Dyer	Mexico, Jalisco	JQ767625	JQ767749	JQ767871
A.monanthes	RD20	R.J.Dyer	Mexico, Jalisco	JQ767626	JQ767750	JQ767872
A.monanthes	RD21	R.J.Dyer	Mexico, Jalisco	JQ767627	JQ767751	-
A.monanthes	RD24	R.J.Dyer	Mexico, Jalisco	JQ767628	JQ767752	JQ767873
A.monanthes	RD25	R.J.Dyer	Mexico, Jalisco	JQ767629	JQ767753	-
A.monanthes	RD26	R.J.Dyer	Mexico, Jalisco	JQ767630	JQ767754	JQ767874
A.monanthes	RD28b	R.J.Dyer	Mexico, Nayarit	JQ767631	JQ767755	JQ767875
A.monanthes	RD29	R.J.Dyer	Mexico, Nayarit	JQ767632	JQ767756	-
A.monanthes	RD30	R.J.Dyer	Mexico, Nayarit	JQ767633	JQ767757	-
A.monanthes	RD32	R.J.Dyer	Mexico, Nayarit	JQ767634	JQ767758	JQ767876
A.monanthes	RD41	R.J.Dyer	Mexico, Jalisco	JQ767635	JQ767759	JQ767877
A.monanthes	RD45	R.J.Dyer	Mexico, Jalisco	JQ767636	JQ767760	JQ767878
A.monanthes	RD53	R.J.Dyer	Mexico, Jalisco	JQ767637	JQ767761	-
A.monanthes	RD70a	R.J.Dyer	Mexico, Guerrero	JQ767638	JQ767762	JQ767879
A.monanthes	RD73a	R.J.Dyer	Mexico, Oaxaca	JQ767639	JQ767763	JQ767880
A.monanthes	RD74	R.J.Dyer	Mexico, Oaxaca	JQ767640	JQ767764	JQ767881
A.monanthes	RD76	R.J.Dyer	Mexico, Oaxaca	JQ767641	JQ767765	JQ767882
A.monanthes	RD80	R.J.Dyer	Mexico, Oaxaca	JQ767642	JQ767766	JQ767883
A.monanthes	RD83a	R.J.Dyer	Mexico, Oaxaca	JQ767643	JQ767767	JQ767884
A.monanthes	RD88a	R.J.Dyer	Mexico, Oaxaca	JQ767644	JQ767768	JQ767885
A.monanthes	RD89	R.J.Dyer	Mexico, Oaxaca	JQ767645	JQ767769	JQ767886
A.monanthes	RD92	R.J.Dyer	Mexico, Oaxaca	JQ767646	JQ767770	JQ767887
A.monanthes	RD94	R.J.Dyer	Mexico, Oaxaca	JQ767647	JQ767771	JQ767888
A.monanthes	RD96	R.J.Dyer	Mexico, Oaxaca	JQ767648	JQ767772	JQ767889
A.monanthes	RD97	R.J.Dyer	Mexico, Oaxaca	JQ767649	JQ767773	-
A.monanthes	RD99	R.J.Dyer	Mexico, Oaxaca	JQ767650	JQ767774	JQ767890
A.monanthes	RD101b	R.J.Dyer	Mexico, Oaxaca	JQ767651	JQ767775	JQ767891
A.monanthes	RD102	R.J.Dyer	Mexico, Oaxaca	JQ767652	JQ767776	JQ767892
A.monanthes	RD103	R.J.Dyer	Mexico, Oaxaca	JQ767653	JQ767777	JQ767893
A.monanthes	RD104	R.J.Dyer	Mexico, Oaxaca	JQ767654	JQ767778	JQ767894
A.monanthes	RD109	R.J.Dyer	Mexico, Mexico DF	JQ767655	-	JQ767895
A.monanthes	RD110	R.J.Dyer	Mexico, Mexico DF	JQ767656	JQ767779	JQ767896
A.monanthes	RD117a	R.J.Dyer	Mexico, Mexico DF	JQ767657	JQ767780	JQ767897
A.monanthes	RD119a	R.J.Dyer	Mexico, Mexico DF	JQ767658	JQ767781	JQ767898
A.monanthes	RD125a	R.J.Dyer	Mexico, Queretaro	JQ767659	JQ767782	JQ767899
A.monanthes	RD126a	R.J.Dyer	Mexico, Queretaro	JQ767660	JQ767783	JQ767900
A.monanthes	RD131	R.J.Dyer	Mexico, Queretaro	JQ767661	JQ767784	JQ767901
A.monanthes	RD132	R.J.Dyer	Mexico, Queretaro	JQ767662	JQ767785	JQ767902
A.monanthes	RD135	R.J.Dyer	Mexico, Queretaro	JQ767663	JQ767786	JQ767903
A.monanthes	RD137	R.J.Dyer	Mexico, Queretaro	JQ767664	JQ767787	JQ767904
A.monanthes	RJ11	R.Jonas	Bolivia	JQ767665	JQ767788	JQ767905
A.monanthes	THO2660	T.Kromer	Mexico	JQ767666	JQ767789	JQ767906

A.monanthes	THO2728	T.Kromer	Mexico	JQ767667	JQ767790	-
A.monanthes	THO2743	T.Kromer	Mexico	JQ767668	JQ767791	JQ767907
A.palmeri	ES486	E.Schuettpelz	USA, Arizona	JQ767669	-	JQ767908
A.palmeri	CJR2494	C.J.Rothfels	USA, Texas	-	JQ767792	JQ767909
A.palmeri	RD130	R.J.Dyer	Mexico, Queretaro	JQ767670	JQ767793	JQ767910
A.polyphyllum	AM5249	A.Monro	Panama, Bocas del toro	JQ767671	JQ767794	JQ767911
A.polyphyllum	ALG08-146	A.L.Grusz	Costa Rica	JQ767672	JQ767795	JQ767912
A.polyphyllum	ALG08-034	A.L.Grusz	Costa Rica	JQ767673	-	-
A.polyphyllum	IJ809	I.Jimenez	Bolivia	JQ767674	-	JQ767913
A.polyphyllum	MC5365	M.Christenhusz	Guatemala	-	-	JQ767914
A.polyphyllum	Mehltreter	K.Mehltreter	Costa Rica	JQ767675	JQ767796	JQ767915
A.polyphyllum	RD95	R.J.Dyer	Mexico, Oaxaca	JQ767676	JQ767797	JQ767916
A.polyphyllum	RD98	R.J.Dyer	Mexico, Oaxaca	JQ767677	-	JQ767917
A.polyphyllum	RD115	R.J.Dyer	Mexico, Mexico DF	JQ767678	JQ767798	JQ767918
A.resiliens	ES428	E.Schuettpelz	USA, Arizona	JQ767679	JQ767799	JQ767919
A.resiliens	ES459	E.Schuettpelz	USA, Arizona	JQ767680	JQ767800	-
A.resiliens	ES469	E.Schuettpelz	USA, Arizona	JQ767681	-	JQ767920
A.resiliens	CJR08-025	C.J.Rothfels	Costa Rica	JQ767682	JQ767801	JQ767921
A.resiliens	CJR2504	C.J.Rothfels	USA, New Mexico	-	-	JQ767922
A.resiliens	MDW3547	M.Windham	USA, Texas	-	-	JQ767923
A.resiliens	RD3b	R.J.Dyer	Mexico, Hidalgo	JQ767683	-	JQ767924
A.resiliens	RD4a	R.J.Dyer	Mexico, Hidalgo	JQ767684	JQ767802	JQ767925
A.resiliens	RD63	R.J.Dyer	Mexico, Guerrero	JQ767685	JQ767803	JQ767926
A.resiliens	RD64	R.J.Dyer	Mexico, Guerrero	JQ767686	JQ767804	JQ767927
A.resiliens	RD72	R.J.Dyer	Mexico, Guerrero	JQ767687	JQ767805	JQ767928
A.resiliens	RD107	R.J.Dyer	Mexico, Oaxaca	JQ767688	JQ767806	JQ767929
A.resiliens	RD121	R.J.Dyer	Mexico, Queretaro	JQ767689	JQ767807	JQ767930
A.resiliens	RD126b	R.J.Dyer	Mexico, Queretaro	JQ767690	JQ767808	JQ767931
A.resiliens	RD127	R.J.Dyer	Mexico, Queretaro	JQ767691	JQ767809	-
A.resiliens	RD128	R.J.Dyer	Mexico, Queretaro	JQ767692	JQ767810	JQ767932
A.resiliens	RD129	R.J.Dyer	Mexico, Queretaro	JQ767693	JQ767811	JQ767933
A.soleirolioides	RD71	R.J.Dyer	Mexico, Guerrero	JQ767694	JQ767812	JQ767934
A.soleirolioides	RD82	R.J.Dyer	Mexico, Oaxaca	JQ767695	-	JQ767935
A.soleirolioides	RD114	R.J.Dyer	Mexico, Mexico DF	JQ767696	JQ767813	JQ767936
Sec.nov.1	JM1339	J.Monterosa	El Salvador	JQ767697	JQ767814	JQ767937
Spec.nov.2	SK10151	S.Knapp	El Salvador	JQ767698	JQ767815	JQ767938

Table A2. Nuclear clone information for nuclear *pgiC* dataset and accession numbers for all clones. Phylogenetic analysis was carried out with reduced datasets with single sequences per unique nuclear copies per specimen. This table shows which clones were designated as unique clones and which were not included in the final analysis. These unique clone sequences are indicated by the presence of values in the unique copy/total copies column. This column shows the unique nuclear copy number and the total number of unique nuclear copies found within the specimen. Each *pgiC* clone has a separate accession number.

Species	Voucher	Clone number	Unique copy/ total copies	Genbank accession number
A.castaneum	RD46b	C1	1/2	JQ767182
A.castaneum	RD46b	C2	2/2	JQ767183
A.castaneum	RD46b	C3		JQ767184
A.castaneum	RD46b	C4		JQ767185
A.castaneum	RD46b	C5		JQ767186
A.castaneum	RD46b	C6		JQ767187
A.castaneum	RD46b	C7		JQ767188

A.castaneum	RD46b	C8		JQ767189
A.castaneum	RD47	C1	1/2	JQ767190
A.castaneum	RD47	C2	2/2	JQ767191
A.castaneum	RD47	C3		JQ767192
A.castaneum	RD47	C4		JQ767193
A.castaneum	RD47	C5		JQ767194
A.castaneum	RD47	C6		JQ767195
A.castaneum	RD47	C7		JQ767196
A.castaneum	RD47	C8		JQ767197
A.castaneum	RD49	C1	1/1	JQ767198
A.castaneum	RD49	C2		JQ767199
A.castaneum	RD49	C3		JQ767200
A.castaneum	RD49	C4		JQ767201
A.castaneum	RD49	C5		JQ767202
A.castaneum	RD49	C6		JQ767203
A.castaneum	RD49	C7		JQ767204
A.castaneum	RD49	C8		JQ767205
A.castaneum	RD52	C1	1/2	JQ767206
A.castaneum	RD52	C2	2/2	JQ767207
A.castaneum	RD52	C3		JQ767208
A.castaneum	RD52	C4		JQ767209
A.castaneum	RD52	C5		JQ767210
A.castaneum	RD52	C6		JQ767211
A.castaneum	RD54	C1		JQ767212
A.fibrillosum	RD10b	C1	1/4	JQ767213
A.fibrillosum	RD10b	C2	2/4	JQ767214
A.fibrillosum	RD10b	C3	3/4	JQ767215
A.fibrillosum	RD10b	C4	4/4	JQ767216
A.fibrillosum	RD10b	C5		JQ767217
A.fibrillosum	RD10b	C6		JQ767218
A.fibrillosum	RD10b	C7		JQ767219
A.fibrillosum	RD10b	C8		JQ767220
A.fibrillosum	RD22	C1	1/2	JQ767221
A.fibrillosum	RD22	C2	2/2	JQ767222
A.fibrillosum	RD22	C3		JQ767223
A.fibrillosum	RD22	C4		JQ767224
A.fibrillosum	RD22	C5		JQ767225
A.fibrillosum	RD22	C6		JQ767226
A.fibrillosum	RD22	C7		JQ767227
A.fibrillosum	RD22	C8		JQ767228
A.formosum	ES1398	C1	1/1	JQ767229
A.formosum	ES1398	C2		JQ767230
A.formosum	ES1398	C3		JQ767231
A.formosum	ES1398	C4		JQ767232
A.formosum	IJ2436	C1	1/1	JQ767233
A.formosum	IJ2436	C2		JQ767234
A.formosum	MK12699	C1	1/2	JQ767235
A.formosum	MK12699	C2	2/2	JQ767236
A.formosum	MK12699	C3		JQ767237
A.formosum	RD27	C1	1/1	JQ767238
A.formosum	RD27	C2		JQ767239
A.formosum	RD27	C3		JQ767240
A.formosum	RD27	C4		JQ767241
A.formosum	RD27	C5		JQ767242
A.formosum	RD27	C6		JQ767243
A.formosum	RD28	C1	1/2	JQ767244
A.formosum	RD28	C2	2/2	JQ767245
A.formosum	RD28	C3		JQ767246

A.formosum	RD28	C4		JQ767247
A.formosum	RD28	C5		JQ767248
A.formosum	RD28	C6		JQ767249
A.formosum	RD28	C7		JQ767250
A.formosum	RD33	C1	1/1	JQ767251
*A.*aff.*hallbergii*	RD85	C1	1/4	JQ767252
*A.*aff.*hallbergii*	RD85	C2	2/4	JQ767253
*A.*aff.*hallbergii*	RD85	C3	3/4	JQ767254
*A.*aff.*hallbergii*	RD85	C4	4/4	JQ767255
*A.*aff.*hallbergii*	RD85	C5		JQ767256
*A.*aff.*hallbergii*	RD85	C6		JQ767257
*A.*aff.*hallbergii*	RD85	C7		JQ767258
*A.*aff.*hallbergii*	RD90	C1	1/3	JQ767259
*A.*aff.*hallbergii*	RD90	C2	2/3	JQ767260
*A.*aff.*hallbergii*	RD90	C3	3/3	JQ767261
*A.*aff.*hallbergii*	RD90	C4		JQ767262
*A.*aff.*hallbergii*	RD90	C5		JQ767263
*A.*aff.*hallbergii*	RD90	C6		JQ767264
*A.*aff.*hallbergii*	RD90	C7		JQ767265
*A.*aff.*hallbergii*	RD90	C8		JQ767266
A.hallbergii	RD18	C1	1/3	JQ767267
A.hallbergii	RD18	C2	2/3	JQ767268
A.hallbergii	RD18	C3	3/3	JQ767269
A.hallbergii	RD18	C4		JQ767270
A.hallbergii	RD18	C5		JQ767271
A.hallbergii	RD18	C6		JQ767272
A.hallbergii	RD18	C7		JQ767273
A.hallbergii	RD23	C1	1/3	JQ767274
A.hallbergii	RD23	C2	2/3	JQ767275
A.hallbergii	RD23	C3	3/3	JQ767276
A.hallbergii	RD23	C4		JQ767277
A.hallbergii	RD23	C5		JQ767278
A.hallbergii	RD23	C6		JQ767279
A.hallbergii	RD23	C7		JQ767280
A.hallbergii	RD23	C8		JQ767281
A.hallbergii	RD81	C1	1/3	JQ767282
A.hallbergii	RD81	C2	2/3	JQ767283
A.hallbergii	RD81	C3	3/3	JQ767284
A.hallbergii	RD81	C4		JQ767285
A.hallbergii	RD81	C5		JQ767286
A.hallbergii	RD81	C6		JQ767287
A.hallbergii	RD81	C7		JQ767288
A.hallbergii	RD81	C8		JQ767289
A.hallbergii	RD111	C1	1/3	JQ767290
A.hallbergii	RD111	C2	2/3	JQ767291
A.hallbergii	RD111	C3	3/3	JQ767292
A.hallbergii	RD111	C4		JQ767293
A.hallbergii	RD111	C5		JQ767294
A.hallbergii	RD111	C6		JQ767295
A.hallbergii	RD111	C7		JQ767296
A.hallbergii	RD112	C1	1/3	JQ767297
A.hallbergii	RD112	C2	2/3	JQ767298
A.hallbergii	RD112	C3	3/3	JQ767299
A.hallbergii	RD112	C4		JQ767300
A.hallbergii	RD112	C5		JQ767301
A.hallbergii	RD112	C6		JQ767302
A.hallbergii	RD112	C7		JQ767303
A.hallbergii	RD136	C1	1/2	JQ767304

A.hallbergii	RD136	C2	2/2	JQ767305
A.hallbergii	RD136	C3		JQ767306
A.hallbergii	RD136	C4		JQ767307
A.hallbergii	RD136	C5		JQ767308
A.hallbergii	RD136	C6		JQ767309
A.hallbergii	RD136	C7		JQ767310
*A.*aff.*heterochroum*	RD9a	C1	1/2	JQ767311
*A.*aff.*heterochroum*	RD9a	C2	2/2	JQ767313
*A.*aff.*heterochroum*	RD9a	C3		JQ767312
*A.*aff.*heterochroum*	RD9a	C4		JQ767314
*A.*aff.*heterochroum*	RD9a	C5		JQ767315
*A.*aff.*heterochroum*	RD9a	C6		JQ767316
*A.*aff.*heterochroum*	RD9a	C7		JQ767317
*A.*aff.*heterochroum*	RD9a	C8		JQ767318
*A.*aff.*heterochroum*	RD75	C1	1/1	JQ767319
*A.*aff.*heterochroum*	RD75	C2		JQ767320
A.monanthes	ALG08-145	C1	1/3	JQ767321
A.monanthes	ALG08-145	C2	2/3	JQ767322
A.monanthes	ALG08-145	C3	3/3	JQ767323
A.monanthes	ALG08-145	C4		JQ767324
A.monanthes	ALG08-145	C5		JQ767325
A.monanthes	ALG08-145	C6		JQ767326
A.monanthes	ALG08-145	C7		JQ767327
A.monanthes	ALG08-145	C8		JQ767328
A.monanthes	RD1a	C1	1/2	JQ767329
A.monanthes	RD1a	C2	2/2	JQ767330
A.monanthes	RD1a	C3		JQ767331
A.monanthes	RD1a	C4		JQ767332
A.monanthes	RD2a	C1	1/3	JQ767333
A.monanthes	RD2a	C2	2/3	JQ767334
A.monanthes	RD2a	C3	3/3	JQ767335
A.monanthes	RD2a	C4		JQ767336
A.monanthes	RD2a	C5		JQ767337
A.monanthes	RD8a	C1	1/2	JQ767338
A.monanthes	RD8a	C2	2/2	JQ767339
A.monanthes	RD8a	C3		JQ767340
A.monanthes	RD8a	C4		JQ767341
A.monanthes	RD8a	C5		JQ767342
A.monanthes	RD8a	C6		JQ767343
A.monanthes	RD10a	C1	1/2	JQ767344
A.monanthes	RD10a	C2	2/3	JQ767345
A.monanthes	RD10a	C3	3/3	JQ767346
A.monanthes	RD10a	C4		JQ767347
A.monanthes	RD10a	C5		JQ767348
A.monanthes	RD16	C1	1/3	JQ767349
A.monanthes	RD16	C2	2/3	JQ767350
A.monanthes	RD16	C3	3/3	JQ767351
A.monanthes	RD16	C4		JQ767352
A.monanthes	RD16	C5		JQ767353
A.monanthes	RD16	C6		JQ767354
A.monanthes	RD16	C7		JQ767355
A.monanthes	RD16	C8		JQ767356
A.monanthes	RD17	C1	1/2	JQ767357
A.monanthes	RD17	C2	2/2	JQ767358
A.monanthes	RD17	C3		JQ767359
A.monanthes	RD17	C4		JQ767360
A.monanthes	RD17	C5		JQ767361
A.monanthes	RD17	C6		JQ767362

A.monanthes	RD17	C7		JQ767363
A.monanthes	RD17	C8		JQ767364
A.monanthes	RD19	C1	1/3	JQ767365
A.monanthes	RD19	C2	2/3	JQ767366
A.monanthes	RD19	C3	3/3	JQ767367
A.monanthes	RD19	C4		JQ767368
A.monanthes	RD19	C5		JQ767369
A.monanthes	RD19	C6		JQ767370
A.monanthes	RD19	C7		JQ767371
A.monanthes	RD19	C8		JQ767372
A.monanthes	RD20	C1	1/2	JQ767373
A.monanthes	RD20	C2	2/2	JQ767374
A.monanthes	RD24	C1	1/2	JQ767375
A.monanthes	RD24	C2	2/2	JQ767376
A.monanthes	RD24	C3		JQ767377
A.monanthes	RD24	C4		JQ767378
A.monanthes	RD24	C5		JQ767379
A.monanthes	RD24	C6		JQ767380
A.monanthes	RD24	C7		JQ767381
A.monanthes	RD24	C8		JQ767382
A.monanthes	RD25	C1	1/3	JQ767383
A.monanthes	RD25	C2	2/3	JQ767384
A.monanthes	RD25	C3	3/3	JQ767385
A.monanthes	RD25	C4		JQ767386
A.monanthes	RD25	C5		JQ767387
A.monanthes	RD25	C6		JQ767388
A.monanthes	RD25	C7		JQ767389
A.monanthes	RD25	C8		JQ767390
A.monanthes	RD26	C1	1/3	JQ767391
A.monanthes	RD26	C2	2/3	JQ767392
A.monanthes	RD26	C3	3/3	JQ767393
A.monanthes	RD26	C4		JQ767394
A.monanthes	RD26	C5		JQ767395
A.monanthes	RD26	C6		JQ767396
A.monanthes	RD26	C7		JQ767397
A.monanthes	RD26	C8		JQ767398
A.monanthes	RD28b	C1	1/3	JQ767399
A.monanthes	RD28b	C2	2/3	JQ767400
A.monanthes	RD28b	C3	3/3	JQ767401
A.monanthes	RD28b	C4		JQ767402
A.monanthes	RD28b	C5		JQ767403
A.monanthes	RD28b	C6		JQ767404
A.monanthes	RD28b	C7		JQ767405
A.monanthes	RD28b	C8		JQ767406
A.monanthes	RD45	C1	1/2	JQ767407
A.monanthes	RD45	C2	2/2	JQ767408
A.monanthes	RD45	C3		JQ767409
A.monanthes	RD45	C4		JQ767410
A.monanthes	RD45	C5		JQ767411
A.monanthes	RD53	C1	1/2	JQ767412
A.monanthes	RD53	C2	2/2	JQ767413
A.monanthes	RD74	C1	1/2	JQ767414
A.monanthes	RD74	C2	2/2	JQ767415
A.monanthes	RD74	C3		JQ767416
A.monanthes	RD74	C4		JQ767417
A.monanthes	RD74	C5		JQ767418
A.monanthes	RD74	C6		JQ767419
A.monanthes	RD76	C1	1/3	JQ767420

A.monanthes	RD76	C2	2/3	JQ767421
A.monanthes	RD76	C3	3/3	JQ767422
A.monanthes	RD76	C4		JQ767423
A.monanthes	RD76	C5		JQ767424
A.monanthes	RD76	C6		JQ767425
A.monanthes	RD80	C1	1/3	JQ767426
A.monanthes	RD80	C2	2/3	JQ767427
A.monanthes	RD80	C3	3/3	JQ767428
A.monanthes	RD80	C4		JQ767429
A.monanthes	RD80	C5		JQ767430
A.monanthes	RD80	C6		JQ767431
A.monanthes	RD97	C1	1/2	JQ767432
A.monanthes	RD97	C2	2/2	JQ767433
A.monanthes	RD97	C3		JQ767434
A.monanthes	RD97	C4		JQ767435
A.monanthes	RD97	C5		JQ767436
A.monanthes	RD97	C6		JQ767437
A.monanthes	RD97	C7		JQ767438
A.monanthes	RD99	C1	1/3	JQ767439
A.monanthes	RD99	C2	2/3	JQ767440
A.monanthes	RD99	C3	3/3	JQ767441
A.monanthes	RD99	C4		JQ767442
A.monanthes	RD99	C5		JQ767443
A.monanthes	RD99	C6		JQ767444
A.monanthes	RD110	C1	1/3	JQ767445
A.monanthes	RD110	C2	2/3	JQ767446
A.monanthes	RD110	C3	3/3	JQ767447
A.monanthes	RD110	C4		JQ767448
A.monanthes	RD110	C5		JQ767449
A.monanthes	RD117a	C1	1/3	JQ767450
A.monanthes	RD117a	C2	2/3	JQ767451
A.monanthes	RD117a	C3	3/3	JQ767452
A.monanthes	RD117a	C4		JQ767453
A.monanthes	RD117a	C5		JQ767454
A.palmeri	CJR2494	C1	1/3	JQ767455
A.palmeri	CJR2494	C2	2/3	JQ767456
A.palmeri	CJR2494	C3	3/3	JQ767457
A.palmeri	CJR2494	C4		JQ767458
A.palmeri	CJR2494	C5		JQ767459
A.palmeri	CJR2494	C6		JQ767460
A.palmeri	CJR2494	C7		JQ767461
A.palmeri	RD130	C1	1/1	JQ767462
A.palmeri	RD130	C2		JQ767463
A.palmeri	RD130	C3		JQ767464
A.palmeri	RD130	C4		JQ767465
A.palmeri	RD130	C5		JQ767466
A.polyphyllum	ALG08-146	C1	1/1	JQ767467
A.polyphyllum	ALG08-146	C2		JQ767468
A.polyphyllum	ALG08-146	C3		JQ767469
A.polyphyllum	ALG08-146	C4		JQ767470
A.polyphyllum	ALG08-146	C5		JQ767471
A.polyphyllum	ALG08-146	C6		JQ767472
A.polyphyllum	ALG08-146	C7		JQ767473
A.polyphyllum	ALG08-146	C8		JQ767474
A.polyphyllum	Mehltreter	C1	1/1	JQ767475
A.polyphyllum	Mehltreter	C2		JQ767476
A.polyphyllum	Mehltreter	C3		JQ767477
A.polyphyllum	Mehltreter	C4		JQ767478

A.polyphyllum	Mehltreter	C5		JQ767479
A.polyphyllum	Mehltreter	C6		JQ767480
A.polyphyllum	Mehltreter	C7		JQ767481
A.polyphyllum	Mehltreter	C8		JQ767482
A.polyphyllum	RD95	C1	1/2	JQ767483
A.polyphyllum	RD95	C2	2/2	JQ767484
A.polyphyllum	RD95	C3		JQ767485
A.polyphyllum	RD95	C4		JQ767486
A.polyphyllum	RD95	C5		JQ767487
A.polyphyllum	RD95	C6		JQ767488
A.polyphyllum	RD95	C7		JQ767489
A.polyphyllum	RD95	C8		JQ767490
A.polyphyllum	RD98	C1	1/1	JQ767491
A.polyphyllum	RD98	C2		JQ767492
A.polyphyllum	RD98	C3		JQ767493
A.polyphyllum	RD98	C4		JQ767494
A.polyphyllum	RD98	C5		JQ767495
A.polyphyllum	RD98	C6		JQ767496
A.polyphyllum	RD98	C7		JQ767497
A.polyphyllum	RD115	C1	1/2	JQ767498
A.polyphyllum	RD115	C2	2/2	JQ767499
A.polyphyllum	RD115	C3		JQ767500
A.polyphyllum	RD115	C4		JQ767501
A.polyphyllum	RD115	C5		JQ767502
A.polyphyllum	RD115	C6		JQ767503
A.polyphyllum	RD115	C7		JQ767504
A.polyphyllum	RD115	C8		JQ767505
A.resiliens	CJR2504	C1	1/3	JQ767506
A.resiliens	CJR2504	C2	2/3	JQ767507
A.resiliens	CJR2504	C3	3/3	JQ767508
A.resiliens	CJR2504	C4		JQ767509
A.resiliens	CJR2504	C5		JQ767510
A.resiliens	CJR2504	C6		JQ767511
A.resiliens	RD3b	C1	1/2	JQ767512
A.resiliens	RD3b	C2	2/2	JQ767513
A.resiliens	RD3b	C3		JQ767514
A.resiliens	RD3b	C4		JQ767515
A.resiliens	RD4a	C1	1/2	JQ767516
A.resiliens	RD4a	C2	2/2	JQ767517
A.resiliens	RD4a	C3		JQ767518
A.resiliens	RD4a	C4		JQ767519
A.resiliens	RD4a	C5		JQ767520
A.resiliens	RD4a	C6		JQ767521
A.resiliens	RD63	C1	1/3	JQ767522
A.resiliens	RD63	C2	2/3	JQ767523
A.resiliens	RD63	C3	3/3	JQ767524
A.resiliens	RD63	C4		JQ767525
A.resiliens	RD63	C5		JQ767526
A.resiliens	RD63	C6		JQ767527
A.resiliens	RD63	C7		JQ767528
A.resiliens	RD63	C8		JQ767529
A.resiliens	RD72	C1	1/2	JQ767530
A.resiliens	RD72	C2	2/2	JQ767531
A.resiliens	RD72	C3		JQ767532
A.resiliens	RD72	C4		JQ767533
A.resiliens	RD72	C5		JQ767534
A.resiliens	RD121	C1	1/2	JQ767535
A.resiliens	RD121	C2	2/2	JQ767536

A.resiliens	RD121	C3		JQ767537
A.resiliens	RD127	C1	1/2	JQ767538
A.resiliens	RD127	C2	2/2	JQ767539
A.resiliens	RD127	C3		JQ767540
A.resiliens	RD127	C4		JQ767541
A.resiliens	RD127	C5		JQ767542
A.resiliens	RD127	C6		JQ767543
A.resiliens	RD127	C7		JQ767544
A.resiliens	RD128	C1	1/3	JQ767545
A.resiliens	RD128	C2	2/3	JQ767546
A.resiliens	RD128	C3	3/3	JQ767547
A.resiliens	RD128	C4		JQ767548
A.resiliens	RD128	C5		JQ767549
A.soleirolioides	RD71	C1	1/2	JQ767550
A.soleirolioides	RD71	C2	2/2	JQ767551
A.soleirolioides	RD71	C3		JQ767552
Spec.nov.1	JM1339	C1	1/2	JQ767553
Spec.nov.1	JM1339	C2	2/2	JQ767554
Spec.nov.1	JM1339	C3		JQ767555
Spec.nov.1	JM1339	C4		JQ767556
Spec.nov.1	JM1339	C5		JQ767557
Spec.nov.1	JM1339	C6		JQ767558
Spec.nov.2	SK10151	C1	1/1	JQ767559
Spec.nov.2	SK10151	C2		JQ767560
Spec.nov.2	SK10151	C3		JQ767561
Spec.nov.2	SK10151	C4		JQ767562
Spec.nov.2	SK10151	C5		JQ767563
Spec.nov.2	SK10151	C6		JQ767564
Spec.nov.2	SK10151	C7		JQ767565
Spec.nov.2	SK10151	C8		JQ767566

Table A3. Haplotype information for combined plastid dataset. Phylogenetic analysis was carried out with reduced datasets of a single representative per haplotype. Haplotypes that are represented by their corresponding single voucher numbers are show here.

Haplotype	Taxa	Vouchers
RD46b	*A.castaneum*	RD46a
	A.castaneum	RD91
	A.castaneum	RD113a
	A.castaneum	RD116
RD95	*A.polyphyllum*	AM5249
RD49	*A.castaneum*	RD46c
	A.castaneum	RD48
	A.castaneum	RD50b
RD9a	*A.heterochroum*	ML601
	A.resiliens	ES428
RD63	*A.resiliens*	CJR08-025
	A.resiliens	RD64
	A.resiliens	RD107
	A.resiliens	RD126b
	A.resiliens	RD129

	A.monanthes	RD32
	A.monanthes	RD88a
RD28b	*A.monanthes*	RD101b
	A.monanthes	RD104
	A.monanthes	RD70a
	A.monanthes	RD94
RD117a	*A.monanthes*	RD73a
RD80	*A.monanthes*	RD89
RD2a	*A.monanthes*	RD103
	A.monanthes	RD126a
	A.monanthes	RD132
	A.monanthes	THO2660
	A.monanthes	THO2743
	A.monanthes	PA14
	A.monanthes	Heiko2
RJ11	*A.monanthes*	RD20
RD19	*A.monanthes*	RD131
	A.monanthes	RD41
	A.monanthes	RD102
RD24	*A.monanthes*	RD125
	A.monanthes	ES462
	A.monanthes	LJ03-38
ALG08-145	*A.monanthes*	RD83
	A.monanthes	RD92
	A.monanthes	RD96
	A.monanthes	RD119
	A.monanthes	RD135
	A.monanthes	RD137
	A.hallbergii	MK13519
	A.hallbergii	RD101a
RD23	*A.hallbergii*	RD120
	A.hallbergii	RD138

Table A4. Information on the phylogenetic analyses of the different datasets. Samples = number of specimens/ sequences included; Nucleotides = maximum number of base-pairs per sequence; results of JModeltest for datasets AIC and BIC criterion. Model abbreviations as in Posada (2008).

Dataset	Samples	Nucleotides	AIC	BIC
psbA-trnH	132	560	-	-
trnl- F1	123	946	-	-
rps4-trnS	117	1,047	-	-
Plastid combined	54	2,550	TVM+I	TPM3uf+G
pgiC 14FN-16RN	141	776	TPM1uf+I+G	HKY+I+G

Table A5. Summary table providing information on phylogenetic relations and counted spore number. Species classified as in Mickel & Smith (2004), voucher specimen as given Table S1. Plastid subclades are presented according to the combined analysis of the plastid regions. For specimens not included in this analysis, subclades are inferred from analysis of the individual plastid regions. Clone number = total number of nuclear clones sequenced. Copy number = total number of unique clones or nuclear copies per specimen (unique nuclear copies interpreted as different alleles, indicating the presence of multiple genomes, i.e. polyploidy). Nuclear copy sub-clade distribution = unique nuclear copy distribution according to sub-clade. Plastid = plastid sub-clade type. Sub-clades are labelled according to Fig. 2. Spore number per sporangium and number of sporangia sampled is given for each specimen sampled, NS indicates; no sporangia present and NPS indicates; no sporangia present and proliferous buds present.

Species	Voucher	Plastid	Clone number	Copy Number	Nuclear copy sub-clade distribution				Spore number	Sporangia counted
A.formosum	ES1398	pFO	4	1	nFO					
A.formosum	IJ2436	pFO	2	1	nFO					
A.formosum	MK12699	pFO	3	2	nFO	nFO				
A.formosum	LO20	pFO								
A.formosum	RD27	pFO	6	1	nFO				64	1
A.formosum	RD28	pFO	7	2	nFO	nFO			64	7
A.formosum	RD33	pFO	1	1	nFO				64	10
A.formosum	L2304	pFO								
A.blepharodes	JL4079	pFI								
A.fibrillosum	RD10b	pFI	8	4	nFI	nFI	nFI	nPA	64	1
A.fibrillosum	RD22	pFI	8	2	nFI	nFI			64	4
A.castaneum	RD46a	pCA2							64	2
A.castaneum	RD91	pCA2							64	5
A.castaneum	RD113a	pCA2							64	4
A.castaneum	RD116	pCA2							64	5
A.castaneum	RD46b	pCA2	8	2	nCA	nPO				
A.castaneum	RD46c	pCA1								
A.castaneum	RD47	pCA2	8	2	nCA	nPO			64	2
A.castaneum	RD48	pCA1							64	5
A.castaneum	RD49	pCA1	8	1	nSO				64	6
A.castaneum	RD50a	pCA1							64	2
A.castaneum	RD50b	pCA1							64	4
A.castaneum	RD52	pCA2	6	2	nCA	nPO			64	5
A.castaneum	RD54	pCA1	1	1	nCA				64	5
A.polyphyllum	AM5249	pPO								
A.polyphyllum	ALG08-146	pPO	8	1	nPO					
A.polyphyllum	ALG08-034	pPO								

A.polyphyllum	IJ809	pPO								
A.polyphyllum	MC5365	pPO								
A.polyphyllum	Mehlttreter	pPO	8	1	nPO					
A.polyphyllum	RD115	pPO	8	2	nPO	nSO			64	3
A.polyphyllum	RD95	pPO	8	2	nPO	nSO			64	3
A.polyphyllum	RD98	pPO	7	1	nPO				64	3
A.soleirolioides	RD114	pSO								
A.soleirolioides	RD71	pSO	8	2	nSO	nSO			32	3
A.soleirolioides	RD82	pSO							NWS	na
A.aff.heterochroum	RD9a	pPA	8	2	nPA	nPA			32	2
A.aff.heterochroum	RD75	pPA	2	1	nPA				32	3
A.heterochroum	ML601	pPA								
A.palmeri	RD130	pPA	5	1	nPA				NSP	NSP
A.resiliens	CJR2504	pPA	6	3	nRE1	nRE1	nPA			
A.resiliens	RD121	pRE1	3	2	nRE2	nRE2			32	3
A.resiliens	RD128	pRE1	5	3	nRE1	nRE2	nRE2		32	4
A.resiliens	RD4a	pRE1	6	2	nRE1	nRE2			32	5
A.resiliens	ES428	pRE2								
A.resiliens	ES459	pRE2								
A.resiliens	ES469	pRE2								
A.palmeri	ES486	pRE2								
A.resiliens	CJR08-025	pRE2								
A.palmeri	CJR2494	pRE2	7	3	nPA	nPA	nRE1			
A.resiliens	MDW3547	pRE2								
A.resiliens	RD107	pRE2							32	3
A.resiliens	RD126b	pRE2							32	6
A.resiliens	RD127	pRE2	7	2	nRE1	nRE2			32	3
A.resiliens	RD129	pRE2								
A.resiliens	RD3b	pRE2	4	2	nRE1	nRE2			32	2
A.resiliens	RD63	pRE2	8	3	nRE1	nRE1	nRE2		32	2
A.resiliens	RD64	pRE2							NS	NS
A.resiliens	RD72	pRE2	5	2	nRE1	nRE1			32	3
A.aff.hallbergii	RD85	pHA	7	4	nHA	nHA	nMO2	nMO2	32	4
A.aff.hallbergii	RD90	pHA	8	3	nHA	nHA	nMO2		32/64	11
A.hallbergii	MK13519	pHA								
A.hallbergii	RD18	pHA	7	3	nHA	nHA	nMO2		32	4
A.hallbergii	RD23	pHA	8	3	nHA	nHA	nHA		32	7
A.hallbergii	RD81	pHA	8	3	nHA	nHA	nMO2		32	6
A.hallbergii	RD93	pHA							32	10

A.hallbergii	RD101a	pHA						NS	NS
A.hallbergii	RD111	pHA	7	3	nHA	nHA	nMO2	32	12
A.hallbergii	RD112	pHA	7	3	nHA	nHA	nMO2	32	3
A.hallbergii	RD113b	pHA						32	1
A.hallbergii	RD120	pHA						32	1
A.hallbergii	RD136	pHA	7	2	nHA	nMO2		32	6
A.hallbergii	RD138	pHA						32	5
A.hallbergii	THO2730	pHA							
A.hallbergii	THO2731	pHA							
A.monanthes	CJR3673	pMO1							
A.monanthes	DT-D4945	pMO1							
A.monanthes	Heiko2	pMO1							
A.monanthes	IJ1269	pMO1							
A.monanthes	ML741	pMO1							
A.monanthes	PA14	pMO1							
A.monanthes	RD1a	pMO1	4	2	nMO1	nMO2		32	8
A.monanthes	RD2a	pMO1	5	3	nMO1	nMO1	nMO2	32	6
A.monanthes	RD8a	pMO1	6	2	nMO1	nMO2		32	1
A.monanthes	RD10a	pMO1	5	3	nMO1	nMO1	nMO2	32	2
A.monanthes	RD17	pMO1	8	2	nMO1	nMO2		32	3
A.monanthes	RD19	pMO1	8	3	nMO1	nMO1	nMO2	32	3
A.monanthes	RD20	pMO1	2	2	nMO1	nMO2		32	2
A.monanthes	RD21	pMO1						32	4
A.monanthes	RD25	pMO1	8	3	nMO1	nMO1	nMO2	NS	NS
A.monanthes	RD26	pMO1	8	3	nMO1	nMO1	nMO2	32	2
A.monanthes	RD28b	pMO1	8	3	nMO1	nMO1	nMO2	NS	NS
A.monanthes	RD29	pMO1						NS	NS
A.monanthes	RD30	pMO1						32	2
A.monanthes	RD32	pMO1						NSP	NSP
A.monanthes	RD70a	pMO1						32	3
A.monanthes	RD73a	pMO1						32	5
A.monanthes	RD74	pMO1	6	2	nMO1	nMO2		32	3
A.monanthes	RD76	pMO1	6	3	nMO1	nMO1	nMO2	32	2
A.monanthes	RD80	pMO1	6	3	nMO1	nMO1	nMO2	32	3
A.monanthes	RD88a	pMO1						32	5
A.monanthes	RD89	pMO1						32	3
A.monanthes	RD94	pMO1						32	4
A.monanthes	RD97	pMO1	6	2	nMO1	nMO2		32	5
A.monanthes	RD101b	pMO1						32	1

A.monanthes	RD103	pMO1						32	3
A.monanthes	RD104	pMO1						32	3
A.monanthes	RD110	pMO1	5	3	nMO1	nMO1	nMO2	32	4
A.monanthes	RD117a	pMO1	5	3	nMO1	nMO1	nMO2	NS	NS
A.monanthes	RD126a	pMO1							
A.monanthes	RD131	pMO1						32	2
A.monanthes	RD132	pMO1						32	1
A.monanthes	RJ11	pMO1							
A.monanthes	THO2660	pMO1							
A.monanthes	THO2743	pMO1							
A.monanthes	AM26	pMO2							
A.monanthes	ES462	pMO2							
A.monanthes	ALG08-145	pMO2	8	3	nMO2	nMO2	nMO2		
A.monanthes	IJ2419	pMO2							
A.monanthes	LJ03-38	pMO2							
A.monanthes	MADBU1	pMO2							
A.monanthes	MC5290	pMO2							
A.monanthes	RD16	pMO2	8	3	nMO2	nMO2	nMO2	NS	NS
A.monanthes	RD24	pMO2	8	2	nMO2	nMO2		32	1
A.monanthes	RD41	pMO2						32	3
A.monanthes	RD45	pMO2	5	2	nMO2	nMO2		32	1
A.monanthes	RD53	pMO2	2	2	nMO2	nMO2		32	6
A.monanthes	RD83a	pMO2							
A.monanthes	RD92	pMO2						32	3
A.monanthes	RD96	pMO2						32	6
A.monanthes	RD99	pMO2	6	3	nMO1	nMO2	nHA	32	3
A.monanthes	RD102	pMO2						32	2
A.monanthes	RD109	pMO2						32	4
A.monanthes	RD119a	pMO2							
A.monanthes	RD125a	pMO2						32	4
A.monanthes	RD135	pMO2						32	1
A.monanthes	RD137	pMO2						32	2
A.monanthes	THO2728	pMO2							
Spec.nov.1	JM1339	pSP1	6	2	nMO1	nMO1			
Spec.nov.2	SK10151	pSP2	8	1	nMO2				

Table A6. Table summarising voucher accessions, and plastid and nuclear subclade information for the hypothesised species forms presented in Fig. 4, and Appendix, Fig. A6. NC= Nuclear copy.

Terminal label	Voucher	Nuclear copy number	Plastid	NC1	NC2	NC3	NC4
A.formosum	IJ2436	1	pFO	nFO			
	ES1398	1	pFO	nFO			
	RD27	1	pFO	nFO			
	RD33	1	pFO	nFO			
	MK12699	2	pFO	nFO	nFO		
	RD28	2	pFO	nFO	nFO		
A.resiliens. R1	RD4a	2	pRE1	nRE1	nRE2		
	RD121	2	pRE1	nRE2	nRE2		
	RD128	3	pRE1	nRE1	nRE2	nRE2	
A.resiliens. R2	RD72	2	pRE2	nRE1	nRE1		
	RD127	2	pRE2	nRE1	nRE2		
	RD3b	2	pRE2	nRE1	nRE2		
	RD63	3	pRE2	nRE1	nRE1	nRE2	
A.palmeri. CJR2494	CJR2494	3	pRE2	nPA	nPA	nRE1	
A.resiliens. CJR2504	CJR2504	3	pPA	nRE1	nRE1	nPA	
A.palmeri	RD130	1	pPA	nPA			
*A.*aff.*heterochroum*	RD75	1	pPA	nPA			
	RD9a	2	pPA	nPA	nPA		
A.fibrillosum. RD10b	RD10b	4	pFI	nFI	nFI	nFI	nPA
A.fibrillosum. RD22	RD22	2	pFI	nFI	nFI		
A.soleirolioides	RD71	2	pSO	nSO	nSO		
A.castaneum. RD49	RD49	1	pCA1	nSO			
A.polyphyllum	RD115	2	pPO	nPO	nSO		
	RD95	2	pPO	nPO	nSO		
A.polyphyllum	ALG08-146	1	pPO	nPO			
	Mehlttreter	1	pPO	nPO			
	RD98	1	pPO	nPO			
A.castaneum	RD46b	2	pCA2	nCA	nPO		
	RD47	2	pCA2	nCA	nPO		
	RD52	2	pCA2	nCA	nPO		
A.castaneum. RD54	RD54	1	pCA1	nCA			
A.aff.hallbergii	RD90	3	pHA	nHA	nHA	nMO2	
	RD85	4	pHA	nHA	nHA	nMO2	nMO2
A.hallbergii	RD136	2	pHA	nHA	nMO2		
	RD18	3	pHA	nHA	nHA	nMO2	
	RD23	3	pHA	nHA	nHA	nHA	
	RD81	3	pHA	nHA	nHA	nMO2	
	RD111	3	pHA	nHA	nHA	nMO2	
	RD112	3	pHA	nHA	nHA	nMO2	
Spec.nov.2	SK10151	1	pSP2	nMO2			
A.monanthes. MO2	RD24	2	pMO2	nMO2	nMO2		
	RD45	2	pMO2	nMO2	nMO2		
	RD53	2	pMO2	nMO2	nMO2		
	ALG08-145	3	pMO2	nMO2	nMO2	nMO2	
	RD16	3	pMO2	nMO2	nMO2	nMO2	
A.monanthes. RD99	RD99	3	pMO2	nMO1	nMO2	nHA	
A.monanthes. MO1	RD1a	2	pMO1	nMO1	nMO2		
	RD8a	2	pMO1	nMO1	nMO2		
	RD17	2	pMO1	nMO1	nMO2		
	RD20	2	pMO1	nMO1	nMO2		
	RD74	2	pMO1	nMO1	nMO2		
	RD97	2	pMO1	nMO1	nMO2		

	RD2a	3	pMO1	nMO1	nMO1	nMO2
	RD10a	3	pMO1	nMO1	nMO1	nMO2
	RD19	3	pMO1	nMO1	nMO1	nMO2
	RD25	3	pMO1	nMO1	nMO1	nMO2
	RD26	3	pMO1	nMO1	nMO1	nMO2
	RD28b	3	pMO1	nMO1	nMO1	nMO2
	RD76	3	pMO1	nMO1	nMO1	nMO2
	RD80	3	pMO1	nMO1	nMO1	nMO2
	RD110	3	pMO1	nMO1	nMO1	nMO2
	RD117a	3	pMO1	nMO1	nMO1	nMO2
Spec.nov.1	JM1339	2	pSP1	nMO1	nMO1	

Table A7. Evidence for reproductive mode. Information given: Species, Voucher number, Apogamous growth = absent or present, plus position and stage of Apogamous growth, Number of samples studies, antheridia = absent or present, archegonia = absent or present, prothallus shape = shape of the mature prothallus. All observations are based on cultivated gametophytes. Callus = early stages of the apomictic sporophyte; locations: apical = outgrowth at or close to the gamtophyte meristem cell, basal = outgrowth at the basal (opposite to the meristem, close to the protonema), part of the prothallus, central = outgrowth along the central part of the prothallus. Apical extension and Apical Ext = an elongate extension originating from the prothallus meristem.

Species	Voucher	Apogamous growth	Sample number	Antheridia	Archegonia	Prothallus shape
A.formosum	RD28	Absent	4	Present	Present	Regular heart shaped
A.formosum	RD33	Absent	1	Present	Present	Regular heart shaped
A.hallbergii	RD118	Apical + central callus	5	Absent	Absent	Heart shaped, Long winged
A.hallbergii	RD93	Basal callus	5	Absent	Absent	Heart shaped, Long winged
*A.*aff.*hallbergii*	RD90	Central callus	2	Absent	Absent	Regular heart shaped with rough edges
A.monanthes	RD1a	Basal callus	9	Absent	Absent	Irregular shaped, callus-like
A.monanthes	RD101b	Basal callus	2	Absent	Absent	Heart shaped, Long winged
A.monanthes	RD103	Central callus	1	Absent	Absent	Regular heart shaped
A.monanthes	RD104	Central sporopyte	5	Absent	Absent	Regular heart shaped with rough edges
A.monanthes	RD110	Central callus	4	Absent	Absent	Heart shaped, slightly Long winged
A.monanthes	RD125a	Apical extension	3	Absent	Absent	Irregular shaped with long outgrowths
A.monanthes	RD132	Apical Ext + central callus	3	Absent	Absent	Irregular shaped with long outgrowths
A.monanthes	RD135	Apical Ext + central callus	5	Absent	Absent	Heart shaped, Long winged
A.monanthes	RD20	Basal callus	1	Absent	Absent	Abnormal with long outgrowths
A.monanthes	RD74	Central callus	8	Absent	Absent	Regular heart shaped with rough edges
A.monanthes	RD76	Apical Ext + central callus	3	Absent	Absent	Irregular shaped with long outgrowths
A.monanthes	RD89	Apical Ext + central callus	2	Absent	Absent	Irregular shaped with long outgrowths
A.monanthes	RD94	Apical extension	2	Absent	Absent	Irregular shaped with long outgrowths
A.resiliens	RD107	Apical extension	5	Absent	Absent	Heart shaped, Long winged
A.resiliens	RD127	Basal callus	1	Absent	Absent	Heart shaped, slightly Long winged
A.resiliens	RD128	Apical Ext + central callus	7	No	No	Heart shaped, slightly Long winged.
A.resiliens	RD63	Apical Ext + central callus	6	No	No	Heart shaped, Long winged
*A.*aff.*heterochroum*	RD75	Apical Ext + central callus	5	No	No	Heart shaped, Long winged
*A.*aff.*heterochroum*	RD9a	Central callus	6	No	No	Heart shaped, Long winged

Table A8. Summary of spore size measurements. Average spore length (μm) and width (μm), and standard deviations (S.D.) for each specimen measured. An average of 25 spores was measured for each specimen.

Species	Voucher	Length	Length S.D	Width	Width S.D
A.castaneum	RD50b	36.54	3.21	28.39	4.22
A.castaneum	RD54	42.33	4.2	34.1	3.78
A.castaneum	RD52	44.48	3.94	35.86	3.1
A.castaneum	RD49	44.91	4	36.29	3.21
A.castaneum	RD47	46.53	4.81	37.69	3.73
A.castaneum	MC5271	38.19	2.09	28.75	2.23
A.fibrillosum	RD22	44.34	3.77	34.85	4.75
A.fibrillosum	RD10b	47.9	8.14	37.97	6.57
A.formosum	RD28	27.85	1.26	20.64	1.25
A.formosum	RD33	32.2	3.8	25.02	4.52
*A.*aff.*halbergii*	RD90	43.32	3.1	30.45	3.39
*A.*aff.*halbergii*	RD85	44.97	4	31.86	2.31
A.hallbergii	RD81	39.15	5.01	27.07	3.27
A.hallbergii	RD137	39.97	2.15	27.25	3.41
A.hallbergii	RD112	44.91	3.15	32.84	3.29
A.hallbergii	RD118	45.73	3.38	32.71	1.78
A.hallbergii	RD136	46.6	3.51	30.57	2.66
A.hallbergii	RD125b	46.83	3.55	32.01	3.49
A.hallbergii	RD18	45.76	2.89	30.48	2.68
*A.*aff.*heterochroum*	RD75	37.43	3.19	25.89	1.92
*A.*aff.*heterochroum*	RD9a	38.62	3.35	27.83	3.87
A.heterochroum	ML601	39.5	4.5	26.51	3.29
A.monanthes	RD73	38.09	2.42	26.68	2.5
A.monanthes	RD70	39.03	3.35	28.47	2.85
A.monanthes	RD17	40.31	3.34	29.7	2.61
A.monanthes	RD117a	42.55	4.43	32.2	3.81
A.monanthes	RD74	44.44	3.14	33.57	3.44
A.monanthes	RD110	44.54	2.85	31.58	2.3
A.monanthes	RD20	45.53	3.38	32.08	2.83
A.monanthes	RD103	46.39	3.54	30.46	2.05
A.monanthes	RD2a	47.38	4.06	30.55	2.9
A.monanthes	RD80	43.15	4.53	31.56	3.53
A.monanthes	RD24	38.45	6.14	29.46	3.01
A.monanthes	RD16	40.18	2.35	26.63	1.87
A.monanthes	RD45	40.23	3.45	31.13	2.86
A.monanthes	RD41	40.4	2.5	29.11	1.48
A.monanthes	ALG08-145	44.87	2.9	29.77	2.68
A.monanthes	RD53	47.76	4.27	31.98	3.35
A.monanthes	RD99	48.54	5.88	34.72	4.75
Spec.nov.1	JM1339	31.26	2.61	21.42	1.15
Spec.nov.2	SK10151	29.22	2.03	20.77	2.04
A.polyphyllum	RD95	35.87	5.03	25.06	6.04
A.polyphyllum	RD116	37.32	2.18	27.79	2.18
A.polyphyllum	RD115	39.87	6.48	30.06	5.29
A.resiliens	RD63	42.39	2.93	28.54	1.77
A.resiliens	RD72	43.45	2.86	31.1	1.96
A.resiliens	RD121	39.78	2.65	28.17	1.84
A.resiliens	RD4a	44.7	4.71	29.11	3.44
A.soleirolioides	RD71	36.88	2.69	27.55	2.11

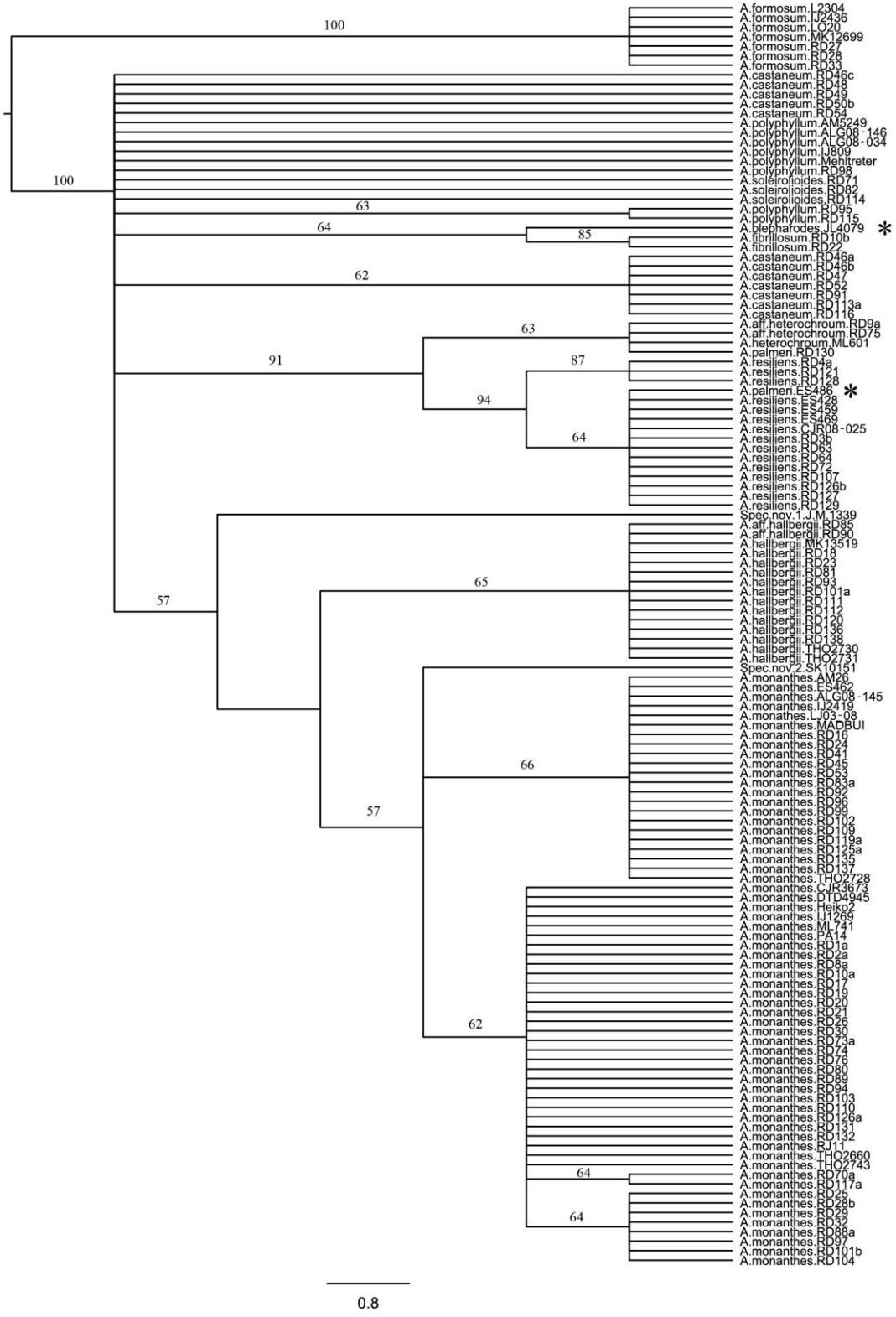

Figure A1. Phylogenetic analysis of the *psbA-trnH* intergenic spacer (IGS) region using maximum parsimony. Bootstrap values are shown above branches.Terminals are labelled with species name and voucher accession number. Stars symbols next to tip labels indicate taxanomic inconsistancies discussed in the results section.

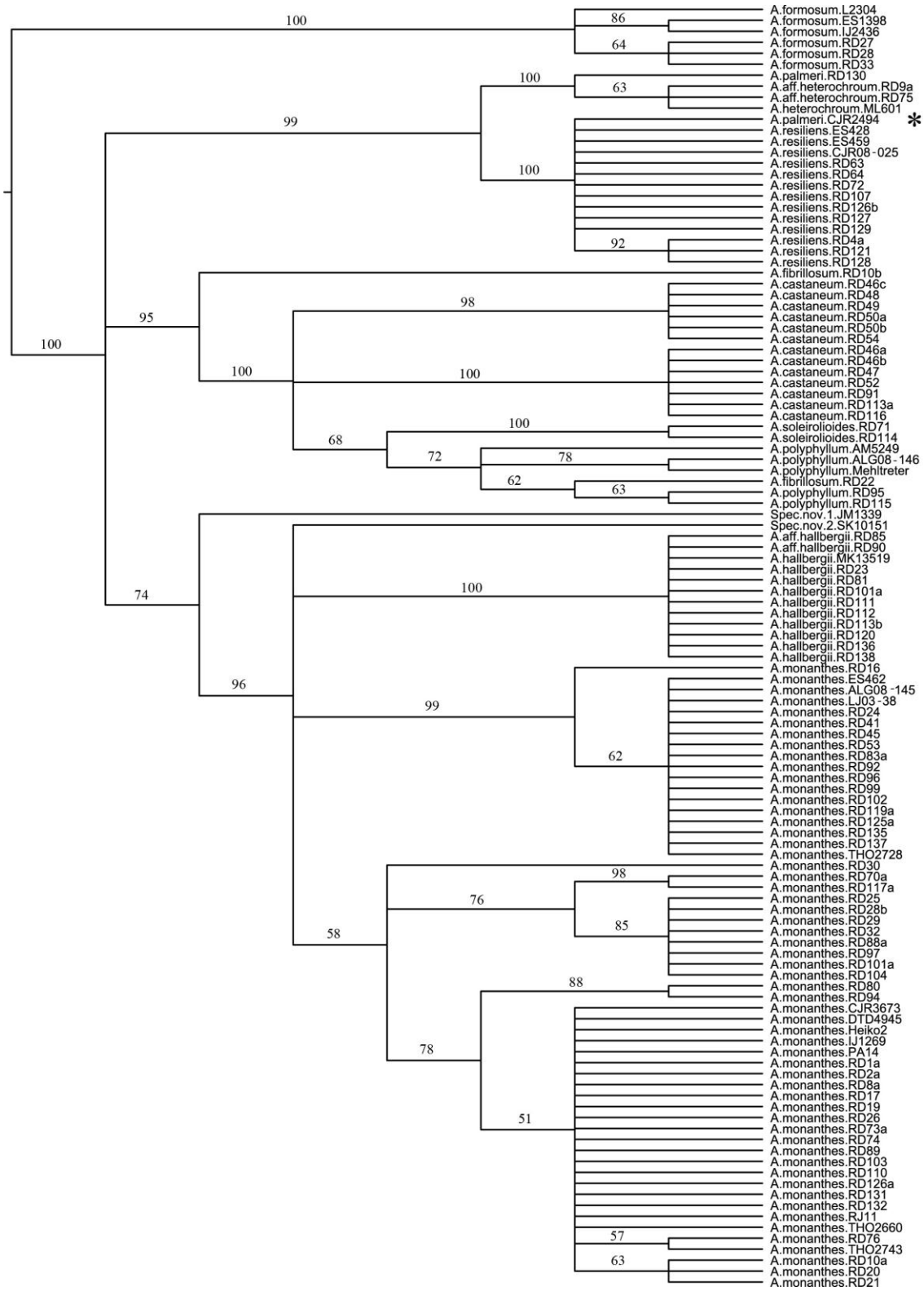

Figure A2. Phylogenetic analysis of the *rps4* plus *rps4-trnS IGS* region using maximum parsimony. Bootstrap values are shown above branches.Terminals are labelled with species name and voucher accession number. Stars symbols next to tip labels indicate taxanomic inconsistancies discussed in the results section.

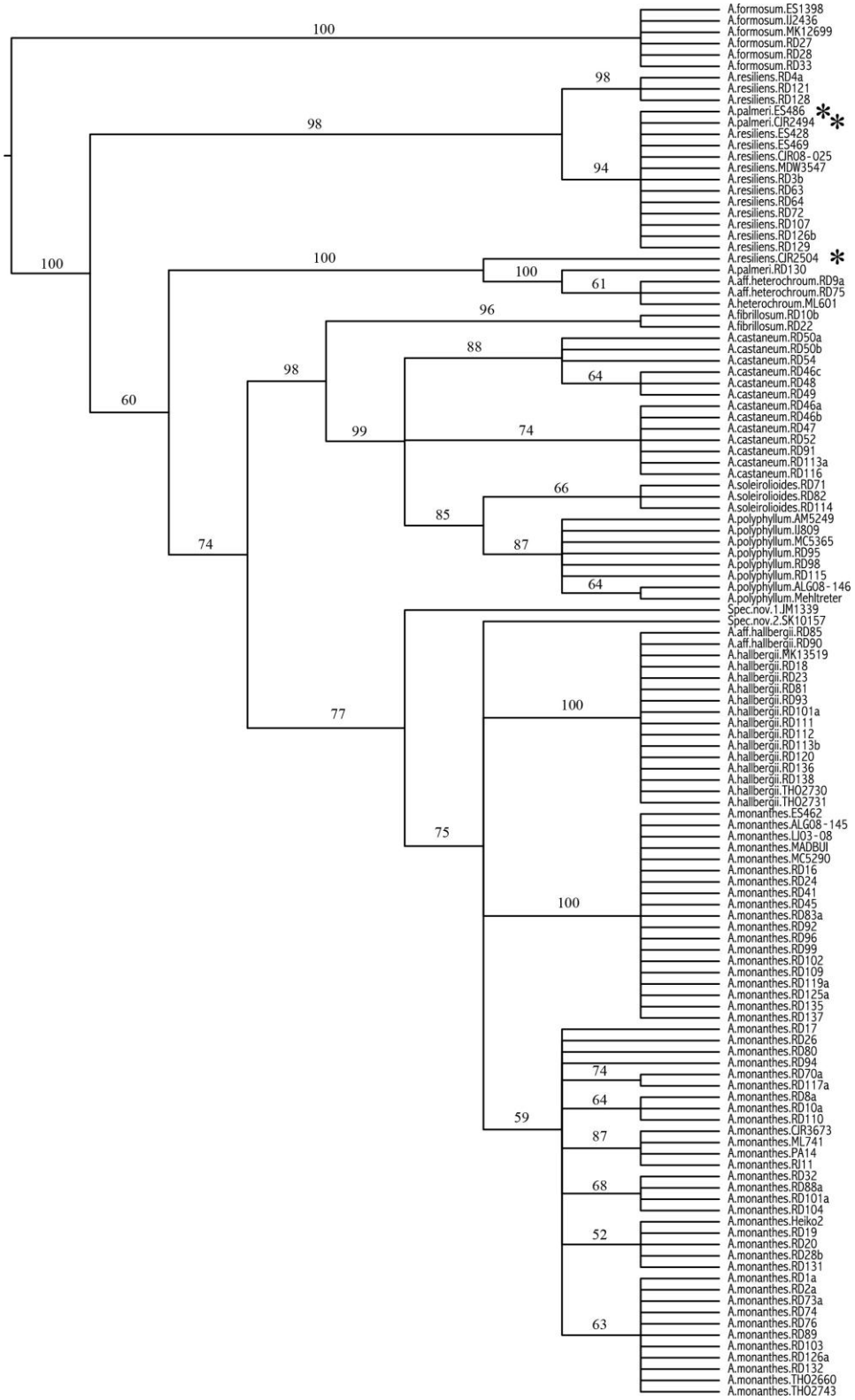

Figure A3. Phylogenetic analysis of the *trnL-trnF* region, including the *trnL* intron and the *trnL-trnF* IGS region, using maximum parsimony. Bootstrap values are shown above branches.Terminals are labelled with species name and voucher accession number. Stars symbols next to tip labels indicate taxanomic inconsistancies discussed in the results section.

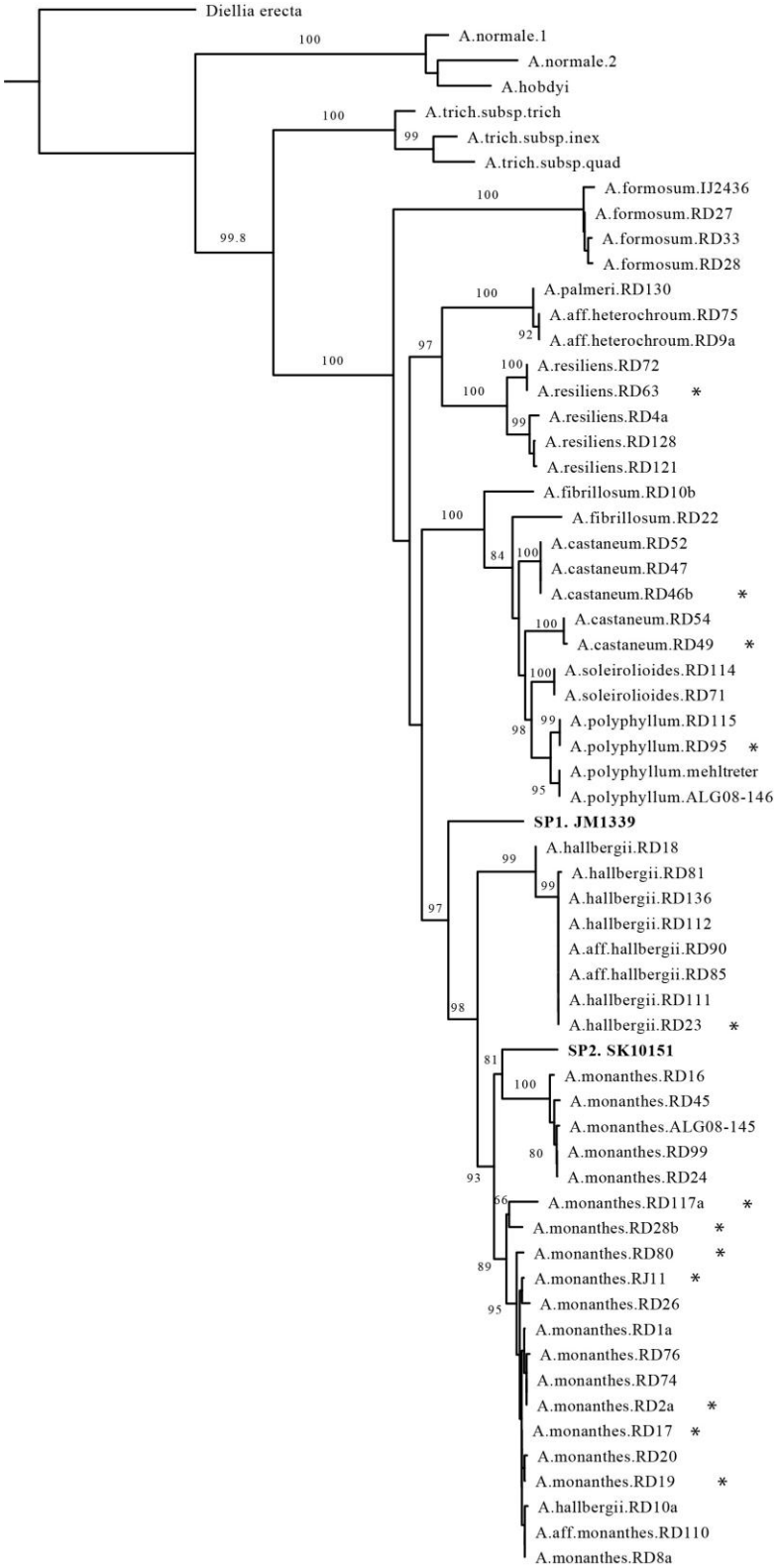

Figure A4. The phylogenetic hypotheses of the plastid sequence datasets of the *A.monanthes* complex as obtained by Maximum likelihood analysis of the combined plastid datasets of: *psbA-trnH*, *rps4*F-*trnS*, and *trnL–trnF* regions. Bootstrap support for values >50% are shown. Stars next to tip labels indicates nodes that represent multiple haplotypes (Appendix, Table A3).

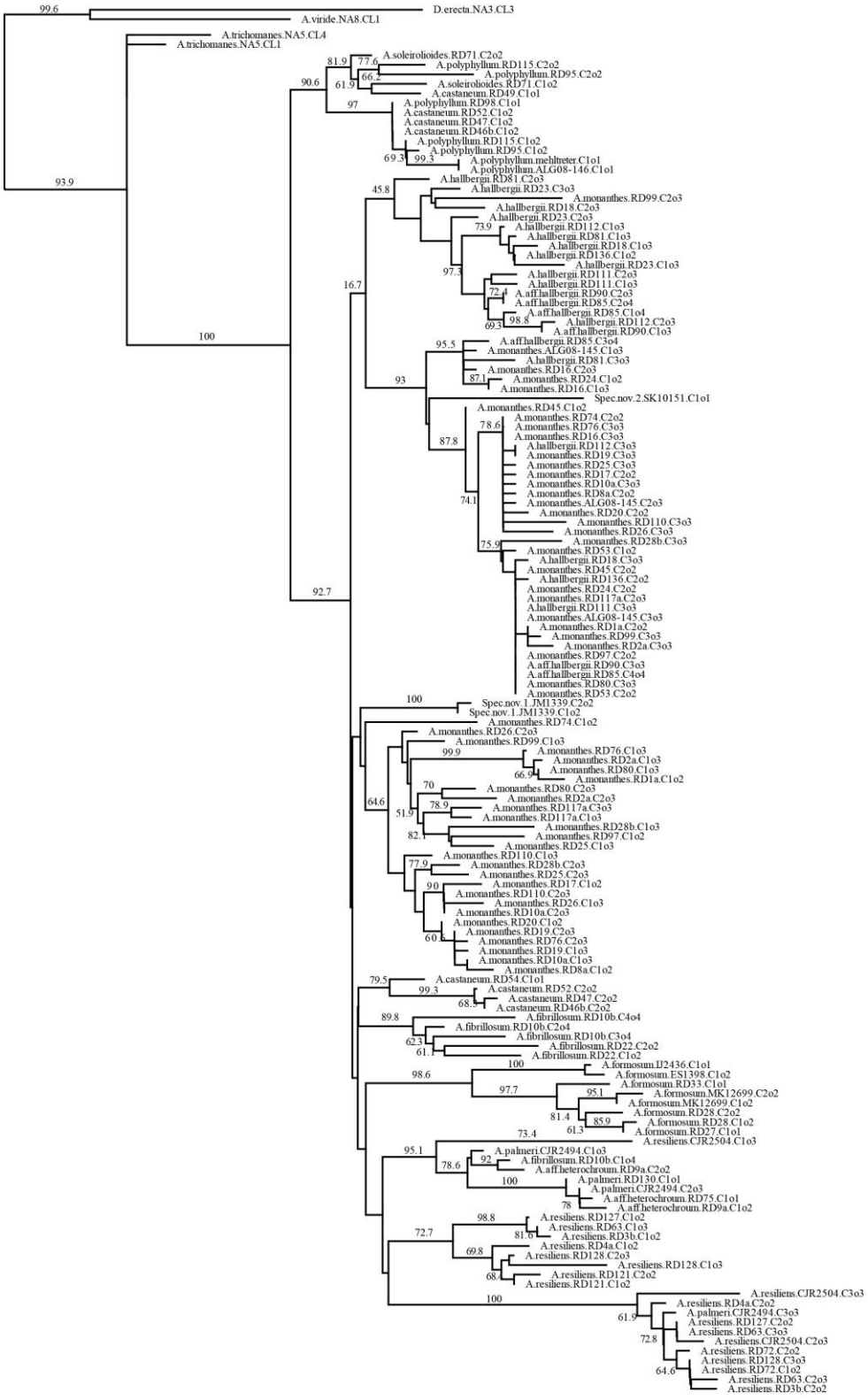

Figure A5. The phylogenetic hypotheses of the nuclear sequence dataset of the *A.monanthes* complex as obtained by Maximum likelihood analysis of the nuclear *pgiC14FN -16RN* region. Bootstrap support for values >50% are shown. Nuclear clone information is given in Appendix, Tables A2 and A6.

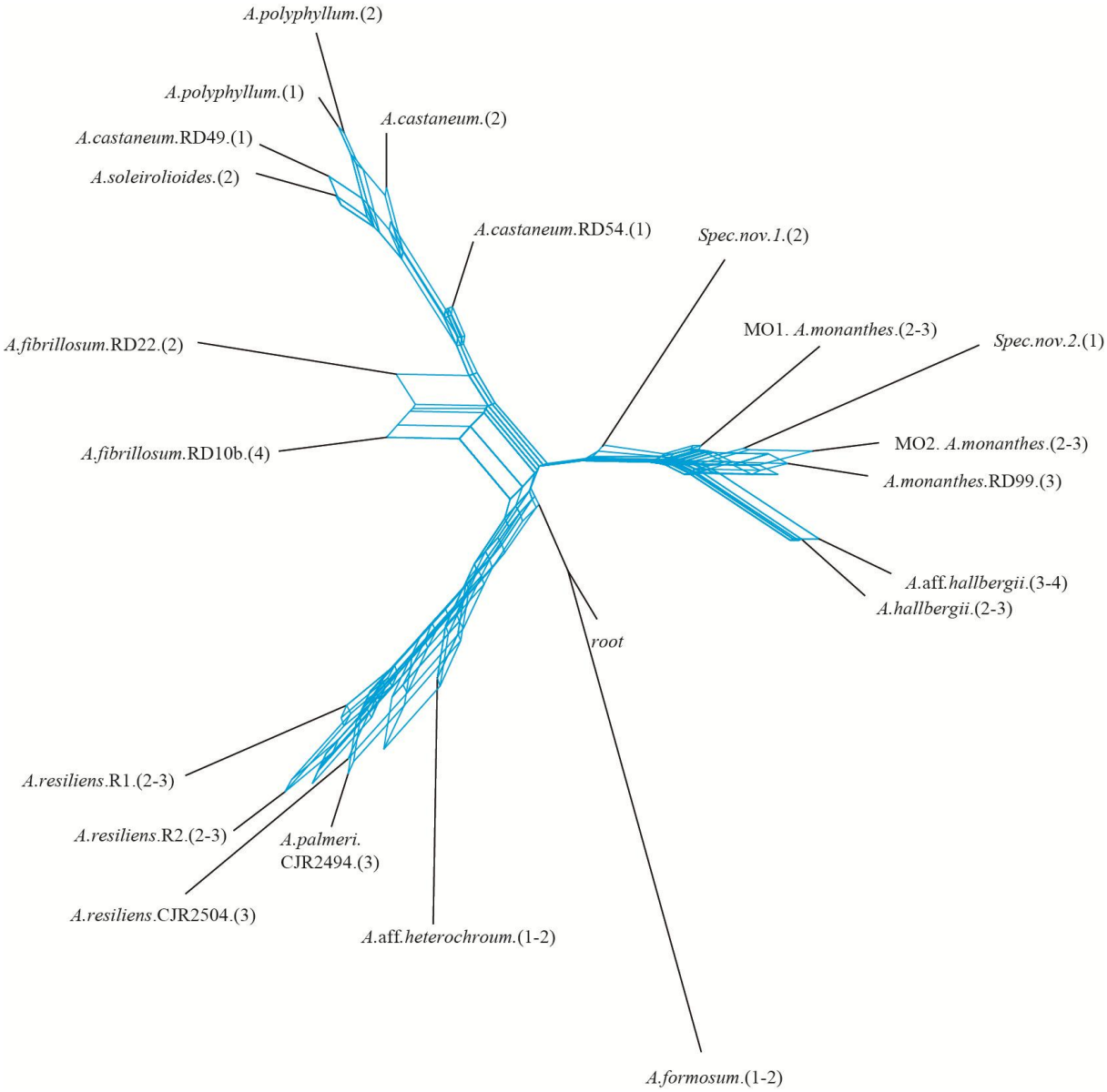

Figure A6. Hybridisation network computed in SplitsTree version 4.12.6 from ML consensus trees of plastid and nuclear datasets. Samples chosen based on unique combinations of plastid and nuclear copies observed within species (Appendix, Fig. A6).

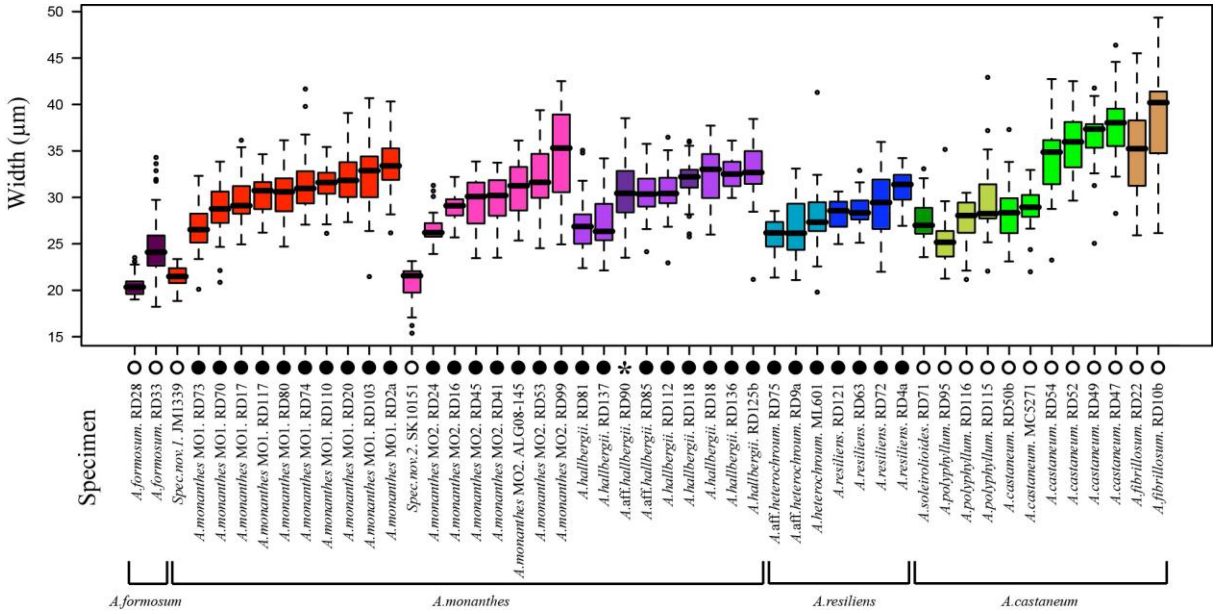

Figure A7. Spore width of taxa of the *A.monanthes* complex. Boxplots illustrating the variation in spore length of species and specimens. Each boxplot is labelled below with its corresponding specimen voucher and coloured according to species. Boxplots are grouped together according to species and phylogenetic clades and ordered from lowest mean length to highest mean length. Colour differences within clades are the same as described in Fig. 2. Each boxplot represents the variation of measurements of spores within each specimen, the thick horizontal line represents the median, the box represents variation observed between the 25th and 75th percentiles and the whiskers represent the variation range with extreme outliers represented by small black circles. Large Filled black circles indicate apomictic specimens that produce 32 spores per sporangium. Large unfilled circles indicate specimens that produce 64 spores sporangium and are inferred to have a sexual mode of reproduction. The star indicates a specimen that produces both 32 and 64 spores per sporangium**.**

BIBLIOGRAPHY

Abraham A, Ninan C. **1954**. The chromosomes of *Ophioglossum reticulatum* L. *Current Science* **23**: 213–214.

Adams CD. **1995**. *Asplenium*. In: Davidse G, Sousa M, Knapp S, eds. Flora Mesoamericana. Mexico: Universidad Nacional Autónoma de México, 290–324.

Aldrich J, Cherney BW, Merlin E, Christopherson L. **1988**. The role of insertions deletions in the evolution of the intergenic region between *psbA* and *trnH* in the chloroplast genome. *Current Genetics* **14**: 137–146.

Althoff D. **2007**. The utility of amplified fragment length polymorphisms in phylogenetics: A comparison of homology within and between genomes. *Systematic Biology* **56**: 477–484.

Ammal LS, Bahavanandan K V. **1991**. Cytological studies on the genus *Asplenium* Linn. *Indian Fern Journal* **8**: 69–73.

Anderson MJ. **2003**. PCO: A FORTRAN computer program for principal coordinate analysis.

Asker SE, Jerling L. **1992**. *Apomixis in Plants*. London: CRC Press.

Bachtrog D. **2003**. Adaptation shapes patterns of genome evolution on sexual and asexual chromosomes in *Drosophila*. *Nature Genetics* **34**: 215–219.

Bainard JD, Henry TA, Bainard LD, Newmaster SG. **2011a**. DNA content variation in monilophytes and lycophytes: large genomes that are not endopolyploid. *Chromosome Research* **19**: 763–775.

Bainard JD, Husband BC, Baldwin SJ, Fazekas AJ, Gregory TR, Newmaster SG, Kron P. **2011b**. The effects of rapid desiccation on estimates of plant genome size. *Chromosome Research* **19**: 825–842.

Barcaccia G, Arzenton F, Sharbel TF, Varotto S, Parrini P, Lucchin M. **2006**. Genetic diversity and reproductive biology in ecotypes of the facultative apomict *Hypericum perforatum* L. *Heredity* **96**: 322–334.

Barker MS. **2009**. Evolutionary genomic analyses of ferns reveal that high chromosome numbers are a product of high retention and fewer rounds of polyploidy relative to angiosperms. *American Fern Journal* **99**: 136–141.

Barker MS. **2013**. Karyotype and genome evolution in pteridophytes. In: Leitch IJ, Greilhuber J, Doležel J, Wendel JF, eds. Plant genome diversity, vol 2, Physical structure, behaviour and evolution of plant genomes. Wien: Springer-Verlag, 245–253.

Barker MS, Wolf PG. **2010**. Unfurling fern biology in the genomics age. *BioScience* **60**: 177–185.

Barraclough TG, Fontaneto D, Ricci C, Herniou EA. **2007**. Evidence for inefficient selection against deleterious mutations in cytochrome oxidase I of asexual bdelloid rotifers. *Molecular Biology and Evolution* **24**: 1952–1962.

Barrington DS, Paris CA, Ranker TA. **1986**. Systematic inferences from spore and stomate size in the ferns. *American Fern Journal* **76**: 149–159.

Barton NH, Charlesworth B. **1998**. Why sex and recombination? *Science* **281**: 1986–1990.

Beaulieu JM, Leitch IJ, Patel S, Pendharkar A, Knight CA. **2008**. Genome size is a strong predictor of cell size and stomatal density in angiosperms. *The New Phytologist* **179**: 975–986.

Beaulieu JM, Moles AT, Leitch IJ, Bennett MD, Dickie JB, Knight CA. **2007**. Correlated evolution of genome size and seed mass. *The New Phytologist* **173**: 422–437.

Beck JB, Alexander PJ, Allphin L, Al-Shehbaz IA, Rushworth C, Bailey CD, Windham MD. **2011a**. Does hybridization drive the transition to asexuality in diploid *Boechera*? *Evolution* **66**: 985–995.

Beck JB, Allison JR, Pryer KM, Windham MD. **2012**. Identifying multiple origins of polyploid taxa: A multilocus study of the hybrid cloak fern (*Astrolepis integerrima*; Pteridaceae). *American Journal of Botany* **99**: 1–9.

Beck JB, Windham MD, Pryer KM. **2011b**. Do asexual polyploid lineages lead short evolutionary lives? A case-study from the fern genus *Astrolepis*. *Evolution* **65**: 3217–3229.

Beck JB, Windham MD, Yatskievych G, Pryer KM. **2010**. A diploids-first approach to species delimitation and interpreting polyploid evolution in the fern genus *Astrolepis* (Pteridaceae). *Systematic Botany* **35**: 223–234.

Bennett M, Leitch IJ. **2001**. Nuclear DNA amounts in Pteridophytes. *Annals of Botany* **87**: 335–345.

Bennett M, Leitch IJ. **2010**. Pteridophyte DNA C-values database (release 4.0, Dec. 2010). *http://www.kew.org/cvalues/homepage.html*.

Benson DA, Karsch-Mizrachi I, Lipman DJ, Ostell J, Sayers EW. **2011**. GenBank. *Nucleic Acids Research* **39**: D32–D37.

Birky C, Adams J, Gemmel M, Perry J. **2010**. Using population genetic theory and DNA sequences for species detection and identification in asexual organisms. *PLoS One* **5**: 1–11.

Blanco-Pastor JL, Vargas P, Pfeil BE. **2012**. Coalescent simulations reveal hybridization and incomplete lineage sorting in Mediterranean Linaria. *PloS One* **7**: e39089.

Blomberg SP, Garland TJ, Ives AR. **2003**. Testing for phylogenetic signal in comparative data: behavioral traits are more labile. *Evolution* **57**: 717–745.

Bonin A, Ehrich D, Manel S. **2007**. Statistical analysis of amplified fragment length polymorphism data: a toolbox for molecular ecologists and evolutionists. *Molecular Ecology* **16**: 3737–3758.

Braithwaite A. **1964**. A new type of apogamy in ferns. *The New Phytologist* **63**: 293–305.

Brandes A, Heslop-Harrison JS, Kamm A, Kubis S, Doudrick RL, Schmidt T. **1997**. Comparative analysis of the chromosomal and genomic organization of Ty1-copia-like retrotransposons in pteridophytes, gymnosperms and angiosperms. *Plant Molecular Biology* **33**: 11–21.

Britton D. **1953**. Chromosome studies on ferns. *American Journal of Botany* **40**: 575–583.

Brownsey PJ, Lovis J. **1987**. Chromosome numbers for the New Zealand species of *Psilotum* and *Tmesipteris*, and the phylogenetic relationships of the Psilotales. *New Zealand Journal of Botany* **25**: 439–454.

Brysting A, Mathiesen C, Marcussen T. **2011**. Challenges in polyploid phylogenetic reconstruction: A case story from the arctic-alpine *Cerastium alpinum* complex. *Taxon* **60**: 333–347.

Bures P, Tichy L, Wang Y-F, Bartos J. **2003**. Occurrence of *Polypodium* × *mantoniae* and new localities for *P.interjectum* in the Czech Republic confirmed using flow cytometry. *Preslia* **75**: 293–310.

Carman J. **1997**. Asynchronous expression of duplicate genes in angiosperms may cause apomixis, bispory, tetraspory, and polyembryony. *Biological Journal of the Linnean Society* **61**: 51–94.

Chao Y, Dong S, Chiang Y, Chiou W-L. **2012**. Extreme multiple reticulate origins of the *Pteris cadieri* Complex (Pteridaceae). *International Journal of Molecular Sciences* **13**: 4523–4544.

Cherry-Garrard A. **1922**. *The Worst Journey in the World*. London: Constable.

Cires E, Cuesta C, Peredo EL, Revilla MÁ, Prieto JAF. **2009**. Genome size variation and morphological differentiation within *Ranunculus parnassifolius* group (Ranunculaceae) from calcareous screes in the Northwest of Spain. *Plant Systematics and Evolution* **281**: 193–208.

Connolly JA, Oliver MJ, Beaulieu JM, Knight CA, Tomanek L, Moline MA. **2008**. Correlated evolution of genome size and cell volume in diatoms (Bacillariophyceae). *Journal of Phycology* **44**: 124–131.

Cronquist A. **1987**. A botanical critique of cladism. *The Botanical Review* **53**: 1–52.

Crow JF. **1992**. An advantage of sexual reproduction in a rapidly changing environment. *Journal of Heredity* **83**: 169–173.

Darnaedi D, Kato M, Iwatsuki K. **1990**. Electrophoretic evidence for the origin of *Dryopteris yakusilvicola* (Dryopteridaceae). *Botanical Magazine (Tokyo)* **103**: 1–10.

Dasmahapatra KK, Hoffman JI, Amos W. **2009**. Pinniped phylogenetic relationships inferred using AFLP markers. *Heredity* **103**: 168–77.

Després L, Gielly L, Redoutet B, Taberlet P. **2003**. Using AFLP to resolve phylogenetic relationships in a morphologically diversified plant species complex when nuclear and chloroplast sequences fail to reveal variability. *Molecular Phylogenetics and Evolution* **27**: 185–196.

Van Dijk PJ. **2003**. Ecological and evolutionary opportunities of apomixis: insights from *Taraxacum* and *Chondrilla*. *Philosophical transactions of the Royal Society of London. Series B, Biological sciences* **358**: 1113–1121.

Doležel J, Greilhuber J, Lucretti S. **1998**. Plant genome size estimation by flow cytometry: Inter-laboratory comparison. *Annals of Botany* **82**: 17–26.

Doležel J, Greilhuber J, Suda J. **2007**. Estimation of nuclear DNA content in plants using flow cytometry. *Nature Protocols* **2**: 2233–2244.

Van Doninck K, Schon I, Martens K, Backeljau T. **2004**. Clonal diversity in the ancient asexual ostracod *Darwinula stevensoni* assessed by RAPD-PCR. *Heredity* **93**: 154–160.

Doyle. **1987**. A rapid DNA isolation procedure for small quantities of fresh leaf tissue. *Phytochemical Bulletin* **19**: 11–15.

Drummond AJ, Suchard MA, Xie D, Rambaut A. **2012**. Bayesian phylogenetics with BEAUti and the BEAST 1.7. *Molecular Biology and Evolution* **29**: 1969–1973.

Dyer RJ, Savolainen V, Schneider H. **2012**. Apomixis and reticulate evolution in the *Asplenium monanthes* fern complex. *Annals of Botany* **110**: 1515–1529.

Döpp W. **1932**. Die Apogamie bei *Aspidium remotum* Al.Br. *Planta* **17**: 86–152.

Ekrt L, Holubová R, Trávnícek P, Suda J. **2010**. Species boundaries and frequency of hybridization in the *Dryopteris carthusiana* (Dryopteridaceae) complex: A taxonomic puzzle resolved using genome size data. *American Journal of Botany* **97**: 1208–1219.

Ekrt L, Stech M. **2008**. A morphometric study and revision of the *Asplenium trichomanes* group in the Czech Republic. *Preslia* **80**: 325–347.

Ekrt L, Trávníček P, Jarolímová V, Vít P, Urfus T. **2009**. Genome size and morphology of the *Dryopteris affinis* group. *Preslia* **81**: 261–280.

Evanno G, Regnaut S, Goudet J. **2005**. Detecting the number of clusters of individuals using the software STRUCTURE: a simulation study. *Molecular Ecology* **14**: 2611–2620.

Ezard T, Fujisawa T, Barraclough TG. **2009**. splits: SPecies' LImits by Threshold Statistics.

Falster DS, Warton DI, Wright IJ. **2006**. SMATR: Standardised major axis tests and Routines, ver 2.0.

Falush DS, Stephens M, Pritchard JK. **2007**. Inference of population structure using multilocus genotype data: dominant markers and null alleles. *Molecular Ecology Notes* **7**: 574–578.

Felsenstein J. **1974**. The evolutionary advantage of recombination. *Genetics* **78**: 737–756.

Felsenstein J. **1985a**. Confidence-limits on phylogenies: An approach using the bootstrap. *Evolution* **39**: 783–791.

Felsenstein J. **1985b**. Phylogenies and the comparative method. *American Naturalist* **125**: 1–15.

Fisher RA. **1930**. *The genetical theory of natural selection: A complete variorum edition*. Oxford UK: Oxford University Press (OUP).

Fontaneto D, Herniou EA, Boschetti C, Caprioli M, Melone G, Ricci C, Barraclough TG. **2007**. Independently evolving species in asexual bdelloid rotifers. *PLoS Biology* **5**: 914–921.

Fraley C, Raftery A. **1998**. How many clusters? Which clustering method? Answers Via model-based cluster analysis. *The Computer Journal* **41**: 578–588.

García-Pereira MJ, Caballero A, Quesada H. **2010**. Evaluating the relationship between evolutionary divergence and phylogenetic accuracy in AFLP data sets. *Molecular Biology and Evolution* **27**: 988–1000.

Garland TJ, Díaz-Uriarte R. **1999**. Polytomies and phylogenetically independent contrasts: examination of the bounded degrees of freedom approach. *Systematic Biology* **48**: 547–558.

Garland TJ, Harvey PH, Ives AR. **1992**. Procedures for the analysis of comparative data using phylogenetically independent contrasts. *Systematic Biology* **41**: 18–32.

Gastony GJ. **1988**. The Pellaea-glabella complex: Electrophoretic evidence for the derivations of the agamosporous taxa and a revised taxonomy. *American fern journal* **78**: 44–67.

Gastony GJ, Gottlieb LD. **1985**. Genetic variation in the homosporous fern *Pellaea andromedifolia*. *American Journal of Botany* **72**: 257–267.

Gastony GJ, Haufler CH. **1976**. Chromosome numbers and apomixis in the fern genus *Bommeria* (Gymnogrammaceae). *Biotropica* **8**: 1–11.

Gastony GJ, Windham MD. **1989**. Species concepts in pteridophytes: the treatment and definition of agamosporous species. *American Fern Journal* **79**: 65–77.

Ghatak J. **1977**. Biosystematic survey of Pteridophytes from Shevaroy Hills, South India. *The Nucleus* **20**: 105–108.

Grafen A. **1989**. The phylogenetic regression. *Philosophical transactions of the Royal Society of London. Series B, Biological sciences* **326**: 119–157.

Grandbastien M-A, Audeon C, Bonnivard E, Casacuberta J, Chalhoub B, Costa A-P, Le Q, Melayah D, Petit M, Poncet C, *et al.* 2005. Stress activation and genomic impact of *Tnt1* retrotransposons in Solanaceae. *Cytogenetic and genome research* **110**: 229–241.

Greilhuber J, Doležel J, Lysák MA, Bennett MD. **2005**. The origin, evolution and proposed stabilization of the terms "genome size" and "C-value" to describe nuclear DNA contents. *Annals of Botany* **95**: 255–260.

Greilhuber J, Leitch IJ. **2013**. Genome size and the phenotype. In: Leitch IJ, Greilhuber J, Doležel J, Wendel JF, eds. Plant genome diversity, vol 2, Physical structure, behaviour and evolution of plant genomes. Wien: Springer-Verlag, 323–344.

Grime J, Hodson J, Hunt R. **1988**. *Coparative Plant Ecology: A functional approach to common British species*. London: Unwin Hyman.

Grover CE, Wendel JF. **2010**. Recent insights into mechanisms of genome size change in plants. *Journal of Botany*: 1–8.

Grusz AL, Windham MD, Pryer KM. **2009**. Deciphering the origins of apomictic polyploids in the *Cheilanthes yavapensis* complex (Pteridaceae). *American Journal of Botany* **96**: 1636–1645.

Guillon J-M. **2007**. Molecular phylogeny of horsetails (Equisetum) including chloroplast *atpB* sequences. *Journal of Plant Research* **120**: 569–574.

Guillén RH, Daviña JR. **2005**. Estudios cromosómicos en especies de *Asplenium* (Aspleniaceae) de la Argentina. *Darwiniana* **43**: 44–51.

Guindon S, Dufayard JF, Lefort V, Anisimova M, Hordijk W, Gascuel O. **2010**. New algorithms and methods to estimate maximum-likelihood phylogenies: Assessing the performance of PhyML 3.0. *Systematic Biology* **59**: 307–321.

Guindon S, Lethiec F, Duroux P, Gascuel O. **2005**. PHYML Online: A web server for fast maximum likelihood-based phylogenetic inference. *Nucleic Acids Research* **33**: 557–559.

Guo Y-P, Vogl C, Van Loo M, Ehrendorfer F. **2006**. Hybrid origin and differentiation of two tetraploid *Achillea* species in East Asia: molecular, morphological and ecogeographical evidence. *Molecular Ecology* **15**: 133–144.

Gustafsson Å. **1946**. Apomixis in higher plants. I. The mechanism of apomixis. *Lunds Universitet Årsskrift* **42**: 1–66.

Gustafsson Å. **1947a**. Apomixis in higher plants. III. Biotype and species formation. *Lunds Universitet Årsskrift* **43**: 183–370.

Gustafsson Å. **1947b**. Apomixis in higher plants. II. The causal aspets of apomixis. *Lunds Universitet Årsskrift* **43**: 71–178.

Hamming R. **1950**. Error detecting and error correcting codes. *Bell System Technical Journal* **29**: 147–160.

Hartfield M, Keightley PD. **2012**. Current hypotheses for the evolution of sex and recombination. *Intergrative Zoology* **7**: 192–209.

Haufler CH. **1987**. Electrophoresis is modifying our concepts of evolution in homosporous pteridophytes. *American Journal of Botany* **74**: 953–966.

Haufler CH. **2002**. Homospory 2002: An odyssey of progress in pteridophyte genetics and evolutionary biology. *BioScience* **52**: 1081–1093.

Haufler CH, Soltis DE. **1984**. Obligate outcrossing in a homosporous fern: Filed confirmation of a labarotory prediction. *American Journal of Botany* **71**: 878–881.

Haufler CH, Soltis D. **1986**. Genetic evidence suggests that homosporous ferns with high chromosome numbers are diploid. *Proceedings of the National Academy of Sciences of the United States of America* **83**: 4389–4393.

Hausdorf B. **2011**. Progress toward a general species concept. *Evolution* **65**: 923–31.

Hausdorf B, Hennig C. **2010**. Species delimitation using dominant and codominant multilocus markers. *Systematic Biology* **59**: 491–503.

Hennig C, Hausdorf B. **2012**. prabclus: Functions for clustering of presence-absence, abundance and multilocus genetic data.

Hodgson JG, Sharafi M, Jalili A, Díaz S, Montserrat-Martí G, Palmer C, Cerabolini B, Pierce S, Hamzehee B, Asri Y, *et al.* 2010. Stomatal vs. genome size in angiosperms: the somatic tail wagging the genomic dog? *Annals of Botany* **105**: 573–584.

Huang Y, Hsu SM, Hsieh TS, Chou HU, Chiou WL. **2011**. Three Pteris species (Pteridaceae: Pteridophyta) reproduce by apogamy. *Botanical Studies* **52**: 79–87.

Hubisz MJ, Falush DS, Stephens M, Pritchard JK. **2009**. Inferring weak population structure with the assistance of sample group information. *Molecular Ecology Resources* **9**: 1322–1332.

Huelsenbeck JP, Ronquist F. **2001**. MRBAYES: Bayesian inference of phylogenetic trees. *Bioinformatics* **17**: 754–755.

Huelsenbeck JP, Ronquist F. **2005**. Bayesian analysis of molecular evolution using MrBayes. *Statistical Methods in Molecular Evolution*: 183–232.

Huson DH, Bryant D. **2006**. Application of phylogenetic networks in evolutionary studies. *Molecular Biology and Evolution* **23**: 254–267.

Huson DH, Scornavacca C. **2011**. A survey of combinatorial methods for phylogenetic networks. *Genome Biology and Evolution* **3**: 23–35.

Hörandl E. **1998**. Species concepts in agamic complexes: Applications in the *Ranunculus auricomus* and general perspectives. *Folia Geobotanica*: 335–348.

Hörandl E, Emadzade K. **2012**. Evolutionary classification: A case study on the diverse plant genus *Ranunculus* L. (Ranunculaceae). *Perspectives in Plant Ecology, Evolution and Systematics* **14**: 310–324.

Hörandl E, Greilhuber J, Klimová K, Paun O, Temsch E, Emadzade K, Hodálová I. **2009**. Reticulate evolution and taxonomic concepts in the *Ranunculus auricomus* complex (Ranunculaceae): insights from analysis of morphological, karyological and molecular data. *Taxon* **58**: 1194–1215.

Hörandl E, Hojsgaard D. **2012**. The evolution of apomixis in Angiosperms: a reappraisal. *Plant Biosystems*: 37–41.

Hörandl E, Paun O, Johansson JT, Lehnebach C, Armstrong T, Chen L, Lockhart P. **2005**. Phylogenetic relationships and evolutionary traits in *Ranunculus* s.l. (Ranunculaceae) inferred from *ITS* sequence analysis. *Molecular Phylogenetics and Evolution* **36**: 305–27.

Ishikawa H, Ito M, Watano Y, Kurita S. **2003**. Electrophoretic evidence for homoeologous chromosome pairing in the apogamous fern species *Dryopteris nipponensis* (Dryopteridaceae). *Journal of Plant Research* **116**: 165–167.

Ishikawa H, Watano Y, Kano K, Ito M, Kurita S. **2002**. Development of primer sets for PCR amplification of the *pgiC* gene in ferns. *Journal of Plant Research* **115**: 65–70.

Jaccard P. **1908**. Nouvelles recherches sur la distribution florale. *Bulletin de la Société Vaudoise des Sciences Naturelles* **44**: 223–270.

Janko K, Drozd P, Flegr J, Pannell JR. **2008**. Clonal turnover versus clonal decay: A null model for observed patterns of asexual longevity, diversity and distribution. *Evolution* **62**: 1264–1270.

Judson OP, Normark BB. **1996**. Ancient asexual scandal. *Trends in Ecology and Evolution* **11**: 41–46.

Juslén A, Väre H, Wikström N. **2011**. Relationships and evolutionary origins of polyploid *Dryopteris* (Dryopteridaceae) from Europe inferred using nuclear *pgiC* and plastid *trnL-F* sequence data. *Taxon* **60**: 1284–1294.

Jørgensen P, Nee M, Beck SG. **2010**. Catálogo de las plantas vasculares de Bolivia. *Monographs in Systematic Botany from the Missouri Botanical Garden*.

Kalendar R, Tanskanen J, Immonen S, Nevo E, Schulman AH. **2000**. Genome evolution of wild barley (*Hordeum spontaneum*) by *BARE-1* retrotransposon dynamics in response to sharp microclimatic divergence. *Proceedings of the National Academy of Sciences of the United States of America* **97**: 6603–6607.

Kawakami SM, Kawakami S, Kondo K, Shmakov A. **2011**. Cytological studies of Russian Altai ferns and the haploid sporophyte formation. *Chromosome Botany* **6**: 21–23.

Kembel SW, Cowan PD, Helmus MR, Cornwell WK, Morlon H, Ackerly DD, Blomberg SP, Webb CO. **2010**. Picante: R tools for integrating phylogenies and ecology. *Bioinformatics* **26**: 1463–1464.

Kessler M, Smith AR. **2011**. Ferns of Bolivia. *http://www.systbot.uzh.ch/static/fernsofbolivia/* **2011**.

Kimura M, Crow J. **1964**. The number of alleles that can be maintained in a finite population. *Genetics* **49**: 725.

Klekowski EJ. **1970**. Populational and genetic studies of a homosporous fern – *Osmunda regalis*. *American Journal of Botany* **57**: 1122–1138.

Klekowski EJ. **1973**. Sexual and subsexual systems in homosporous pteridophytes: A new hypothesis. *American Journal of Botany* **3**: 535–544.

Klekowski EJ, Baker HG. **1966**. Evolutionary significance of polyploidy in the Pteridophyta. *Science* **153**: 305–307.

Klekowski EJ, Hickok LG. **1974**. Nonhomologous chromosome pairing in the fern *Ceratopteris*. *American Journal of Botany* **61**: 422–432.

Kloepper TH, Huson DH. **2008**. Drawing explicit phylogenetic networks and their integration into SplitsTree. *BMC Evolutionary Biology* **8**: 22.

Knight CA, Beaulieu JM. **2008**. Genome size scaling through phenotype space. *Annals of Botany* **101**: 759–766.

Knobloch IW. **1966**. A preliminary review of spore number and apogamy within the genus *Cheilanthes*. *American Fern Journal* **56**: 163–167.

Kondrashov A. **1982**. Selection against harmful mutations in large sexual and asexual populations. *Genetics Research* **40**: 325–332.

Koopman WJM. **2005**. Phylogenetic signal in AFLP data sets. *Systematic Biology* **54**: 197–217.

Kosman E, Leonard KJ. **2005**. Similarity coefficients for molecular markers in studies of genetic relationships between individuals for haploid, diploid, and polyploid species. *Molecular Ecology* **14**: 415–424.

Kropf M, Comes HP, Kadereit JW. **2009**. An AFLP clock for the absolute dating of shallow-time evolutionary history based on the intraspecific divergence of southwestern European alpine plant species. *Molecular Ecology* **18**: 697–708.

Kruskal JB. **1964**. Multidimensional scaling by optimizing goodness of fit to a nonmetric hypothesis. *Psychometrika* **29**: 1–27.

Laird S, Sheffield E. **1986**. Antheridia and archegonia of the apogamous fern *Pteris cretica*. *Annals of Botany* **57**: 139–143.

Legendre P, Legendre L. **1998**. *Numerical Ecology* (SE Edition, Ed.). Elsevier.

Leitch IJ, Bennett M. **2004**. Genome downsizing in polyploid plants. *Biological Journal of the Linnean Society* **82**: 651–663.

Leitch AR, Leitch IJ. **2012**. Ecological and genetic factors linked to contrasting genome dynamics in seed plants. *The New Phytologist* **194**: 629–646.

Leitch IJ, Leitch AR. **2013**. Genome size diversity and evolution in land plants. In: Leitch IJ, Greilhuber J, Doležel J, Wendel JF, eds. Plant genome diversity, vol 2, Physical structure, behaviour and evolution of plant genomes. Wien: Springer-Verlag, 307–322.

Lin S, Kato M, Iwatsuki K. **1992**. Diploid and triploid offspring of triploid agamosporous fern *Dryopteris pacifica*. *Botanical Magazine (Tokyo)* **105**: 443–452.

Liu H-M, Dyer RJ, Guo Z-Y, Meng Z, Li J-H, Schneider H. **2012**. The evolutionary dynamics of apomixis in ferns: A case study from Polystichoid ferns. *Journal of Botany* **2012**: 1–11.

Liu L, Pearl DK, Brumfield RT, Edwards S V. **2008**. Estimating species trees using multiple-allele DNA sequence data. *Evolution* **62**: 2080–2091.

Lloyd RM. **1973**. Faculative apomixis and polyploidy in *Matteuccia orientalis*. *American Fern Journal* **63**: 43–48.

Lloyd RM. **1974**. Reproductive biology and evolution in the Pteridophyta. *Annals of the Missouri Botanical Garden* **61**: 318–331.

Lockton S, Ross-Ibarra J, Gaut BS. **2008**. Demography and weak selection drive patterns of transposable element diversity in natural populations of *Arabidopsis lyrata*. *Proceedings of the National Academy of Sciences of the United States of America* **105**: 13965–13970.

Loureiro J, Rodriguez E, Doležel J, Santos C, Article T. **2007**. Two new nuclear isolation buffers for plant DNA flow cytometry: A test with 37 species. *Annals of Botany* **100**: 875–888.

Lovis J. **1977**. Evolutionary patterns and processes in ferns. In: Preston RD, Woolhouse HW, eds. Advances in Botanical Research.402–402.

Lovis J, Rasbach H, Rasbach K, Reichstein T. **1977**. *Asplenium azoricum* and other ferns of the *A. trichomanes* group from the Azores. *American Fern Journal* **67**: 81–93.

Maddison WP, Maddison DR. **1989**. Interactive analysis of phylogeny and character evolution using the computer program MacClade. *Folia Primatologica* **53**: 190–202.

Maddison DR, Maddison WP. **2005**. MacClade 4: Analysis of phylogeny and character evolution. Version 4.08a. *http://macclade.org*.

Maddison WP, Maddison DR. **2011**. Mesquite: A modular system for evolutionary analysis. Version 2.5. *http://mesquiteproject.org*.

Manton I. **1950**. *Problems of Cytology and Evolution in the Pteridophyta*. Cambridge : The syndics of the Cambridge University Press.

Manton I. **1959**. Cytological Information of the Ferns of West Tropical Africa. In: Alston AHG, ed. The Ferns and Fern Allies of West Tropical Africa. Cambridge, 75–81.

Manton I, Vida G. **1968**. Cytology of the ferns flora of Tristan da Cunha. *Proceedings of the Royal Society of London, Series B* **170**: 361–371.

Manton I, Vida G, Gibby M. **1986**. Cytology of the fern flora of Madeira. *Bulletin of the British Museum (Natural History). Botany.* **15**: 123–161.

Mason-Gamer RJ, Kellogg EA. **1996**. Testing for phylogenetic conflict among molecular data sets in the tribe Triticeae (Gramineae). *Systematic Biology* **45**: 524–545.

Matzk F, Hammer K, Schubert I. **2003**. Coevolution of apomixis and genome size within the genus *Hypericum*. *Sexual Plant Reproduction* **16**: 51–58.

Maynard Smith J. **1978**. *The Evolution of Sex*. Cambridge: Cambridge University Press.

McDade L. **1990**. Hybrids and phylogenetic systematics I. Patterns of character expression in hybrids and their implications for cladistic analysis. *Evolution* **44**: 1685–1700.

McGrath JM, Hickok LG. **1999**. Multiple ribosomal RNA gene loci in the genome of the homosporous fern *Ceratopteris richardii*. *Canadian Journal of Botany* **77**: 1199 –1202.

McGrath JM, Hickok LG, Pichersky E. **1994**. Assessment of gene copy number in the homosporous ferns *Ceratopteris thalictroides* and *C. richardii* (Parkeriaceae) by restriction fragment length polymorphisms. *Plant Systematics and Evolution* **189**: 203–210.

Mechanda S, Baum B. **2004**. Sequence assessment of comigrating AFLP™ bands in Echinacea — implications for comparative biological studies. *Genome* **25**: 15–25.

Meudt HM. **2011**. Amplified fragment length polymorphism data reveal a history of auto- and allopolyploidy in New zealand endemic species of Plantago (Plantaginaceae): New perspectives on a taxonomically challenging group. *International Journal of Plant Sciences* **172**: 220–237.

Meudt HM, Clarke AC. **2007**. Almost forgotten or latest practice? AFLP applications, analyses and advances. *Trends in Plant Science* **12**: 106–117.

Meudt HM, Lockhart PJ, Bryant D. **2009**. Species delimitation and phylogeny of a New Zealand plant species radiation. *BMC Evolutionary Biology* **9**: 111.

Mickel JT, Smith AR. **2004**. *The Pteridophytes of Mexico*. New York: New York Botanical Gardens Press.

Midford P, Garland TJ, Maddison W. **2005**. PDAP Package of Mesquite. *http://mesquiteproject.org*.

Mogie M. **1990**. Homospory and the cost of asexual reproduction. *Evolution* **44**: 1707–1710.

Mogie M. **1992**. *The Evolution of Asexual Reproduction in Plants*. London: Chapman and Hall.

Monaghan MT, Wild R, Elliot M, Fujisawa T, Balke M, Inward DJG, Lees DC, Ranaivosolo R, Eggleton P, Barraclough TG, *et al.* 2009. Accelerated species inventory on Madagascar using coalescent-based models of species delineation. *Systematic Biology* **58**: 298–311.

Monterrosa JS, Pena-chocarro M, Knapp S, Lechuga RE. **2009**. *Guia de identificacion de Helechos de El Salvador*. Antiguo Cuscatlan: Jardin Botanico La Laguna.

Moran RC. **1982**. The *Asplenium trichomanes* Complex in the United States and adjacent Canada. *American Fern Journal* **72**: 5–11.

Morzenti V. **1966**. Morphological and cytological data on southeastern United States species of the *Asplenium heterochroum-resiliens* complex. *American Fern Journal* **56**: 167–177.

Morzenti V, Wagner W. **1962**. Southeastern American blackstem spleenworts of the *Asplenium heterochroum-resiliens* complex. *The Association of Southeastern Biologsts Bulletin* **9**: 40–41.

Muller H. **1932**. Some genetic aspects of sex. *The American Naturalist* **66**: 118–138.

Muller H. **1964**. The relation of recombination to mutational advance. *Mutation Research* **106**: 2–9.

Nakazato T, Barker MS, Rieseberg LH, Gastony GJ. **2008**. Evolution of the nuclear genome of ferns and lycophytes. In: Ranker TA, Haufler CH, eds. Biology and Evolution of Ferns and Lycpohytes. Cambridge Unversity Press, 175–198.

Nakazato T, Jung M-K, Housworth EA, Rieseberg LH, Gastony GJ. **2006**. Genetic map-based analysis of genome structure in the homosporous fern *Ceratopteris richardii*. *Genetics* **173**: 1585–1597.

Nei M, Li WH. **1979**. Mathematical model for studying genetic variation in terms of restriction endonucleases. *Proceedings of the National Academy of Sciences of the United States of America* **76**: 5269–5273.

Niemiller ML, Near TJ, Fitzpatrick BM. **2012**. Delimiting species using multilocus data: diagnosing cryptic diversity in the southern cavefish, *Typhlichthys subterraneus* (Teleostei: Amblyopsidae). *Evolution* **66**: 846–866.

Nitta JH, Ebihara A, Ito M. **2011**. Reticulate evolution in the *Crepidomanes minutum* species complex (Hymenophyllaceae). *American Journal of Botany* **98**: 1–19.

Obermayer R, Leitch IJ, Hanson L, Bennett MD. **2002**. Nuclear DNA C-values in 30 species double the familial representation in pteridophytes. *Annals of Botany* **90**: 209–217.

Oksanen J, Blanchet FG, Kindt R, Legendre P, MInchin PR, O'Hara RB, Simpson GL, Solymos P, Stevens MHH, Wagner H. **2012**. vegan: Community Ecology Package. *R package version* **1**: R package version 2.0–4.

Ootsuki R, Sato H, Nakato N, Murakami N. **2012**. Evidence of genetic segregation in the apogamous fern species *Cyrtomium fortunei* (Dryopteridaceae). *Journal of Plant Research* **125**: 605–612.

Ootsuki R, Shinohara W, Suzuki T, Murakami N. **2011**. Genetic variation in the apogamous fern *Cyrtomium fortunei* (Dryopteridaceae). *Acta Phytotaxonomica et Geobotanica* **62**: 1–14.

Orr H, Presgraves D. **2000**. Speciation by postzygotic isolation: forces, genes and molecules. *BioEssays* **22**: 1085–1094.

Otto SP, Lenormand T. **2002**. Resolving the paradox of sex and recombination. *Nature Reviews Genetics* **3**: 252–261.

Otto S, Whitton J. **2000**. Polyploid incidence and evolution. *Annual Review of Genetics* **34**: 401–437.

O'Meara BC. **2010**. New heuristic methods for joint species delimitation and species tree inference. *Systematic Biology* **59**: 59–73.

O'Meara BC, Ané C, Sanderson MJ, Wainwright PC. **2006**. Testing for different rates of continuous trait evolution using likelihood. *Evolution* **60**: 922–933.

Pagel MD. **1992**. A method for the analysis of comparative data. *Journal of Theoretical Biology* **156**: 431–442.

Paradis E, Claude J, Strimmer K. **2004**. APE: analyses of phylogenetics and evolution in R language. *Bioinformatics* **20**: 289–290.

Park C-HH, Kato M. **2003**. Apomixis in the interspecific triploid hybrid fern *Cornopteris christenseniana* (Woodsiaceae). *Journal of Plant Research* **116**: 93–103.

Paun O, Greilhuber J, Temsch EM, Hörandl E. **2006**. Patterns, sources and ecological implications of clonal diversity in apomictic *Ranunculus carpaticola* (*Ranunculus auricomus* complex, Ranunculaceae). *Molecular Ecology* **15**: 897–910.

Pellicer J, Fay MF, Leitch IJ. **2010**. The largest eukaryotic genome of them all? *Botanical Journal of the Linnean Society* **164**: 10–15.

Pelser PB. **2003**. Phylogeny reconstruction in the gap between too little and too much divergence: the closest relatives of *Senecio jacobaea* (Asteraceae) according to DNA sequences and AFLPs. *Molecular Phylogenetics and Evolution* **29**: 613–628.

Petit M, Guidat C, Daniel J, Denis E, Montoriol E, Bui Q, Lim K, Kovarik A, Leitch AR, Grandbastien M-A, *et al.* 2010. Mobilization of retrotransposons in synthetic allotetraploid tobacco. *The New Phytologist* **186**: 135–147.

Pichersky E, Soltis DE, Soltis PS. **1990**. Defective chlorophyll a/b-binding protein genes in the genome of a homosporous fern. *Proceedings of the National Academy of Sciences of the United States of America* **87**: 195–199.

Pichot C, El Maâtaoui M, Raddi S, Raddi P. **2001**. Surrogate mother for endangered Cupressus. *Nature* **412**: 39.

Pirie MD, Humphreys AM, Barker NP, Linder HP. **2009**. Reticulation, data combination, and inferring evolutionary history: an example from Danthonioideae (Poaceae). *Systematic Biology* **58**: 612–628.

Pons J, Barraclough TG, Gomez-Zurita J, Cardoso A, Duran D, Hazell S, Kamoun S, Sumlin W, Vogler A. **2006**. Sequence-Based Species Delimitation for the DNA Taxonomy of Undescribed Insects. *Systematic Biology* **55**: 595–609.

Posada D. **2008**. jModelTest: Phylogenetic model averaging. *Molecular Biology and Evolution* **25**: 1253–1256.

Posada D. **2009**. Selection of Models of DNA Evolution with jMODELTEST. *Bioinformatics for DNA Sequence Analysis*: 93–112.

Posada D, Crandall KA. **1998**. MODELTEST: testing the model of DNA substitution. *Bioinformatics* **14**: 817–818.

Pritchard JK, Stephens M, Donnelly P. **2000**. Inference of population structure using multilocus genotype data. *Genetics* **155**: 945–959.

Pryer KM, Schuettpelz E, Wolf PG, Schneider H, Smith AR, Cranfill R. **2004**. Phylogeny and evolution of ferns (Monilophytes) with a focus on the early Leptosporangiate divergences. *American Journal of Botany* **91**: 1582–1598.

Quader S, Isvaran K, Hale RE, Miner BG, Seavy NE. **2004**. Nonlinear relationships and phylogenetically independent contrasts. *Journal of Evolutionary Biology* **17**: 709–715.

De Queiroz K. **2007**. Species concepts and species delimitation. *Systematic Biology* **56**: 879–886.

R Core Development Team. **2011**. R: a language and environment for statistical computing.

Rambaut A, Drummond A. **2007**. Tracer v1.5. *http://beast.bio.ed.ac.uk/Tracer*.

Read A, Nee S. **1995**. Inference from binary comparative data. *Journal of Theoretical Biology* **173**: 99–108.

Reeves PA, Richards CM. **2011**. Species delimitation under the general lineage concept: an empirical example using wild North American hops (Cannabaceae: *Humulus lupulus*). *Systematic Biology* **60**: 45–59.

Regalado Gabancho L, Prada C, Gabriel y Galán J. **2010**. Sexuality and apogamy in the Cuban *Asplenium auritum–monodon* complex (Aspleniaceae). *Plant Systematics and Evolution* **289**: 137–146.

Rieseberg LH, Wood TE, Baack EJ. **2006**. The nature of plant species. *Nature* **440**: 524–527.

Robson NKB. **2006**. Studies in the genus *Hypericum* L. (Clusiaceae). Section 9. *Hypericum* sensu lato (part 3): subsection 1. *Hypericum* series 2. *Senanensia*, subsection 2. *Erecta* and section 9b. *Graveolentia*. *Systematics and Biodiversity* **4**: 19–98.

Roe AD, Rice A V, Bromilow SE, Cooke JEK, Sperling FAH. **2010**. Multilocus species identification and fungal DNA barcoding: insights from blue stain fungal symbionts of the mountain pine beetle. *Molecular Ecology Resources* **10**: 946–959.

Roe AD, Sperling FAH. **2007**. Population structure and species boundary delimitation of cryptic *Dioryctria* moths: an integrative approach. *Molecular Ecology* **16**: 3617–3633.

Ronquist F, Huelsenbeck JP. **2003**. MrBayes 3: Bayesian phylogenetic inference under mixed models. *Bioinformatics* **19**: 1572–1574.

Sauer J, Hausdorf B. **2010**. Reconstructing the evolutionary history of the radiation of the land snail genus *Xerocrassa* on Crete based on mitochondrial sequences and AFLP markers. *BMC Evolutionary Biology* **10**: 299–311.

Sauer J, Hausdorf B. **2012**. A comparison of DNA-based methods for delimiting species in a Cretan land snail radiation reveals shortcomings of exclusively molecular taxonomy. *Cladistics* **28**: 300–316.

Schneider H, Ranker TA, Russell SJ, Cranfill R, Geiger JMO, Aguraiuja R, Wood KR, Grundmann M, Kloberdanz K, Vogel JC. **2005**. Origin of the endemic fern genus Diellia coincides with the renewal of Hawaiian terrestrial life in the Miocene. *Proceedings. Biological sciences / The Royal Society* **272**: 455–460.

Schneider H, Russell S, Cox C, Bakker F, Henderson S, Rumsey F, Barrett J, Gibby M, Vogel J. **2004a**. Chloroplast phylogeny of Asplenioid ferns based on *rbcL* and *trnL-F* spacer sequences (Polypodiidae, Aspleniaceae) and its implications for biogeography. *Systematic Botany* **29**: 260–274.

Schneider H, Schuettpelz E, Pryer KM, Cranfill R, Magallon S, Lupia R, Magallón S. **2004b**. Ferns diversified in the shadow of angiosperms. *Nature* **428**: 553–557.

Schneider H, Smith AR, Pryer KM. **2009**. Is morphology really at odds with molecules in estimating fern phylogeny? *Systematic Botany* **34**: 455–475.

Schneller J, Krattinger K. **2010**. Genetic composition of Swiss and Austrian members of the apogamous *Dryopteris affinis* complex (Dryopteridaceae, Polypodiopsida) based on ISSR markers. *Plant Systematics and Evolution* **286**: 1–6.

Schwander T, Henry L, Crespi B. **2011**. Molecular evidence for ancient asexuality in *Timema* stick insects. *Current Biology* **21**: 1129–1134.

Shaw J, Lickey EB, Schilling EE, Small RL. **2007**. Comparison of whole chloroplast genome sequences to choose noncoding regions for phylogenetic studies in angiosperms: The tortoise and the hare III. *American Journal of Botany* **94**: 275–288.

Sigel EM, Windham MD, Huiet L, Yatskievych G, Pryer KM. **2011**. Species relationships and farina evolution in the cheilanthoid fern genus *Argyrochosma* (Pteridaceae). *Systematic Botany* **36**: 554–564.

Smith AR, Cranfill RB. **2002**. Intrafamilial relationships of the thelypteroid ferns (Thelypteridaceae). *American Fern Journal* **92**: 131–149.

Smith AR, Kessler M, Gonzales J. **1999**. New records of Pteridophytes from Bolivia. *American Fern Journal* **89**: 244–266.

Smith AR, Mickel JT. **1977**. Chromosome counts for Mexican ferns. *Brittonia* **29**: 391–398.

Smith AR, Pryer KM, Schuettpelz E, Korall P, Schneider H, Wolf PG. **2006**. A classification for extant ferns. *Taxon* **55**: 705–731.

Soltis DE, Soltis PS. **1987**. Polyploidy and breeding systems in homosporous pteridophyta: a reevaluation. *The American Naturalist* **130**: 219–232.

Somer M, Arbesú R, Menéndez V, Revilla MA, Fernández H. **2009**. Sporophyte induction studies in ferns in vitro. *Euphytica* **171**: 203–210.

Stebbins GL. **1950**. *Variation and evolution in plants.* Columbia University Press, New York.

Stebbins GL. **1957**. Self-fertilization and population variation in higher plants. **91**: 337–354.

Stolze RG. **1981**. *Ferns and Fern Allies of Guatemala. Part II. Polypodiaceae*.

Stolze RG, Pacheco L, Øllgaard B. **1994**. 14(5B). Polypodiaceae - Dryopteridoideae - Physematieae. In: Harling G, Andersson L, eds. Flora of Ecuador. Goteborg: University of Goteborg, 108.

Suda J, Krahulcová A, Trávnícek P, Krahulec F. **2006**. Ploidy level versus DNA ploidy level: an appeal for consistent terminology. *Taxon* **55**: 447–450.

Suzuki T, Iwatsuki K. **1990**. Genetic variation in agamosporous fern *Pteris cretica* L . in Japan. *Heredity* **65**: 221–227.

Swofford DL. **1993**. PAUP: A computer-program for phylogenetic inference using maximum parsimony. *Journal of General Physiology* **102**.

Swofford DL. **2002**. PAUP* Phylogenetic Analysis Using Parsimony (* and other methods) Version 4.0b10, Sinauer Associates, Sunderland.

Sánchez-Jiménez I, Hidalgo O, Canela MÁ, Siljak-Yakovlev S, Šolić ME, Vallès J, Garnatje T. **2012**. Genome size and chromosome number in *Echinops* (Asteraceae, Cardueae) in the Aegean and Balkan regions: technical aspects of nuclear DNA amount assessment and genome evolution in a phylogenetic frame. *Plant Systematics and Evolution* **298**: 1085–1099.

Taberlet P, Gielly L, Pautou G, Bouvet J. **1991**. Universal primers for amplification of 3 non-coding regions of chloroplast DNA. *Plant Molecular Biology* **17**: 1105–1109.

Trewick SA, Morgan-Richards M, Russell SJ, Henderson S, Rumsey FJ, Pinter I, Barrett JA, Gibby M, Vogel JC. **2002**. Polyploidy, phylogeography and Pleistocene refugia of the rockfern *Asplenium ceterach*: Evidence from chloroplast DNA. *Molecular Ecology* **11**: 2003–2012.

Tryon R. **1956**. A revision of the American species of *Notholaena*. Contr. *Gray Herb.* **179**: 1–106.

Tryon A. **1957**. A revision of the fern genus *Pellaea* section *Pellaea*. *Annals of the Missouri Botanical Garden* **44**: 125–193.

Tryon R, Stolze R, Leon B. **1993**. Pteridophyta of Peru. Part V. 18: Aspleniaceae - 21. Polpodiaceae. *Fieldiana, Botany* **32**: 1–190.

Tryon R, Voeller B, Tryon A, Riba R. **1973**. Fern Biology in Mexico (A Class Field Program). *BioScience* **23**: 28–33.

Tutin TG, Burges NA, Chater AO, Edmondson JR, Heywood VH, Moore DM, Valentine DH, Walters SM, Webb DA. **1993**. *Flora Europea*.

Vekemans X, Beauwens T, Lemaire M, Roldán-Ruiz I. **2002**. Data from amplified fragment length polymorphism (AFLP) markers show indication of size homoplasy and of a relationship between degree of homoplasy and fragment size. *Molecular ecology* **11**: 139–151.

Verduijn MH, Van Dijk PJ, Van Damme JMM. **2004**. Distribution, phenology and demography of sympatric sexual and asexual dandelions (*Taraxacum officinale* s.l.): geographic parthenogenesis on a small scale. *Biological Journal of the Linnean Society* **82**: 205–218.

Verhoeven KJF, Dijk PJ van, Biere A, Van Dijk PJ. **2010**. Changes in genomic methylation patterns during the formation of triploid asexual dandelion lineages. *Molecular Ecology* **19**: 315–324.

Vida G. **1970**. The nature of polyploidy in *Asplenium ruta-muraria* L. and *A.lepidium* C. *Presl. Caryologia* **23**: 525–547.

Vos P, Hogers R, Bleeker M, Reijans M, Vandelee T, Hornes M, Frijters A, Pot J, Peleman J, Kuiper M, *et al.* 1995. AFLP: A new technique for DNA fingerprinting. *Nucleic Acids Research* **23**: 4407–4414.

Wagner W. **1963**. A biosystematic study of United States ferns - preliminary abstract. *American Fern Journal* **53**: 1–16.

Wagner W. **1966**. Two new species of ferns from the United states. *American Fern Journal* **56**: 3–17.

Wagner W, Farrar D, McAlpin B. **1970**. Pteridology of the Highlands Biological Station Area, Southern Appalachians. *Journal of the Elisha Mitchell Scientific Society* **86**: 1–24.

Wagner W, Moran R, Werth C. **1993**. Aspleniaceae. Flora of North America. New York: Oxford University Press, 237–238.

Wagner W, Wagner F. **1966**. Pteridophytes of the mountain lake aras, Gilles Co., Virginia: Biosystematic Studies 1964-65. *Castanea* **31**: 121–140.

Wagner W, Wagner F. **1980**. Polyploidy in pteridophytes. In: Lewis WH, ed. Polyploidy, biological relevance. Plenum Press, 199–214.

Walker TG. **1962**. Cytology and evolution in the fern genus *Pteris* L. *Evolution* **16**: 27–43.

Walker TG. **1966a**. Apomixis and vegetative reproduction in ferns. In: Hawkes JG, ed. Reproductive Biology and Taxonomy of Vascular Plants. Hampton, Middlesex: Bot.Soc.Brit.Isles, 152–161.

Walker TG. **1966b**. A cytotaxonomic survey of the pteridophytes of Jamaica. *Transacions of the Royal Society of Edinburgh* **66**: 169–237.

Walker TG. **1979**. The cytogenetics of ferns. In: Dyer AF, ed. The Experimental Biology of Ferns. New York: Academic Press, 87–132.

Warton DI, Duursma RA, Falster DS, Taskinen S. **2011**. SMATR 3- an R package for estimation and inference about allometric lines. *Methods in Ecology and Evolution*: 1–3.

Watano Y, Iwatsuki K. **1988**. Genetic variation in the "Japanese apogamous form" of the fern *Asplenium unilaterale* Lam. *Botanical Magazine (Tokyo)* **101**: 213–228.

Webb CO, Ackerly DD, Kembel SW. **2008**. Phylocom: software for the analysis of phylogenetic community structure and trait evolution. *Bioinformatics* **24**: 2098–2100.

Weber HE. **1996**. Former and modern taxonomic treatment of the apomictic *Rubus* complex. *Folia Geobotanica & Phytotaxonomica* **31**: 373–380.

Welch DM, Meselson M. **2000**. Evidence for the evolution of bdelloid rotifers without sexual reproduction or genetic exchange. *Science* **288**: 1211–1215.

Whitton J, Sears CJ, Baack EJ, Otto SP. **2008**. The dynamic nature of apomixis in the angiosperms. *International Journal of Plant Sciences* **169**: 169–182.

Williams GC. **1975**. Sex and evolution. *Monogr Popul Biol*: 3–200.

Windham MD. **1983**. The ferns of Elden Mountain, Arizona. *American Fern Journal* **73**: 85–93.

Winkler H. **1908**. *Parthenogenesis und apogamie im pflanzenreich* (G Fisher, Ed.). Jena.

Wood TE, Takebayashi N, Barker MS, Mayrose I, Greenspoon PB, Rieseberg LH. **2009**. The frequency of polyploid speciation in vascular plants. *Proceedings of the National Academy of Sciences* **106**: 13875–13879.

Wubs ERJ, De Groot GA, During HJ, Vogel JC, Grundmann M, Bremer P, Schneider H. **2010**. Mixed mating system in the fern *Asplenium scolopendrium* : implications for colonization potential. *Annals of Botany* **106**: 583–90.

Yao-Moan Huang YMH, Hsueh-Mei Chou HMC, Tsung-Hsin Hsieh THH, Jenn-Che Wang JCW, Wen-Liang Chiou WLC. **2006**. Cryptic characteristics distinguish diploid and triploid varieties of *Pteris fauriei* (Pteridaceae). *Canadian Journal of Botany* **84**: 261–268.

Zedek F, Smerda J, Smarda P, Bureš P. **2010**. Correlated evolution of LTR retrotransposons and genome size in the genus *Eleocharis*. *BMC Plant Biology* **10**: 265–274.

Zuloaga FO, Morrone O, Belgrana MJ. **2008**. *Catalogo de las Plantas Vasculares del Cono Sur*. St. Louis: MBG Press.